# Molecular genetic investigations of histone deacetylase inhibitors

# as potential neurotherapeutics

# for autosomal recessive proximal spinal muscular atrophy (SMA)

**I n a u g u r a l - D i s s e r t a t i o n**

**zur**

**Erlangung des Doktorgrades**

**der Mathematisch-Naturwissenschaftlichen Fakultät**

**der Universität zu Köln**

**vorgelegt von**

**Lars Brichta**

**aus Lutherstadt Eisleben**

**2006**

**Für meine Eltern**

# Acknowledgements

# Table of contents

# List of abbreviations

| | |
|---|---|
| A | adenine |
| APS | ammonium persulfate |
| bp | base pair |
| BSA | bovine serum albumin |
| C | cytosine |
| CD | cluster of differentiation |
| cDNA | complementary DNA |
| cen | centromeric |
| CK | creatine kinase |
| cM | centimorgan |
| cm | centimeter |
| CNS | central nervous system |
| CPDA-1 | citrate, phosphate, dextrose-adenine (solution) |
| DEPC | diethylpyrocarbonate |
| D-MEM | Dulbecco's modified Eagle medium |
| DMSO | dimethylsulfoxide |
| DNA | deoxyribonucleic acid |
| EBV | Epstein-Barr virus |
| EDTA | ethylenediaminetetraacetic acid |
| e.g. | exempli gratia |
| EMG | electromyography |
| ESE | exonic splicing enhancer |
| ESS | exonic splicing silencer |
| *et al.* | et alii |
| FCS | fetal calf serum |
| FDA | Food and Drug Administration |
| FITC | fluorescein isothiocyanate |
| FL | full length |
| G | guanine |
| *g* | acceleration due to gravity |
| GGT | gamma-glutamyltransferase |
| GPT | glutamic-pyruvic transaminase |
| h | hours |
| HAT | histone acetyltransferase |
| HBSS | Hanks' balanced salt solution |
| HDAC | histone deacetylase |
| HMT | histone methyltransferase |
| i.e. | id est |
| ISS | intronic splicing silencer |

| | |
|---|---|
| kb | kilobases |
| kDa | kilodalton |
| l | liter |
| LAT | lysine acetyltransferase |
| LLN | lower limit of normal |
| M | molar |
| m | milli- |
| Mb | megabases |
| MDa | megadalton |
| min | minutes |
| ml | milliliter |
| mm | millimeter |
| mM | millimolar |
| mRNA | messenger RNA |
| NCV | nerve conduction velocity |
| n.d. | not determined |
| ng | nanogram |
| nm | nanometer |
| nmol | nanomol |
| OHSC | organotypic hippocampal slice culture |
| OMIM | Online Mendelian Inheritance in Man |
| PAA | polyacrylamide |
| PAGE | polyacrylamide gel electrophoresis |
| PBMC | peripheral blood mononuclear cells |
| PBS | phosphate-buffered saline |
| PCR | polymerase chain reaction |
| pH | power of hydrogen |
| PI | propidium iodide |
| pmol | picomol |
| RNA | ribonucleic acid |
| RNAi | RNA interference |
| rpm | revolutions per minute |
| RT | reverse transcription |
| SAHA | suberoylanilide hydroxamid acid |
| SD | standard deviation |
| SDS | sodium dodecyl sulfate |
| SEM | standard error of the mean |
| siRNA | small interfering RNA |
| SMA | autosomal recessive spinal muscular atrophy |
| SMN | survival motor neuron |
| T | thymidine |
| TEMED | N,N,N',N'-tetramethylethylenediamine |

| | |
|---|---|
| ter | telomeric |
| UV | ultraviolet |
| VPA | valproic acid |
| μ | micro- |
| μg | microgram |
| μl | microliter |
| μM | micromolar |
| μm | micrometer |
| # | number |

# 1    Introduction

The spinal muscular atrophies constitute a genetically and clinically heterogeneous group of neuromuscular disorders in humans sharing the common pathological feature of degeneration of lower motor neurons in the anterior horns of the spinal cord. Other neurologic systems (including brain and sensory nerves) or other organs are rarely involved. Intelligence of affected individuals is normal. In all spinal muscular atrophy patients, the progressive loss of innervating α-motor neurons causes denervation especially of voluntary muscles, leading to weakness and muscle atrophy as central disease symptoms. The different forms of lower motor neuron diseases covered by the term 'spinal muscular atrophies' are classified according to clinical features (including age of onset, disease severity and distribution of muscle weakness) and on their modes of inheritance (autosomal or X-linked, recessive or dominant). However, the majority of patients (80-90%) demonstrate autosomal recessive inheritance with proximal manifestation of muscle weakness and atrophy of limbs and trunk, which is defined as *autosomal recessive proximal spinal muscular atrophy (SMA)*.

With an incidence of approximately 1 in 6,000-10,000 live births and a heterozygosity frequency of 1 in 35 among Europeans, proximal SMA is the second most common autosomal recessive disorder after cystic fibrosis. Worldwide, it represents the leading genetic cause of death in childhood and early youth. In order to analyze the molecular genetic basis and the pathophysiological mechanisms of SMA, research focused on the identification of the disease determining gene. In 1990, the application of positional cloning strategies and segregation analyses revealed mapping of proximal SMA to a candidate region on the long arm of human chromosome 5 (5q11.2-13.3). There was a major breakthrough in the understanding of the disease in 1995, when a gene was identified which was found to be homozygously deleted in most SMA patients. According to the typical degeneration of α-motor neurons in SMA, this gene was named *survival of motor neuron* gene (*SMN*). There are two nearly identical gene copies of *SMN* located within the ~750 kb SMA region on chromosome 5q13: one telomeric copy termed *SMN1*, and a second copy of the gene closer to the centromer termed *SMN2*. While homozygous deletion or mutation of *SMN1* has been determined to cause SMA, each patient retains at least one *SMN2* copy. *SMN2* is the result of duplication events in the human genome and differs from *SMN1* by five nucleotides, only one of which is located in the translated region. This nucleotide exchange in exon 7 has been characterized as a silent mutation without impact on the amino acid sequence. Consequently, *SMN1* and *SMN2* encode identical proteins. However, in contrast to *SMN1*, which exclusively produces full-length mRNA transcripts, *SMN2* undergoes alternative splicing and mainly generates transcripts lacking exon 7. The latter encode an unstable, only partially functional protein. Hence, *SMN2* is not able to fully compensate for the loss of *SMN1* in SMA patients. Insufficient amounts of functional SMN protein lead to α-motor neuron degeneration.

To date, a causal therapy for SMA is not available. *SMN2* is the only SMA modifying gene known so far. Milder disease phenotypes correlate with increased *SMN2* copy numbers. Since *SMN2* is present in each patient, ubiquitously expressed in all tissues and encodes the same protein like *SMN1*, it has been identified as major target for a potential SMA therapy.

## 1.1    Diagnostic criteria and clinical picture of proximal SMA

### 1.1.1    Diagnostic criteria

The diagnosis of SMA is carried out by the help of clinical, biochemical, electrophysiological, histopathological and molecular genetic criteria (Munsat and Davies 1992; Zerres and Davies 1999). The key symptom of proximal SMA is a symmetrical and progressive muscle weakness and atrophy affecting the limbs positioned closer to the body, such as upper arms and legs, rather than more distant body parts such as hands, feet, fingers, or toes. The weakness in the legs occurs earlier and is generally greater than the weakness in the arms. Muscle groups in the face and eyes are not involved.

Serum creatine kinase (CK) activity is a sensitive marker of increased muscle membrane permeability for large molecules. CK is a "leakage enzyme" present in high concentrations in the cytoplasm of myocytes and is the most widely used enzyme to diagnose and follow muscle disease. In neuromuscular disorders like proximal SMA, serum CK values are only mildly to moderately elevated. The CK test is used to exclude primary dystrophic processes of the muscle which may lead to extensively increased CK values of 10x normal and above. An elevated serum CK activity above 10x normal indicates a muscle disorder and is an exclusion criterion for proximal SMA.

One of the main diagnostic tools is electromyography (EMG). Contraction of the voluntary muscles is controlled by electrical impulses. They originate from the brain and pass down the motor neurons to the connecting muscles, where the contraction is triggered. The EMG records this electrical impulse and determines whether the electric current and the speed at which the electric impulse passes down the motor neuron are the same as in normal individuals. In SMA patients, EMG demonstrates characteristic spontaneous muscle activity with fibrillations and fasciculations of single muscle fibers and motor units. Nerve conduction velocity (NCV) in SMA patients is normal or mildly reduced, but not lower than 70% compared to age-matched control individuals. A secure diagnosis of proximal SMA always includes an adequate muscle biopsy specimen processed with histochemical stains. Typical histologic and histochemical features allow separation of SMA from other denervating disorders. The vast majority of fibers are atrophic and of both fiber types, with pathologic fiber type grouping the rule. An additional distinctive feature is the presence of a small number of scattered hypertrophic type 1 fibers presumably resulting from physiologic hypertrophy. Normal-appearing fibers may be present. Important in histologic diagnosis is the absence of significant necrosis, degeneration, regeneration, lipid accumulation, or connective tissue proliferation. However, older patients with long-standing SMA may demonstrate some of these features, suggesting a secondary myopathic process.

Since 1995, the clinical diagnosis of SMA can be confirmed by molecular genetic testing. Therefore, the *SMN1* gene on chromosome 5q is screened for specific mutations (deletions/gene conversions of exon 7 or exon 7 and 8). In addition, this molecular investigation is applied in prenatal diagnosis and carrier testing, making it a highly important diagnostic tool.

In 1992, the International SMA Consortium defined diagnostic criteria which allow the secure separation of proximal SMA from other disorders (Munsat and Davies 1992). Due to the gain of knowledge regarding SMA, these criteria were modified in 1999 (Zerres and Davies 1999). The most important inclusion and exclusion criteria for proximal SMA are summarized in table 1.

**Table 1: Diagnostic inclusion and exclusion criteria for proximal SMA (Munsat and Davies 1992), modified by the International SMA Consortium in 1999 (Zerres and Davies 1999). "LLN" is the abbreviation for "lower limit of normal".**

| Inclusion criteria | Exclusion criteria |
| :---: | :---: |
| **Muscle weakness** | involvement of muscle groups of eye and face |
| symmetrical | CNS involvement |
| proximal > distal | involvement of other organs (e.g. ears, eyes) |
| legs > arms | disturbance of sensibility |
| involvement of trunk and intercostals | involvement of diaphragm and myocardium |
| | creatine kinase activity > 10x normal |
| **Denervation** | nerve conduction velocity < 70% of the LLN |
| neurogenic EMG | |
| atrophic fibers in muscle biopsy | |
| fasciculation | |

### 1.1.2    Clinical picture and classification of proximal SMA

The clinical picture of severe infantile proximal SMA was described for the first time by Werdnig in 1891 (Werdnig 1891) and Hoffmann in 1893 (Hoffmann 1893). Many years later, in 1956, Kugelberg and Welander reported a less severe form of SMA. The phenotype of proximal SMA is highly variable. In acute cases, first disease symptoms may occur as early as prenatally, whereas milder forms are characterized by manifestation in adulthood. Depending on the age of onset and disease severity, the International SMA Consortium defined a classification into four types (type I-IV) which is presented in table 2 (Munsat and Davies 1992; Zerres and Rudnik-Schoneborn 1995).

**Type I SMA** patients (acute infantile SMA, Werdnig-Hoffmann disease; OMIM #253300) are most severely affected with generalized muscle weakness and hypotonia ("floppy infants"). Manifestation already occurs by decreased fetal movements in the last trimester of pregnancy in about one third of cases. However, onset is always noted within six months after birth. Affected infants never achieve the ability to sit or walk and normally die before two years of age due to respiratory failure or infection.

**Type II SMA** patients (intermediate form, chronic infantile SMA; OMIM #253550) show first clinical signs after six months but before 18 months of age. They are able to sit independently but never learn to walk. Life expectancy is reduced, the survival rate is about 70% at age 20.

**Type III SMA** patients (Kugelberg-Welander disease, juvenile SMA, OMIM #253400) present a disease onset after 18 months of age and the symptoms can begin to develop as late as adulthood. They are able to sit and walk but often become wheelchair-bound in the course of disease progression. Patients with an age of onset before three years are sub-classified as IIIa, those with an

age of onset after three years as IIIb (Zerres and Rudnik-Schoneborn 1995; Wirth et al. 2006). Life expectancy is almost normal.

**Type IV SMA** patients (adult form of SMA, OMIM #271150) are very rare and characterized by an age of onset >30 years and only very mild signs of muscle weakness. So far, only very few patients with type IV have been identified with homozygous absence of *SMN1* (Brahe et al. 1995; Clermont et al. 1995; Wirth et al. 2006), while the majority of SMA type IV patients do not show any detectable deletions in this gene (Zerres et al. 1995). The life expectancy of SMA type IV patients is not reduced.

**Table 2: Proximal SMA is a clinically heterogenous disorder.**

| SMA type | Age of onset | Motor milestone achievements | Life expectancy |
|---|---|---|---|
| **I** <br> **(Werdnig-Hoffmann)** | ≤ 6 months | never able to sit or walk | < 2 years |
| **II** <br> **(intermediate form)** | ≤ 18 months | able to sit but never learn to walk | youth to adulthood |
| **III** <br> **(Kugelberg-Welander)** | > 18 months | able to sit and walk at one time | slightly reduced |
| **IV** <br> **(adult form)** | > 30 years | normal development | normal |

Due to the ongoing degeneration of α-motor neurons, motor milestones which have been achieved by a patient at one time may be lost again in the course of disease progression. In particular in SMA type I and II patients, weakness of the muscles involved in breathing and coughing increases the susceptibility for respiratory infections. Thus, respiratory insufficiency is the most frequent cause of death.

Although the clinical spectrum of onset and severity is broad, all autosomal-recessively inherited forms of proximal SMA are genetically homogenous (Gilliam et al. 1990). Siblings affected with SMA present identical courses of disease progression and are assigned to the same SMA type. The finding of siblings with discordant phenotypes is a very rare exception (Brahe et al. 1993; Rudnik-Schöneborn et al. 1994; Cobben et al. 1995; Hahnen et al. 1995; Wang et al. 1996; Helmken et al. 2003).

## 1.2    Molecular basis of proximal SMA

### 1.2.1    Mapping of the SMA region

In 1990, SMA types I, II and III were mapped by linkage analysis to one single region of about 10 cM on chromosome 5q (5q11.2-13.3) (Brzustowicz et al. 1990; Gilliam et al. 1990; Melki et al. 1990). The development of many new highly polymorphic markers during the following five years allowed the critical SMA locus to be refined to a size less than 1 Mb (Melki et al. 1993; Soares et al. 1993; DiDonato et al. 1994; Melki et al. 1994; Wirth et al. 1994; Wirth et al. 1995). This region was shown to contain a highly complex genomic structure consisting of a duplicated and inverted DNA segment of about 500 kb (Lefebvre et al. 1995), which considerably hampered the construction of a uniform

physical map (Thompson et al. 1993; Melki et al. 1994; Lefebvre et al. 1995; Roy et al. 1995b). As we know nowadays, the SMA region is prone to *de novo* genomic rearrangements including unequal crossing-over, inter- and intrachromosomal rearrangements and gene conversions (Melki et al. 1994; Wirth et al. 1997; Schmutz et al. 2004). Each of the two 500 kb segments can be present in 0 to 4 copies per chromosome and contains five genes which were assumed to be candidates for determination of SMA (figure 1): the *survival motor neuron* gene [*SMN*, (Lefebvre et al. 1995)], the *baculoviral IAP repeat-containing protein 1* gene (*BIRC1*), also known as *neuronal apoptosis inhibitory protein* gene [*NAIP*, (Roy et al. 1995a)], the *small EDRK-rich factor 1* gene [*SERF1*, (Scharf et al. 1998)], also known as *H4F5,* the *general transcription factor IIH* or *p44* gene (*GTF2H2*) which encodes a subunit of the transcription factor TFIIH (Burglen et al. 1997; Carter et al. 1997)*,* and the *occludin* gene [*OCLN*, (Lefebvre et al. 1995; Schmutz et al. 2004)]. The polymorphic region which contains the duplicated and inverted five candidate genes is proximally flanked by the unique gene *RAD17* (Deimling von et al. 1999) and distally flanked by *TFNR* (Kelter et al. 2000).
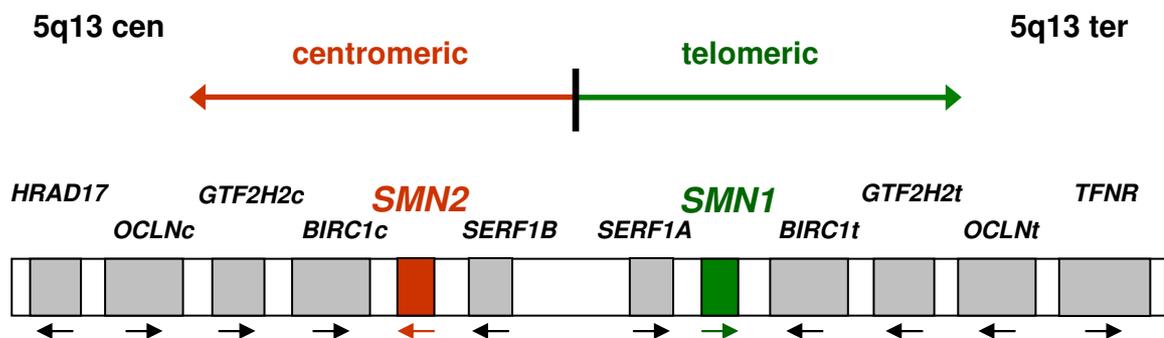


**Figure 1: Schematic of the duplicated and inverted SMA region on chromosome 5q13.**

### 1.2.2    *Survival motor neuron (SMN)*, the SMA determining gene in humans

In 1995, Lefebvre and colleagues identified the *survival motor neuron gene 1* (*SMN1)* as the SMA determining gene (Lefebvre et al. 1995). Although each of the genes that are located in the SMA region may be deleted in SMA patients (Roy et al. 1995a; Burglen et al. 1997; Scharf et al. 1998), it has been conclusively demonstrated that only homozygous mutation of the telomeric *SMN1* is causative for SMA. The ultimate proof was given by the identification of subtle (and in particular missense) mutations located in the *SMN1* gene [reviewed in (Wirth 2000)]. The number of centromeric *SMN2* copies modifies the disease severity (Lefebvre et al. 1995; Burghes 1997; Wirth et al. 1999; Brahe 2000; Wirth 2000; Feldkötter et al. 2002; Mailman et al. 2002; Wirth et al. 2006).

On genomic level, each *SMN* copy spans a region of about 28 kb (Chen et al. 1998) and consists of nine exons (1-2a, 2b-8) with an open reading frame of 882 bp (294 codons). *SMN1* and *SMN2* are almost identical except for five nucleotide differences at their 3' ends (figure 2): one in exon 7, one in exon 8, one in intron 6 and another two in intron 7, respectively (Lefebvre et al. 1995; Burglen et al. 1996; Chen et al. 1998; Monani et al. 1999a). Applying a PCR-based assay followed by restriction digestion or direct sequencing, the genomic differences allow molecular genetic diagnostics of SMA

(Lefebvre et al. 1995; van der Steege et al. 1995; Wirth et al. 1999). The vast majority of SMA type I-III patients (96%) show homozygous absence of *SMN1* exon 7 and 8 or exon 7 only (Wirth 2000). This phenomenon is due to two mechanisms: deletions of *SMN1* or gene conversion of *SMN1* into *SMN2* (Wirth et al. 1997). Deletions are typically observed in type I SMA patients. Conversions of *SMN1* into *SMN2* which result in an increased number of *SMN2* genes are predominantly found in type II and III SMA patients. Gene conversion is a common mutational mechanism in the SMA region (Lefebvre et al. 1995; Hahnen et al. 1996; van der Steege et al. 1996). It may also cause the conversion of *SMN2* into *SMN1*. In rare cases, it has been described as a *de novo* event (Raclin et al. 1997; Wirth et al. 1997; Wirth et al. 1999) and can affect the complete *SMN* gene as well as only a part of it. Besides homozygous absence of *SMN1*, a minority of SMA patients (~4%) exhibit intragenic *SMN1* mutations which result in a disturbed gene function. Typically, these patients are compound heterozygotes with a deletion on one and a subtle mutation on the other chromosome 5 (Bussaglia et al. 1995; Lefebvre et al. 1995; Rodrigues et al. 1995; Hahnen et al. 1997; Simard et al. 1997; Wirth et al. 1999; Wirth 2000; Ogino and Wilson 2002; Clermont et al. 2004; Sun et al. 2005). The presence of at least one fully functional *SMN1* gene is sufficient to protect from SMA. Homozygous absence of *SMN2*, a genotype found in about 3-5% of control individuals, has no apparent phenotypical consequences (Lefebvre et al. 1995).

None of the five nucleotides which allows *SMN1* and *SMN2* to be distinguished on genomic level leads to an amino acid exchange on protein level. While the C to T transition in exon 7 is a silent mutation, the nucleotide exchange in exon 8 is located in the 3' untranslated region of the *SMN* mRNA.

### 1.2.3    Alternative splicing of *SMN* transcripts

The roughly 1.5 kb *SMN1* and *SMN2* transcripts are ubiquitously expressed (Lefebvre et al. 1995). However, subsequent processing of *SMN1* and *SMN2* pre-mRNA is markedly different (Gennarelli et al. 1995; Lefebvre et al. 1995) (figure 2). The disease determining *SMN1* gene almost exclusively produces full-length transcripts (FL-*SMN1*) that contain each single exon (1-2a, 2b-8), whereas *SMN2* undergoes alternative splicing and generates only 10% of FL transcripts (FL-*SMN2*) but 90% of transcripts that lack exon 7 (Δ7-*SMN2*). In the FL transcripts, the translation termination codon is located at the end of exon 7. FL-*SMN1* transcripts and FL-*SMN2* transcripts code for an identical FL-SMN protein composed of 294 amino acids. The Δ7-*SMN2* transcripts lack exon 7 and therefore encode a truncated SMN protein of only 282 amino acids. Skipping of exon 7 forces the translation machinery to use an alternative stop codon located in exon 8. Thus, a protein is generated with a C-terminus that lacks the 16 amino acids encoded by exon 7 but contains four amino acids encoded by exon 8. This truncated protein is biochemically unstable and shows a reduced oligomerization capacity which is essential for proper SMN function (Lorson et al. 1998; Lorson and Androphy 2000).

Additionally, both *SMN* genes produce very low amounts of alternatively spliced transcripts lacking exon 5 (Δ5-*SMN*) or exon 3 (Δ3-*SMN*) or exons 5 and 7 (Δ5,7-*SMN*) (Gennarelli et al. 1995; Chang et al. 2001; Singh et al. 2006). Skipping of these exons leads to the synthesis of an SMN protein which is truncated but in frame. The loss of exon 3 is of particular interest, since the corresponding protein

sequence contains a so-called *Tudor domain* that is essential for the interaction with Sm (Smith antigen) proteins (see chapter 1.2.5). Absence of the Tudor domain or the presence of missense mutations within the encoding genomic region either abolishes or reduces the ability of SMN to interact with Sm proteins (Buhler et al. 1999; Mohaghegh et al. 1999; Sun et al. 2005).
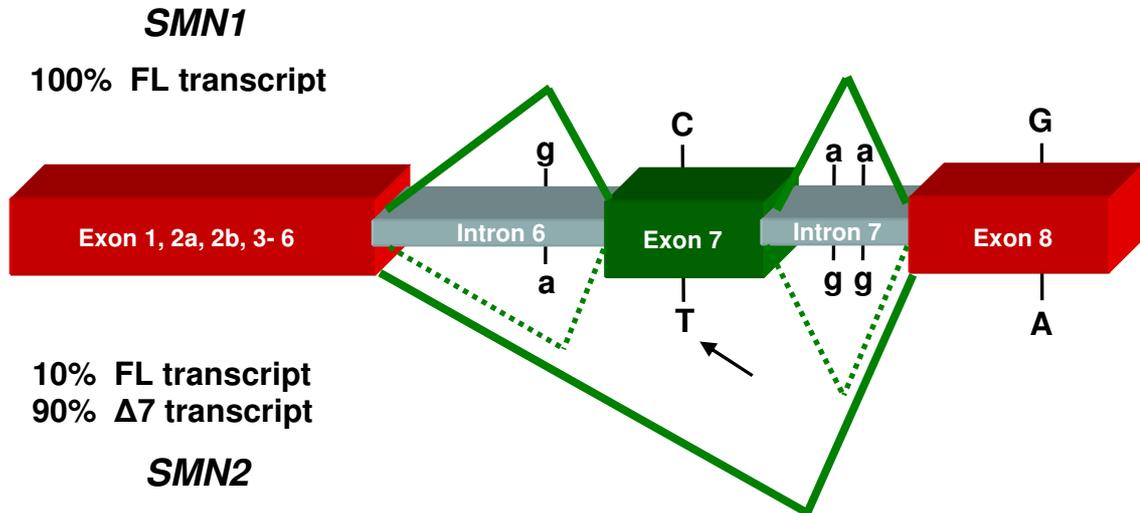


**Figure 2: The genomic sequences of *SMN1* and *SMN2* are almost identical except for five nucleotide variants: one in intron 6 (44 bp upstream of exon 7: c.835-44G>A), one in exon 7 (bp number 6: c.840C>T), two in intron 7 (100 bp downstream of exon 7: c.888+100A>G, and 214 bp downstream of exon 7: c.888+214A>G), and one in the 3' untranslated region in exon 8 (bp 234: c.1121G>A). In contrast to *SMN1* which mainly produces FL transcripts, *SMN2* undergoes alternative splicing of exon 7 and generates only minor amounts of a FL transcript, but large numbers of truncated Δ7 transcripts.**

### 1.2.4    Splicing regulation of *SMN* exon 7

*SMN* exon 7 spans 54 nucleotides and harbors a translation termination codon at positions 49 to 51. The last nucleotide at the exon/intron border is an adenosine residue, which places exon 7 into the minor group of internal exons lacking a guanosine residue at the 3'-end (Burge et al. 1999). Exon 7 is characterized by a weak 3' splice site due to a suboptimal polypyrimidine tract (Lim and Hertel 2001). Correct splicing of exon 7 depends on a number of cis-acting elements (splicing enhancers and silencers) that are localized within exon 7 itself and the adjacent introns 6 and 7. They are recognized by various trans-acting splicing factors which belong to the family of serine(S)–arginine(R)–rich proteins (SR and SR-like proteins) as well as to the family of heterogeneous nuclear ribonucleoproteins (hnRNPs) (Lorson et al. 1999; Hofmann et al. 2000; Lorson and Androphy 2000; Cartegni and Krainer 2002; Hofmann and Wirth 2002; Miyajima et al. 2002; Young et al. 2002b; Kashima and Manley 2003; Miyaso et al. 2003). Most of these elements seem to be highly conserved and also play a role in processing of the murine *Smn* pre-mRNA (DiDonato et al. 2001).

In 1999, it was demonstrated that only the C to T transition in *SMN2* exon 7 is responsible for skipping of this exon in the majority of *SMN2* transcripts, regardless of the cell type or tissue that was

investigated (Lorson et al. 1999). Subsequent studies by Cartegni et al. revealed that the C to T exchange disrupts the conserved heptamer motif of an exonic splicing enhancer (ESE). In *SMN1* transcripts, this ESE is recognized directly by the SR-rich splicing factor SF2/ASF. Binding of SF2/ASF to *SMN1* exon 7 facilitates the generation of FL transcripts. However, the altered ESE sequence in *SMN2* derived transcripts fails to recruit SF2/ASF leading to inefficient exon 7 inclusion (Cartegni and Krainer 2002). In contrast to these findings, Kashima et al. demonstrated that the C to T exchange in *SMN2* creates a new exonic splicing silencer (ESS) for the repressor protein hnRNP A1 rather than disrupting an ESE for SF2/ASF (Kashima and Manley 2003). Binding of hnRNP A1 to the ESS in *SMN2* exon 7 results in skipping of this exon. It was shown that the reduction of hnRNP A1 by RNA interference in HeLa cells promotes exon 7 inclusion into *SMN2* RNA. Moreover, by using *in vitro* UV cross-linking, hnRNP A1 was found to bind exon 7 of *SMN2* but not of *SMN1*. In 2006, results obtained from further extensive testing of the enhancer-loss and the silencer-gain models were presented by Cartegni et al. (Cartegni et al. 2006). They support the hypothesis of the enhancer-loss model and confirm that *SMN2* exon 7 skipping primarily results from the loss of the SF2/ASF-dependent ESE. It was found that hnRNP A1 indeed has a strong inhibitory effect on exon 7 inclusion, but this observation is independent of the C to T transition and, therefore, an indirect event not specific to *SMN2*. The finding that SF2/ASF and hnRNP A1 antagonize each other is well known (Eperon et al. 2000; Zhu et al. 2001; Black 2003) and may cause tissue-specific differences in the extent of exon 7 inclusion based on the relative concentration of these two proteins.

Furthermore, an investigation of the first 16 nucleotides of *SMN2* exon 7 revealed that the 5' end of this exon contains a so-called extended inhibitory context (Singh et al. 2004a; Singh et al. 2004b). This context covers a larger sequence than the disrupted SF2/ASF-ESE and hnRNP A1-ESS. The abrogation of this inhibitory context promotes exon 7 inclusion even in the absence of the SF2/ASF binding motif as well as the presence of the hnRNP A1 binding site. Another inhibitory tract consisting of seven nucleotides was found near the 3' end of exon 7 (Singh et al. 2004b).

In addition to the 5' end ESE and ESS, another GA-rich ESE is localized in the center of exon 7 of *SMN1* and *SMN2* (Lorson and Androphy 2000). This ESE binds the SR-like splicing factor Htra2-β1, the ortholog of Drosophila melanogaster transformer-2 (Tra2) (Hofmann et al. 2000). In Drosophila, Tra2 is essential for the regulation of sex-differentiation by alternative splicing (Baker 1989). Mutations in the ESE in the center of exon 7 abolish the capacity of *SMN1* to produce correctly spliced transcripts (Lorson and Androphy 2000). In addition, the SR protein SRp30c as well as hnRNP G and RBM (belonging to the group of hnRNPs) directly bind Htra2-β1 and further enhance the inclusion of exon 7 (Hofmann and Wirth 2002; Young et al. 2002b). This network of splicing factors binding to the central ESE in exon 7 is most likely responsible for the 10-15% of FL mRNA generated by *SMN2*. Over-expression of these splicing factors either separate or in combination restores the splicing capacity of *SMN2* minigenes up to 80% and substantially increases endogenous SMN protein levels (Hofmann et al. 2000; Hofmann and Wirth 2002; Young et al. 2002b). In consideration of the regulatory proteins known so far, figure 3 displays two models which summarize the splicing of exon 7 in *SMN1* and *SMN2* pre-mRNA.

Alternative splicing of *SMN2* exon 7 is furthermore regulated by an intronic splicing silencer localized in intron 6 (element 1; 112 to 68 bp upstream of exon 7) and by an intronic splicing enhancer localized in intron 7 (element 2; 59 to 72 bp downstream of exon 7) (Miyajima et al. 2002; Miyaso et al. 2003).

However, deletion or mutation of these elements does not affect the correct splicing of wild-type *SMN1* pre-mRNA, suggesting that their function depends on the presence of the C to T transition in *SMN2* exon 7. A 33 kDa protein has been shown to interact with element 1 of *SMN2* but not of *SMN1*. Element 2 in intron 7 possesses a characteristic stem-loop structure, in which correct matching of the nucleotides within the stem is essential. Data base analysis revealed matching of the nucleotide sequence of the stem-loop structure to intronic sequences of several other genes, however, the experimental proof for a role in the regulation of splicing still has to be given.
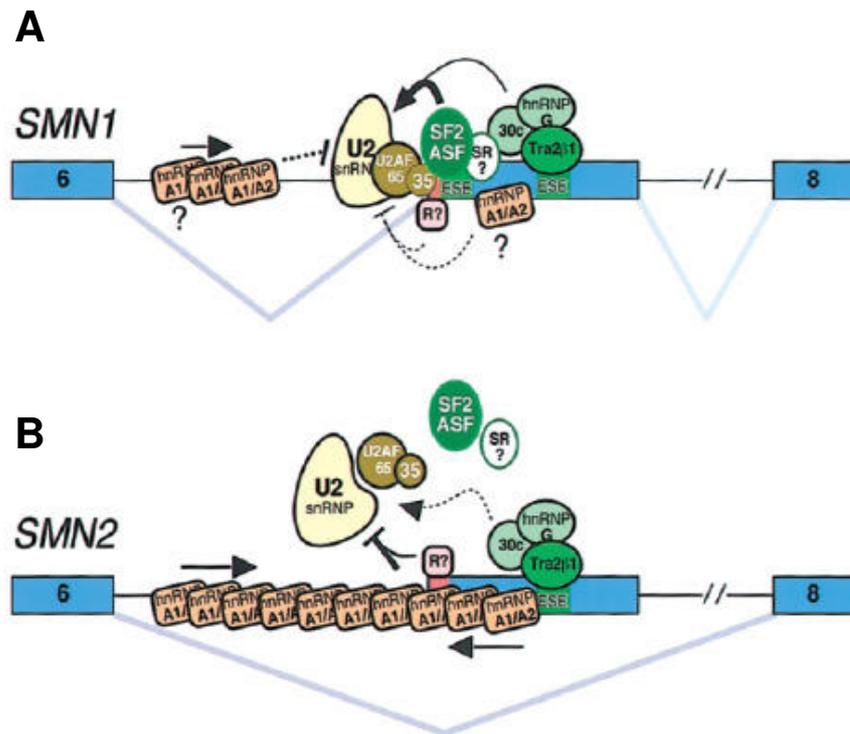


**Figure 3: Model for the impact of the *SMN2* C to T transition on splicing of exon 7 in *SMN* pre-mRNA (Cartegni et al. 2006). *(A)* In *SMN1*, binding of U2 snRNP and efficient splicing of exon 7 is due to binding of SF2/ASF to the ESE at the 5' end of the exon which contains the C at position +6. Further splicing factors (Htra2-β1, SRp30c, hnRNP G, and yet unknown proteins termed "SR?") binding to enhancer motifs localized downstream additionally promote exon 7 inclusion and the generation of FL transcripts. This network of splicing proteins prevents an inhibitory action of hnRNP A1 and/or additional repressor proteins ("R?") on *SMN1* exon 7 splicing. *(B)* In contrast to the *SMN1* context, the C to T nucleotide exchange and abrogation of the ESE for SF2/ASF in *SMN2* allows a markedly increased inhibitory effect of hnRNP A1 and/or further suppressors termed "R?". Thus, exon 7 is skipped in the majority of *SMN2* transcripts. This inhibitory effect can not be overcome by the remaining positive elements which are still able to bind downstream in exon 7, except they are over-expressed.**

Very recently, another inhibitory element was discovered in intron 7 (Singh et al. 2006). The element was called intronic splicing silencer N1 (ISS-N1) and is located 10 to 24 bp downstream of exon 7. ISS-N1 is not present in mouse *Smn* and therefore evolutionary nonconserved. Deletion or mutation of ISS-N1 resulted in the correction of the pathologic *SMN2* splicing such that substantially increased amounts of FL transcript and a splicing pattern similar to that of *SMN1* were obtained.

The existence of different *SMN* genes that are differently spliced is specific for humans. Mice and rats carry only one *Smn* gene and primates have several *SMN* gene copies, however, non of these genes is subject to alternative splicing and therefore they represent orthologs of the human *SMN1* (DiDonato et al. 1997; Rochette et al. 2001).

## 1.2.5   The SMN protein

The SMN protein consists of 294 amino acids, is ubiquitously expressed and has a molecular weight of 38 kDa. Investigations of adult human tissue revealed high SMN protein levels in spinal cord, kidney, liver and brain, whereas skeletal and cardiac muscle tissues, fibroblasts and lymphocytes presented lower expression levels (Coovert et al. 1997; Lefebvre et al. 1997). A comparison of SMN expression in various human fetal and postnatal tissues revealed that protein levels markedly decrease during the postnatal period, suggesting a requirement of high SMN levels during embryo-fetal development (Burlet et al. 1998). A similar expression pattern and developmental regulation of Smn, the counterpart to human SMN, was observed in rats and mice (Battaglia et al. 1997; Bergin et al. 1997; La Bella et al. 1998; Jablonka et al. 2000). Postnatal down-regulation of the murine Smn protein has recently been attributed to a decreased acetylation of histone proteins associated with the *Smn* promoter which in part results in silencing of *Smn* expression (Kernochan et al. 2005).

The SMN protein localizes both in the nucleus and the cytoplasm. Immunostaining of various cell types demonstrated that cytoplasmic distribution of SMN is diffuse, whereas it is found in prominent dot-like structures in the nucleus (Liu and Dreyfuss 1996; Coovert et al. 1997; Burlet et al. 1998). These SMN-containing structures are often observed in close proximity to or completely overlapping with the coiled bodies [also Cajal bodies; nuclear domains that are enriched in spliceosomal U snRNPs (Fakan et al. 1984)], and therefore are termed gemini of coiled bodies (gems) (Liu and Dreyfuss 1996; Liu et al. 1997; Young et al. 2000).

FL-*SMN1* and FL-*SMN2* transcripts encode an identical SMN protein. Thus, both genes *SMN1* and *SMN2* contribute to the amount of functional SMN protein present in each cell (Coovert et al. 1997; Lefebvre et al. 1997). However, due to the skipping of exon 7 during pre-mRNA splicing, *SMN2* produces only minor amounts of FL-SMN protein but predominantly generates a truncated, unstable Δ7-SMN2 protein (Lorson et al. 1998; Lorson and Androphy 2000). Consequently, *SMN2* is unable to compensate for the homozygous loss of *SMN1* in SMA patients, resulting in a lack of functionable SMN protein. This has been confirmed by several studies which demonstrated that SMA patients show substantially lower SMN levels in lymphoblastoid cell lines, fibroblasts, liver, muscle and spinal cord than control individuals (Coovert et al. 1997; Lefebvre et al. 1997; Helmken et al. 2003). Moreover, the number of gems was found to be decreased in subjects affected by SMA.

SMN forms large multi-subunit macromolecular complexes of ~1MDa that contain numerous SMN-interacting proteins. The components of the SMN complex are divided into two subgroups. A set of at least seven proteins associate with the SMN complex in a stable and stoichiometric manner. They are termed 'core components'. Because they colocalize with SMN in the gems in the nucleus, they are also called 'Gemins2-8'. In addition to these core components, another set of interacting partners associates transiently or in a substoichiometric manner with the SMN complex including the Sm

proteins which form part of the U snRNPs that are involved in pre-mRNA splicing. A comprehensive overview of the SMN complex components known so far is given in table 3. In figure 4, a model for the complex of SMN and the core components is presented. In addition to the ability of SMN to bind other proteins, it is also known that SMN binds nucleic acids (Lorson and Androphy 1998; Bertrandy et al. 1999).
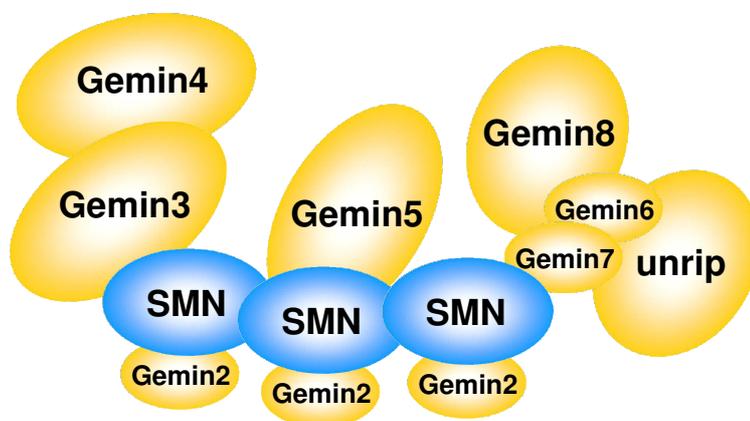


**Figure 4: The SMN protein forms a functional entity termed SMN complex. The major protein components have been grouped as Gemins2-8, and a factor termed unrip. SMN binds directly to Gemin2, Gemin3, Gemin5, and Gemin7. The interactions of Gemin3 with Gemin4 and of Gemin7 with Gemin6 mediate the close association of these two proteins with the SMN complex. Gemin8 and unrip are bound to the complex via direct interaction with the Gemin6-Gemin7 heterodimer. The precise stoichiometry of the SMN complex components is not known so far, and with regard to this aspect figure 4 remains a model.**

The SMN protein is involved in several essential cellular processes. There are seven main functions of the protein known so far:

1. The SMN complex catalyzes the assembly of spliceosomal U snRNPs (uridine-rich small nuclear ribonucleoprotein particles). U snRNPs are composed of one (U1, U2, and U5) or two (U4 and U6) uridine-rich RNAs and characteristic sets of proteins (Will and Luhrmann 2001). Together with other non-snRNP proteins (Jurica and Moore 2003), the U snRNPs form the subunits of the spliceosome, which is the macromolecular machinery that promotes and controls the splicing of pre-mRNAs. During the splicing process, U snRNPs are responsible for the recognition and activation of intronic sites for splicing (Blencowe 2000). The core structure of the U snRNPs is formed by the transfer of seven Sm proteins, which are common to all spliceosomal U snRNPs, onto the U snRNA molecule. In several studies, it has been demonstrated that this process requires the assistance of the SMN complex *in vivo* (Meister et al. 2001; Meister and Fischer 2002; Pellizzoni et al. 2002). Moreover, the SMN complex is also able to promote the maturation of other snRNPs such as U7 snRNP which is involved in histone-mRNA processing rather than pre-mRNA splicing, assigning the SMN complex with the potential role of 'master RNP assembler' (Terns and Terns 2001; Pillai et al. 2003).

2. Several studies suggest that SMN has a crucial function as recycling factor that regenerates U snRNPs after splicing catalysis and thus maintains the U snRNPs in an active form (Pellizzoni et al. 1998; Meister et al. 2000; Mourelatos et al. 2001).

**Table 3: The SMN protein is present as part of a large macromolecular complex containing a number of common core components and a set of transiently or substoichiometrically interacting partners.**

| SMN complex component [suggested protein function] | Direct SMN interaction | Reference |
|---|---|---|
| **Core components** | | |
| Gemin1 (SMN) | | (all references from this table) |
| Gemin2 (SIP 1) [snRNP biogenesis and pre-mRNA splicing] | + | (Liu et al. 1997) |
| Gemin3 (DP103) [snRNP biogenesis and pre-mRNA splicing] | + | (Charroux et al. 1999; Campbell et al. 2000) |
| Gemin4 (GIP1) [snRNP biogenesis and pre-mRNA splicing] | - | (Charroux et al. 2000; Meister et al. 2000) |
| Gemin5 (p175) [snRNP biogenesis and pre-mRNA splicing] | + | (Gubitz et al. 2002) |
| Gemin6 [snRNP biogenesis and pre-mRNA splicing] | - | (Pellizzoni et al. 2001b) |
| Gemin7 [snRNP biogenesis and pre-mRNA splicing] | + | (Baccon et al. 2002) |
| Gemin8 [snRNP biogenesis and pre-mRNA splicing] | - | (Carissimi et al. 2006) |
| Unrip [snRNP biogenesis and pre-mRNA splicing] | - | (Meister et al. 2001; Grimmler et al. 2005b) |
| **Substoichiometric components** | | |
| Sm proteins [snRNP biogenesis and pre-mRNA splicing] | + | (Liu et al. 1997; Friesen and Dreyfuss 2000) |
| LSm4 [snRNP biogenesis and pre-mRNA splicing] | + | (Friesen and Dreyfuss 2000; Brahms et al. 2001) |
| Fibrillarin [assembly of snoRNPs] | + | (Jones et al. 2001; Pellizzoni et al. 2001a) |
| GAR1 [assembly of snoRNPs] | + | (Pellizzoni et al. 2001a) |
| Coilin [recruitment of SMN to Cajal bodies] | + | (Hebert et al. 2001) |
| U1-A, U2-A' [snRNP biogenesis] | unknown | (Liu et al. 1997) |
| Profilin [control of actin dynamics] | + | (Giesemann et al. 1999) |
| ZPR1 (zinc-finger protein 1) [caspase activation and apoptosis ; snRNP assembly/maturation] | + | (Gangwani et al. 2001) |
| OSF (osteoclast-stimulating factor) [regulation of osteoclast formation and activity] | + | (Kurihara et al. 2001) |
| Nucleolin and B23 [cell growth and control of proliferation; programmed cell death, cell surface signal transduction; differentiation and maintenance of neural tissues] | - | (Lefebvre et al. 2002) |

| SMN complex component<br>[suggested protein function] | Direct SMN interaction | Reference |
|---|---|---|
| RNA helicase A<br>[transcription] | + | (Pellizzoni et al. 2001c) |
| RNA polymerase II<br>[transcription] | - | (Pellizzoni et al. 2001c) |
| hnRNP Q and R<br>[RNA transport along axons] | + | (Mourelatos et al. 2001; Rossoll et al. 2002) |
| hsc70 (heat-shock protein 70)<br>[posttranslational protein transport] | unknown | (Meister et al. 2001) |
| snurportin and importin β<br>[transport of snRNPs to nucleus] | - and + | (Narayanan et al. 2002) |
| galectin 1 and 3<br>[snRNP biogenesis and pre-mRNA splicing] | - | (Park et al. 2001) |
| p53<br>[apoptosis] | + | (Young et al. 2002a) |
| ISG20<br>[degradation of single-stranded RNA] | unknown | (Espert et al. 2006) |
| FGF-2 (fibroblast growth factor 2)<br>[neurotrophic factor for motor neurons] | + | (Claus et al. 2004) |
| mSin3A<br>[transcriptional regulation] | unknown | (Zou et al. 2004) |
| EWS (Ewing Sarcoma)<br>[transcriptional regulation] | + | (Young et al. 2003) |
| Bcl-2<br>[anti-apoptosis] | + | (Iwahashi et al. 1997) |
| FUSE binding protein<br>[regulator of transcription, mRNA stability, and RNA metabolism] | + | (Williams et al. 2000; Rothe et al. 2006) |
| TIA-1 and TIAR<br>[RNA metabolism; translation regulation; assemblers of stress granules] | unknown | (Hua and Zhou 2004b) |
| Rpp20<br>[RNA metabolism; component of stress granules] | + | (Hua and Zhou 2004a) |
| PPP4 (protein phosphatase 4)<br>[dephosphorylation of serine and threonine residues] | - | (Carnegie et al. 2003) |
| TGS1 (trimethylguanosine synthase 1)<br>[snRNA cap hypermethylase] | + | (Mouaikel et al. 2003) |
| **Viral proteins** | | |
| Papilloma virus E2<br>[nuclear transcription activation] | + | (Strasswimmer et al. 1999) |
| Minute virus NS1 and NS2<br>[viral replication and transcriptional activation] | unknown | (Young et al. 2002c; Young et al. 2002d; Young et al. 2005) |
| Epstein-Barr virus nuclear antigen 6<br>[EBV-induced immortalization of primary human B-lymphocytes *in vitro*; transcriptional regulator] | unknown | (Krauer et al. 2004) |

3. Other studies revealed that SMN is associated with RNA helicase A and RNA polymerase II (Strasswimmer et al. 1999; Pellizzoni et al. 2001c; Voss et al. 2001). Over-expression of a dominant SMN mutant was shown to inhibit transcription *in vivo*, whereas wild-type SMN stimulated gene transcription (Pellizzoni et al. 2001c). These results raise the possibility that the SMN protein plays a role in gene transcription. This hypothesis is further supported by the finding that SMN interacts with the protein mSin3A (Zou et al. 2004). mSin3A is a transcriptional co-repressor and known to be associated with a number of interacting partners in a multiprotein complex, including histone deacetylase (HDAC) 1, HDAC 2, methyltransferases, silencing mediator of retinoid and thyroid hormone receptor (SMRT), and nuclear receptor co-repressor (N-CoR) (Alland et al. 1997; Hassig et al. 1997; Heinzel et al. 1997; Laherty et al. 1997). In particular HDACs and methyltransferases are directly involved in the regulation of chromatin accessibility and gene expression. Several studies revealed that the recruitment of an HDAC-containing complex is a common transcriptional repression mechanism used by transcription factors belonging to various functional classes, e.g. nuclear hormone receptors (Heinzel et al. 1997; Nagy et al. 1997) and the methyl CpG-binding protein MeCP2 (Jones et al. 1998; Nan et al. 1998). All together, these data suggest that the SMN protein might play a role in the repression of gene activity via interaction with the co-repressor protein mSin3A.

4. In addition, it has been proposed that SMN is a critical factor involved in axonal mRNA transport in neurons. First hints for such an activity of the SMN protein came from the finding that SMN interacts with hnRNP R, a protein that binds to the 3' untranslated region of β-actin mRNA (Mourelatos et al. 2001; Rossoll et al. 2002). In a subsequent study, it was demonstrated that over-expression either of Smn or of hnRNP R in the rat pheochromocytoma cell line PC12 enhances cell differentiation and their axonal outgrowth (Rossoll et al. 2003). In addition, motor neurons isolated from an SMA mouse model are characterized by reduced levels of β-actin mRNA at the distal axons and growth cones, which underlines the assumption that Smn and hnRNP R modulate axonal mRNA transport. Strikingly, it has been shown that the SMN protein is indeed localized in dendrites and axons (Bechade et al. 1999; Pagliardini et al. 2000). In neuritis and growth cones of cultured neuronal cells, SMN is localized in granules that are able to bidirectionally travel along axons which is a prerequisite for the function of SMN in axonal trafficking (Zhang et al. 2003). These observations are supported by the finding that SMN interacts with profilin II, a neuron-specific factor required for actin polymerization (Giesemann et al. 1999; Sharma et al. 2005). Thus, SMN, hnRNP R and profilin II all together might be involved in axonal transport processes.

5. The SMN protein interacts with TIA-1 and TIAR and co-localizes with these proteins in specific cellular substructures called stress granules (Hua and Zhou 2004b). This suggests a role for SMN in translation regulation. Stress granules are formed in the cytoplasm under stressed conditions. In response to stress, about 50% of the total cellular mRNA is actively recruited to stress granules (Kedersha et al. 1999). The mRNA in the stress granules is not translated, but rather stored and protected. Once the stress is released, stress granules are disassembled, and the mRNAs are available for protein synthesis (Nover et al. 1989). It has been clearly demonstrated that both TIA-1 and TIAR regulate the translation of various mRNAs in the

cytoplasm by binding to AU-rich elements located in the 3' untranslated regions of these molecules (Piecyk et al. 2000; Dixon et al. 2003; Yu et al. 2003; Kandasamy et al. 2005), suggesting a similar mechanism of action in the stress granules (Rothe et al. 2006). Moreover, the SMN protein is known to interact with FUSE binding protein (Williams et al. 2000). FUSE binding protein has also been identified as interaction partner of TIA-1 and TIAR and was shown to migrate into TIA-1-containing stress granules upon oxidative stress (Rothe et al. 2006). These findings suggest the presence of a protein network which includes SMN and fulfills key functions in RNA metabolism and translation regulation in the cell.

6. It is assumed that the SMN protein is involved in the regulation of apoptotic pathways in the cell. This idea is based on the finding that the zinc-finger protein ZPR1 belongs to the SMN complex components (Gangwani et al. 2001). SMN mutations disrupt the interaction between the two proteins, and SMA patients express reduced levels of ZPR1 (Helmken et al. 2003). It has been reported that mutation or silencing of the murine *Zpr1* gene causes caspase activation and apoptosis which results in massive cell death and early embryonic death in mice (Gangwani et al. 2005). The interaction between SMN and ZPR1 and the simultaneous regulation of the two proteins found in SMA patients suggests that they both may represent components of a common functional apoptotic pathway. Additionally, SMN was found to interact with the tumor suppressor protein p53 (Young et al. 2002a). p53 can stimulate apoptosis through multiple mechanisms (Vousden 2000). It has been suggested that wild-type SMN prevents p53-mediated apoptosis, while Δ7-SMN and mutated SMN fail to associate with p53, allowing the activation of p53-dependent apoptotic pathways (Young et al. 2002a). The idea of a role for SMN in apoptosis is further supported by the finding that SMN can function as anti-apoptotic factor in neuronal cells (Kerr et al. 2000) and interacts with the anti-apoptotic factor Bcl-2 in a tissue culture model (Iwahashi et al. 1997).

7. It has been demonstrated that SMN interacts with various viral proteins, including Papilloma virus E2, a nuclear regulator of viral gene expression (Strasswimmer et al. 1999), minute virus of mice NS1 which performs critical functions in viral gene expression and genome replication (Young et al. 2002c), and Epstein-Barr virus nuclear antigen 6, a transcriptional regulator which also plays a role in the EBV-induced immortalization of primary B-lymphocytes *in vitro* (Krauer et al. 2004). The association with SMN is assumed to be required to maintain the function of these viral proteins.

## 1.3    Animal models of proximal SMA

The use of animal models is a key aspect of scientific research, especially in numerous fields of medicine. Animal models of human pathophysiological processes and disorders are desired to simulate human conditions and study the cause, nature and cure of human diseases. The advantage of animal models is that they represent simpler systems than humans, which often allows a faster understanding of the disease underlying molecular mechanisms. Moreover, they are easy to breed such that a large number of animals can be obtained within a relatively short period of time. Additionally, animal models provide the opportunity to carry out investigations which are essential but

unethical to be carried out in humans. However, there is no guaranty that knowledge gained from animal models can always be transferred one-to-one to humans.

In 1997, the murine homolog of the *SMN* gene was identified and characterized (DiDonato et al. 1997; Viollet et al. 1997). In contrast to humans, mice carry only one *Smn* gene copy which is not subject to alternative splicing. To create a mouse model of SMA, *Smn* was homozygously knocked out (Schrank et al. 1997). However, these experiments did not lead to a model of SMA because the mice (genotype: *Smn*^{-/-}) displayed massive cell death and lethality during early embryogenesis, indicating that *SMN* is an essential gene required for cellular survival and function. This observation is consistent with the finding that each SMA patient carries at least one intact *SMN2* gene and the complete absence of both *SMN1* and *SMN2* has never been reported.

To overcome the embryonic lethality in *Smn*^{-/-} mice, two approaches were developed. A conditional knockout of the murine *Smn* gene was created by using the Cre-LoxP system. Mice carrying *Smn* exon 7 flanked by LoxP sites were crossbred with mice transgenic for Cre recombinase which is expressed under the control of the *neuron-specific enolase* (NSE) promoter (Frugier et al. 2000). These double transgenic mice presented a phenotype with many typical features seen in SMA patients, which underlined the fatal consequences of *SMN* exon 7 skipping in SMA. However, the main disadvantage of this mouse model is the continual depletion of FL-*Smn* in neuronal cells, whereas SMA patients display uniformely low levels of FL-*SMN2* transcripts. Moreover, depending on the number of *SMN2* copies, the amount of FL-*SMN2* varies among SMA patients, resulting in a variation of disease severity. This phenomenon could not be modeled in the conditional *Smn* exon 7 knockout mice. Application of a different strategy led to the generation of transgenic mice which are characterized by homozygous deletion of the murine *Smn* gene but express the human *SMN2* gene (genotype: *Smn*^{-/-}; *SMN2*) (Hsieh-Li et al. 2000; Monani et al. 2000). In these animals, *SMN2* was able to prevent the embryonic lethality observed in *Smn*^{-/-} mice. *Smn*^{-/-};*SMN2* mice carrying one or two copies of the transgene showed a substantial degeneration of motor neurons and muscle atrophy by postnatal day 5 and subsequently died which closely resembles a severe type I SMA phenotype in humans. These mice produce low levels of SMN protein and gems are undetectable in spinal motor neurons. An increased number of *SMN2* transgenes increased the levels of SMN protein. When eight copies of *SMN2* were introduced into *Smn*^{-/-} mice, the transgenes completely rescued the disease phenotype, which is consistant with the disease modifying character of *SMN2* in humans (Monani et al. 2000).

Additional mouse models were generated which rather resemble the milder type II to III SMA phenotypes. Therefore, *SMN* cDNA lacking exon 7 was placed under the control of an *SMN* promoter and introduced onto a severe SMA genetic background (genotype: *Smn*^{-/-}; *SMN2*; *SMNΔ7*) (Le et al. 2005). A similar phenotype was achieved by expression of a known mild SMA missense mutation (p.A2G) on the severe SMA mouse background (genotype: *Smn*^{-/-}; *SMN2*; *SMN A2G*) (Monani et al. 2003). Mice heterozygous for endogenous mouse *Smn* display features which are similar to human type III SMA (Jablonka et al. 2000).

A *Drosophila melanogaster* model of SMA has been described in 2003 (Chan et al. 2003). Fly larvae were identified which contain *dSmn* missense mutations on both alleles. The mutations are localized in a highly conserved region of the encoded protein. Due to the presence of maternal mRNA coding for wild-type dSmn protein which is contributed to the embryo by the mother, low levels of wild-type

protein will be present in the larvae and thus allow survival up to late larvae stages. The mutant fly larvae present severe motor abnormalities and therefore may serve as a very simple invertebrate disease model. Another model of SMA was established in zebrafish (*Danio rerio*) by knockdown of the Smn protein using antisense morpholinos (McWhorter et al. 2003). Due to its well-characterized nervous system, the relatively simple neuromuscular organization and the transparency of the embryos which allows a close inspection of neurons, zebrafish are a well-suited model for the analysis of neuromuscular diseases like proximal SMA. Furthermore, *Caenorhabditis elegans* is known to be a powerful model organism to study neurobiology, development, and cell death (Wood 1988; Riddle 1997). It is easy to grow and maintain, the entire genome has been sequenced (The-*C.elegans*-Sequencing-Consortium 1998), and the whole organism consists of a low number of cells (Wood 1988). The use of RNA interference to down-regulate Smn protein levels in *Caenorhabditis elegans* led to a phenotype that included a marked negative effect on embryonic viability and locomotive defects in the progeny, suggesting that the nematode can also serve as model organism for the study of SMA (Miguel-Aliaga et al. 1999).

## 1.4     Biology of motor neuron degeneration in proximal SMA

Spinal muscular atrophy is characterized by specific degeneration of α-motor neurons in the anterior horns of the spinal cord. Other cell types are not known to be affected in SMA patients. Thus, the discovery of the *SMN* gene in 1995 raised the question whether this gene might have an exclusively neuronal function and impairment of this tissue-specific function causes the disease phenotype. If this were the case, expression of *SMN* should also be restricted to α-motor neurons only. However, *SMN* is ubiquitously expressed in all types of cells, rather suggesting that it belongs to the group of housekeeping genes which are crucial for the survival of each single cell type in an organism. So the question is: Why does the reduced expression of the ubiquitous protein SMN cause a tissue-specific phenotype? Considering that spinal cord is one of the tissues showing particularly high levels of SMN, it is reasonable to speculate that α-motor neurons are more vulnerable to substantially reduced SMN protein levels than other cell types, but the question remains: Which function(s) of the SMN protein is so essential for α-motor neurons that only these cells degenerate upon homozygous loss of the *SMN1* gene and not other cell types?

Based on the current knowledge about the cellular functions of the SMN protein (see chapter 1.2.5), several models are proposed which try to give the reason for the specific defect of α-motor neurons in SMA patients. Two of these models are considered as most likely to explain the underlying pathophysiologic mechanism. One prediction is that SMA indeed is the result from the disruption of a neuron-specific function assigned to the SMN protein, such as the essential role in β-actin mRNA trafficking along axons (Rossoll et al. 2003; Briese et al. 2005). Insufficient transport of β-actin mRNA to neuronal growth cones would lead to defects in axonal outgrowth, i.e. truncation and early branching of motor axons, finally resulting in insufficient innervation of muscles, a typical feature in SMA patients. This hypothesis is supported by the observation that actin polymerization in axons requires the interaction between functionable SMN protein and profilin II (Giesemann et al. 1999; Sharma et al. 2005).

The second model suggests that the impairment of snRNP biogenesis (which decreases the amount of active spliceosomes available for pre-mRNA splicing) is the causative reason for motor neuron degeneration. In contrast to mRNA trafficking which is specifically required in motor neurons, snRNP biogenesis is a basic function of every cell. However, it is believed that motor neurons are more vulnerable to a defect in U snRNP assembly, because they exhibit a high turnover of mRNAs encoding proteins with tissue-specific activities (Chisholm and Tessier-Lavigne 1999; Tear 1999). A hypothesis suggests that tissue-specific pre-mRNAs are spliced less efficiently than pre-mRNAs of constitutive genes (Faustino and Cooper 2003). Thus, a group of tissue-specific mRNAs with suboptimal splice sites might be more sensitive to reduced SMN levels and reduced snRNP levels than other mRNAs. Consequently, it might be possible that motor neurons are not able anymore to meet the demand for such tissue-specific proteins, resulting in specific motor neuron degeneration.

Both scenarios are attractive and sound convincing. However, further experiments are needed to check which of the models gives the reason for the tissue-specific pathology in SMA. It has to be carefully evaluated if β-actin mRNA transport and actin-polymerization are linked directly to reduced levels of SMN. A direct link between reduced levels of SMN and the impaired ability of these cells to promote U snRNP assembly has already been demonstrated in non-neuronal cell cultures (Feng et al. 2005; Shpargel and Matera 2005; Wan et al. 2005; Winkler et al. 2005) and fibroblasts derived from SMA patients (Wan et al. 2005). Moreover, this hypothesis was supported using zebrafish as a model for SMA. Silencing of Gemin2, a component of the SMN complex, resulted in the same motor-axon phenotype as obtained by knock-down of SMN expression (Winkler et al. 2005). This motor-axon phenotype of zebrafish lacking either Gemin2 or SMN could be prevented by addition of purified U snRNPs, the end product of the SMN-mediated snRNP biogenesis. However, future studies now have to focus on the search for tissue-specific pre-mRNAs with splicing patterns that are offset to prove the idea that they are more sensitive to reduced snRNP levels and lead to reduced levels of proteins which are specifically required by motor neurons.

In addition, there is a third model which is based on the findings that (i) the SMN protein is located in stress granules, interacts with the TIA-1, the TIAR, and the FUSE-binding proteins and therefore might have a role in translation regulation (Williams et al. 2000; Hua and Zhou 2004b; Rothe et al. 2006), and (ii) SMN interacts with the transcriptional co-repressor mSin3A and therefore may be involved in the regulation of gene activity and transcription (Zou et al. 2004). It is assumed that reduced levels of the SMN protein might result in the dysregulation of genes and their transcripts which are specific of and essential for α-motor neurons in the spinal cord, subsequently leading to their degeneration. However, to confirm this hypothesis, future studies will have to prove whether such genes can indeed be identified.

## 1.5    State-of-the-art of SMA treatment and therapeutic prospects

So far, a cure for SMA is not available. Most care for patients is focused on symptomatic control and preventive rehabilitation, including physical therapy to maintain joint mobility and to decrease the incidence of contractures. However, the extensive knowledge gained about the pathological disease mechanisms and the underlying molecular principles allows the development of therapeutic strategies

which might lead to an improvement of the SMA phenotype or even prevent disease onset. The therapeutic approaches which have been established until now are summarized in figure 5. So-called non-targeted strategies aim at the discovery of neuroprotective or neurotrophic agents which are able to protect α-motor neurons from degeneration (figure 5f). Another idea is the application of replacement therapies to SMA. By the means of embryonic stem cell transfer or gene therapy, motor
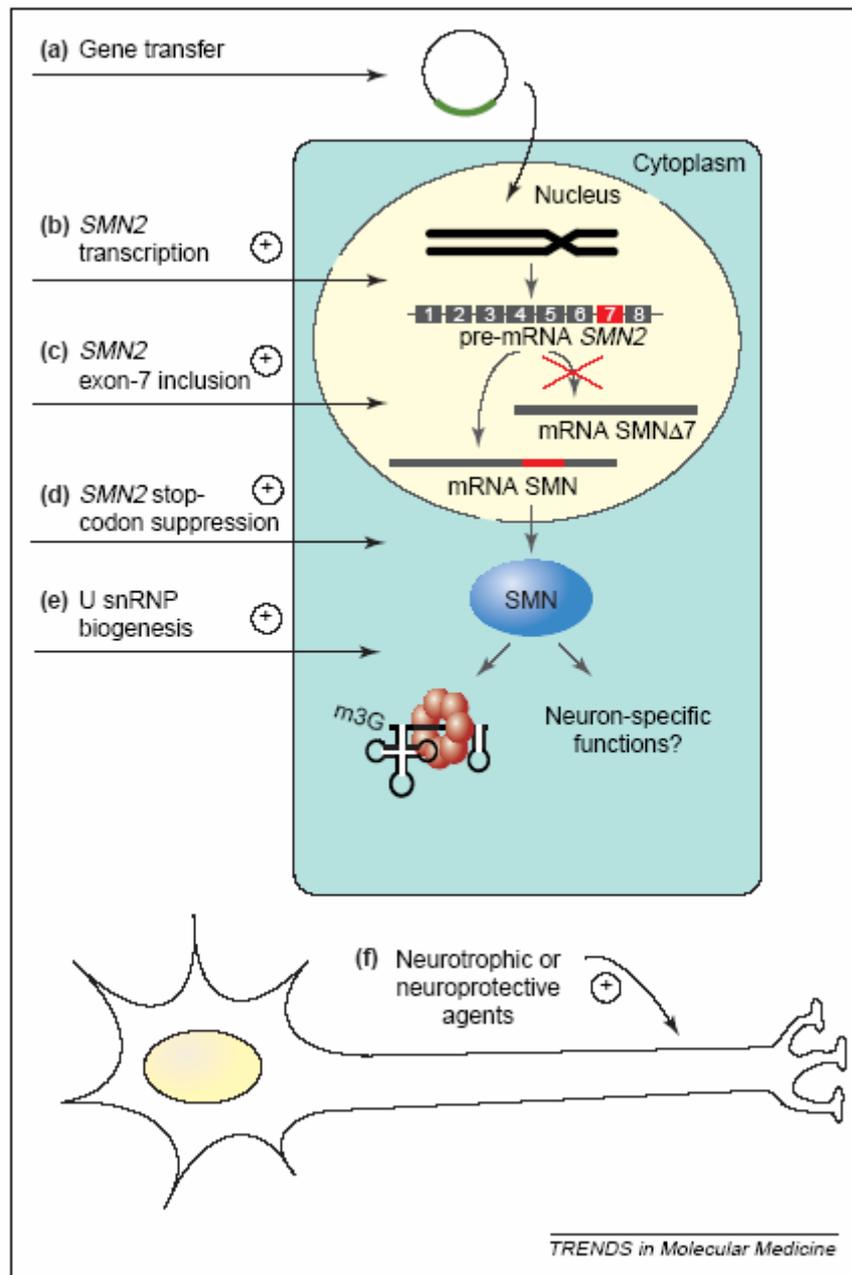


**Figure 5: Potential therapeutic strategies for the treatment of SMA (Eggert et al. 2006).**

neurons containing functional *SMN1* genes or functional *SMN1* copies per se could be introduced into the spinal cord of SMA patients and compensate for the inherited loss of *SMN1* (figure 5a). The therapeutic approaches considered most promising, however, are so-called targeted strategies which focus on the *SMN2* gene. *SMN2* is ubiquitously expressed and present at least once in each SMA patient. Importantly, FL-SMN2 protein is identical to FL-SMN1 protein. Thus, it seems reasonable to

believe that increasing the amount of endogenous FL-SMN2 may compensate for the lack of FL-SMN1, resulting in a clinical benefit for SMA patients. An up-regulation of FL-SMN2 protein levels might be achieved by increasing the overall transcription rate of the *SMN2* gene (figure 5b) or by promoting the inclusion of exon 7 into *SMN2* mRNA such that the pathological *SMN2* splicing pattern shifts toward the wild-type pattern of *SMN1* (figure 5c). Moreover, it is assumed that suppression of the use of the stop codon in exon 8 of the Δ7-*SMN2* transcripts leads to the synthesis of a protein containing additional amino acids at the C-terminus, which possibly increases stability and oligomerization ability of the Δ7-SMN2 protein (figure 5d). Another idea is to elevate the activity of functional FL-SMN2 protein remaining in SMA patients to improve the efficacy of processes catalyzed by SMN, e.g. the assembly of snRNPs and axonal mRNA trafficking (figure 5e).

## 1.6     Chromatin structure and epigenetic regulation

The genetic code for proteins is defined by the nucleotide sequence of the DNA. The DNA transfers this information to mRNA, which is translated into a protein macromolecule. However, the DNA code alone is not sufficient for the generation and regulation of the complex gene expression pattern in eukaryotic organisms. Multiple transcription factors bind to specific nucleotide sequences in the chromatin, which is the condensed structure of the DNA in the nucleus, and recruit chromatin modifiers and further transcription complexes. These modifiers and complexes provide additional regulatory information, mainly consisting of the posttranslational modification of histones which are proteins complexed to the DNA in the nuclei of all eukaryotic cells. The information is printed on the N-termini of the histone proteins in the form of acetylation, phosphorylation and/or methylation, thereby extending the information given by the nucleotide sequence in the DNA code. One of the major differences between the DNA code and the so-called histone code is that the DNA code is permanent while the histone code is temporal. Importantly, the DNA encodes the information for printing the histone code (Jenuwein and Allis 2001; Agalioti et al. 2002; Richards and Elgin 2002).

The term epigenetics refers to the study of heritable, potentially reversible changes in the expression of genes (e.g. due to histone modification) that occur without a change of the DNA sequence but rather provide an "extra" layer of transcriptional control that regulates how genes are expressed (Egger et al. 2004; Galm et al. 2006; Rodenhiser and Mann 2006).

### 1.6.1     DNA packaging in the eukaryotic nucleus

In the nuclei of all eukaryotic cells, the genomic DNA is associated with histone proteins and non-histone proteins, forming a highly folded, complex structure called chromatin (Kornberg 1974; Luger et al. 1997; Spotswood and Turner 2002; Felsenfeld and Groudine 2003) (figure 6). The basic repeating unit of the chromatin is called nucleosome (Kornberg 1974; Oudet et al. 1975). Nucleosomes are composed of approximately 146 bp of two superhelical turns of DNA wrapped around an octamer of core histone proteins (Luger et al. 1997). Core histones are among the most highly conserved eukaryotic proteins known, presumably because of specific structural properties required for the

interaction with DNA, with one another, and with other non-histone proteins (Sandman et al. 1998). This histone core consists of pairs of histones H4, H3, H2A, and H2B (Thomas and Kornberg 1975; Eickbush and Moudrianakis 1978). The H3 and H4 subunits form a H3-H4 heterotetramer which interacts with two H2A-H2B dimers (Burlingame et al. 1985; Arents et al. 1991). The nucleosomes are
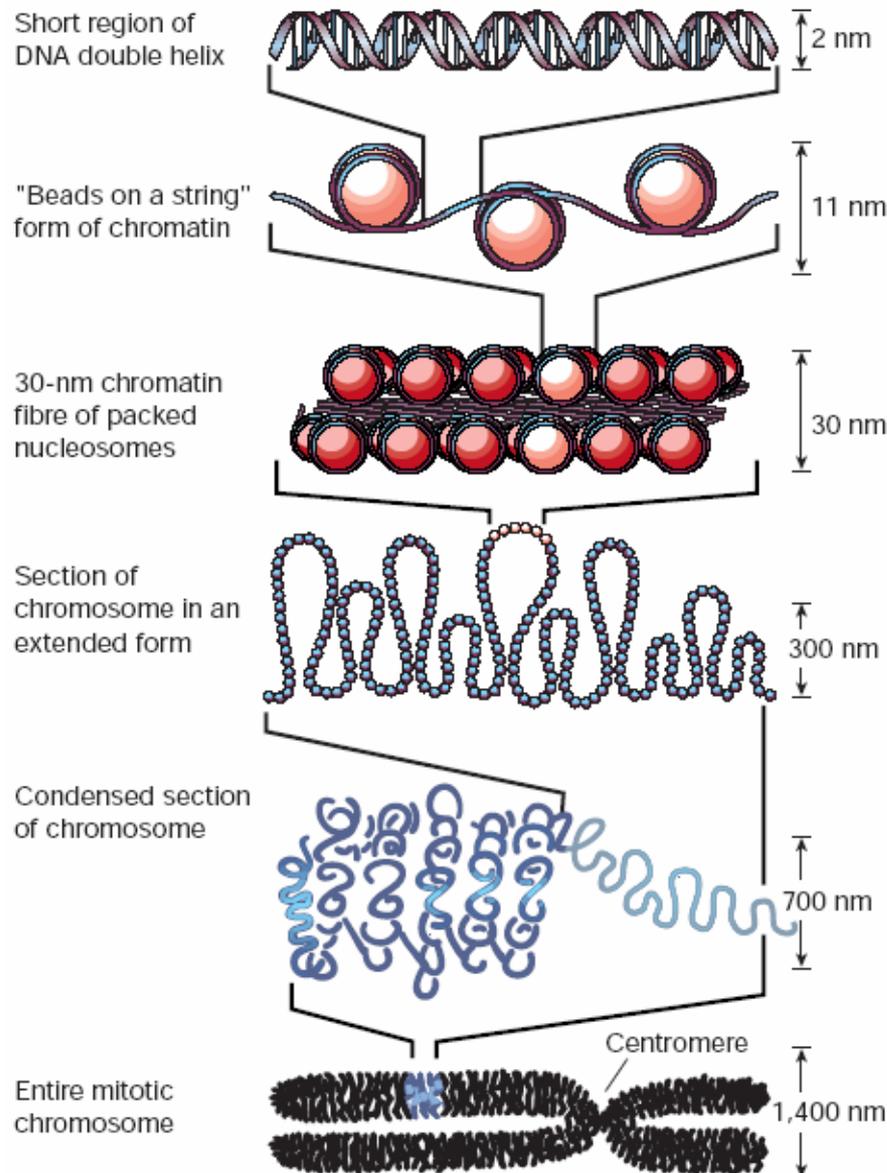


**Figure 6: Eukaryotes package their DNA inside cells in the nucleus. There, the DNA is associated with histone and non-histone proteins to form a highly folded, complex structure called chromatin (Felsenfeld and Groudine 2003).**

separated by DNA pieces consisting of 10-80 bp which are also called linker-DNA. The resulting chromatin fiber is characterized by a diameter of about 10 nm and may also be described as "beads-on-a-string" arrangement (Olins and Olins 1974) which is folded into even more condensed chromatin fibers with a diameter of ~30 nm. These 30-nm fibers are stabilized by binding of a linker histone protein H1 to each nucleosome and its adjacent linker. Histone H1 shows a greater degree of

evolutionary variability than the core histones and might be expressed in several variants in different cell types of an organism (Noll and Kornberg 1977; Widom 1998; Thomas 1999; Felsenfeld and Groudine 2003). Further condensation of the DNA occurs *in vivo* to form 100-400 nm thick interphase coiled chromatin fibers or more highly compacted metaphase chromosome structures. Non-histone proteins, including the class of high mobility group (HMG) proteins which are ubiquitous in mammalian cells, are also able to bind to chromatin, thereby acting as architectural elements that may modify the chromatin structure (Bustin and Reeves 1996; Bustin 1999; Bustin 2001a; Bustin 2001b).

### 1.6.2    Epigenetic modification of DNA and histone proteins

The highly condensed DNA which is organized into chromatin fibers is inaccessible for enzymes such as RNA polymerases. They are denied access to chromatin, and biochemical reactions such as transcription are inhibited. Consequently, the chromatin structure must be dynamic: Genes are silent when the chromatin is condensed, and they are transcribed as soon as the chromatin structure is (partially) disrupted and unfolded (Felsenfeld and Groudine 2003; Rodenhiser and Mann 2006). Consistent with this idea, it has been demonstrated that nucleosomes which are associated with transcriptionally active genes are better accessible to enzymes that digest DNA than those associated with inactive genes (Weintraub and Groudine 1976).

The dynamics of the chromatin structure is obtained by specific reversible changes in the epigenetic pattern, most importantly including DNA methylation and posttranslational modification of histone proteins (Feinberg and Tycko 2004). The methylation of DNA is carried out by covalent addition of a methyl group to cytosines within CpG (cytosine/guanine) pairs by a family of cytosine-methyltransferases (Ehrlich and Wang 1981; Laird and Jaenisch 1994; Feinberg and Tycko 2004; Rodenhiser and Mann 2006). DNA methylation occurs almost exclusively at CpG pairs. Clusters of CpG pairs are also called CpG islands. Unmethylated CpGs are located in tissue-specific genes and genes that are constitutively expressed in all tissues because they are required for the maintenance of basic cell functions (housekeeping genes). They are target for proteins that specifically bind to unmethylated CpGs and initiate gene transcription. In contrast, methylated CpGs can block binding of these proteins, are target for a distinct subset of binding proteins which mediate transcription repression and thus play an important role in gene silencing. DNA methylation is a mechanism of high relevance for X-chromosome inactivation (Avner and Heard 2001). The disruption of the normal DNA methylation pattern is an important epigenetic cause of disease. Already in 1983, DNA extracted from normal and cancer tissues was compared by digestion with methylation-sensitive restriction enzymes (Feinberg and Vogelstein 1983a). It was demonstrated that a large proportion of CpGs which are methylated in normal tissues were unmethylated in cancer cells, suggesting that hypomethylation may cause cancer by activation of oncogenes that promote proliferation (Feinberg and Vogelstein 1983b; Nakamura and Takenaga 1998; Cho et al. 2001; Akiyama et al. 2003). On the other hand, also hypermethylation may lead to cancer by silencing of tumor-suppressor genes. The first link between hypermethylation and tumor-suppressor genes was demonstrated on the retinoblastoma gene *RB* in 1989 and 1991 (Greger et al. 1989; Sakai et al. 1991). In 1993 and 1994, further studies confirmed that *RB* expression is reduced by 92% in tumors with promoter hypermethylation (Ohtani-Fujita et al.

1993; Greger et al. 1994). Today, a large number of tumor-suppressor genes is known to be linked to cancer in case of hypermethylation (Rodenhiser and Mann 2006).

In addition to DNA methylation, posttranslational modification of histone proteins is another factor with substantial impact on DNA structure and gene expression. Each of the core histones harbors a globular domain which mediates histone-histone interactions within the octamer and a flexible amino-terminal charged tail that is rich in basic amino acids and protrudes from the surface of the nucleosome (Luger et al. 1997; Jenuwein and Allis 2001; Peterson and Laniel 2004). Many amino acids of the histone proteins may be chemically modified: lysines may be acetylated, mono-/di-/tri-methylated, ubiquitylated or sumoylated; arginines may be acetylated or mono-/di-methylated; serine and threonine residues are subject to phosphorylation (Grant 2001; Peterson and Laniel 2004). The majority of posttranslational modifications occurs at the amino-terminal histone tails, however, a
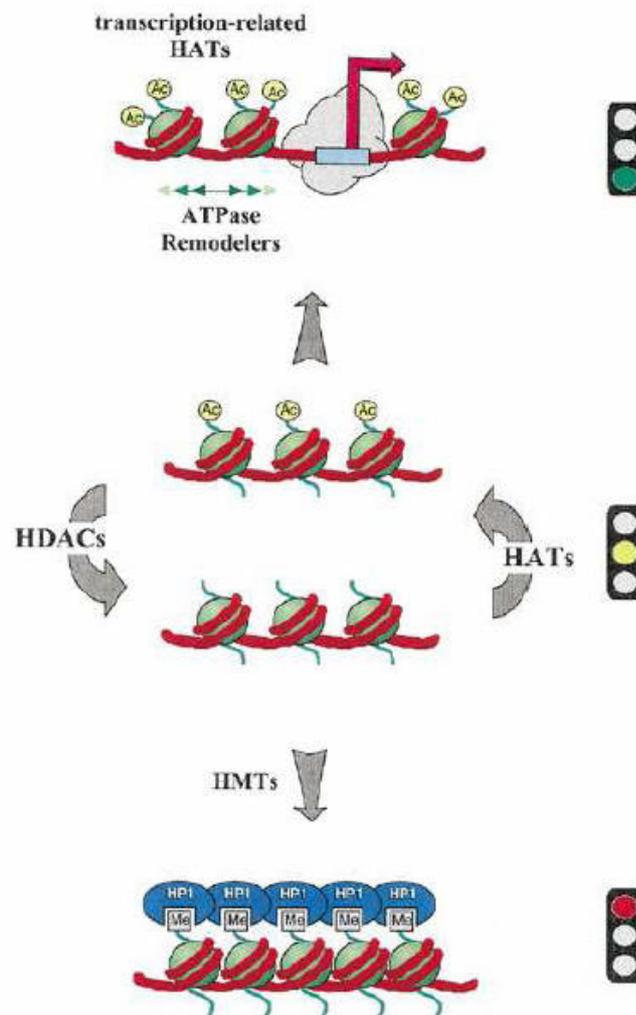


**Figure 7: Histone methylation and acetylation are two key factors that regulate gene expression. Deacetylation of histones by histone deacetylases (HDACs) and subsequent methylation by histone methyltransferases (HMTs) provides a solid base for highly repressive structures, such as heterochromatin (red traffic light). Unmethylated histones which are acetylated by histone acetyltransferases (HATs) (yellow traffic light) permit ATP-dependent chromatin remodeling factors to open promoters which activates gene transcription activity (green traffic light). Methyl groups (Me) are indicated as gray rectangles, and acetyl groups (Ac) are presented as yellow circles (Eberharter and Becker 2002).**

number of marks has also been discovered at the carboxy-terminal tail and even within the central histone domains. Histone modifications have long been linked to DNA function and regulation of transcription (Allfrey et al. 1964). All histone modifications together constitute the so-called histone code (Jenuwein and Allis 2001; Peterson and Laniel 2004). They can affect one another, and they are often correlated with each other. A specific combination of single histone marks results in specific functional consequences and correlates with certain biological functions. Interestingly, one and the same combination of histone marks may lead to different or opposite biological consequences, depending on the gene of interest and the cellular context. In contrast, the DNA code is always the same, no matter in which cell type or tissue a gene is analyzed. The first enzyme which catalyzes histone modifications was identified not earlier than 1996 (Brownell et al. 1996). The yeast protein Gcn5, a transcriptional co-activator protein, was demonstrated to possess histone acetyltransferase (HAT) activity which provided strong molecular evidence of the link between histone modification and regulation of transcription. Today, histone modification enzymes are subdivided into several groups, including histone acetyltransferases (HATs), histone deacetylases (HDACs), histone methyltransferases (HMTs) and histone kinases. Histone modifying enzymes do not bind directly to DNA, but are recruited to DNA by DNA-sequence specific transcription factor protein complexes (Cress and Seto 2000; Urnov et al. 2000; Gray and Ekstrom 2001; de Ruijter et al. 2003). A specific set of site-specific posttranslational histone modifications is achieved by targeting histone modifying enzymes to specific promoter regions and by the specificity of the recruited enzymes themselves for individual histone tails and histone residues. Once a pattern of histone modification is established, histone tails are able to specifically interact with nonhistone proteins which in turn can also regulate chromatin structure and the accessibility of certain DNA regions for further enzymes (Strahl and Allis 2000; Wu and Grunstein 2000).

In general, transcriptionally active chromatin regions (euchromatin) are characterized by unmethylated DNA and high levels of acetylated histones. In contrast, inactive DNA regions (heterochromatin) show deacetylated histones and methylated CpG islands (figure 7). However, this is not an overall rule.

E.g., although methylated histone H3 recruits the heterochromatin protein 1 (HP1) and is mainly associated with transcriptionally silent DNA regions, HP1 also interacts with a number of transcriptional coactivators involved in gene regulation in euchromatin (Wallrath 1998; Jones et al. 2000). Likewise, whereas histone hypoacetylation is commonly found in inactive chromatin regions, acetylation of specific lysine residues of histone H4 has been reported to be a characteristic for heterochromatin too (Turner et al. 1992; Braunstein et al. 1996; Turner 2000). This suggests that histone methylation not exclusively corresponds with gene silencing, and histone acetylation mostly stimulates, but may also repress gene transcription (Jenuwein and Allis 2001).

### 1.6.3   Histone deacetylases (HDACs) and histone acetyltransferases (HATs)

The acetylation and deacetylation of the amino groups of lysine residues in histone tails is the most intensively studied posttranslational histone modification (Grant 2001). Histone acetylation is catalyzed by a category of enzymes called histone acetyltransferases (HATs), whereas deacetylation is carried out by a group of enzymes termed histone deacetylases (HDACs). In addition to the specific and

targeted acetylation and deacetylation of histone sites which, e.g., takes place throughout the normal cell cycle, it is suggested that there is a constant battle among HATs and HDACs in a global, non-targeted manner to maintain a baseline, equilibrium level of histone acetylation throughout the genome (Peterson and Laniel 2004).

In 1996, HDAC 1 was the first mammalian histone deacetylase to be identified (Taunton et al. 1996). Based on their similarity to various yeast histone deacetylases, all mammalian HDACs which have been identified so far can be separated into three classes (table 4) (Khochbin et al. 2001; de Ruijter et al. 2003; Marks et al. 2003; Yang and Gregoire 2005). Class I includes HDACs 1, 2, 3, and 8. These enzymes are related to yeast deacetylase RPD3 (reduced potassium dependency 3) and share

**Table 4: Classification of mammalian histone deacetylases (HDACs). The homologous yeast deacetylase is given in brackets.**

| Class I (RPD3) | Class II (HDA1) | Class III (Sir2) |
|:---:|:---:|:---:|
| HDAC 1 | HDAC 4 | SIRT 1 |
| HDAC 2 | HDAC 5 | SIRT 2 |
| HDAC 3 | HDAC 6 | SIRT 3 |
| HDAC 8 | HDAC 7 | SIRT 4 |
| (HDAC 11) | HDAC 9 | SIRT 5 |
|  | HDAC 10 | SIRT 6 |
|  |  | SIRT 7 |

homologous catalytic sites. Class II includes HDACs 4, 5, 6, 7, 9, and 10. With a molecular mass between 120 and 135 kDa, they are larger molecules than class I HDACs which have a mass ranging between 22 and 55 kDa. Class II HDACs are homologs of yeast deacetylase HDA1. The class II enzymes may be subdivided into members with only one catalytic domain (HDACs 4, 5, 7, 9) and members with two catalytic domains (HDACs 6, 10) (Fischer et al. 2002; Hubbert et al. 2002). HDAC 11 contains conserved residues in the catalytic region which are shared by both class I and II HDACs (Gao et al. 2002). Therefore, HDAC 11 has homology to both HDAC classes and is sometimes grouped into a separate category termed HDAC class IV (Yang and Gregoire 2005). Class I HDACs display some sequence homology to members of class II, but not to those of class III. Class III HDACs are enzymes with homology to yeast Sir2 (silent information regulator 2). In contrast to the zinc-dependent activity of class I and II HDACs, class III acts $NAD^+$-dependent. SIRT 1-7 appear not to act on histones but rather deacetylate non-histone proteins such as p53, α-tubulin, forkhead and other transcription factors (Marks et al. 2004; Marmorstein 2004). HDACs are not redundant in function. Class I HDACs are almost exclusively localized in the nucleus, whereas class II HDACs shuttle between the nucleus and the cytoplasm (Marks et al. 2004). Among the members of class III, SIRT 1, 6, and 7 are localized in the nucleus, SIRT 2 in the cytoplasm, and SIRT 3, 4, and 5 in the mitochondria (Michishita et al. 2005).

Proteins with histone acetyltransferase (HAT) activity are more diverse than HDACs (Roth et al. 2001; Carrozza et al. 2003). Some of the known HATs are also able to acetylate non-histone proteins (Kouzarides 2000; Sterner and Berger 2000) which was first discovered in 1997 when p53 was found to be acetylated at specific lysine residues in its C-terminus (Gu and Roeder 1997). Likewise, not all of

the proteins which possess lysine acetyltransferase activity are able to acetylate histones (Yang 2004). Enzymes which are able to acetylate specific lysine residues within histones and/or other proteins are termed lysine acetyltransferases (LATs). Mammalian LATs are subclassified into a number of families: Hat1, Gcn5/PCAF, p300/CBP, MYST, p160, CIITA, ATFII; $TAF_{II}250$, TFIIIC, Elp3, CDY, TFIIB, MCM3AP, Eco1, and ARD1 (Yang 2004). The majority of proteins known to be modified by LATs are histones and transcriptional regulators. Other cellular proteins in which this modification has been observed include DNA metabolic enzymes (Hasan et al. 2001; Tini et al. 2002), the signaling regulator Smad7 (Gronroos et al. 2002), and α-tubulin (Doenecke and Gallwitz 1982). Most HATs exist as multisubunit complexes *in vivo*. One HAT can be the catalytic subunit of multiple complexes which adds another level of complexity to the already diverse superfamily of LATs (Yang 2004).

### 1.6.4    Chemical substances that inhibit the activity of HDACs

In 1990, trichostatin A (TSA, a Streptomyces product) was the first substance reported to have an effect on cell proliferation and cell differentiation and to directly inhibit HDACs (Yoshida et al. 1990). However, due to its unfavorable bioavailability, TSA was never considered as promising anticancer drug. Independent from this discovery, in screens for promising drugs for cancer therapy which were carried out a few years later, several novel compounds were identified to inhibit proliferation and induce differentiation of tumor cell lines *in vitro* (Yoshida et al. 1987; Ueda et al. 1994a; Ueda et al. 1994b; Ueda et al. 1994c; Richon et al. 1996). The mechanism of action of these substances was unclear. It was after their identification as potential anticancer agents that these compounds were identified as inhibitors of HDACs (Nakajima et al. 1998; Richon et al. 1998). Thus, a novel class of agents termed HDAC inhibitors was established. According to their chemical structure, the HDAC inhibitors discovered so far are divided into four classes: hydroxamic acids, cyclic peptides, aliphatic acids, and benzamids (table 5) (Miller et al. 2003). The structural details of the HDAC inhibitor – enzyme interaction have been elucidated in 1999. Crystallographic studies using TSA and SAHA indicated that these compounds inhibit HDAC activity by interacting with the catalytic site of HDACs, thereby blocking substrate access (Finnin et al. 1999). Thus, HDAC inhibitors consist of a metal-binding domain which chelates zinc and blocks enzymatic activity; a linker domain which mimics the substrate and occupies the enzymatic channel; and a surface domain which makes contacts with the rim (Miller et al. 2003). For some of the cyclic peptides, an irreversible action of HDAC inhibition is discussed, however, the ultimate proof is still lacking (Kijima et al. 1993; Meinke and Liberator 2001; Miller et al. 2003). All HDAC inhibitors known so far work equally well against class I and II HDACs (Marks et al. 2004). Only a few compounds (MS-275 and cyclic peptides) seem to be preferential inhibitors of class I versus class II HDACs (Furumai et al. 2001; Furumai et al. 2002; Matsuyama et al. 2002; Miller et al. 2003), none of the compounds known to date is selective for a single enzyme (Marks et al. 2004).

The mechanisms by which HDAC inhibitors facilitate their antitumor activites involve hyperacetylation of histone proteins, thereby directly altering the chromatin structure and activating the expression of genes. Moreover, the activity of transcription factors can be modulated by acetylation which may exert additional effects on gene transcription (Cress and Seto 2000; Marks et al. 2001; Marks et al. 2004).

On the basis of promising results obtained in cell cultures *in vitro* and favorable bioavailability data, a small number of HDAC inhibitors which are not toxic has been promoted to clinical trials to prove their potency against cancer *in vivo* (Miller et al. 2003; Marks et al. 2004).

**Table 5: Classification of histone deacetylase inhibitors (HDACs).**

| Hydroxamic acids | Cyclic peptides | Aliphatic acids | Benzamids |
|---|---|---|---|
| - Trichostatin A (TSA) | - Depsipeptide | - Valproic acid | - MS-275 |
| - Suberoylanilide | - Apicidin | - Butyrate | - CI-994 |
|   hydroxamid acid | - Trapoxin-hydroxamid | - Phenylbutyrate | - M344 |
|   (SAHA) |   acid analog | | |
| - Pyroxamide | | | |
| - m-Carboxycinnamic | | | |
|   acid bishydroxamide | | | |
|   (CBHA) | | | |
| - LAQ-824 | | | |
| - PXD-101 | | | |
| - Oxamflatin | | | |
| - Scriptaid | | | |

A substance which has long been known to induce hyperacetylation of chromatin in cell culture and also belongs to the earliest discovered HDAC inhibitors is sodium butyrate (Riggs et al. 1977). It has been suggested that, at least in part, this observation is due to a suppression of histone deacetylase activity (Boffa et al. 1978; Vidali et al. 1978; McCaffrey et al. 1997). Sodium butyrate has been shown to stimulate the expression of a number of genes and to induce differentiation in cancer cell lines (Leder and Leder 1975; Kruh 1982; Byrd and Alho 1987). It also has been demonstrated that butyrate increases the production of fetal-hemoglobin which is able to functionally substitute for the beta-globin chains that are defective or absent in patients suffering from beta-thalassemias (Perrine et al. 1993; McCaffrey et al. 1997). In 2001, the treatment of Epstein-Barr-Virus transformed lymphoblastoid cell lines derived from SMA type I, II, and III patients with sodium butyrate revealed increased full-length *SMN2* transcript and SMN protein levels (Chang et al. 2001). In addition, when sodium butyrate was administered to the pregnant mothers of SMA transgenic mice ($Smn^{-/-}$; *SMN2*), it improved survival in their offspring. This was the first study which suggested that HDAC inhibitors might be able to exert an effect on *SMN2* expression. However, due to a terminal half-life of only six minutes in human serum after systemic administration, butyrate would never reach its potential target in sufficient amounts and therefore was never considered as potential candidate neither for a long-term SMA therapy in patients, nor for cancer treatment (Miller et al. 1987; Newmark et al. 1994; Newmark and Young 1995; Engelhard et al. 2001).

Interestingly, it was discovered in 2001 that valproic acid is a powerful HDAC inhibitor which causes hyperacetylation of histones in cultured cells, relieves HDAC-dependent transcriptional repression, activates transcription from diverse exogenous and endogenous promoters and inhibits growth and induces differentiation of carcinoma cell lines *in vitro*, and of tumors in animal experiments *in vivo* (Gottlicher et al. 2001; Phiel et al. 2001). Valproic acid is a well-known drug which is used in long-term

treatment of epilepsy, mood disorders and migraine, is characterized by a suitable terminal half-life of 9-18 h in human serum, rarely shows severe side effects and possesses an excellent bioavailability (Johannessen 2000; Johannessen and Johannessen 2003). Thus, the drug is considered as excellent candidate for cancer therapy by HDAC inhibition (Gottlicher et al. 2001).

# 2 Aims

Proximal spinal muscular atrophy is the leading genetic cause of death in early childhood. Until now, a cure is not available. Since *SMN1* was identified as the SMA determining gene in 1995, comprehensive knowledge regarding the pathological disease mechanisms and the underlying molecular principles was gained, most importantly including the discovery and characterization of the *SMN2* copy gene in SMA patients. This knowledge about the molecular basis of SMA enables the design of therapeutic strategies which might lead to a clinical benefit for patients with SMA.

The aim of this work was to focus on the *SMN2* copy gene as a promising target for an SMA therapy. The basic question was whether inhibitors of histone deacetylases (HDACs) are able to stimulate the transcription of *SMN2*, thereby increasing the level of FL-*SMN2* transcript and SMN2 protein. HDAC inhibitors are exogenous compounds that have been previously identified as promising agents for the treatment of cancer. They have been demonstrated to activate the expression of genes which suppress proliferation and induce cell differentiation.

In a first step, this work was supposed to concentrate on the *in vitro* investigation of the HDAC inhibitor valproic acid (VPA). VPA is a well-known drug used for the long-term therapy of epilepsy in humans. To evaluate whether VPA is able to exert an effect on the human *SMN2* gene *in vitro*, an assay was planned to be established in which cell lines derived from SMA patients are treated with varying amounts of VPA. A potential effect of VPA should be uncovered and characterized in more detail by analysis of *SMN2* RNA and protein levels in the treated cell lines. Moreover, this work aimed at the investigation of a potential *ex vivo* effect of VPA on *SMN2* expression in neuronal tissue, the target tissue for an SMA therapy.

In a second step, it was an aim of this work to select additional HDAC inhibitors which are not yet available for application to humans but are tested for their anticancer potency in clinical trials, and to evaluate whether these drugs are able to elevate FL-*SMN2* transcript and protein levels in SMA cell lines *in vitro*. This drug screening should serve as a tool to identify promising candidates which might have a chance to be further considered for a potential SMA therapy.

In case the treatment of SMA cell lines with VPA should reveal an up-regulation of the SMN2 protein level, it was planned to further investigate VPA *in vivo*. The existing approval of VPA for the application in humans would allow the treatment of a small number of probands within a pilot trial to investigate whether the drug exerts an effect on *SMN* gene expression *in vivo*. Therefore, this work also aimed at the development of bioanalytical methods to reliably detect *SMN* transcript and SMN protein levels in peripheral blood. These methods would not only be essential to analyze the samples collected throughout the pilot trial with VPA, but also to establish a clinical biomarker to distinguish between drug responders and nonresponders in larger clinical trials and future therapies in SMA patients.

# 3      Subjects, Materials, and Methods

## 3.1      Human material derived from control subjects, SMA carriers, and SMA patients

Whenever human material was collected and a genetic analysis was carried out, informed written consent was given by the respective subjects or their legal guardians. All SMA type I, II, and III patients who donated human material fulfilled the diagnostic criteria for SMA (Munsat and Davies 1992), and carry homozygous deletions of *SMN1* as determined by routine molecular diagnostic testing. The number of genomic *SMN1* copies (controls, SMA carriers) and the number of genomic *SMN2* copies (controls, SMA carriers, SMA type I, II, and III patients) was determined in DNA isolated from an EDTA blood sample which has been collected from the respective donor (for details regarding the quantitative analysis of *SMN1* and *SMN2* copies, see also chapter 3.8.9.2).

### 3.1.1      Cell lines derived from SMA patients

In Professor Dr. Brunhilde Wirth's laboratory, a collection of about 50 primary fibroblast cell lines and about 400 Epstein-Barr-Virus (EBV) transformed lymphoblastoid cell lines derived from SMA patients, SMA carriers, and controls is available. The fibroblast lines were obtained from skin biopsies. The EBV cell lines are derived from EDTA blood samples.

### 3.1.2      Blood samples derived from untreated controls, SMA carriers, and SMA patients

From a number of 41 untreated individuals (including control subjects, SMA carriers and SMA type I, II, and III patients), blood samples were collected to serve for the isolation of total RNA or mRNA.

### 3.1.3      Blood samples derived from SMA carriers treated with valproic acid

Twelve SMA carriers were treated with valproic acid within a pilot trial that was approved by the local Ethics Committee of the University of Bonn (Approval number 13804). Written informed consent was obtained from each subject according to the Declaration of Helsinki. Blood samples were collected to serve either for the isolation of total RNA or for the isolation of protein.

### 3.1.4      Blood samples derived from SMA patients treated with valproic acid

A number of 20 SMA patients were treated with valproic acid by their local doctors in individual experimental curative approaches throughout Germany according to section 41 of the German Drug Act (AMG). Blood samples were collected to serve for the isolation of total RNA.

### 3.1.5 Human Blood Fractions MTC Panel

The Human Blood Fractions Multiple Tissue cDNA (MTC) Panel is a set of nine cDNA samples prepared from isolated human blood cell fractions and was obtained from *Clontech*, Saint-Germain-en-Laye (France). According to the information provided by the manufacturer, all blood was obtained from normal healthy donors tested negative for HIV-1 and -2, hepatitis B and syphilis, the ratio male/female being approximately 2:1. Cell fractions were isolated either from whole blood treated with the anticoagulant CPDA-1 or from platelet-depleted buffy coats. The purity was more than 98% for each cell population, as it was evaluated by staining fixed smears of freshly isolated cells with hematoxylin. Activation was performed with pokeweed mitogen and concanavalin A or phytohemagglutinin while cells were maintained in culture medium. RNA was prepared by *Clontech* using the RNeasy Midi Kit (*Qiagen*) followed by DNase treatment with RNase-free DNase (*Epicentre*).

## 3.2 Organotypic hippocampal slices prepared from rats

Five-day-old Wistar rats were used for the preparation of organotypic hippocampal slice cultures. Animals were decapitated, brains were rapidly removed and placed into ice-cold preparation medium (see chapter 3.4.2). After dissection of the frontal pole of the hemispheres and the cerebellum, brains were continuously kept in preparation medium and cut into 350 $\mu$m thick horizontal slices using a vibratome (*Leica*).

## 3.3 Equipment and Chemicals

### 3.3.1 Equipment

Isolation and analysis of nucleic acids:
- Centrifuges:
    Allegra X22-R, *Beckman Coulter*
    5415 D, *Eppendorf*
- Heating block: HTMR-133, *HLC*
- Spectrophotometers:
    BioPhotometer, *Eppendorf*
    NanoDrop ND-1000, *Peqlab*
- Cuvettes: UV-Vette, *Eppendorf*
- Thermocycler:
    GeneAmp 9600, *Perkin Elmer*
    GeneAmp 9700, *Applied Biosystems*
    LightCycler 1.5, *Roche*
    ABI Prism 7700, *Applied Biosystems*

- Polyacrylamide gel electrophoresis chamber:
    Multigel-long G47, *Biometra*
- Agarose gel electrophoresis chamber:
    SGE-020-02, *CBS Scientific*
- Power supplies:
    PowerPac 1000, *Biorad*
    PowerPac HC, *Biorad*
- Shaker: 3015, *GFL*
- Imaging systems:  ChemiDoc XRS, *Biorad*
                    Gel Doc 2000, *Biorad*
- Sequencer: ABI 3730, *Applied Biosystems*
- Microplate reader: Safire[2], *Tecan*

Isolation and analysis of proteins:

- Centrifuges:

    Allegra X22-R, *Beckman Coulter*

    5415 D, *Eppendorf*

    5415 R, *Eppendorf*

- Heating block: HTMR-133, *HLC*

- Spectrophotometer: BioPhotometer, *Eppendorf*

- Cuvettes: UV-Vette, *Eppendorf*

- pH meter: pH Level 1, *inoLab*

- SDS gel electrophoresis chamber:

    Mini-Protean 3 Cell, *Biorad*

- Western Blot transfer chamber:

    Mini Trans-Blot Cell, *Biorad*

- Power supply: PowerPac 1000, *Biorad*

- Shakers:

    3015, *GFL*

    VSR23, *Grant BOEKEL*

- Autoradiography cassette, *Agfa*

- Developer machine: CURIX 60, *Agfa*

- Imaging system: ChemiDoc XRS, *Biorad*

- Heat sealer: polystar 423, *Rische und Herfurth*

- Flow cytometer:

    FACScalibur, *Becton Dickinson*

Cell and tissue culture:

- Tissue culture hood: Hera Safe, *Heraeus*

- Microscope: Leica DMIL, *Leica*

- Centrifuge: Allegra X22-R, *Beckman Coulter*

- Incubator: Hera Cell 150, *Heraeus*

- Neubauer counting chamber, *Optik-Labor*

Further equipment:

- Nucleofector II, *Amaxa*

- MACS Multi Stand, *Miltenyi Biotec*

- MiniMACS Separation Unit, *Miltenyi Biotec*

- µMACS Separation Unit, *Miltenyi Biotec*

- Vibratome: VT 1000S, *Leica*

### 3.3.2 Chemicals

Whenever possible, only chemicals with the purity grade "pro analysi" were used for the experiments described in this work. All standard chemicals and organic solvents were purchased from the following companies: *Roche Molecular Biochemicals*, Mannheim; *Difco Lab.*, Michigan (USA); *Invitrogen*, Niederlande BV, Leek (Netherlands); *Merck*, Darmstadt; *MWG*, Ebersberg; *Amersham*, Freiburg; *Promega*, Mannheim; *Riedel de Haen AG*, Seelze; *Sigma Chemie*, Taufkirchen; *Serva*, Heidelberg; *Stratagene*, La Jolla (USA); *Applichem*, Darmstadt; *Roth*, Karlsruhe. For RNA isolation and analysis, only chemicals free of RNases have been used.

## 3.4     Solutions and Media

### 3.4.1     Frequently used buffers and solutions

| 10% PAA gel stock solution, native: | for 500 ml: |
|---|---|
| Acrylamide | 49.0 g |
| Bisacrylamide | 1.0 g |
| 1 x TBE buffer | to a final volume of 500 ml |
| TEMED | 500 µl |
| | store at 4°C; prior to use, add 200 µl APS |
| | per 20 ml stock solution |

| Ammonium Persulfate (APS) solution (10%): | for 10 ml: |
|---|---|
| APS | 1.0 g |
| deionized $H_2O$ | to a final volume of 10 ml |
| | store at -20°C |

| Blocking solution (6%): | for 100 ml: |
|---|---|
| Nonfat dry milk | 6 g |
| TBS Tween buffer | to a final volume of 100 ml |

| Bradford solution: | for 1l: |
|---|---|
| Coomassie Brilliant Blue G250 | 100 mg |
| $H_3PO_4$ (85%) | 100 ml |
| Ethanol (95%) | 50 ml |
| deionized $H_2O$ | to a final volume of 1 l |
| | store at 4°C |

| Diethylpyrocarbonate (DEPC) treated $H_2O$: | for 1 l: |
|---|---|
| DEPC | 1 ml |
| deionized $H_2O$ | to a final volume of 1 l |
| | mix overnight and autoclave |

(other solutions can be treated with DEPC
in a similar way, except for Tris solutions)

| DNA loading buffer (10 x): | for 50 ml: |
|---|---|
| 100 mM EDTA (pH 7.2-8.5) | 10 ml 0.5 M EDTA (pH 7.2-8.5) |
| 1% SDS | 2.5 ml 20% SDS |
| 50% Glycerol | 28.7 ml 87% Glycerol |
| 0.1% Bromphenol Blue | 0.05 g |
| deionized $H_2O$ | to a final volume of 50 ml |

| dNTP mix: | for 1 ml: |
|---|---|
| dNTP (100 mM) | 12.5 µl of each dNTP (total volume: 50 µl) |
| deionized $H_2O$ | to a final volume of 1000 µl |

| Electrophoresis buffer (10 x): | for 1 l: |
|---|---|
| Tris-Base | 30.29 g |
| Glycine | 144.13 g |
| SDS | 10.0 g |
| deionized $H_2O$ | to a final volume of 1 l |

| Ethidium bromide solution (1%): | for 100 ml: |
|---|---|
| Ethidium bromide | 1.0 g |
| deionized $H_2O$ | to a final volume of 100 ml |
| | store at 4°C in the dark |

| FACS buffer: | for 50 ml: |
|---|---|
| 0.1% Sodium azide | 0.05 g |
| 5% Fetal calf serum | 2.5 ml |
| 1 x PBS | to a final volume of 50 ml |

| Laemmli buffer for SDS PAGE (2x): | for 100 ml: |
|---|---|
| Tris-Base | 0.757 g |
| Glycerol | 20 ml |
| Bromphenol Blue | 10 mg |
| SDS | 6 g |
| *(prior to use: β-Mercaptoethanol* | *10 ml)* |
| deionized $H_2O$ | to a final volume of 90 ml without |
| | β-Mercaptoethanol, store at room temperature |
| | *(100 ml with β-Mercaptoethanol, store at 4°C and* |
| | *use not longer than 2 weeks)* |

| Lysis buffer (pH 7.4): | for 500 ml: |
|---|---|
| 155 mM $NH_4Cl$ | 77.5 ml 1 M $NH_4Cl$ |
| 10 mM $KHCO_3$ | 5 ml 1 M $KHCO_3$ |
| 0.1 mM EDTA | 100 µl 0.5 M EDTA |
| deionized $H_2O$ | 400 ml |
| | adjust pH to 7.4 with HCl |
| deionized $H_2O$ | to a final volume of 500 ml |
| | store at 4°C |

MACS buffer:                                for 50 ml:

2 mM EDTA                                   0.2 ml 0.5 M EDTA

0.5% Fetal calf serum                       0.25 ml

1 x PBS                                     to a final volume of 50 ml

                                            store at 4°C


Nucleus lysis buffer:                       for 1000 ml:

10 mM Tris                                  10 ml 1 M Tris-HCl (pH 8.0)

400 mM NaCl                                 80 ml 5 M NaCl

2 mM $Na_2EDTA$                             4 ml 0.5 M $Na_2EDTA$ (pH 7.0)

deionized $H_2O$                            700 ml

                                            adjust pH to 8.2

deionized $H_2O$                            to a final volume of 1000 ml

                                            store at 4°C


PCR buffer (10 x):                          for 500 ml:

500 mM KCl                                  250 ml 1 M KCl

100 mM Tris-HCl (pH 8.3)                    50 ml 1 M Tris (pH 8.3)

15 mM $MgCl_2$                              7.5 ml 1 M $MgCl_2$

0.1% gelatin                                0.5 g gelatin

deionized water                            to a final volume of 500 ml

                                            adjust to pH 8.3, sterile filtration


Phosphate buffered saline (PBS) (10 x):     for 1000 ml:

NaCl                                        80.0 g

KCl                                         2.0 g

$Na_2HPO_4$                                 14.4 g

$KH_2PO_4$ (pH 7.3)                         2.4 g

deionized $H_2O$                            to a volume of 800 ml

                                            adjust pH to 7.4

deionized $H_2O$                            to a final volume of 1000 ml, autoclave


Ponceau solution:                           for 100 ml:

0.5% Ponceau S                              0.5 g

1% Acetic acid glacial                      1 ml

deionized $H_2O$                            to a final volume of 100 ml

RIPA buffer:                                              for 50 ml:

150 mM NaCl                                               1.5 ml 5 M NaCl

1% IGEPAL                                                 5 ml 10% IGEPAL

0.5% DOC (Deoxycholic acid)                              2.5 ml 10% DOC

0.1% SDS (Sodium Dodecyl Sulfate)                       0.5 ml 10% SDS

50 mM Tris (pH 8.6)                                      2.5 ml 1 M Tris (pH 8.6)

deionized $H_2O$                                         deionized $H_2O$ to a final volume of 50 ml


RT mix:                                                  for 1000 µl:

5 x buffer (supplied with reverse transcriptase)        400 µl

DTT (100 mM)                                            200 µl

dNTP (100 mM)                                           25 µl of each dNTP (total volume: 100 µl)

DEPC treated deionized $H_2O$                           300 µl


Separation gel for SDS PAGE 12%:                        for 1 gel:

deionized $H_2O$                                        1.7 ml

acrylamide-bisacrylamide mix (29:1, 30%)               2.0 ml

Tris (1.5M, pH 8.8)                                    1.3 ml

SDS (10%)                                               0.05 ml

APS (10%)                                               0.05 ml

TEMED                                                   0.002 ml


Sodium Dodecyl Sulfate (SDS) solution 10%:             for 100 ml:

SDS                                                     10.0 g

deionized $H_2O$                                       to a final volume of 100 ml

                                                        dilute at 65°C, store at room temperature


Stacking gel for SDS PAGE:                             for 1 gel:

deionized $H_2O$                                       0.68 ml

acrylamide-bisacrylamide mix (29:1, 30%)               0.17 ml

Tris (1 M, pH 6.8)                                     0.13 ml

SDS (10%)                                               0.01 ml

APS (10%)                                               0.01 ml

TEMED                                                   0.001 ml


TBE buffer (5 x):                                      for 1 l:

445 mM Tris base                                       54 g Tris base

445 mM Borate                                          27.5 g Boric acid

10 mM EDTA                                             20 ml 0.5 M EDTA (pH 8.0)

deionized $H_2O$                                       to a final volume of 1000 ml

| TBS Tween buffer: | for 5 l: |
|---|---|
| 20 mM Tris | 12.1 g Tris |
| 137 mM NaCl | 40.0 g NaCl |
| 0.5% Tween 20 | 25 ml Tween 20 |
| deionized $H_2O$ | deionized $H_2O$ to a final volume of 5 l |
| adjust to pH 7.56 | |

| $TE^{-4}$ buffer: | for 100 ml: |
|---|---|
| Tris (1 M, pH 8.0) | 1 ml |
| EDTA (0.5 M, pH 8.0) | 20 µl |
| deionized $H_2O$ | to a final volume of 100 ml |

| Transfer buffer: | for 5 l: |
|---|---|
| Tris-Base | 12.1 g |
| Glycine | 56.3 g |
| Methanol | 1000 ml |
| deionized $H_2O$ | to a final volume of 5 l |

| Tris-HCl (1 M, pH 6.8): | for 400 ml: |
|---|---|
| Tris-HCl | 60.0 g |
| deionized $H_2O$ | to a final volume of 400 ml |
| | adjust pH to 6.8 with concentrated HCl |

| Tris-HCl (1.5 M, pH 8.8): | for 400 ml: |
|---|---|
| Tris-HCl | 90.5 g |
| deionized $H_2O$ | to a final volume of 400 ml |
| | adjust pH to 8.8 with concentrated HCl |

### 3.4.2 Media for eukaryotic cell and tissue culture procedures

| Medium for human fibroblasts: | for 556.4 ml: |
|---|---|
| D-MEM with 4500 mg/l Glucose, L-Glutamine, Pyruvate (#41966-029, *Invitrogen*) | 500.0 ml |
| Fetal calf serum (*Biochrom*) | 50.0 ml |
| Penicillin-Streptomycin (*Invitrogen*) | 5.0 ml |
| Amphotericin B (*PromoCell*) | 1.4 ml of a stock with the concentration 250 µg/ml |

Medium for human EBV-transformed
lymphoblastoid cells:                          for 631.4 ml:
RPMI 1640 Medium without L-Glutamine
(#31870-025, *Invitrogen*)                     500.0 ml
Fetal calf serum (*Biochrom*)                  120.0 ml
Penicillin-Streptomycin (*Invitrogen*)         5.0 ml
Amphotericin B (*PromoCell*)                    1.4 ml of a stock with the concentration 250 µg/ml
L-Glutamine (*Invitrogen*)                      5.0 ml of a stock with the concentration 200 mM


Media for lipofection of human fibroblasts:


OptiMEM I (#31985-047, Invitrogen)


D-MEM with 4500 mg/l Glucose, L-Glutamine,
Pyruvate (#41966-029, *Invitrogen*)            500.0 ml
Fetal calf serum (*Biochrom*)                  50.0 ml


Preparation medium for organotypic
hippocampal slices from rat:                   for 540.0 ml
MEM (#11012-028, *Invitrogen*)                 8.0 g
deionized autoclaved $H_2O$                    500.0 ml
Tris-Base (1 M, *Sigma*)                       5.0 ml
L-Glutamine (*Invitrogen*)                     5.0 ml of a stock with the concentration 200 mM
Glucose (10%, *Merck*)                         5.0 ml
                                               sterile filtration
Horse serum (*Biochrom*)                       25.0 ml


Medium for culture of organotypic
hippocampal slices from rat:                   for 105.46 ml:
MEM (#11012-028, *Invitrogen*)                 0.8 g
deionized autoclaved $H_2O$                    50.0 ml
HBSS (#24020-091, *Invitrogen*)                25.0 ml
Glucose                                        1.2 ml of 10% Glucose
L-Glutamine (*Invitrogen*)                     2.0 ml of a stock with the concentration 200 mM
Penicillin-Streptomycin (*Sigma*)              1.0 ml
0.8 µg/ml Vitamin C
10 µg/ml Insulin-transferrin-sodium selenite
Sodium bicarbonate (7.5%)                      580 µl
Tris-Base (1 M, *Sigma*)                       500 µl
                                               sterile filtration
25% Horse serum (*Biochrom*)                   25.0 ml

## 3.5    Primers and siRNAs

The primers and probes listed in table 6 were purchased from the companies MWG or Metabion and used for semi-quantitative PCRs, quantitative real-time PCRs, or sequencing. They were delivered in lyophilized form and subsequently diluted in deionized, autoclaved H$_2$O to achieve primer stock solutions with a concentration of 100 pmol/µl. Stock solutions were stored at -20°C and served for the preparation of working solutions with the concentration 10 pmol/µl.

**Table 6: Primers and probes used for semiquantitative PCRs and quantitative real-time PCRs. "No." indicates the internal laboratory number of the respective primer, "F" and "R" are the abbreviations for "forward" and "reverse", "°C" is the annealing temperature, and "bp" indicates the expected length of the PCR product using the respective primer pair. Lowercase letters in the primer sequences indicate mutations introduced to obtain adequate gene-specific primer binding. *SFRS10* is the human gene encoding *Htra2-β* transcripts.**

| Locus | No. | | °C | Sequence 5'→3' | bp |
|---|---|---|---|---|---|
| Human *SMN* exon 6 | 1837 | F | 55 | ATA ATT CCC CCA CCA CCT C | FL: 432 |
| Human *SMN* exon 8 | 1841 | R | | GCC TCA CCA CCG TGC TGG | Δ7: 378 |
| Human *GAPDH* exon 1 | 1879 | F | 55 | TCC GCG CAG CCG AGC CA | 334 |
| Human *GAPDH* exon 4 | 1876 | R | | ACG CCA GTG GAC TCC ACG | |
| Human *SFRS10* exon 1 | 1093 | F | 55 | CCA GGA GTC ATG AGC GAC AG | Htra2-β1: 222 Htra2-β3: 87 Htra2-β4: 303 |
| Human *SFRS10* exon 4 | 1094 | R | | GAC CGG GTA TAA TGC CTT CG | |
| Human *SFRS10* exon 1 | 1970 | F | 55 | GCG ACA GCG GCG AGC AG | Htra2-β2: 112 |
| Human *SFRS10* exon 2 | 1986 | R | | CAC TTA TTC CTG AGC TTC AAA T | |
| Human *SFRS10* exon 1 | 1970 | F | 55 | GCG ACA GCG GCG AGC AG | Htra2-β1: 165 Htra2-β4: 246 |
| Human *SFRS10* exon 3 | 1971 | R | | TAG ATT CAG ATC GGA CCT G | |
| Rat *Smn* exon 5 | - | F | 60 | GGA TGC CTC CGT TCC CTT | 59 |
| Rat *Smn* exon 6 | | R | | TCC AGA CAG TCG GGA GAT ATG G | |
| Rat *Smn* probe | | | | FAM-AGG ACC ACC AAT AAT TCC TCC ACC CCC T-TAMRA | |
| Rat *β-actin* exon 3 | - | F | 60 | AGG CCC CTC TGA ACC CTA AG | 118 |
| Rat *β-actin* exon 4 | | R | | CCA GAG GCA TAC AGG GAC AAC | |
| Rat *β-actin* probe | | | | FAM-TTT GAG ACC TTC AAC ACC CCA GCC A-TAMRA | |

| Locus | No. | | °C | Sequence 5'→3' | bp |
|---|---|---|---|---|---|
| Human *SMN1* intron 6/exon 7 | 1127 | F | 58 | TTT ATT TTC CTT ACA GGG TTT C | 307 |
| Human *SMN1* intron 7 | 1133 | R | | GTG AAA GTA TGT TTC TTC CAC gTA | |
| Human *SMN2* intron 6/exon 7 | 1263 | F | 58 | TTT ATT TTC CTT ACA GGG TTT TA | 307 |
| Human *SMN2* intron 7 | 1268 | R | | GTG AAA GTA TGT TTC TTC CAC gCA | |
| Human *CTLA1* exon 2 | 2048 | F | 60 | TGA TAC GAG ACG ACT TCG TGC | 194 |
| Human *CTLA1* exon 3/4 | 2049 | R | | CTT TCT CTC CAG CTG CAG TA | |
| Human *RPLP0* exon 2/3 | 2939 | F | 63 | GAC CTG GAA GTC CAA CTA CTT C | 258 |
| Human *RPLP0* exon 4 | 2940 | R | | GTC CCT GAT CTC AGT GAG GTC | |
| Human *PPIB* exon 2/3 | 2935 | F | 65 | CTT AGC TAC AGG AGA GAA AGG A | 199 |
| Human *PPIB* exon 4 | 2936 | R | | GCC TGC GTT GGC CAT GCT C | |
| Human *B2M* exon 2 | 1967 | F | 61 | TGT CTT TCA GCA AGG ACT GG | 148 |
| Human *B2M* exon 3 | 1968 | R | | GAT GCT GCT TAC ATG TCT CG | |
| Human *GUSB* exon 10 | 2937 | F | 69 | CTA CTA CTC TTG GTA TCA CGA C | 174 |
| Human *GUSB* exon 11 | 2938 | R | | TCT TCA GTG AAC ATC AGA GGT G | |
| Human *SMN* exon 7 | 2075 | F | 62 | GAA GGT GCT CAC ATT CCT TAA AT | 186 |
| Human *SMN* exon 8 | 2076 | R | | ATC AAG AAG AGT TAC CCA TTC CA | |
| Human *SMN* exon 5 | 1449 | F | 61 | CCA CCA CCC CAC TTA CTA TCA | 183 |
| Human *SMN* exon 6/8 | 1450 | R | | GCT CTA TGC CAG CAT TTC CAT A | |
| Human *SFRS10* exon 4 | 2690 | F | 68 | CTC CCG AAG GCA TTA TAC CCG GTC | 196 |
| Human *SFRS10* exon 5 | 2691 | R | | GTA CAA GCT CAG CCC AAA TAC T | |

In addition, a number of small interfering RNAs (siRNAs) have been used for transfection experiments of human fibroblasts. They are listed below (*SFRS10* is the human gene encoding *Htra2-β* transcripts):

- Hs_SFRS10_3_HP siRNA, #SI00065807, *Qiagen* (target: *Htra2-β* transcripts; target
  sequence located in exon 4/5: TCG GGC AAA TCC TGA TCC TAA)
- Hs_SFRS10_5_HP validated siRNA, #SI02653252, *Qiagen* (target: *Htra2-β* transcripts; target
  sequence located in exon 7: CGG GAC TAC TAT AGC AGA TCA)
- siCONTROL Non-Targeting siRNA, *Dharmacon* (control siRNA)
- siCONTROL TOX Transfection Control, *Dharmacon* (siRNA to check transfection efficiency)
- siCONTROL Cyclophilin B siRNA, *Dharmacon* (target: *Cyclophilin B* transcripts)

All siRNAs were pre-designed by the respective company. The siRNAs purchased from Qiagen were delivered in lyophilized form. To obtain a 20 µM stock solution, 250 µl siRNA Suspension Buffer (*Qiagen*) were added to 5 nmol siRNA. Subsequently, the dilution was incubated at 90 °C for 1 min and at 37 °C for another 60 min according to the manufacturer's protocol to disrupt higher aggregates.

Stocks were stored at -20 °C and further diluted with siRNA Suspension Buffer to obtain 1 µM working dilutions prior to use.

The siRNAs purchased from Dharmacon were also delivered in lyophilized form and dissolved in 1 x siRNA Buffer (*Dharmacon*) to obtain a stock dilution of 20 µM. Stocks were stored at -20 °C. Prior to transfection of fibroblasts, stocks were further diluted with siRNA Buffer to obtain working dilutions with a concentration of 1 µM.

## 3.6 Software, internet programs, and databases

Microsoft® Office Professional Edition 2003, *Microsoft Corporation* (word processing, data analysis)

Adobe Photoshop 8.0.1, *Adobe Systems Inc.* (image editing)

EndNote 9, *Thomson ResearchSoft* (organization of references)

SigmaPlot 9.0, *Systat Software, Inc.* (creation of graphs)

OneDScan, *Scanalytics* (densitometric analysis of PAA gels and western blots)

Quantity One 4.5.1, *Biorad* (scanning and densitometric analysis of gels and western blots)

FinchTV Version 1.3.1, *Geospiza Inc.* (analysis of DNA sequencing results)

Editseq/PrimerSelect/SeqBuilder, *DNASTAR Inc.* (DNA/protein sequence analysis, primer selection)

BioEdit 7.0.4.1, *Tom Hall* (DNA sequence alignment and analysis)

LightCycler Software, *Roche* (documentation/analysis of real-time PCR data)

Sequence Detection Software, *Applied Biosystems* (documentation/analysis of real-time PCR data)

Multi-Analyst Version 1.1, *Biorad* (scanning and densitometric analysis of gels and western blots)

XFluor4SafireII software, *Tecan* (analysis of absorption/fluorescence using microtiter plates)

BD CellQuest software Version 3.3, *Becton Dickinson* (flow cytometry analysis)

NCBI, www.ncbi.nlm.nih.gov

ENSEMBL, www.ensembl.org

UCSC Genome Browser, www.genome.ucsc.edu/cgi-bin/hgGateway

Medline, www.ncbi.nlm.gov/PubMed

OMIM, www.ncbi.nlm.nih.gov/entrez/query.fcgi?db=OMIM

Gene Expression Atlas database, expression.gnf.org

## 3.7 Cell culture and tissue culture procedures

To avoid any contaminations with fungi or bacteria, all cell culture work was carried out under a tissue culture hood using only sterile solutions and materials. To further increase the protection of the cells and tissues from contamination, amphotericin B and/or penicillin and streptomycin were added to the culture medium. Fetal calf serum or horse serum served as important sources of essential growth factors.

### 3.7.1    Cell culture of primary fibroblasts derived from SMA patients

Fibroblasts were routinely grown as adherent cultures in medium described in chapter 3.4.2. Cells were kept in an atmosphere with 5% $CO_2$ at 37 °C using tissue culture flasks of either 25 cm$^2$ or 75 cm$^2$ surface. Medium was changed once or twice a week depending on the cell division rate of the respective fibroblast line. The requirement of fresh medium was indicated by a color change of the medium in the cell culture flasks which occurs as soon as the nutrients are used up and the metabolic products of the cells cause a change of the pH in the medium.

When the fibroblasts in the culture flasks were confluent, they were washed with PBS and released from the bottom of the flask by treatment with trypsin. Trypsinization was stopped by addition of fresh culture medium and cells were split into several new flasks. Depending on the cell division rate of the respective cell line, the fibroblasts from one 75 cm$^2$ flask were split in two to four new 75 cm$^2$ flasks.

To store the fibroblasts, cells were washed with PBS and trypsinized. After addition of culture medium and centrifugation at 1200 rpm for 10 min, the cell pellet was suspended in a sterile mix consisting of 90% FCS and 10% dimethylsulfoxide (DMSO) and frozen at -196 °C in liquid nitrogen. At any time, these aliquots can be thawed and cells can be grown again in culture medium using the conditions described above.

### 3.7.2    Stimulation of primary fibroblast cell lines with chemical substances

Fibroblast cultures derived from SMA patients were grown in tissue culture flasks to a confluence of ~80%. Cells were washed with PBS and released with trypsin. After addition of culture medium and vigoros mixing to obtain a homogeneous suspension; cells were counted and the cell number adjusted

**Table 7: Drug solvents, final drug concentrations used in cell cultures, and incubation time of the cells with the respective drug. For clarification: Throughout this thesis, the common term "valproic acid" and the corresponding abbreviation "VPA" are used. However, all *in vitro* and *ex vivo* experiments were carried out with a solution of the salt sodium valproate.**

| Drug | Solvent | Final drug concentrations in fibroblast cultures | Incubation time |
|---|---|---|---|
| **Sodium valproate** (#P4543, *Sigma*) | $H_2O$ | 0, 0.5, 5, 50, 500, 1000 µM | 16 h (no pre-incubation) |
| **Sodium butyrate** (#B-5887, *Sigma*) | $H_2O$ | 0, 0.5, 5, 50, 500, 1000 µM | 24 h (no pre-incubation) |
| **SAHA** (#270-288, *Alexis*) | DMSO | 0, 0.05, 0.5, 1, 5, 10 µM | 24 h (24 h pre-incubation) |
| **MS-275** (#382147, *Calbiochem*) | DMSO | 0, 0.05, 0.25, 0.5, 1, 5 µM | 24 h (no pre-incubation) |

with additional culture medium to some $2 \times 10^5$ cells / 8 ml.

Subsequently, some $2 \times 10^5$ cells of fibroblasts from SMA patients were transferred into 10 cm petri dishes. The respective drug was dissolved either in deionized and autoclaved $H_2O$ or DMSO and added dropwise to each dish. For each experiment, to one of the dishes only solvent (deionized and autoclaved $H_2O$ or DMSO) was added to serve as a control (mock). Cells were incubated with the respective drug at 5% $CO_2$ and 37 °C. For details about the solvent for the respective drug, the final drug concentrations used in the fibroblast cultures, and the incubation times used, see table 7. Each drug treatment experiment was always repeated at least twice in different passages of the respective fibroblast cell line and the final results are given as mean ± SEM.

### 3.7.3    Cell culture of EBV-transformed lymphoblastoid lines derived from SMA patients

EBV-transformed lymphoblastoid cell lines were maintained as suspension cultures in medium described in chapter 3.4.2. Cells were grown in an atmosphere with 5% $CO_2$ at 37 °C using tissue culture flasks of 25 $cm^2$ surface which were kept in an upright position. Cultures were fed with 4 ml of medium twice a week.

### 3.7.4    Stimulation of lymphoblastoid cell lines with chemical substances

EBV cell lines derived from SMA patients were maintained in tissue culture flasks. To obtain well-growing suspension cultures with a medium cell density, a part of the stock cell culture was transferred to a new flask and fed with fresh culture medium two days before setting up the experiment.
On the day of the experiment, the cell culture was mixed vigorosly to obtain a homogeneous suspension. Subsequently, cells were counted, the cell number adjusted by addition of fresh culture medium, and aliquots containing the respective number of cells were transferred into new culture flasks. Valproic acid or butyrate were dissolved in deionized and autoclaved $H_2O$ and added dropwise to each flask. For each experiment, to one of the flasks only solvent was added to serve as a control (mock). Cells were incubated with the respective drug at 5% $CO_2$ and 37 °C for varying time periods.

### 3.7.5    MTT assay

Thiazolyl blue tetrazolium bromide (MTT) is converted into violet formazan crystals by living cells, but not by dead cells. The absorption maxima of MTT and formazan are different. Thus, MTT can be added to cell cultures treated with a chemical substance, and subsequent photometric measurement of the newly synthesized formazan can give evidence of cell survival under drug treatment and the cytotoxicity of the drug (Mosmann 1983).

In each well of a 96-well plate, some 8000 fibroblasts were plated in 250 µl culture medium and incubated with different drugs at 5% $CO_2$ and 37 °C. The solvent for the respective drug, the final drug

concentrations, and the incubation times are identical to the conditions used for the stimulation experiments described in chapter 3.7.2 (table 7). After incubation of the cells with the drug, old medium was removed and replaced by 225 µl of fresh culture medium and 25 µl MTT stock solution (50 mg MTT in 10 ml PBS). Cells were incubated for another 3 h to induce the production of formazan crystals. After replacing the medium with 100 µl iso-stock [50 ml Isopropanol (100%) + 165 µl HCl (37%)], photometric absorption was measured at 550 nm using a microplate reader (Safire[2], *Tecan*). For each drug concentration, results were averaged from a number of eight wells. To evaluate the mock values, a number of sixteen wells were used. Results are always given as mean ± standard error of the mean (SEM).

### 3.7.6   Transient transfection of primary human fibroblasts

The technique of transient transfection is applied to (over-)express a desired protein or to knock-down specific target RNA transcripts in cell cultures. For protein expression, a so-called mammalian expression vector has to be delivered to the cells. This vector contains a strong promoter [e.g. the human Cyto-Megalo-Virus (CMV) promoter] and the cDNA of the desired protein to be expressed. To knock-down target RNA transcripts in cell cultures, small interfering RNAs (siRNAs) have to be introduced into the cells. They are able to specifically silence gene expression via a pathway called RNA interference (RNAi). RNAi has originally been discovered as cellular defense mechanism against double-stranded viral RNA which is present in the cell upon viral invasion. However, introduction of long double-stranded RNAs (>30 nucleotides) initiates a general antiviral response, including nonspecific inhibition of protein synthesis and RNA degradation. In contrast, delivery of the functional intermediates in the RNAi pathway, small interfering RNAs (siRNAs) which are usually generated from long double-stranded RNAs by an RNase III-like enzyme called Dicer, is able to achieve specific gene silencing of the target without a general cellular response. Double-stranded siRNAs are 19-25 bp in length, and assemble into endoribonuclease-containing complexes known as RNA-induced silencing complexes (RISCs) after entering the cell. There, they are unwinded. The siRNA strands subsequently guide the RISCs to complementary RNA transcripts, which are cleaved and destroyed.

To transiently transfect cells, the calcium phosphate method is frequently used. This method is simple and cost-saving, however, transfection efficiency reached in primary human fibroblasts is very low. Therefore, different approaches have to be applied for this type of cells.

Electroporation of fibroblasts derived from SMA patients was carried out using the Nucleofector technique (*Amaxa*). During electroporation, cells are treated with a current pulse that temporarily disrupts the cell membrane and electrophoreses DNA into cells. According to the information provided by the manufacturer, plasmids are directly delivered to the nucleus of treated cells, resulting in a very fast protein expression which is already visible a few hours after the transfection procedure. The same technique can be applied to transfect siRNA oligos into the target cells. To transiently transfect fibroblasts, the Human Dermal Fibroblast Nucleofector Kit (*Amaxa*) and the Basic Nucleofector Kit for Primary Fibroblast Cells (*Amaxa*) were used according to the manufacturer's protocols. In brief, fibroblasts were harvested, counted, and a volume containing the required amount of cells was

centrifuged at 1200 rpm for 10 min. For each single transfection reaction, a number of $0.5 \times 10^6$ cells were used. Cell pellet was suspended in Nucleofector Solution (100 µl for each $0.5 \times 10^6$ cells), and after addition of 2 µg pmaxGFP expression vector (*Amaxa*) for each $0.5 \times 10^6$ cells, aliquots of 100 µl were transferred to cuvettes and treated with the respective electroporation program (A24, T16, U12, U23, V13). After electroporation in cuvettes, aliquots were added to 1.5 ml of culture medium which was pre-warmed in 6-well plates. A number of additional control transfection reactions was performed: (i) cells suspended in Nucleofector Solution without adding vector were treated with a strong program to check the reaction of cells to the electroporation program, and (ii) cells suspended in Nucleofector Solution with vector were not treated with any program to check for a potential toxicity of the vector. Cells were kept at 37°C and 5% $CO_2$ up to 48 h.

Lipofection is another way to deliver plasmids or siRNAs to cells in culture. Lipofection is a technique which injects genetic material into cells by means of liposomes which are vesicles that can easily merge with the cell membrane since they are both made of a phospholipid bilayer (Felgner et al. 1987). They are able to complex DNA or RNA in their inner space and deliver these molecules to the cell upon merge with the membrane.

For lipofection experiments, fibroblasts were grown to a confluency of ~80% in tissue culture flasks, washed with PBS, and released with trypsin. After addition of culture medium, cells were counted, and an aliquot containing the required amount of fibroblasts was transferred to a 50 ml Falcon tube. Cells were centrifuged at 1200 rpm for 10 min, the supernatant was removed, and the cell pellet was suspended in culture medium to obtain a concentration of $1 \times 10^5$ cells / 2 ml. A number of $1 \times 10^5$ cells were transferred to each well of a 6-well plate and maintained at 5% $CO_2$ and 37°C for 24 h.

Prior to transient transfection, siRNA stocks (see chapter 3.5) were diluted in suspension buffer to a final concentration of 1 µM. Dharmafect 1 (*Dharmacon*) was used for all transfection experiments. This agent is optimized for the delivery of siRNAs into cells. Transfection was carried out according to the manufacturer's protocol. In brief, 100 µl of each 1 µM siRNA dilution was mixed with 100 µl OptiMEM I in a 1.5 ml tube. In a 2 ml tube, 4 µl of Dharmafect 1 were mixed with 196 µl OptiMEM I. After incubation for 5 min, the contents of both tubes were mixed, followed by another incubation period of 20 min. Subsequently, 1.6 ml of fibroblast culture medium without antibiotics was added to the 0.4 ml mixture containing the respective siRNA and Dharmafect 1 to a final volume of 2 ml. After removal of old medium, the 2 ml transfection preparation was added to the fibroblasts of one well. Cells were kept at 5% $CO_2$ and 37°C for another 72 h to allow for delivery of siRNAs into fibroblast cells and knock-down of RNA transcripts. During the last 16 h of incubation, a part of the cells was treated with an aqueous dilution of valproic acid for a final drug concentration of 1000 µM. After cell harvest, RNA was isolated as described in chapter 3.8.3, and protein was isolated as described in chapter 3.9.1. For each combination of a specific siRNA with/without drug treatment, experiments were performed in triplicates and results are given as mean ± standard error of the mean (SEM). Whenever the analysis of RNA and protein was required for a specific combination of siRNA with/without drug treatment, two triplicates were performed (corresponding to six wells). The cells from each two wells were pooled, mixed and separated again into two equal parts for subsequent RNA or protein isolation.

### 3.7.7 Tissue culture of organotypic hippocampal slices from rat

A number of three 350 $\mu$m thick hippocampal brain slices from rat were transferred into a culture plate insert membrane dish (*BD Biosciences*) and thereafter into 6-well culture dishes (*BD Biosciences*) containing 1.2 ml culture medium (chapter 3.4.2), according to the interface technique described by Stoppini et al. (Stoppini et al. 1991) and modified by Savaskan et al. (Savaskan et al. 2000). The slices were cultivated at 35°C and 5% $CO_2$. The medium was changed one day after preparation and every second day thereafter.

(These experiments have been performed in collaboration with Prof. Dr. I. Blümcke from the Institute of Neuropathology and Dr. I.Y. Eyüpoglu from the Department of Neurosurgery at the University Erlangen-Nuremberg in Erlangen).

### 3.7.8 Stimulation of rat hippocampal slices with chemical substances

After six days *in vitro*, sodium valproate (diluted in deionized, autoclaved $H_2O$) was added to the culture medium of the organotypic hippocampal slice cultures from rat to obtain final drug concentrations of 0, 50, 500 and 2000 µM. For each concentration, a number of three slices was treated with the drug. The slices were incubated with the drug for 12, 24, 36, and 48 h and subsequently harvested and snap-frozen in liquid nitrogen.

## 3.8 Molecular biology methods

### 3.8.1 Isolation of genomic DNA from whole blood

Human genomic DNA can be extracted from leukocytes which are nucleated and present in whole blood. Extraction can be performed applying either the phenol/chloroform method or the salting out procedure (Miller et al. 1988). Due to the toxicity of phenol, the salting out procedure is more commonly used and is also preferred in our lab. This method includes the collection of blood in tubes containing EDTA as anticoagulant, lysis and removal of erythrocytes, subsequent lysis of leukocytes, removal of cell debris including proteins by enzymatic digestion, and precipitation of the leukocyte DNA.

A volume of 5-10 ml whole blood was transferred to a 50 ml Falcon tube and supplemented with lysis buffer to a final volume of 50 ml. After mixing and incubation on ice for 15 min, samples were centrifuged at 4°C and 2000 rpm for 15 min. The supernatant was discarded and the remaining leukocyte pellet was suspended in 10 ml of nucleus lysis buffer. After addition of 0.7 ml 10% SDS solution (denaturation of DNA-binding proteins) and 400 µl Pronase E solution (20 mg/ml), samples were shaken at 37°C in a water bath overnight. On the next day, digested cell lysates were supplemented with 3.2 ml saturated NaCl solution, vigorosly mixed and centrifuged two times at 4000 rpm for 10 min. The supernatant was transferred to a new 50 ml Falcon tube, the protein pellet was

discarded. After precipitating the DNA from the supernatant using isopropanol, the DNA was fished with a glass stick, washed with 70% ethanol, air dried, and finally diluted in 200 to 600 µl TE$^{-4}$.

### 3.8.2  Determination of the DNA concentration

The DNA concentration was determined by measuring the absorption at a wave length of 260 nm ($A_{260}$) on a photometer (*Eppendorf*). The absorption is expected to be 1 when measuring a dilution of double-stranded DNA with a concentration of 50 µg/ml, using a cuvette with a path length of 1 cm (Current Protocols in Molecular Biology, 2001, Appendix A.3D.1). To determine the concentration of the DNA stocks, dilutions (e.g. 1:10, 1:20) with a volume of 50 µl were prepared prior to photometric analysis. Purity of the DNA was determined by measuring the ratio of the absorption at 260 nm and the absorption at 280 nm. The ratio is recommended to range between 1.8 and 2.0. Higher values suggest contamination with RNA, while lower values point to contamination with proteins or ethanol. After measuring the background absorption of the solvent, the absorption of the DNA dilutions was determined and the concentration (in µg DNA/ml) was calculated as follows: factor of the dilution x (absorption at 260 nm – background) x 50 µg. Measurements were performed in triplicates and the concentration calculated as mean of the single values.

Alternatively, a NanoDrop ND-1000 Spectrophotometer (*Peqlab*) was used to determine the DNA concentration. Therefore, a 1 µl DNA sample was pipetted onto the end of a fiber optic cable and a second fiber optic cable was brought into contact with the liqid. Absorption was measured at wave lengths of 260 nm and 280 nm utilizing a pathlength of 0.2 mm, and the DNA concentration and purity was calculated by the software based on the same principles as described above. Measurements were performed in triplicates and the concentration calculated as mean of the single values.

### 3.8.3  Isolation of total RNA from primary fibroblast cell cultures

From fibroblast cultures treated with various drugs, total RNA was isolated using the EZNA Total RNA Kit (*Peqlab*) according to the manufacturer's protocol.

To isolate total RNA from fibroblasts used for siRNA transfection experiments, the RNeasy Kit (*Qiagen*) and the QIAshredder (*Qiagen*) were used according to the manufacturer's protocols. The QIAshredder reduces viscosity of the samples which is due to the presence of DNA in the cell lysates and may disturb the RNA isolation with the RNeasy Kit. As recommended for RNA samples which are planned to be investigated by quantitative real-time PCR, a DNase digest was carried out by use of the RNase-Free DNase set (*Qiagen*) according to the protocol included in the RNeasy Kit.

### 3.8.4 Isolation of total RNA from organotypic hippocampal slice cultures (OHSCs) from rat

Total RNA was extracted from every three pooled rat OHSCs using the RNeasy Kit (*Qiagen*) and the QIAshredder (*Qiagen*) according to the manufacturer's protocols. Again, the QIAshredder was applied to reduce viscosity of the tissue lysates before proceeding with the RNA isolation (see chapter 3.8.3).

### 3.8.5 Isolation of total RNA from peripheral whole blood

A volume of 2.5 ml of peripheral whole blood was collected in PAXgene Blood RNA tubes (*PreAnalytiX*). These tubes contain 6.9 ml of a liquid additive which stabilizes the cellular RNA profile in blood cells up to five days. After blood sampling, the tubes were stored at room temperature as recommended by the manufacturer. Total RNA isolation from blood samples was carried out on day three after blood sampling using the PAXgene Blood RNA Kit (*PreAnalytiX*) according to the manufacturer's protocol with two exceptions: Digestion of the proteins in the sample after addition of Proteinase K was carried out for 15 min (instead of 10 min) in a shaker-incubator, and subsequent centrifugation was performed for 10 min (instead of 3 min). Only 2 ml reaction tubes were used during the RNA isolation procedure. Because the RNA samples were planned to be analyzed by quantitative real-time PCR, a DNase digest was included by use of the RNase-Free DNase set (*Qiagen*) according to the protocol included in the PAXgene Blood RNA Kit.

### 3.8.6 Isolation of mRNA from peripheral blood mononuclear cells (PBMCs)

PBMCs were obtained from 4 ml peripheral whole blood which was collected in BD Vacutainer® CPT Cell Preparation Tubes with Sodium Citrate (*Becton Dickinson*). After separation of monocytes and lymphocytes (see chapter 3.9.9), mRNA was isolated from each of the two cell fractions using the µMACS mRNA Isolation Kit (*Miltenyi*) according to the manufacturer's protocol. The procedure is based on magnetic labeling of polyA-mRNA with MACS Oligo(dT) MicroBeads. After binding, bound mRNA is washed, eluted and may then serve for downstream applications.

### 3.8.7 Determination of the RNA concentration

The most commonly used technique for measuring nucleic acid concentration is the determination of absorbance at 260 nm ($A_{260}$). The major disadvantages of this method are the large relative contribution of proteins and free nucleotides to the signal, the interference caused by contaminants commonly found in nucleic acid preparations and the relative insensitivity of the assay (an $A_{260}$ of 0.1 corresponds to a 4 µg/ml RNA solution). The use of RiboGreen® RNA quantitation reagent alleviates many of these problems. It allows detection and quantification of small amounts of RNA without detecting proteins, free nucleotides or other contaminants.

### 3.8.7.1  Photometric RNA concentration analysis

The concentration of the RNAs isolated from fibroblast cultures treated with various drugs and from organotypic hippocampal rat brain slices treated with valproic acid was determined by measuring the absorption at a wave length of 260 nm on a photometer (*Eppendorf*). The absorption is expected to be 1 when measuring an aqueous dilution of single-stranded RNA with a concentration of 40 µg/ml using a cuvette with a path length of 1 cm (Current Protocols in Molecular Biology, 2001, Appendix A.3D.1). However, a concentration of 44 µg/ml is expected when measuring a dilution of RNA in 10 mM Tris-HCl. According to the manufacturer's protocol provided with the PAXgene Blood RNA Kit (*PreAnalytiX*), dilution of the RNA sample in RNase-free water may lead to inaccurately low values.
To determine the concentration of the RNA stocks, 1:16 dilutions with a final volume of 80 µl were prepared prior to photometric analysis. Purity of the RNA was determined by measuring the ratio of the absorption at 260 nm and the absorption at 280 nm. The ratio is recommended to range between 1.8 and 2.1. Higher values suggest presence of degraded RNA or free nucleotides, lower values point to contamination with protein. After measuring the background absorption of the solvent, the absorption of the RNA samples was determined and the concentration (in µg RNA / ml) calculated as follows: factor of the dilution x (absorption at 260 nm – background) x 44 µg. Measurements were performed in triplicates and the concentration calculated as mean of the single values.

### 3.8.7.2  Fluorimetric RNA concentration analysis with RiboGreen® dye

Fluorimetric determination of the exact RNA concentration was carried out on all RNA samples extracted from peripheral whole blood derived from controls, SMA carriers, and SMA type I, II, and III patients, on mRNA samples isolated from PBMCs, and on RNA samples isolated from fibroblast cultures used for siRNA transfection experiments. This method is ~1000fold more sensitive than photometric absorption measurement at 260 nm, and therefore more appropriate for the relatively small amounts of RNA isolated from the blood samples. Importantly, the concentration of RNA can be determined very precisely without detecting contaminants, proteins or free nucleotides. This is essential if normalization of target transcript numbers measured by real-time PCR is performed with the amount of total RNA used for reverse transcription. For fluorimetric measurement, the RiboGreen® RNA Quantitation Kit (*Molecular Probes*) was used according to the manufacturer's protocol. All samples were pre-treated with RNase-free DNase (see chapter 3.8.3 and 3.8.5) to ensure that the entire sample fluorescence is due to dye bound to RNA. The kit is using the phenomenon that RiboGreen is non-fluorescent when free in solution. Upon binding RNA, the fluorescence of the RiboGreen reagent increases more than 1000fold. The RNA bound to RiboGreen reagent has an excitation maximum of ~500nm and an emission maximum of ~525nm similar to Fluorescein. Based on an estimated RNA concentration of the samples ranging between ~40 to 150 ng/µl, the high-range assay and high-range standard curve were performed. The assay was set up in 96-well plates (FIA-Plate, Black, flat bottom, medium binding, #655076, *Greiner bio-one*). Fluorescence of the RNA-RiboGreen®-complexes was determined on a TECAN Safire[2] monochromator-based microplate

reader (*Tecan*). All RNA stocks were analyzed in triplicates and the concentration calculated as average of these measurements.

### 3.8.8    Reverse transcription (cDNA synthesis)

Reverse transcription is a tool to generate double-stranded complementary DNA (cDNA) from single-stranded RNA templates using an RNA-dependent DNA polymerase.

Each reverse transcription was performed in a 1.5 ml tube. The total reaction volume was 10 µl, containing an amount of 150 ng total RNA (or 8 ng mRNA), 5 µl RT mix (see chapter 3.4.1), 0.5 µl oligo-dT primer (0.5 mg/ml, *Operon*), 0.25 µl RNase Inhibitor (40 U/µl, *Invitrogen*), 0.25 µl Superscript II Reverse Transcriptase (50 U/µl, *Invitrogen*), and DEPC-treated $H_2O$. The reaction mix was incubated at 42 °C for 60 min and subsequently used for PCR. The use of oligo-dT primers allowed the specific reverse transcription of mRNA molecules. They are all characterized by a polyA-tail, providing the complementary sequence for oligo-dT primers.

### 3.8.9    Polymerase chain reaction (PCR)

The polymerase chain reaction (PCR) is a method which allows the enzymatic amplification of specific single-stranded DNA regions (Mullis and Faloona 1987). The reaction uses a DNA-dependent DNA polymerase which synthesizes copies from a denatured, single-stranded DNA template, starting from sequence specific oligonucleotides (primers). The primers specifically hybridize to the complementary sequence in the DNA template and are elongated at their free 3'-hydroxy group. The program of cycles including repeated DNA denaturation, primer hybridization, and DNA synthesis is performed in a thermocycler.

### 3.8.9.1  Analysis of gene expression by semi-quantitative multiplex PCR

During PCR, an increase of the amount of newly synthesized DNA can be observed. Theoretically, there should be a quantitative relationship between the amount of starting target sample and the amount of PCR product at any given cycle number. However, a basic PCR can be broken up into three phases. During the exponential phase, exact doubling of product is occurring with every cycle (assuming 100% reaction efficiency). The reaction is very specific and precise in all samples, all reagents are fresh and available. This phase is followed by the linear phase in which the PCR reaction already slows down, PCR components are being consumed as a result of amplification, and products start to degrade. In the linear phase, the PCR is not as precise anymore because the slow down of the reaction might be different among all samples. Thus, samples are not completely comparable anymore. During the final plateau phase, the reaction eventually has stopped, a saturation is reached, and a further increase of the DNA amount is barely visible. This is due to a lack of primers, nucleotides, and functionable DNA polymerase at higher PCR cycle numbers. Moreover, products

undergo degradation. Due to different reaction kinetics, each PCR sample will plateau at a different point, making a quantitative comparison impossible.

Thus, to compare samples in a semi-quantitative manner, the PCR has to be stopped at lower cycle numbers during the exponential phase. The optimal number of cycles depends on the respective template and the primer combinations and has to be determined for each PCR setup.

In addition, semi-quantitative PCR requires amplification not only of the target transcript (target cDNA), but also of a transcript (cDNA) derived from a gene which is assumed to be equally expressed in different samples. Such a gene is called housekeeping gene or endogenous control gene. The resulting PCR product serves as loading control and ensures that equal amounts of template have been used to compare the expression of target transcripts in different samples. The use of several primer pairs within one and the same PCR reaction is termed multiplex PCR.

After synthesis of cDNA, semi-quantitative multiplex PCR was performed on all samples derived from repeated experiments in different passages of each fibroblast cell line treated with various drugs. Each reaction was set up in a final volume of 25 µl, containing 12.2 µl deionized and autoclaved $H_2O$, 2.5 µl 10 x PCR buffer, 4 µl dNTP mix, a total volume of 2 µl primer working dilutions (target and endogenous control, see table 8), 0.3 µl Taq polymerase (5 U/µl, *Invitrogen*), and 4 µl of the cDNA generated as described in chapter 3.8.8. As endogenous control, the *glyceraldehyde-3-phosphate dehydrogenase* (*GAPDH*) *gene* was co-amplified in all PCR reactions. The PCR conditions were as follows: 95°C for 5 min, followed by 23 cycles to ensure quantitative PCR conditions before reaching saturation (95°C for 15 s, 55°C for 30 s, 72°C for 45 s), and final extension at 72°C for 10 min.

**Table 8: Primer combinations and amounts of the 10 pmol/µl primer working dilutions used for multiplex PCRs. For more details on primers, see chapter 3.5.**

| Amplified transcripts (target + endogenous control) | Numbers of forward and reverse primers | Volume of primer working dilutions |
|---|---|---|
| **FL-*SMN2*/Δ7-*SMN2*** | 1837 and 1841 | 1.7 µl each |
| **+** | | |
| ***GAPDH*** | 1879 and 1876 | 0.3 µl each |
| ***Htra2-β1*** | 1093 and 1094 / 1970 and 1971 | 1.7 µl each |
| **+** | | |
| ***GAPDH*** | 1879 and 1876 | 0.3 µl each |
| ***Htra2-β2*** | 1970 and 1986 | 1.8 µl each |
| **+** | | |
| ***GAPDH*** | 1879 and 1876 | 0.2 µl each |

### 3.8.9.2 Analysis of the number of genomic *SMN1* and *SMN2* copies by quantitative real-time PCR

Real-time PCR makes quantitation of genomic DNA or RNA (cDNA) easier and much more precise than traditional PCR (see also chapter 3.8.9.1). Real-time PCR detects the accumulation of amplicon

after each PCR cycle. Thus, for each PCR sample, the exponential, linear, and plateau phases are detected, summarized as amplification plot (amount of PCR product versus number of PCR cycles), and analyzed. Consequently, the exponential phase of each PCR reaction can be detected much more accurate than with traditional PCR and quantitative comparison of several samples is much more precise. Real-time PCR can be performed with a dye (SYBR Green I) that is non-fluorescent when free in solution, but forms fluorescent complexes with double-stranded PCR products. Another way to detect the amount of PCR product is the use of fluorescently labeled probes.

To characterize individuals regarding their *SMN1* and/or *SMN2* copy numbers, a quantitative test can be applied which includes the analysis of genomic DNA isolated from an EDTA blood sample by quantitative real-time PCR (Feldkötter et al. 2002). The procedure is based on the exact measurement of the DNA concentration of each sample. Each real-time PCR reaction contains an amount of 7.5 ng DNA with unknown *SMN1* or *SMN2* copy number. DNAs from individuals with a known number of *SMN1* or *SMN2* copies which are prepared in the same way as the unknown samples are used to create standard curves. The standard curve serves to determine the *SMN1* or *SMN2* copy number in the unknown DNA samples.

Prior to the measurement of the *SMN1* or *SMN2* copy number, the genomic DNA isolated from EDTA blood samples was stored at room temperature for five days to allow for complete dilution of the DNA in TE$^{-4}$ buffer. Subsequently, the DNA concentration was measured in triplicates on a photometer (*Eppendorf*) and a DNA dilution of 20 ng/µl was prepared. After storage of the 20 ng/µl dilution at room temperature for another 24h, this dilution was measured on a photometer (*Eppendorf* or *Peqlab*) and served for the preparation of two independent 5 ng/µl dilutions. They were analyzed by real-time PCR at least twice on a LightCycler 1.5 instrument (*Roche*) using the Fast Start DNA Master SYBR Green I Kit (*Roche*). Each single real-time PCR reaction was set up in a 20 µl LightCycler Capillary (*Roche*) and performed in a total volume of 10 µl, containing 4.3 µl H$_2$O, 1.2 µl 4 mM MgCl$_2$, 1.0 µl of each primer working dilution, 0.833 µl SYBR Green I reaction mix, 0.166 µl polymerase, and 1.5 µl of the 5 ng/µl DNA sample. Primers were able to distinguish between *SMN1* and *SMN2*, ending on or very close to the nucleotide differences between the two copies in exon 7 at position +6 and intron 7 at

**Table 9: Conditions for the analysis of the number of genomic *SMN1* and *SMN2* copies by quantitative real-time PCR.**

| PCR step | SMN1 | SMN2 |
|---|---|---|
| Heating | 95°C for 10 min | |
| Amplification | 95°C for 15 s | |
| | 58°C for 5 s | |
| | 72°C for 25 s | |
| | 76°C for 1 s | |
| Melting curve | 95°C for 15 s | |
| | 65°C for 15 s | |
| | Temperature increase to 85°C, hold for 0 s | |
| Cooling | 40°C for 30 s | |

position +214. For primer sequence and localization, see table 6 (*SMN1* primers: #1127 and #1133; *SMN2* primers: #1263 and #1268). Standard curves for *SMN1* or *SMN2* were performed using 1.5 µl of genomic DNA in concentrations of 1.25, 2.5, 5, and 7.5 ng/µl. The PCR conditions are given in table 9. The quantification program was followed by a melting step to detect the melting points for every PCR product. Analysis of the PCR curves was performed with the second derivative maximum method of the LightCycler software (*Roche*).

### 3.8.9.3 Analysis of gene expression by quantitative real-time PCR

According to the principles and advantages of real-time PCR explained in chapter 3.8.9.2, the comparative analysis of gene expression in a set of samples by real-time PCR is more exact than the application of semi-quantitative multiplex PCR. Moreover, real-time PCR is a high-throughput method which allows analysis of a large number of samples in a relatively short period of time. Thus, real-time PCR was applied to quantitatively investigate the expression of various transcripts in peripheral whole blood samples, in PBMCs, in the blood fractions included in the Human Blood Fractions MTC Panel (*Clontech*), and in fibroblast cells used for siRNA transfection experiments. The transcripts (cDNA templates) which have been amplified together with the primers and PCR conditions are given in table 10. For primer sequences and localization, see table 6.

**Table 10: Transcripts that were investigated by quantitative real-time PCR. For each transcript, the respective primer pair and the PCR conditions are given.**

| | FL-*SMN* | Δ7-*SMN* | GUSB | PPIB | B2M | RPLP0 | CTLA1 | Htra2-β |
|---|---|---|---|---|---|---|---|---|
| **Primer numbers** | 2075 2076 | 1449 1450 | 2937 2938 | 2935 2936 | 1967 1968 | 2939 2940 | 2048 2049 | 2690 2691 |
| **PCR conditions** | | | | | | | | |
| **Heating** | 95℃ for 10 min | | | | | | | |
| **Amplification** | 95℃,10s 62℃,10s 72℃,10s 78℃,1s | 95℃,10s 61℃,15s 72℃,12s 80℃,1s | 95℃,10s 69℃,12s 72℃,12s 82℃,1s | 95℃,10s 65℃,15s 72℃,12s 85℃,1s | 95℃,10s 61℃,15s 72℃,10s 76℃,1s | 95℃,10s 63℃,15s 72℃,12s 86℃,1s | 95℃,10s 60℃,15s 72℃,12s 82℃,1s | 95℃,10s 68℃,15s 72℃,12s 84℃,1s |
| **Melting curve** | 95℃,15s 65℃,15s 92℃,0s | 95℃,15s 65℃,15s 92℃,0s | 95℃,15s 65℃,15s 94℃,0s | 95℃,15s 65℃,15s 95℃,0s | 95℃,15s 65℃,15s 95℃,0s | 95℃,15s 65℃,15s 95℃,0s | 95℃,15s 65℃,15s 95℃,0s | 95℃,15s 65℃,15s 95℃,0s |
| **Cooling** | 40℃ for 30s | | | | | | | |

Samples were measured on a Lightcycler 1.5 machine (*Roche*) using the Fast Start DNA Master SYBR Green I Kit (*Roche*). Prior to analysis, cDNAs to be analyzed were diluted in TE$^{-4}$ buffer. For each amplified transcript (cDNA template), a standard curve was established using RNA prepared in the same way as the unknown samples. Reactions were performed in 20 µl LightCycler Capillaries (*Roche*) in a total volume of 10 µl, containing 2.8 µl $H_2O$ (Δ7-*SMN*: 1.3 µl), 1.2 µl 4 mM $MgCl_2$, 1.0 µl of

each primer working dilution, 0.833 µl SYBR Green I reaction mix, 0.166 µl polymerase, and 3.0 µl (Δ7-*SMN*: 4.5 µl) of the cDNA dilution. The quantification program was followed by a melting step to detect the melting points for every PCR product. Analysis of the PCR curves was performed with the second derivative maximum method of the LightCycler software (*Roche*). Correct identity of all PCR products was confirmed by sequencing (see chapter 3.8.13). Controls (RNA without reverse transcription step) were included to rule out any unspecific binding of primers to remaining DNA or RNA. All sample measurements were repeated at least twice and results are given as mean ± standard error of the mean (SEM).

### 3.8.9.4  Analysis of gene expression by one-step reverse transcription - quantitative real-time PCR

Reverse transcription of RNA into cDNA and quantitative real-time PCR using cDNA as template can be combined and performed in one and the same tube. Therefore, RNA is incubated with all reagents required for reverse transcription (including the reverse transcriptase) and all reagents required for subsequent PCR (including the DNA-dependent DNA polymerase). The reaction mix is incubated at conditions which allow the reverse transcriptase to become active and to synthesize cDNA. Then, by heating up the reaction mix, the reverse transcriptase is inactivated. Thereafter, the DNA-dependent DNA polymerase is activated and the quantitative real-time PCR takes place. One-step reverse transcription - quantitative real-time PCR is less time-consuming than separate reactions and minimizes pipette steps.

One-step reverse transcription - quantitative real-time PCR was performed on RNA samples derived from organotypic hippocampal rat brain slices treated with VPA. The TaqMan EZ RT-PCR Core Reagents Kit (*Applied Biosystems*) was used according to the manufacturer's protocol. Each reaction used 100 ng of total RNA, 300 nM primers and 100 nM probe. Rat *Smn* was amplified as the target transcript. In a separate reaction, rat *β-actin* was amplified as the endogenous control which was expected to be equally expressed in all of the samples. For probes, primer sequences, and primer localization, see table 6. Cycling conditions were 50 °C for 2 min, 60 °C for 30 min (reverse transcription step), 95 °C for 5 min followed by 40 cycles of 94 °C for 20 s and 60 °C for 1 min. Analysis of the real-time raw data and normalization of *Smn* data with *β-actin* data for each sample was performed using the Sequence Detection Software, version 1.7 (*Applied Biosystems*). All sample measurements were repeated at least twice and results are given as mean ± standard error of the mean (SEM).

### 3.8.10  Gel electrophoresis for separation of DNA fragments

Gel electrophoresis is based on the migration of charged molecules across the gel when an electric current is applied. The negative charge of DNA fragments is mainly due to the phosphate groups which are part of the alternating sugar-phosphate-backbone. Depending on their size, the DNA fragments will move differently through the gel matrix: short fragments will more easily fit through the

pores of the gel and migrate faster, while larger ones will have more difficulty and thus migrate slower. Additionally, the speed of migration depends on the current applied to the gel and the size of the pores of the gel. To separate DNA fragments which have different size, gel electrophoresis can be performed using an agarose gel matrix or a polyacrylamide (PAA) gel matrix.

### 3.8.10.1   Agarose gel electrophoresis

Whenever a new real-time PCR assay with new primers was developed to investigate the expression of a particular transcript (chapter 3.8.9.3), the real-time PCR product was sequenced (chapter 3.8.13) to confirm the correct identity before a large number of samples was analyzed with the new method. Therefore, the real-time PCR product was run on an 1.5% agarose gel to separate it from remaining PCR reagents like nucleotides and enzyme. An amount of 4.5 g agarose was dissolved in 300 ml TBE buffer by boiling in a microwave. After a short cool down and addition of 15 µl ethidium bromide solution (1%), agarose solution was transferred into a chamber supplied with an appropriate comb. After solidifying of the agarose solution, the gel was transferred to a gel electrophoresis chamber. TBE buffer was added, PCR samples were supplemented with DNA loading buffer and pipetted into the gel slots. Separation was carried out at 100 V for ~1 h. In a separate lane on the gel, a 100 bp DNA ladder (*Invitrogen*) was run together with the samples to estimate the length of the real-time PCR products. DNA fragments were finally visualized with UV light (wavelength 254 nm) on a ChemiDoc XRS Imaging system (*Biorad*).

### 3.8.10.2   Polyacrylamide (PAA) gel electrophoresis

PAA gel electrophoresis was performed to separate the PCR products in the samples derived from different passages of each fibroblast cell line treated with various drugs. PAA gels are formed by co-polymerization of acrylamide and N,N'-methylenbisacrylamid. Polymerization is initiated by ammonium persulfate and TEMED: TEMED accelerates the rate of formation of free radicals from persulfate, and these in turn catalyze polymerization. The persulfate free radicals convert acrylamide monomers to free radicals which react with unactivated monomers to begin the polymerization chain reaction (Shi and Jackowski 1998). The elongating polymer chains are randomly crosslinked, resulting in a gel in which the pore size depends on the polymerization conditions and monomer concentrations. In this work, only native 10% PAA gels (without urea) were prepared between glass plates (supplied with an appropriate comb) using 20 ml PAA gel stock solution and 200 µl APS to start polzmeriyation. After solidifying, the glass plates with the gel in between were transferred to a gel electrophoresis chamber. TBE buffer was added, PCR samples were supplemented with DNA loading buffer and inserted into the gel slots. Separation was carried out at 20 mA for ~3 h. In a separate lane on the gel, a 100 bp DNA ladder (*Invitrogen*) was run together with the samples to estimate the length of the PCR products. After electrophoresis, PAA gels were stained in 100 ml TBE buffer supplemented with 15 µl ethidium bromide solution (1%) for 30 min. DNA fragments were finally visualized with UV light (wavelength 254 nm) on a Gel Doc 2000 Imaging system (*Biorad*).

### 3.8.11   Densitometric analysis of DNA bands

Densitometric analysis of the separated PCR products obtained from the samples derived from repeated drug treatment of fibroblast cell lines was carried out using the ONE-DScan program (*Scanalytics*) and the gel scans obtained from the Gel Doc 2000 Imaging system (see chapter 3.8.10.2). With the help of the ONE-DScan program, a densitometric value was calculated for each single PCR band. Resulting data are given as mean (average of repeated experiments) ± SEM.

### 3.8.12   Extraction of DNA from agarose gels

Prior to sequencing of PCR products separated on a 1.5% agarose gel, bands were visualized with UV light (wave length 302 nm), cut with a scalpel, and the piece of gel containing the respective PCR product was transferred to a 2 ml reaction tube. Extraction of the PCR product was carried out according to the manufacturer's protocol out using the QIAquick Gel Extraction Kit (*Qiagen*). DNA was eluted from the column with deionized autoclaved $H_2O$.

### 3.8.13   Automatic, non-radioactive sequencing of DNA (Sanger 1977)

DNA was sequenced with chain-terminating inhibitors (Sanger et al. 1977) using the BigDye® Terminator v1.1 Cycle Sequencing Kit (*Applied Biosystems*). Each sequencing reaction contained ~30 ng PCR product to be sequenced, 3 µl 5 x sequencing buffer, 1 µl primer working dilution, 1 µl reaction mix and deionized, autoclaved $H_2O$ to a final volume of 20 µl. Cycle sequencing was performed on a thermocycler using the following conditions: 95 °C for 30 s, followed by 25 cycles of 95 °C for 10 s, 50 °C for 5 s, and 60 °C for 4 min. The annealing temperature was set up to 50 °C which is low enough to be universal for all primers used. The separation of the fragments which were synthesized throughout the cycle sequencing was performed on an ABI 3730 sequencer machine (*Applied Biosystems*). Results were analyzed using the Finch TV or BioEdit software.

## 3.9      Proteinbiochemical and immunological methods

### 3.9.1   Extraction of proteins from primary fibroblast cell cultures

After incubation of different passages from each fibroblast line with various drugs, the culture medium was removed, and cells were washed twice in 1 x PBS buffer. Thereafter, fibroblasts in each petri dish were lysed by addition of 50 µl RIPA buffer. Dishes were kept on ice for 20 min to complete lysis. Subsequently, cell lysates were harvested, transferred to 1.5 ml reaction tubes, and protein extracts prepared by centrifugation at 4 °C and 12,000 rpm for 20 min. The pellet containing cell debris was discarded, and the supernatant containing the protein was frozen at -80 °C.

Fibroblasts used for siRNA experiments underwent a similar protocol for protein extraction. After pooling and aliquoting the cells, a volume of 20 μl RIPA buffer was used for each cell pellet obtained from the respective well of the culture plate.

### 3.9.2    Extraction of proteins from organotypic hippocampal slice cultures (OHSCs) from rat

Proteins were extracted from rat OHSCs by homogenization of three pooled slices for each experiment in 100 μl lysis buffer containing 50 mM Tris (pH 8.0), 150 mM NaCl, 1% Triton-X 100, 1 mM EDTA (pH 8.0), 0.1% SDS, 1 mM PMFS, and 1 pill Complete-Mini (*Roche*) per 10 ml. After lysis, samples were centrifuged at 4 °C and 12,000 rpm for 20 min. The pellet containing cell debris was discarded, and the supernatant containing the protein was frozen at -80 °C.

### 3.9.3    Extraction of proteins from peripheral blood mononuclear cells (PBMCs)

An amount of 4 ml peripheral whole blood was collected in BD Vacutainer® CPT Cell Preparation Tubes with Sodium Citrate (*Becton Dickinson*). Tubes are intended for the collection of whole blood and the separation of mononuclear cells. The cell separation medium is comprised of a polyester gel and a density gradient liquid. This configuration permits cell separation during a single centrifugation step.

Tubes were centrifuged at room temperature and 1500-1800 x g for 20 min. After aspiration of the plasma layer, the layer containing lymphocytes and monocytes (peripheral blood mononuclear cells, PBMCs) was collected with a Pasteur pipette, transferred to a 15 ml Falcon tube, and PBS was added to a final volume of 10 ml. Tubes were inverted 5 times, and centrifuged at 430 x g for 15 min. Supernatant was aspirated, and the cell pellet washed by addition of 10 ml PBS and centrifugation at 430 x g for another 10 min. To the resulting cell pellet, 50 μl RIPA buffer were added. Tubes were kept on ice for 20 min to complete lysis. Subsequently, cell lysates were transferred to 1.5 ml reaction tubes, and protein extracts prepared by centrifugation at 4 °C and 12,000 rpm for 20 min. The pellet containing cell debris was discarded, and the supernatant containing the protein was frozen at -80 °C.

### 3.9.4    Protein contents determined according to the Bradford method

The quantitative determination of the protein concentration was carried out according to the method described by Bradford (Bradford 1976). The method is based on different absorption maxima of unbound Coomassie Brilliant Blue G250 and Coomassie Brilliant Blue G250 which is bound to proteins.

A volume of 2 μl (siRNA experiments: 1 μl) of each protein sample to be analyzed was incubated in 500 μl (siRNA experiments: 100 μl) Bradford solution for 15 min. Subsequently, absorption of the samples was measured at a wavelength of 595 nm. To calculate the protein concentrations in the unknown samples, values obtained for absorption were compared to the values obtained from a standard curve which was prepared from bovine serum albumin (BSA).

### 3.9.5    Discontinuous denaturing polyacrylamide gel electrophoresis (SDS-PAGE)

The separation of proteins in denaturing polyacrylamide gels occurs primarily by length (primary protein structure, number of amino acids) because the use of the anionic detergent SDS linearizes the proteins and applies a negative charge to each protein in proportion to its mass (Laemmli 1970). Without SDS, different proteins with similar molecular weights would migrate differently due to differences in folding, as differences in folding patterns would cause some proteins to better fit through the gel pores than others.

In a first step, the 12% PAA separation gel was prepared between two glass plates (distance 0.5 mm). 70% ethanol was added on top of the gel until solidification. After polymerization, the ethanol was removed and the stacking PAA gel was added on top of the separation gel between the two glass plates. The stacking gel contains less PAA than the separation gel which results in larger gel pores. Moreover, the stacking gel is prepared with a Tris-buffer that differs from the Tris-buffer used for the separation gel in its concentration and pH. The main function of the stacking gel is to focus all of the proteins into a single sharp band shortly after penetration into the gel. Proteins are then resolved in the separation gel which possesses much smaller pores. As soon as an electric current is applied across the gel, the negatively charged proteins start to migrate. Short proteins will more easily fit through the pores in the gel, while larger ones will have more difficulty and migrate slower. The usage of a system with discontinuous buffers and gel pores enhances the sharpness of the protein bands.

Before 7.5 µg of each protein sample were transferred into the slots of the PAA gel, samples were supplemented with Laemmli buffer and boiled at 95℃ for 5 min to enhance denaturation. In a separate lane, marker proteins of known molecular weight were run (Precision Plus Protein All Blue Standards, *Biorad*) to estimate the molecular weight of the unknown proteins in the samples. Gel electrophoresis was performed at 60-80 V in an electrophoresis chamber using 1 x electrophoresis buffer.

### 3.9.6    Transfer of proteins to nitrocellulose membrane by wet blotting (western blot)

To make proteins available for antibody detection, they were moved from within the gel onto a nitrocellulose membrane [Protran BA 83 Cellulosenitrat (E), *Whatman*]. The membrane was equilibrated in transfer buffer, placed face-to-face with the gel, and a gel sandwich was prepared together with two fiber pads and two filter pads all soaked in transfer buffer. The gel sandwich was put into a cassette which then was placed into a module of a Mini Trans-Blot Cell (*Biorad*). Additionally, a frozen cooling unit and transfer buffer were added to the Trans-Blot Cell. Wet blotting was carried out at a current of 30 V overnight. Thus, charged proteins moved onto the membrane while maintaining the organization they had within the gel. As a result of this blotting process, proteins were exposed on a thin surface layer for detection.

### 3.9.7 Ponceau staining of proteins on nitrocellulose membranes

After wet blotting overnight, correct protein transfer was checked by incubation of the membrane in Ponceau solution for 30 s. Subsequently, the membrane was washed in TBS Tween buffer several times to remove Ponceau dye again.

### 3.9.8 Immunostaining of membranes with antibodies and detection of signals with chemiluminescence reagent

Nitrocellulose membranes bind proteins non-specifically. Interactions between the membrane and the antibodies used for detection were prevented by blocking the membrane in 6% blocking solution containing non-fat dry milk for 3 h (after Ponceau staining). Subsequently, the membrane was probed with the primary antibody diluted in 10 ml 1-2% non-fat dry milk in TBS Tween. The primary antibody binds the target protein directly. This was followed by 5 x 5 min washing steps in TBS Tween to remove unbound primary antibody, exposure to the secondary antibody diluted in 10 ml 1-2% non-fat

**Table 11: Conditions used to probe nitrocellulose membranes with primary and secondary antibodies.**

| Primary antibody | Dilution and incubation time |
|---|---|
| anti-SMN, monoclonal mouse (*BD Transduction Laboratories*) | 1:5,000 for 1 h<br>1:1,000 for 1 h (blots with carrier proteins) |
| anti-β-Tubulin, monoclonal mouse (*Sigma*) | 1:2,000 for 1 h |
| anti-Htra2-β1, polyclonal rabbit (Hofmann et al. 2000) | 1:1,000 for 1 h |
| anti-SF2/ASF, monoclonal mouse (*kindly provided by A. Krainer, Cold Spring Harbor Laboratories*) | 1:200 for 4 h |
| anti-SRp20, monoclonal mouse (*Santa Cruz*) | 1:100 for 24 h |
| anti-β-Actin, monoclonal mouse (*Sigma*) | 1:5,000 for 1 h<br>1:40,000 for 1 h (blots with carrier proteins) |
| **Secondary antibody** | **Dilution and incubation time** |
| Goat anti-mouse IgG, peroxidase-conjugated (*Dianova*) | 1:2,500 for 1 h |
| Goat anti-rabbit IgG, peroxidase-conjugated (*Pierce*) | 1:10,000 for 1 h |

dry milk in TBS Tween, and another 5 x 5 min washing steps in TBS Tween to remove unbound secondary antibody. The secondary antibody was linked to a reporter enzyme (horseradish peroxidase) and binds to the primary antibody. The conditions used for incubation of the membrane with various primary and secondary antibodies are given in table 11. Detection of the probes that are

labeled and bound to the protein of interest was performed via chemiluminescent detection. Western blots were incubated with 8 ml SuperSignal® West Pico Chemiluminescent Substrate (*Pierce*) for 5 min. This is a substrate which will fluoresce when exposed to horseradish peroxidase on the secondary antibody. The light was then detected by photographic film (Hyperfilm ECL, *Amersham*) and the image analyzed by densitometry to evaluate the relative amount of protein staining and to quantify the results in terms of optical density. Western blot results obtained from different passages of each fibroblast line treated with various drugs and from triplicates of siRNA transfection experiments are given as mean ± standard error of the mean (SEM).

### 3.9.9    Separation of monocytes and lymphocytes from peripheral whole blood by magnetic cell sorting (MACS)

An amount of 4 ml peripheral whole blood was collected in BD Vacutainer® CPT Cell Preparation Tubes with Sodium Citrate (*Becton Dickinson*). Within two hours after blood drawing, tubes were centrifuged at room temperature and 1500-1800 x g for 20 min. After aspiration of the plasma layer, the layer containing lymphocytes and monocytes (peripheral blood mononuclear cells, PBMCs) was collected with a Pasteur pipette, transferred to a 15 ml Falcon tube, and PBS was added to a final volume of 10 ml. Tubes were inverted 5 times, and centrifuged at 430 x g for 15 min. Supernatant was aspirated, the cells were suspended in 10 ml of PBS and counted. After centrifugation at 430 x g for another 10 min, cell pellet was suspended in MACS buffer (80 µl buffer for each $1 \times 10^7$ PBMCs). Subsequently, the fraction of monocytes was separated by magnetic labeling using CD14 MicroBeads (*Miltenyi*) according to the manufacturer's protocol. The beads are conjugated to a monoclonal mouse antibody against the human protein CD14 which is only present on monocytes but not on other PBMCs. After binding of monocytes to the beads, lymphocytes are obtained in the column flow-through. Purity of the two cell fractions was checked by flow cytometry (see chapter 3.9.11).

### 3.9.10   Immunohistochemistry staining of peripheral blood mononuclear cells (PBMCs)

An amount of 4 ml peripheral whole blood was collected in BD Vacutainer® CPT Cell Preparation Tubes with Sodium Citrate (*Becton Dickinson*). Tubes were centrifuged at room temperature and 1500-1800 x g for 20 min. After aspiration of the plasma layer, the layer containing lymphocytes and monocytes (peripheral blood mononuclear cells, PBMCs) was collected with a Pasteur pipette, transferred to a 15 ml Falcon tube, and PBS was added to a final volume of 10 ml. Tubes were inverted 5 times, and centrifuged at 430 x g for 15 min. Supernatant was aspirated, the cells were suspended in 10 ml of PBS and counted. After centrifugation at 430 x g for another 10 min, cell pellet was suspended in PBS to obtain a concentration of $2.5 \times 10^6$ cells / ml.

Cells were fixed and permeabilized using the Fix&Perm Cell Permeabilization Kit (*Caltag*). 100 µl cell suspension were incubated with 100 µl fixation medium for 15 min. After centrifugation at 430 x g for 5 min, washing with FACS buffer and centrifugation at 430 x g for 5 min, the cell pellet was suspended in 100 µl permeabilization medium. Addition of 2 µg anti-SMN FITC-conjugated antibody (*BD*

*Transduction Laboratories*) or 2 µg of the isotype control (mouse IgG$_1$ FITC-conjugated, *Becton Dickinson*) to check for background staining was followed by short vortexing and incubation at 2-8°C for 1 h. Subsequently, cells were centrifuged at 430 x g for 5 min, the pellet was washed once with FACS buffer, and then reconstituted with 0.2 ml FACS buffer. An aliquot was transferred onto a microscope slide together with DAPI-Mounting-Medium (*Vector*) to stain cell nuclei and analyzed on an Axioskop 2 fluorescence microscope (*Zeiss*).

### 3.9.11   Analysis of peripheral blood mononuclear cells (PBMCs) by flow cytometry

Isolation of PBMCs was carried out as described in chapter 3.9.10. After adjusting the cell suspension to a concentration of 2.5 x 10$^6$ cells / ml, cells were fixed (and permeabilized for SMN stainings) using the Fix&Perm Cell Permeabilization Kit (*Caltag*). After pipetting 0.125 µg PE-conjugated anti-CD14 (*Becton Dickinson*) and 0.125 µg PerCP-conjugated anti-CD45 (*Becton Dickinson*) into a FACS tube, 100 µl cell suspension were added and the tubes vortexed and incubated in the dark for 15 min. To set up parameters for analysis on the flow cytometer and to check background staining, one sample was incubated with the respective isotype controls (0.125 µg PE-conjugated IgG$_{2a}$ and 0.125 µg PerCP-conjugated IgG$_1$, *Becton Dickinson*). CD14 and CD45 are surface markers present on PBMCs. While CD45 is found on monocytes and lymphocytes, CD14 is present exclusively on monocytes. The antibodies are labeled with different dyes which allow for differentiation of the cell fractions by flow cytometry. Subsequently, 100 µl fixation medium were added followed by incubation for 15 min. Cells were centrifuged at 430 x g for 5 min, washed with FACS buffer and again centrifuged at 430 x g for 5 min. To check the purity of the fractions after separation of monocytes and lymphocytes (chapter 3.9.9), the cell pellet was reconstituted with 0.2 ml FACS buffer and measured on a FACScalibur flow cytometer (*Becton Dickinson*). For SMN protein analysis, cell pellet was suspended in 100 µl permeabilization medium. Addition of 2 µg anti-SMN FITC-conjugated antibody (*BD Transduction Laboratories*) or 2 µg of the isotype control (mouse IgG$_1$ FITC-conjugated, *Becton Dickinson*) to check for background staining was followed by short vortexing and incubation at 2-8°C for 1 h. Subsequently, cells were centrifuged at 430 x g for 5 min, the pellet was washed once with FACS buffer, reconstituted with 0.2 ml FACS buffer and measured on a FACScalibur flow cytometer (*Becton Dickinson*). To compare SMN measurements at different time points, Sphero Rainbow Calibration Particles (8 peaks, 3.0 – 3.4 µM, *Becton Dickinson*) were used to perform a standard curve together with each SMN analysis. Rainbow beads are a mixture of particles that are dyed to eight different fluorescent intensities and may be used for the calibration of flow cytometers.

### 3.9.12   Analysis of pmaxGFP-transfected fibroblasts by flow cytometry

Fibroblasts were harvested 24 h after transfection, transferred to a FACS tube, washed once with PBS, centrifuged at 1200 rpm for 10 min, washed once with FACS buffer, and centrifuged again at 1200 rpm for 10 min. Subsequently, the cell pellet obtained from one well of a 6-well plate was reconstituted with 0.2 ml FACS buffer and analyzed on a FACScalibur flow cytometer (*Becton*

*Dickinson*). Due to similar emission maxima, GFP fluorescence was detected in the channel commonly used for the detection of green FITC fluorescence.

## 3.10 Specific methods applied to evaluate the *in vivo* effect of valproic acid in human subjects

### 3.10.1 Pilot trial with SMA carriers

#### 3.10.1.1 Recruitment of probands

Initially, 17 SMA carriers (parents of patients with SMA) were recruited for participation in the VPA pilot trial. The project was approved by the local Ethics Committee of the University of Bonn (Approval number 13804) and written informed consent was obtained from each subject according to the Declaration of Helsinki. Because it is well known that VPA is teratogenic in the first trimester of pregnancy, only males and postmenopausal women were included. Each of the recruited SMA carriers (13 males, four postmenopausal or sterilized females; mean age ± SD: 47.3±9.3 years) presented 1 *SMN1* copy and 1-3 *SMN2* copies as determined by real-time quantitative PCR described in chapter 3.8.9.2. A number of five potential probands had to be rejected since they did not meet the strict inclusion criteria of normal blood values before drug treatment: four subjects revealed slightly elevated GPT and/or GGT levels above the normal range and one individual was diagnosed with Gilbert's syndrome. Based on the fact that VPA rarely causes severe side effects involving liver and pancreas function, only SMA carriers with normal liver function values were included in the protocol.

#### 3.10.1.2 Design of the pilot trial

The remaining eight heterozygous men and four heterozygous women were enrolled in the study. Drug treatment was started with an initial dose of 300 mg/day VPA (Ergenyl® chrono 300, *Sanofi-Synthelabo*). Probands were seen every two weeks and, by gradually increasing the administered VPA dose up to 1200–1800 mg/day, VPA serum levels were individually adjusted to 70–100 mg/l. This is the therapeutic range for epilepsy treatment. After maintaining serum levels at 70–100 mg/l for about five weeks, VPA dose was gradually decreased and medication finally discontinued. Another two probands (one male and one female) quit the study prior to reaching the final VPA serum level due to compliance problems and leg edema, respectively. Consequently, results from a total number of ten carriers finally served as basis for evaluating the study outcome. For clarification: Throughout this thesis, the common term "valproic acid" and the corresponding abbreviation "VPA" are used. However, all *in vivo* investigations in SMA carriers were carried out with sodium valproate which is the active agent in Ergenyl® chrono 300.

### 3.10.1.3 Blood sampling

For analysis of gene expression under VPA treatment, peripheral whole blood was collected from each participant using the PAXgene blood RNA system (*PreAnalytiX*). The first three blood samples were taken prior to VPA medication. In order to evaluate baseline transcript levels, the three measurements for each transcript were averaged and set to 1.0 corresponding to 100%. Blood sampling was then continued throughout the VPA dose escalation period, followed by three samples taken while VPA serum levels were determined to be in the therapeutic range. A final sample was collected from each carrier several weeks after discontinuing VPA medication. All measured values were calculated as multiples of 1.0.

In addition, 9/10 carriers agreed to donate an additional amount of 4 ml peripheral whole blood for SMN protein analysis. From each of these individuals, blood was taken once before VPA treatment and once under therapeutic VPA serum levels and collected in BD Vacutainer® CPT Cell Preparation Tubes with Sodium Citrate (*Becton Dickinson*).

### 3.10.2 Individual experimental curative approaches in SMA patients

### 3.10.2.1 Patient collective

Blood samples in PAXgene blood RNA tubes (*PreAnalytiX*) were obtained from five patients with type I (four males, one female; mean age ± SD: 1.6±0.9 years), 11 patients with type II (seven males, four females; mean age ± SD: 10.3±7.1 years), and four patients with type III SMA (three males, one female; mean age ± SD: 20.8±6.9 years) treated with VPA in individual experimental curative approaches throughout Germany according to section 41 of the German Drug Act (AMG). Informed written consent for genetic analysis of samples was given by all subjects or their legal guardians. All of these patients presented homozygous absence of *SMN1* and varying numbers of *SMN2* copies measured by real-time quantitative PCR as described in chapter 3.8.9.2.

### 3.10.2.2 Blood sampling

In each of the individual experimental curative approaches described above, analysis of FL- and Δ7-*SMN2* mRNA levels was carried out in a total of five blood samples. We obtained two samples taken before VPA treatment within a time period of several weeks allowing us to determine transcript baseline levels by averaging the two measurements and setting the mean to 1.0 corresponding to 100%. Then, at intervals of about four weeks, we received another three samples under drug treatment together with the corresponding VPA serum level. All determined values were calculated as multiples of 1.0.

## 3.11    Statistical methods

A directional student's t-test for uncorrelated samples was carried out to check for differences between data obtained from mock-treated and drug-treated cell cultures and organotypic hippocampal slice cultures, respectively. The same statistical test was applied to evaluate the significance of knocked down RNA and protein levels after siRNA treatment of fibroblasts. A non-directional student's t-test for uncorrelated samples was performed to compare the FL-*SMN2* transcript level, the Δ7-*SMN2* transcript level, and the FL / Δ7 ratio in siRNA-treated cells, the corresponding mock, and the negative siRNA control.

To analyze the differential expression of genes in lymphocytes and monocytes, a non-directional student's t-test for uncorrelated samples was applied.

In all cases, three levels of statistical significance were distinguished: $p<0.05$, $p<0.01$, and $p<0.001$. Significant differences are indicated with different numbers of asterisks within the respective figures and/or are given within the text.

Analysis of variance (ANOVA, F-test) was carried out to check for differences between untreated controls, carriers and SMA types I, II, and III regarding their baseline FL- and Δ7-*SMN* transcript levels and the FL/Δ7-*SMN* ratios. A significant ANOVA ($p<0.05$) was followed by a post-hoc analysis applying the Tukey-Kramer procedure (multiple pairwise comparisons of data sets containing unequal sample sizes). Post-hoc analysis distinguished three levels of statistical significance: $p<0.05$, $p<0.01$ and $p<0.001$. Significant differences are given within the text.

To evaluate the significance of increased/decreased *SMN* transcript levels in each single carrier and SMA patient treated with VPA, individual data were subdivided into values without drug treatment and values obtained under drug therapy. Subsequently, the two data groups were compared by analysis of variance (ANOVA for two data groups, equivalent to a non-directional t-test with $F=t^2$). Statistically significant values were considered $p<0.05$. Significant differences are given within the text.

# 4      Results

Proximal spinal muscular atrophy (SMA) results from homozygous loss of the *survival motor neuron gene 1* (*SMN1*) and pathological splicing of the remaining *SMN2* copy genes. Consequently, SMA patients suffer from a lack of functionable full-length (FL)-SMN protein which results in degeneration of the α-motor neurons in the anterior horns of the spinal cord, subsequently leading to progressive muscle weakness and atrophy. Each SMA patient retains one or more *SMN2* genes. The number of *SMN2* copies inversely correlates with the disease severity.

One of the major challenges in SMA research is to increase the level of FL-*SMN2* transcripts/FL-SMN2 protein derived from the *SMN2* gene. This goal might be achieved by stimulating the transcriptional activity of *SMN2* and/or by correcting the *SMN2* splicing pattern.

In 2001, it was demonstrated for the first time that treatment of EBV-transformed lymphoblastoid cell lines derived from SMA patients with a compound, sodium butyrate, results in elevated FL-*SMN2* transcript and FL-SMN2 protein levels (Chang et al. 2001). Moreover, butyrate treatment prolonged the survival of SMA transgenic mice (*Smn*^{-/-}, *SMN*2). It was suggested that butyrate exerts its effects on *SMN2* expression through the inhibition of histone deacetylases (HDACs). However, the striking disadvantage of butyrate is its very short terminal half-life of only 6 min in human serum, which makes the drug inadequate for SMA therapy.

Independently, valproic acid (VPA) was identified as a powerful HDAC inhibitor with anti-cancer activity in 2001 (Gottlicher et al. 2001). In contrast to butyrate, VPA is a well-known FDA-approved drug with a terminal half-life of 9-18 hours in human serum. The compound has successfully been used in long-term epilepsy therapy for more than three decades. Interestingly, both drugs butyrate and VPA not only share the ability to inhibit HDACs, but they also have similar chemical structures that assign them to the class of short-chain fatty acids. Hypothesizing a connection between the chemical structure of butyrate, it's inhibitory effect on HDACs and the elevated levels of FL-*SMN2* RNA and protein in butyrate-treated lymphoblastoid cell lines, we assumed that the closely related compound VPA could show a similar impact on *SMN2* expression and started to investigate the drug in cell cultures *in vitro*.

## 4.1     *In vitro* experiments with histone deacetylase (HDAC) inhibitors in cell lines derived from SMA patients

### 4.1.1    Treatment of EBV-transformed lymphoblastoid cell cultures with valproic acid

EBV-transformed lymphoblastoid cell lines can be obtained without difficulty from human EDTA blood samples. The cultures are relatively easy to maintain and show rapid growth. In Dr. Brunhilde Wirth's laboratory, a large number of EBV-transformed cell lines are available. To check whether VPA is able to regulate FL-SMN2 protein expression, four different EBV-cell lines were selected for treatment with the compound: cell line B6100a (SMA I, 3 *SMN2* copies), cell line T56/91 (SMA I, 1 *SMN2* copy), cell

line BW332 (SMA IIIb, 3 *SMN2* copies), and cell line BW231 (SMA I, 1 *SMN2* copy). In parallel, experiments were set up to incubate these cell lines with butyrate. Since it had been demonstrated already that butyrate has an impact on SMN2 expression in EBV cell lines (Chang et al. 2001), these experiments served as positive control. The conditions used for drug treatment were based on those which had revealed best results for histone hyperacetylation and anticancer activity of VPA (Gottlicher et al. 2001) and for the regulation of *SMN2* expression with butyrate [(Chang et al. 2001) and personal communication Jan-Gowth Chang], respectively.

The selected EBV cell lines were treated with solvent, 50, 500, and 1000 µM VPA for 16 and 24 h or with solvent, 5, 10, 50, 500, 1000, 2000, 3000, 5000, and 10000 µM butyrate for 16 and 24 h. For each drug concentration, various cell numbers were tested: $2x10^5$ cells/2 ml culture medium, $4x10^5$ cells/4 ml culture medium, $1x10^6$ cells/2 ml or 5 ml culture medium, $1.5x10^6$ cells/2 ml or 5 ml culture medium, and $2x10^6$ cells/2 ml or 5 ml culture medium. The respective drug was added dropwise either immediately after cell counting or 6 to 24 h later. After incubation of the cultures with butyrate or VPA, cells were harvested. Since the ultimate goal of the experiments was an increase of the SMN2 protein level, protein extracts were prepared for analysis, and western blots were performed to stain the SMN protein and β-tubulin. The protein β-tubulin was assumed to be similarly expressed in all cells and therefore served as control to confirm loading of equal protein amounts onto the nitrocellulose membrane. However, regardless of the experimental conditions and despite of multiple repetition of each set up, neither the positive control experiments carried out with butyrate nor the experiments performed with VPA revealed an up-regulation of the SMN protein level (data not shown).

## 4.1.2    Treatment of SMA fibroblast cultures with valproic acid

It has been clearly demonstrated that butyrate is able to stimulate FL-*SMN2* expression in EBV-transformed lymphoblasts (Chang et al. 2001). However, the results could not be reproduced, suggesting that the experimental conditions did not meet all of the requirements. Consequently, a conclusion regarding the ability of VPA to exert an effect on SMN2 expression could not be drawn from the experiments performed in lymphoblastoid cell lines either. Therefore, a different strategy was applied to investigate a potential impact of VPA on SMN2 expression *in vitro*. Besides of EBV-transformed lymphoblastoid cell lines, primary fibroblast cell lines derived from SMA patients were available in the laboratory. These cell lines are obtained from skin biopsies, are also relatively easy to maintain, and show medium to rapid growth as adherent cultures. Several fibroblast cell lines from SMA patients were selected and used for drug treatment experiments.

### 4.1.2.1 Impact of valproic acid on SMN2 protein levels

Fibroblast cultures from three SMA patients with homozygous absence of *SMN1* were used to determine the influence of VPA on *SMN2* expression. One of the cell lines is derived from a type I SMA patient with two *SMN2* copies (ML-17), another cell line is from a type I SMA patient with three *SMN2* copies (ML-16), and the third selected fibroblast line is from a type II SMA patient with three

*SMN2* copies (ML-5). Again, the conditions used for the treatment of the cells with VPA were based on those which had revealed best results for histone hyperacetylation and anticancer activity of VPA (Gottlicher et al. 2001). Moreover, the drug concentrations should cover a broad range which is well tolerated by the cells and not toxic. Thus, fibroblast cultures were treated with solvent (mock) or 0.5, 5, 50, 500, and 1000 $\mu$M of VPA for 16 h. The optimal time period of treatment (16h) was evaluated by a time course experiment which covered 12, 16, 24, 36 and 48 h. The result correlated well with the maximum histone acetylation in F9 teratocarcinoma cells and HeLa cells observed ~12-16 h after addition of VPA (Gottlicher et al. 2001).

Protein extracts of untreated (mock) and treated fibroblasts were analyzed by western blotting. In a first step, all blots were verified for equal amounts of loaded protein by staining with an anti-*β*-tubulin antibody. In a second step, nitrocellulose membranes were probed with anti-SMN antibody. After VPA treatment, in each of the investigated fibroblast lines a significant up-regulation of the SMN protein level was observed with highest values ranging between 2.7-fold and 3.3-fold compared to untreated cells (mock). Mean values ± SEM for SMN protein levels relative to β-tubulin obtained from the treatment of three different passages of each fibroblast line with increasing amounts of VPA are summarized in table 12 and presented as bar graphs in figure 8 A-C. Additionally, representative western blots for each VPA-treated fibroblast culture are presented in figure 8 A-C.

In each fibroblast line, the cumulative data from repeated drug treatment experiments revealed a peak of the SMN protein level either at 5 µM VPA (ML-16), at 50 µM VPA (ML-17) or at 500 µM VPA (ML-5), but never at 1000 µM VPA. In ML-17 and ML-5, the peak is followed by a slight decrease of the SMN protein level under increasing concentrations of VPA. In ML-16, a fluctuation was visible. After reaching a maximum at 5 µM VPA, the SMN protein level decreased at 50 µM VPA. At 500 µM, a second maximum was obtained, followed by another decrease at 1000 µM VPA. Importantly, even the lowest concentration of VPA used (0.5 $\mu$M) still increased the SMN protein level 1.6-fold to 2.3-fold in each treated fibroblast culture (figure 8A-C, table 12).

**Table 12: SMN protein levels (relative to β-tubulin) in SMA fibroblasts after VPA treatment. Average data (± SEM) from repeated experiments are shown and highest levels are marked in bold.**

| Human SMA fibroblast | | Concentration of VPA (µM) | | | | | |
|---|---|---|---|---|---|---|---|
| culture | | Mock | 0.5 | 5 | 50 | 500 | 1000 |
| **ML-17** | (SMA I, 2 *SMN2* copies) | 1.0±0.0 | 1.6±0.1 | 1.8±0.2 | **2.7±0.1** | 2.3±0.3 | 2.4±0.3 |
| **ML-16** | (SMA I, 3 *SMN2* copies) | 1.0±0.0 | 2.1±0.3 | **3.1±0.6** | 2.2±0.3 | 2.9±0.4 | 2.2±0.4 |
| **ML-5** | (SMA II, 3 *SMN2* copies) | 1.0±0.0 | 2.3±0.6 | 2.7±0.7 | 2.8±0.9 | **3.3±0.8** | 2.6±0.6 |

**A**



fibroblast line ML-17

(SMA I, 2 *SMN2* copies)

**B**



fibroblast line ML-16

(SMA I, 3 *SMN2* copies)

**C**



fibroblast line ML-5

(SMA II, 3 *SMN2* copies)
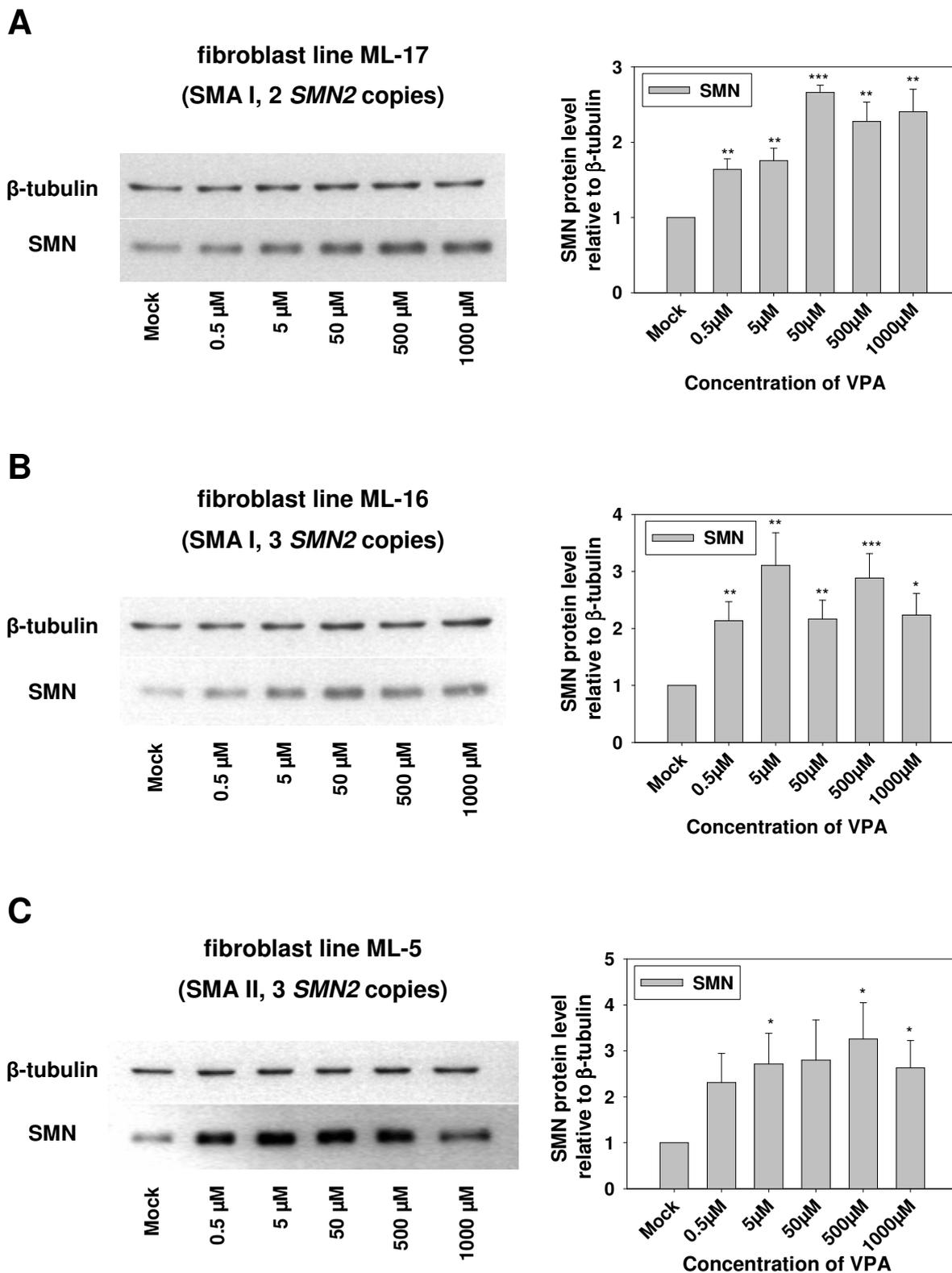
**Figure 8: Increase of the SMN protein level in fibroblast cultures derived from SMA patients treated with solvent (mock) or increasing concentrations of VPA (0.5, 5, 50, 500, and 1000 µM) for 16 h. For the treated fibroblast lines ML-17** *(A)*, **ML-16** *(B)*, **and ML-5** *(C)*, **a representative western blot is given which was probed with antibodies against β-tubulin (loading control) and SMN. Mean values ± SEM for the SMN protein level relative to β-tubulin obtained from repeated experiments are summarized in bar graphs. Significant changes are indicated by asterisks (* p<0.05; ** p<0.01; *** p<0.001).**

Similar to the protocol which was used for the drug treatment experiments in EBV-transformed cell lines (chapter 4.1.1), one of the fibroblast lines was also incubated with butyrate. This drug has been proven already to increase SMN2 expression in lymphoblastoid cells and therefore can be used as a positive control. Based on the published information regarding the most effective butyrate concentrations and the incubation time (Chang et al. 2001), fibroblast experiments were performed with solvent (mock) or 0.5, 5, 50, 500, and 1000 µM butyrate for 24 h. Butyrate treatment of ML-5 revealed significantly elevated SMN protein levels compared to untreated cells (mock). The cumulative data (mean ± SEM) for the SMN protein level relative to the loading control β-tubulin obtained from incubation of different passages with the drug are presented in table 13.

**Table 13: SMN protein level (relative to β-tubulin) in SMA fibroblast line ML-5 after butyrate treatment. Average data (± SEM) from repeated experiments are shown and the highest level is marked in bold.**

| Human SMA fibroblast | Concentration of sodium butyrate (µM) | | | | | |
|---|---|---|---|---|---|---|
| culture | Mock | 0.5 | 5 | 50 | 500 | 1000 |
| **ML-5** (SMA II, 3 *SMN2* copies) | 1.0±0.0 | 1.9±0.1 | 2.1±0.4 | 2.4±0.4 | 2.4±0.0 | **2.7±0.5** |

With increasing concentrations of butyrate, the level of the SMN protein in ML-5 was found to be elevated, peaking in a 2.7-fold increase at 1000 µM. Together with the findings for VPA, this result confirmed that suitable conditions were found to treat fibroblasts with drugs and this assay can be used to screen for drugs which exert an effect on SMN protein expression. A representative western blot together with a bar graph that displays the cumulative data for the treatment of ML-5 with increasing amounts of butyrate is given in figure 9.
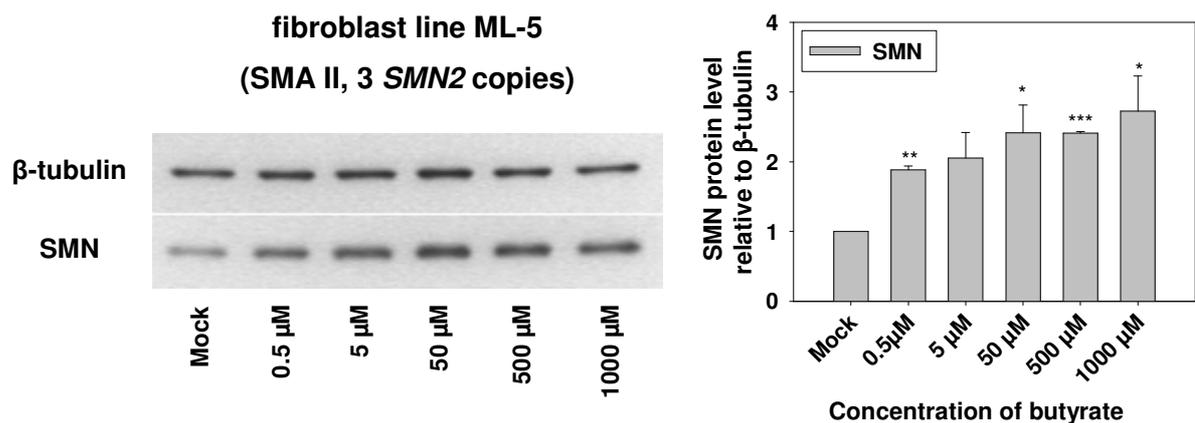


**Figure 9: Increase of the SMN protein level in fibroblast line ML-5 treated with solvent (mock) or increasing concentrations of butyrate (0.5, 5, 50, 500, and 1000 µM) for 24 h. A representative western blot is given which was probed with antibodies against β-tubulin (loading control) and SMN. Mean values ± SEM for the SMN protein level relative to β-tubulin obtained from repeated experiments are summarized as bar graph. Significant changes are indicated by asterisks (* p<0.05; ** p<0.01; *** p<0.001).**

#### 4.1.2.2 *SMN2* RNA expression under valproic acid treatment

To identify the mechanism(s) by which VPA causes the SMN2 protein increase, analysis of *SMN2* mRNA was performed by determining the FL-*SMN2* *versus* Δ7-*SMN2* transcript ratio and by investigating the total amount of *SMN2* transcripts (FL-*SMN2* plu*s* Δ7-*SMN2)* relative to an internal control.

The FL-*SMN2*/Δ7-*SMN2* ratio is a parameter which measures an effect on exon 7 inclusion and therefore indicates a reversion of the *SMN2* splicing pattern. If inclusion of exon 7 is promoted, the amount of FL-*SMN2* transcripts is increased, whereas the amount of Δ7-*SMN2* is decreased at the same time. This would result in elevated FL-*SMN2*/Δ7-*SMN2* ratios. Conversely, a preferential exon 7 skipping would lower the amount of FL-*SMN2* and increase the level of Δ7-*SMN2* transcripts, leading to a decreased FL-*SMN2*/Δ7-*SMN2* ratio. The total amount of *SMN2* transcripts is a parameter for the gene transcription rate. Increased levels of total *SMN2* transcripts would indicate a stimulation of the *SMN2* transcription.

**Table 14: Levels of FL-*SMN2* RNA, Δ7-*SMN2* RNA, total *SMN2* transcripts FL+Δ7 (relative to *GAPDH*) and the FL/Δ7 ratio in the SMA fibroblast lines ML-17, ML-16, and ML-5 which were treated with solvent (mock) or increasing concentrations of VPA. Average data (± SEM) from repeated experiments are shown and highest values are marked in bold.**

| Human SMA fibroblast culture | | Concentration of VPA (µM) | | | | | |
|---|---|---|---|---|---|---|---|
| | | **Mock** | **0.5** | **5** | **50** | **500** | **1000** |
| **ML-17** (SMA I, 2 *SMN2* copies) | **FL-*SMN2*** | 0.38±0.1 | 0.38±0.1 | 0.55±0.1 | 0.63±0.0 | 0.59±0.1 | **0.70±0.2** |
| | **Δ7-*SMN2*** | 0.24±0.0 | 0.24±0.0 | 0.30±0.0 | 0.31±0.1 | 0.35±0.1 | **0.44±0.2** |
| | **ratio FL/ Δ7** | 1.58±0.0 | 1.58±0.1 | 1.83±0.1 | **2.03±0.3** | 1.69±0.1 | 1.59±0.0 |
| | **FL+ Δ7** | 0.62±0.1 | 0.62±0.1 | 0.85±0.1 | 0.94±0.1 | 0.94±0.2 | **1.14±0.4** |
| **ML-16** (SMA I, 3 *SMN2* copies) | **FL-*SMN2*** | 0.30±0.0 | 0.55±0.2 | 0.91±0.2 | 1.12±0.2 | 1.24±0.1 | **1.55±0.5** |
| | **Δ7-*SMN2*** | 0.29±0.0 | 0.44±0.1 | 0.72±0.1 | 0.80±0.2 | 0.84±0.1 | **0.96±0.2** |
| | **ratio FL/ Δ7** | 1.03±0.0 | 1.25±0.1 | 1.26±0.1 | 1.40±0.2 | 1.48±0.0 | **1.61±0.2** |
| | **FL+ Δ7** | 0.59±0.0 | 0.99±0.3 | 1.63±0.3 | 1.92±0.4 | 2.08±0.2 | **2.51±0.7** |
| **ML-5** (SMA II, 3 *SMN2* copies) | **FL-*SMN2*** | 0.40±0.0 | 0.55±0.1 | **0.85±0.1** | 0.73±0.3 | 0.66±0.1 | 0.74±0.0 |
| | **Δ7-*SMN2*** | 0.37±0.1 | 0.43±0.1 | **0.56±0.0** | 0.47±0.1 | 0.42±0.1 | 0.52±0.1 |
| | **ratio FL/ Δ7** | 1.08±0.2 | 1.28±0.1 | 1.52±0.2 | 1.55±0.1 | **1.57±0.4** | 1.42±0.3 |
| | **FL+ Δ7** | 0.77±0.1 | 0.98±0.2 | **1.41±0.1** | 1.20±0.4 | 1.08±0.2 | 1.26±0.1 |

After treatment of fibroblast cultures with VPA, RNA was isolated, transcribed into cDNA using oligo-dT primers, and subsequently, a multiplex PCR was carried out under semi-quantitative conditions (23 cycles) using primers within exon 6 and exon 8 of *SMN2* (primers #1837 and #1841). Values for both FL-*SMN2* and Δ7-*SMN2* mRNA as well as the ratio among them and the total amount of *SMN2* transcripts were calculated relative to the internal control (*GAPDH)*. Similar to the analysis of protein extracts by western blotting, *GAPDH* was assumed to be equally expressed in all cells and therefore served as loading control. A summary of the results obtained from different passages of each investigated SMA fibroblast culture is shown in table 14. A representative gel analysis of the multiplex PCR together with the corresponding bar graphs showing the average data from repeated experiments is given for each fibroblast line in figure 9 A-C.

The data obtained from semi-quantitative RT-PCRs clearly demonstrate that VPA treatment of primary fibroblasts derived from SMA patients resulted in a significant increase of FL-*SMN2* mRNA levels (table 14, figure 9). The maximum level ranged between 1.8-fold (ML-17) and 5.2-fold (ML-16). In ML-17 and ML-16, FL-*SMN2* levels continuously increased with increasing drug concentrations and peaked at 1000 µM VPA. Treatment of ML-5 revealed the maximum FL-*SMN2* level already at 5 µM VPA, followed by slightly lower levels at higher drug concentrations.

The augmentation of FL-*SMN2* transcript levels was only partially achieved by preferential inclusion of *SMN2* exon 7 and a correction of the *SMN2* splicing pattern, since the FL-*SMN2 versus* Δ7-*SMN2* ratio increased up to ~1.5-fold only in each VPA-treated fibroblast line (significant in ML-17 and ML-16) (figure 9, table 14). Moreover, treatment of ML-17 revealed the highest FL-*SMN2* level at 1000 µM VPA, although at this drug concentration the FL-*SMN2* / Δ7-*SMN2* ratio was unchanged compared to mock cells (figure 9 A, table 14). This suggested that another mechanism substantially contributed to the up-regulation of FL-*SMN2* transcripts.

Importantly, in each of the fibroblast cultures, VPA treatment led to an increase of both the Δ7-*SMN2* transcript levels (significant in ML-16) and the levels of total *SMN2* transcripts (significant in ML-16 and ML-5) (figure 9, table 14).The respective maximum was always observed together with the peak of the FL-*SMN2* transcript levels. These observations clearly indicated that the *SMN2* gene transcription activity was stimulated by VPA, resulting in elevated levels of total *SMN2* transcripts.

Thus, a synergistic effect of transcription activation and reversion of the *SMN2* splicing pattern was responsible for the increase of FL-*SMN2* mRNA after treatment of SMA fibroblasts with 0.5-1000 *µ*M VPA.

### 4.1.2.3 Effect of valproic acid on the level of SR and SR-like splicing factors

Recently, it has been demonstrated that increased levels of the SR-like splicing factor Htra2-β1 restore the splicing pattern of *SMN2* pre-mRNA (Hofmann et al. 2000). Over-expression of Htra2-β1 in HEK293 cells and NIH 3T3 murine fibroblasts carrying an *SMN2* minigene dramatically increased the production of FL-*SMN2* transcript. Inclusion of exon 7 was facilitated by specific binding of Htra2-β1 to an AG-rich exonic splicing enhancer in *SMN* exon 7. To explain the preferred processing of *SMN2* pre-mRNA to FL-*SMN2* transcripts and the increased FL-*SMN2*/Δ7-*SMN2* ratio observed in the
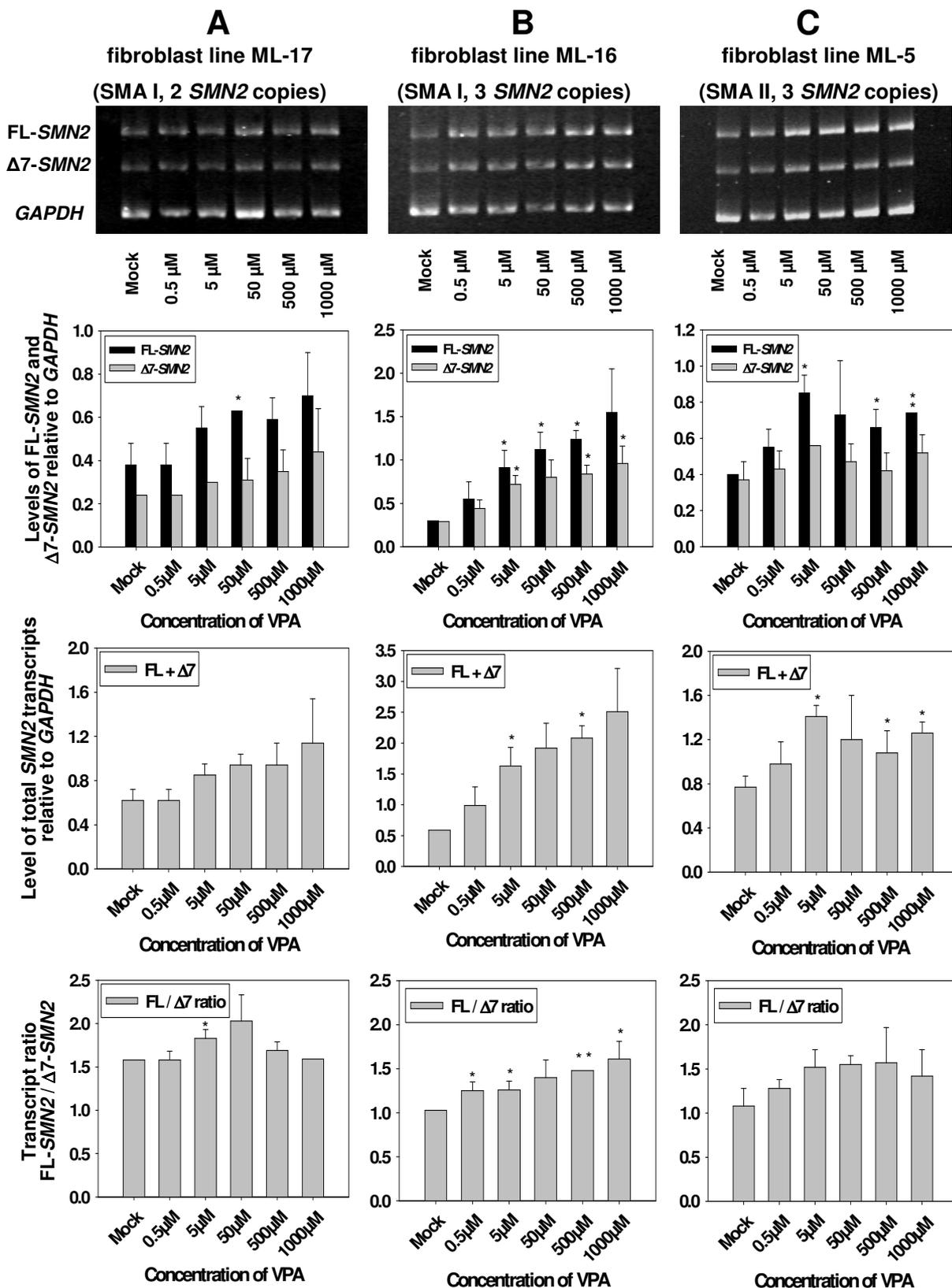
**Figure 9:** *SMN2* RNA analysis in SMA fibroblast cultures ML-17 *(A, first column)*, ML-16 *(B, second column)*, and ML-5 *(C, third column)* after treatment with solvent or increasing concentrations of VPA (0.5, 5, 50, 500, and 1000 µM). For each cell line, a representative gel analysis of the semi-quantitative multiplex RT-PCR is given, showing FL-*SMN2*, Δ7-*SMN2* and the internal standard *GAPDH*. In the bar graphs, mean ± SEM values from repeated experiments are given for the FL-*SMN2* level, the Δ7-*SMN2* level, the level of total *SMN2* transcripts (all of the parameters relative to *GAPDH*), and the FL-*SMN2*/Δ7-*SMN2* ratio. Significant changes are indicated by asterisks (* p<0.05; ** p<0.01; *** p<0.001).

fibroblast cultures treated with VPA, another quantitative western blot analysis was performed on protein extracts isolated from cell cultures after incubation with the drug. Membranes were restained with an antibody against the SR-like splicing factor Htra2-β1. The protein β-tubulin was used as loading control as already described (4.1.2.1). The levels of Htra2-β1 were found significantly up-regulated under increasing concentrations of VPA. The highest levels varied between the 2.7-fold (at 50 µM VPA in ML-17 and ML-16) and the 4.1-fold (at 1000 µM VPA in ML-5) as compared to untreated mock cells (figure 10 and table 15).

**Table 15: Levels of the splicing factors Htra2-β1, SF2/ASF, and SRp20 (relative to β-tubulin) in SMA fibroblasts treated with solvent (mock) or increasing concentrations of VPA (0.5, 5, 50, 500, and 1000 µM). Average data (± SEM) from repeated experiments with different passages of each fibroblast culture are shown with highest values marked in bold.**

| Human SMA fibroblast culture | Splicing factor | Concentration of VPA (µM) | | | | | |
|---|---|---|---|---|---|---|---|
| | | Mock | 0.5 | 5 | 50 | 500 | 1000 |
| **ML-17** (SMA I, 2 *SMN2* copies) | **Htra2-β1** | 1.0±0.0 | 1.7±0.3 | 1.7±0.7 | **2.7±0.3** | 2.7±1.4 | 2.2±0.6 |
| | **SF2/ASF** | 1.0±0.0 | 3.1±1.5 | 3.1±1.4 | 4.0±1.3 | **4.1±2.3** | 3.4±1.8 |
| | **SRp20** | 1.0±0.0 | **2.2±0.7** | 1.6±0.7 | 2.0±0.5 | 1.6±0.9 | 1.9±0.9 |
| **ML-16** (SMA I, 3 *SMN2* copies) | **Htra2-β1** | 1.0±0.0 | 1.9±1.1 | 2.3±0.3 | **2.7±0.9** | 1.5±0.3 | 2.3±0.6 |
| | **SF2/ASF** | 1.0±0.0 | 1.9±0.8 | 2.6±0.6 | **2.9±1.0** | 1.8±0.5 | 1.9±0.3 |
| | **SRp20** | 1.0±0.0 | 2.0±1.0 | 3.0±1.1 | **3.3±1.4** | 2.1±0.9 | 2.1±0.9 |
| **ML-5** (SMA II, 3 *SMN2* copies) | **Htra2-β1** | 1.0±0.0 | 2.9±1.0 | 3.1±0.5 | 3.3±1.1 | 3.2±1.2 | **4.1±1.9** |
| | **SF2/ASF** | 1.0±0.0 | 1.4±0.4 | 1.2±0.1 | 1.2±0.3 | **1.4±0.1** | 1.1±0.2 |
| | **SRp20** | 1.0±0.0 | 2.4±0.7 | **3.1±0.5** | 3.1±0.7 | 3.0±1.3 | 1.7±0.7 |

To investigate whether this effect is specific for Htra2-β1 (because an increased amount of *SMN2* pre-mRNA eventually requires higher levels of Htra2-β1, the most important *trans*-acting splicing factor shown to restore FL-*SMN2* mRNA) or whether VPA treatment of fibroblasts leads to a rather unspecific elevation of the levels of a number of SR/SR-like proteins, the western blot membranes were restained with antibodies against two additional SR splicing factors, SF2/ASF and SRp20. SF2/ASF has been shown to be involved in splicing regulation of *SMN1* pre-mRNA (Cartegni and Krainer 2002), whereas SRp20 was excluded to act in that way (Hofmann et al. 2000; Hofmann and Wirth 2002). Analysis revealed that the levels of both splicing proteins were elevated in fibroblasts after incubation with VPA (table 15, figure 10). In ML-17, an up to 4.1-fold elevation of SF2/ASF was observed at 500 µM VPA. The maximum up-regulation in ML-16 was 2.9-fold compared to untreated cells (mock) and was reached at 50 µM VPA. In contrast, a very weak increase of SF2/ASF levels was observed in ML-5, peaking in a 1.4-fold elevation at 0.5 and 500 µM VPA. SRp20 levels reached an up
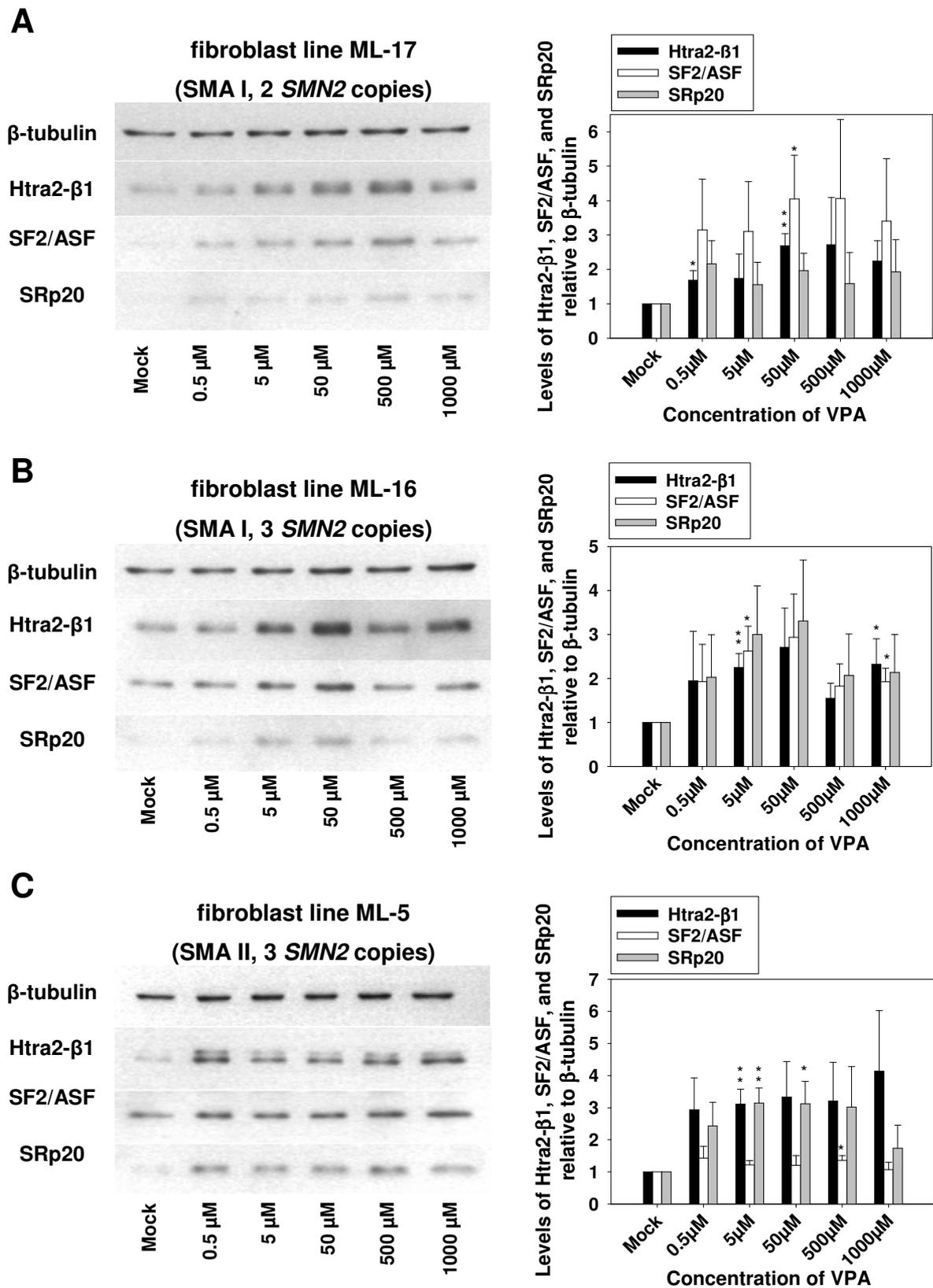
**Figure 10: Levels of the splicing factors Htra2-β1, SF2/ASF, and SRp20 in SMA fibroblast cultures treated with solvent (mock) or increasing concentrations of VPA (0.5, 5, 50, 500, and 1000 µM) for 16 h. For each fibroblast line, a representative western blot is given with β-tubulin serving as loading control. Mean values ± SEM for the level of each splicing factor relative to β-tubulin obtained from repeated experiments are summarized in bar graphs. Two bands for Htra2-β1 on the western blot result from the phosphorylated and the unphosphorylated form of the protein. Significant changes are indicated by asterisks (* p<0.05; ** p<0.01).**

to 2.2-fold increase at 0.5 µM VPA in ML-17, a 3.3-fold increase at 50 µM VPA in ML-16, and a 3.1-fold augmentation at 5 µM VPA in ML-5. The levels of all three investigated splicing factors, however, varied between the passages of one particular fibroblast cell line as demonstrated by the high SEM values in table 15. Moreover, particularly for the splicing factor SF2/ASF, a different response of the fibroblast lines to VPA treatment was observed. While a marked up-regulation was measured in ML-17 and ML-16, ML-5 barely revealed an increase of SF2/ASF levels under drug treatment (table 15, figure 10).

These data obtained from VPA-treated fibroblasts demonstrate that the drug stimulates expression of some SR and SR-like splicing factors regardless whether they are involved in *SMN* pre-mRNA splicing or not. However, based on the data from *in vitro* and *in vivo* splicing experiments published so far, only over-expressed Htra2-β1 is able to restore the splicing pattern of *SMN2* (Hofmann et al. 2000; Hofmann and Wirth 2002).


To elucidate the mechanism which triggers the increase of Htra2-β1 protein levels in VPA-treated SMA fibroblasts, an analysis of the transcripts derived from the *SFRS10* gene was carried out on RNA prepared from fibroblast cultures incubated with increasing drug concentrations for 16h. The *SFRS10* gene consists of ten exons and encodes five different *Htra2-β* transcripts which arise from alternative splicing, alternative polyadenylation and alternative promoter usage: *Htra2-β1* (exons 1 and 3-10), *Htra2-β2* (exons 1-2), *Htra2-β3* (exons 1 and 4-10), *Htra2-β4* (exons 1-10), and *Htra2-β5* (part of intron 2 and exons 3-10). Only *Htra2-β1* and *Htra2-β3* are translated into protein (Stoilov et al. 2004). Two of the mRNA isoforms (*Htra2-β1* and *Htra2-β2*) are ubiquitously expressed, whereas expression of *Htra2-β3* and *Htra2-β4* appears to be tissue-specific and developmentally regulated (Nayler et al. 1998). *Htra2-β5* was firstly described in 2004 (Stoilov et al. 2004), however, this was exclusively based on *in silico* analysis without any evidence for its existence *in vivo* so far.

In a first step, it was checked whether the tissue-specific mRNA isoforms *Htra2-β3* and *Htra2-β4* are expressed in untreated and/or VPA-treated primary human SMA fibroblasts. Treated cells were included for investigation because it was demonstrated already that VPA may exert an effect on transcription and splicing (see chapter 4.1.2.2). A multiplex RT-PCR was carried out on RNA isolated from fibroblasts treated with solvent (mock) or VPA using primers located in exons 1 (#1093) and exon 4 (#1094) of the *SFRS10* gene. An additional RT-PCR was carried out using another pair of primers located in exon 1 (#1970) and exon 3 (#1971). Since *GAPDH* was checked already to be sufficiently expressed in fibroblasts (see chapter 4.1.2.2), it was co-amplified, and served as positive control in each PCR reaction. The analysis revealed that *Htra2-β3* and *Htra2-β4* were not expressed in SMA fibroblast cultures, regardless if they were treated with VPA or not (figure 11 A). Thus, subsequent experiments focused on the ubiquitously expressed *Htra2-β1* and *Htra2-β2* transcripts. On RNA from each of the three fibroblast lines treated with increasing amounts of VPA, a semi-quantitative multiplex PCR was performed. *Htra2-β1* transcripts were amplified using the primers located in exon 1 and 4. *GAPDH* was co-amplified and served as internal control. The gel analysis clearly revealed an elevation of *Htra2-β1* transcripts under VPA treatment (figure 11 B-D, for corresponding data see appendix page IX, table A.1) which explains the increase of Htra2-β1 protein levels under drug treatment. An additional experiment was performed on the sample set derived from

**A**



**B**

fibroblast line ML-17

(SMA I, 2 *SMN2* copies)

**C**

fibroblast line ML-16

(SMA I, 3 *SMN2* copies)

**D**

fibroblast line ML-5

(SMA II, 3 *SMN2* copies)
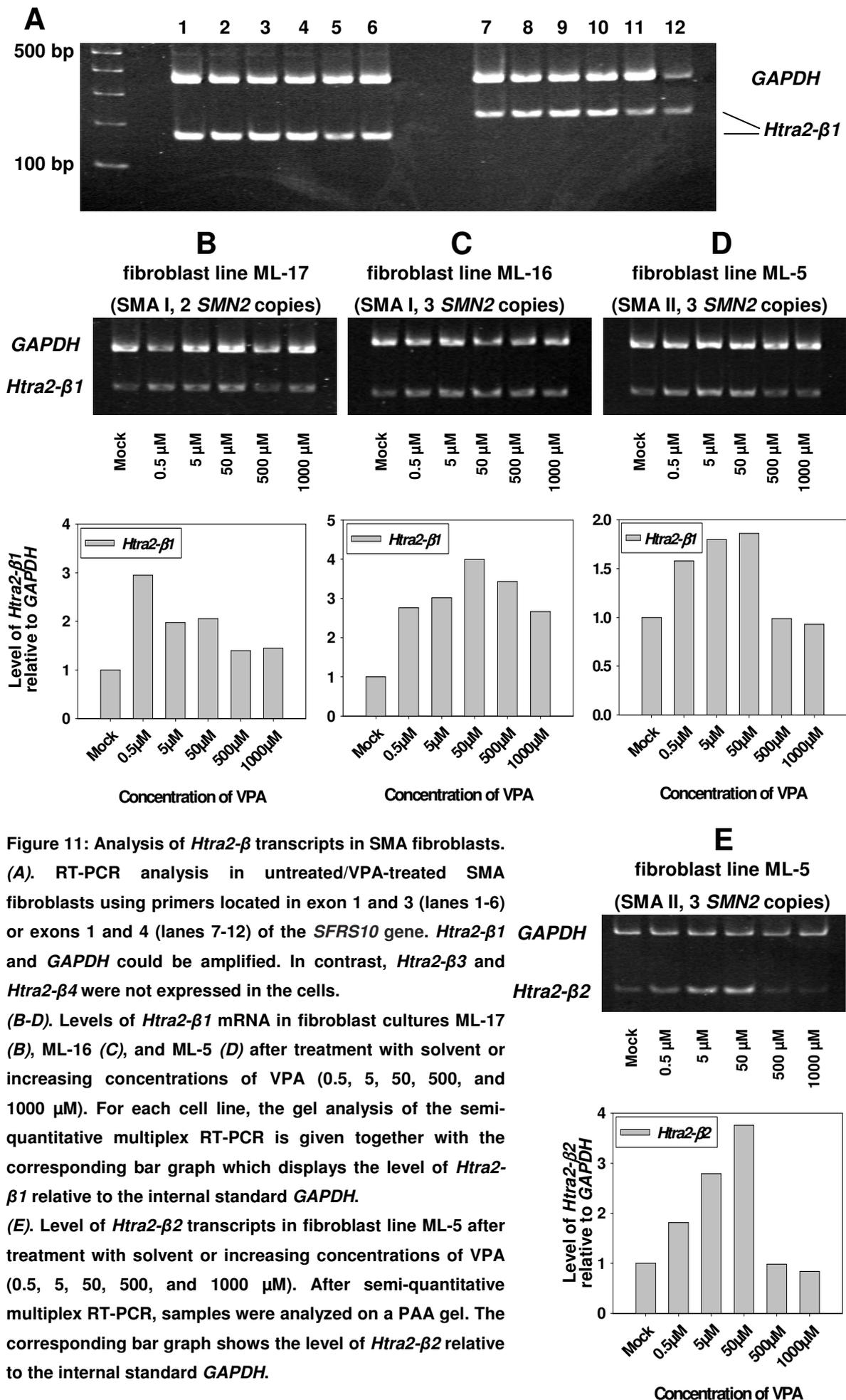


**Figure 11: Analysis of *Htra2-β* transcripts in SMA fibroblasts.**
*(A)*. RT-PCR analysis in untreated/VPA-treated SMA fibroblasts using primers located in exon 1 and 3 (lanes 1-6) or exons 1 and 4 (lanes 7-12) of the *SFRS10* gene. *Htra2-β1* and *GAPDH* could be amplified. In contrast, *Htra2-β3* and *Htra2-β4* were not expressed in the cells.
*(B-D)*. Levels of *Htra2-β1* mRNA in fibroblast cultures ML-17 *(B)*, ML-16 *(C)*, and ML-5 *(D)* after treatment with solvent or increasing concentrations of VPA (0.5, 5, 50, 500, and 1000 μM). For each cell line, the gel analysis of the semi-quantitative multiplex RT-PCR is given together with the corresponding bar graph which displays the level of *Htra2-β1* relative to the internal standard *GAPDH*.
*(E)*. Level of *Htra2-β2* transcripts in fibroblast line ML-5 after treatment with solvent or increasing concentrations of VPA (0.5, 5, 50, 500, and 1000 μM). After semi-quantitative multiplex RT-PCR, samples were analyzed on a PAA gel. The corresponding bar graph shows the level of *Htra2-β2* relative to the internal standard *GAPDH*.

**E**

fibroblast line ML-5

(SMA II, 3 *SMN2* copies)

fibroblast line ML-5 and revealed that the levels of the *Htra2-β2* isoform were similarly increased when the cells were treated with VPA (figure 11 E and appendix page IX, table A.1). This suggested that VPA stimulates the transcription of the *SFRS10* gene in SMA fibroblasts resulting in increased levels of total *Htra2-β* transcripts. However, an additional effect of VPA on the splicing pattern could not be excluded since both transcripts could not be amplified within the same multiplex RT-PCR reaction using one and the same primer pair.

The drug treatment experiments in SMA fibroblasts were not only performed with VPA, but also with butyrate, which was included as positive control (chapter 4.1.2.1). Consistent with the results obtained in EBV-transformed lymphoblastoid cell lines (Chang et al. 2001), incubation of fibroblasts with butyrate led to increased SMN2 protein levels. Moreover, it was demonstrated already that butyrate increases the FL-*SMN2*/Δ7-*SMN2* ratio, and the level of SR proteins (Chang et al. 2001). Consequently, it seemed reasonable to check whether butyrate acts similarly to VPA and is able to increase the levels of Htra2-β1, but also of SF2/ASF and SRp20 in fibroblast cultures. Analysis was performed on the protein extracts isolated from cell cultures after incubation with increasing amounts of butyrate for 24 h. As already described, β-tubulin was used as loading control (chapter 4.1.2.1). Western blot membranes were restained with antibodies against each of the three splicing factors.
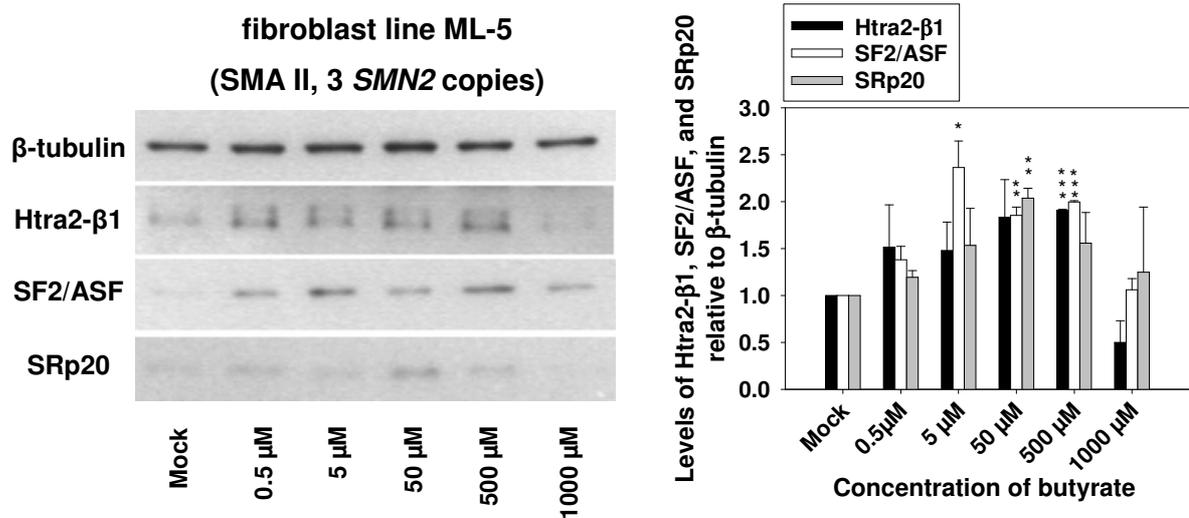


**Figure 12: Levels of Htra2-β1, SF2/ASF, and SRp20 in fibroblast line ML-5 treated with solvent (mock) or increasing concentrations of butyrate (0.5, 5, 50, 500, and 1000 μM) for 24 h. A representative western blot is given with β-tubulin serving as loading control. Mean values ± SEM for the splicing factor levels relative to β-tubulin obtained from repeated experiments are summarized as bar graph. Two bands for Htra2-β1 on the western blot result from the phosphorylated and the unphosphorylated form of the protein. Significant changes are indicated by asterisks (* p<0.05; ** p<0.01; *** p<0.001).**

Indeed, as in case of VPA, butyrate treatment of fibroblasts led to significantly increased Htra2-β1, SF2/ASF, and SRp20 protein levels (table 16, figure 12), demonstrating that both drugs VPA and butyrate share similar pathways of activation and supporting the assumption that elevated amounts of Htra2-β1 are responsible for the change of the *SMN2* splicing pattern observed in fibroblasts under drug treatment.

**Table 16: Htra2-β1, SF2/ASF, and SRp20 protein levels (relative to β-tubulin) in SMA fibroblast line ML-5 treated with solvent (mock) or increasing concentrations of sodium butyrate (0.5, 5, 50, 500, and 1000 µM). Average data (± SEM) from repeated experiments with different passages are shown with highest values marked in bold.**

| Human SMA fibroblast culture | Splicing factor | Concentration of sodium butyrate (µM) | | | | | |
|---|---|---|---|---|---|---|---|
| | | **Mock** | **0.5** | **5** | **50** | **500** | **1000** |
| **ML-5** (SMA II, 3 *SMN2* copies) | **Htra2-β1** | 1.0±0.0 | 1.5±0.5 | 1.5±0.3 | 1.8±0.4 | **1.9±0.0** | 0.5±0.2 |
| | **SF2/ASF** | 1.0±0.0 | 1.4±0.1 | **2.4±0.3** | 1.9±0.1 | 2.0±0.0 | 1.1±0.1 |
| | **SRp20** | 1.0±0.0 | 1.2±0.1 | 1.5±0.4 | **2.0±0.1** | 1.6±0.3 | 1.2±0.7 |

### 4.1.2.4 Cytotoxicity of valproic acid in SMA fibroblast cultures

To investigate the cytotoxicity of VPA in primary SMA fibroblasts, MTT assays were performed and the viability of cells was measured under drug treatment. Therefore, ML-17, ML-16, and ML-5 were
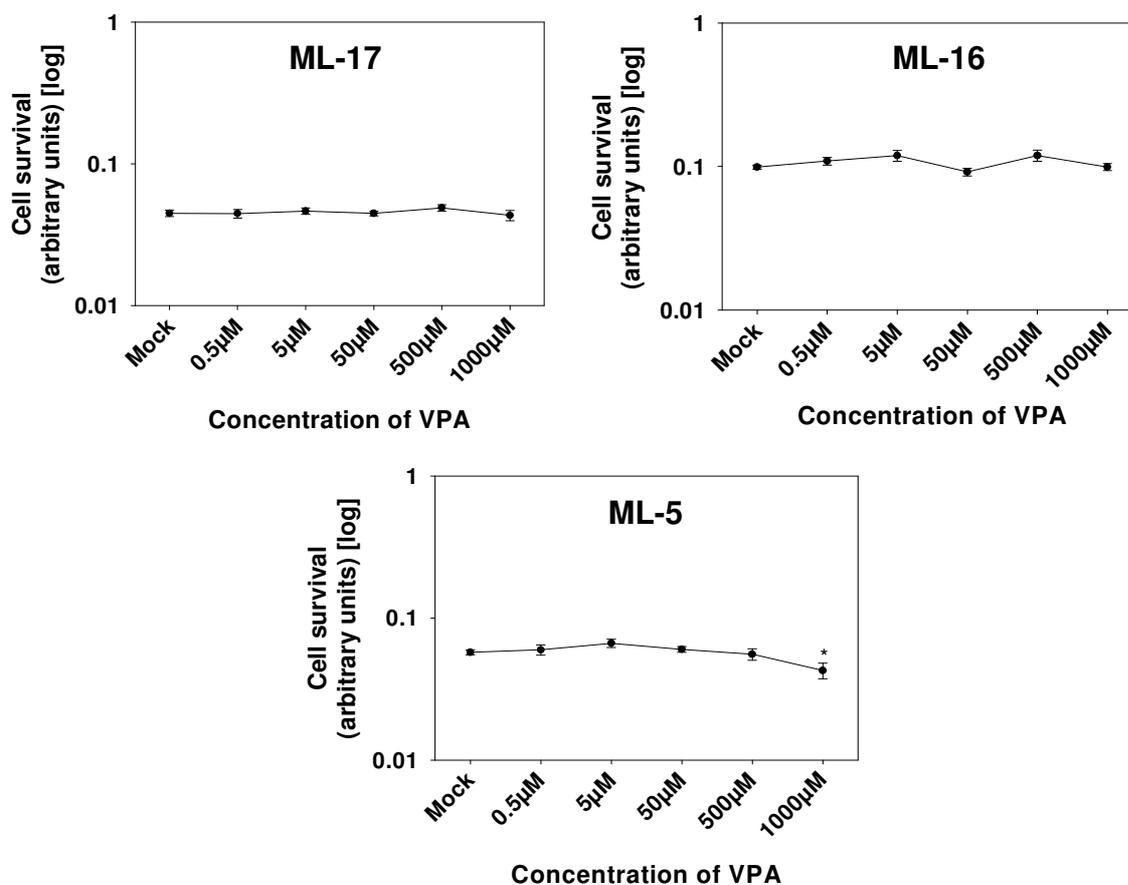


**Figure 13: MTT assays with fibroblast lines ML-17, ML-16, and ML-5. Cells were treated with solvent (mock) or increasing concentrations of VPA (0.5, 5, 50, 500, and 1000 µM). Values for the absorption are given as mean ± SEM. Significant changes are indicated by asterisks (* p<0.05).**

incubated with solvent (mock) or increasing amounts of VPA for 16 h. Subsequently, the number of surviving cells was analyzed using their ability to convert thiazolyl blue tetrazolium bromide into detectable violet formazan crystals. As displayed in figure 13, fibroblast line ML-17 did not show any decreased absorption with increasing concentrations of VPA, indicating that the survival of these cells was not affected during incubation with VPA. Similarly, the values measured for the absorption in cell line ML-16 did not reveal significant changes either, suggesting that VPA was well tolerated by these fibroblasts. Only in ML-5, a significantly decreased absorption (corresponding with a slightly lower cell survival) was observed at 1000 µM VPA. These data indicate that the VPA concentrations used to stimulate *SMN2* expression in primary fibroblasts derived from SMA patients cover a range which is well tolerated by the cells without severely affecting their survival. However, the highest VPA concentration caused significant cell death in 1/3 cell lines, suggesting that treatment of the fibroblasts with even higher VPA concentrations to achieve elevated SMN protein levels would probably be limited by toxic effects.

### 4.1.2.5  Knock-down of Htra2-β1 in primary SMA fibroblast cells

A reasonable experiment to directly approach the correlation between increased Htra2-β1 protein levels and elevated FL-*SMN2* / Δ7-*SMN2* ratios in SMA fibroblasts treated with VPA is the knock-down of Htra2-β1 by siRNA oligos. If elevated Htra2-β1 levels are indeed responsible for the change of the *SMN2* splicing pattern, knock-down of the protein in SMA fibroblasts should prevent the elevation of the FL-*SMN2* / Δ7-*SMN2* ratio observed upon VPA treatment.
In addition, regardless of any drug treatment experiments, it would be interesting to investigate if the knock-down of Htra2-β1 has any consequences for the *SMN2* splicing pattern in SMA fibroblasts (which have not been treated with any drugs). Despite the knowledge about increasing FL / Δ7 ratios in case of Htra2-β1 over-expression, which was gained from studies in HEK293 cells and NIH 3T3 murine fibroblasts (Hofmann et al. 2000; Hofmann and Wirth 2002), a knock-down experiment has not been carried out so far.

To knock down Htra2-β1, siRNA oligos directed against *Htra2-β1* mRNA have to be incorporated into the cells. Since primary fibroblasts are very difficult to transfect with conventional methods, in a first approach electroporation was applied by using the Amaxa Nucleofector technology. To establish a procedure which results in a high transfection efficiency, fibroblasts were transfected with pmaxGFP, a plasmid encoding the green fluorescent protein (GFP) from *Pontenilla p.* To optimize the transfection process, initial experiments were performed with two different nucleofector solutions which are required to electroporate the cells [Human Dermal Fibroblast Nucleofector Kit (NHDF) and Basic Nucleofector Kit for Primary Fibroblast Cells], and five different electroporation programs (A24, T16, U12, V13, U23). From A24 to U23, the current applied for electroporation is increasing. This results in a higher electroporation efficiency, however, the number of dead cells might also be increased. Thus, an electroporation program which balances between these two factors had to be identified. At 24 h after electroporation of ML-16, the cells were checked under the microscope to evaluate if any of the electroporation programs led to massive cell death. However, all of the programs were well tolerated

by the fibroblasts. Subsequently, cells were harvested and the transfection efficiency determined by flow cytometry. Cells expressing GFP were detected by their green fluorescence. Fibroblasts which were treated with program U23 but not transfected with pmaxGFP served as mock to determine the baseline fluorescence level of the cells. Data analysis revealed that the highest transfection efficiency of ML-16 fibroblasts was obtained after electroporation with the Basic Nucleofector Kit for Primary Fibroblast Cells using program U23 and 2 µg of the pmaxGFP plasmid. Depending on the number of the respective cell passage, transfection efficiency varied between 60 and 85% (see appendix page IX, table A.2 for complete data obtained with different kits, different passages, different programs, and different amounts of pmaxGFP plasmid). The highest value of 85% was obtained for the youngest fibroblast passage, and the efficiency of 60% was obtained for the oldest passage, suggesting that younger fibroblast passages are more suitable and easier to electroporate. Electroporation with the Basic Kit and program V13, and the NHDF Kit and program U23 or V13, respectively, also revealed transfection efficiencies above 50%, suggesting that they might be used as alternative programs for transfection.

However, despite the relatively high transfection efficiency of ML-16, electroporation with the Amaxa Nucleofector technology was not considered further to knock-down Htra2-β1. Western blot analysis using an antibody against Htra2-β1 protein revealed that the electroporation procedure itself caused a knock-down of Htra2-β1 protein levels such that the protein was not detectable anymore. This was first observed in initial experiments which aimed at the evaluation of a suitable siRNA oligo directed against Htra2-β1 and the evaluation of the suitable incubation time required to obtain a sufficient knock-down of the Htra2-β1 protein level. Cell extracts derived from these experiments were used to perform western blotting. In all of the samples, β-tubulin and SMN were detected. In contrast, a signal for Htra2-β1 was not obtained in any of the samples, regardless if they were treated with a siRNA oligo
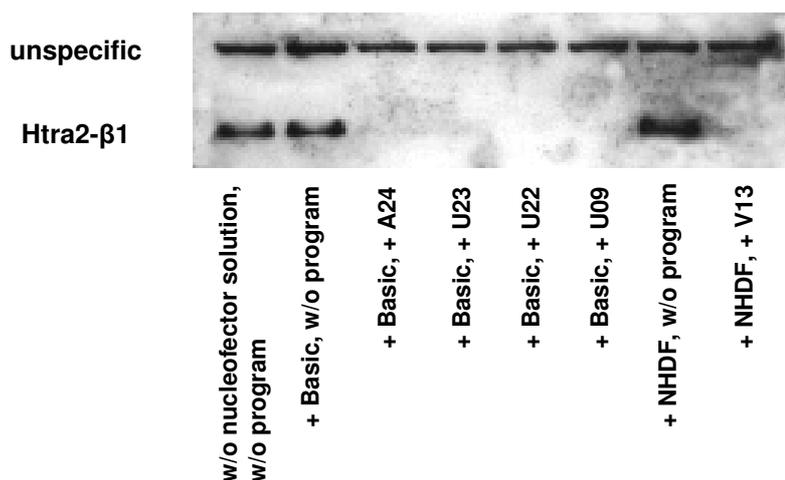


**Figure 14: Western blot analysis of protein extracts obtained from ML-16 using an antibody against Htra2-β1. The protein was only detected in extracts prepared from cells which were not treated with an electroporation program. In contrast, electroporated cells did not show Htra2-β1 expression 24 h after treatment, regardless of the strength of the electroporation program used. "w/o" indicates "without"; "Basic" and "NHDF" are two different nucleofector solutions, and "A24", "U23", "U22", "U09", and "V13" indicate electroporation programs.**

against *Htra2-β1*, a negative control siRNA, or with solvent (see appendix page X, figure A.3). However, all of the samples had in common that they were treated with the electroporation program U23, suggesting that this might be the critical factor which led to a down-regulation of Htra2-β1 protein levels. To confirm this hypothesis in a subsequent experiment, ML-16 fibroblasts were treated with the electroporation programs U23 (strongest program), U22, U09, V13 (slightly milder programs) or A24 (mildest program) without adding pmaxGFP or any siRNA oligos, were subsequently grown at 37°C for 24 h, and finally harvested. Only in the positive control (without nucleofector solution, not treated with any program) and in the cells suspended in nucleofector solution (NHDF Kit or Basic Kit) but not treated with any program, Htra2-β1 was detectable (figure 14). Even five days after electroporation treatment, the splicing factor was undetectable on western blots performed on protein extracts of the cells. This was confirmed using fibroblast line ML-5 (see appendix page XI, figure A.4).

Since the observed knock-down of Htra2-β1 after electroporation without using siRNAs was most likely stress-dependent and therefore unspecific, a similar downregulation had to be assumed for additional proteins (including other splicing factors). This made the electroporation procedure inappropriate to investigate the consequences of an Htra2-β1 knock-down on the *SMN2* splicing pattern in primary fibroblasts. Thus, further methods were evaluated to identify a suitable transfection procedure to deliver siRNAs against *Htra2-β1* to SMA fibroblasts. Recently, a new class of lipofection reagents (Dharmafect 1, 2, and 3) has been developed by *Dharmacon*. These reagents were optimized for the transfection of siRNA oligos, and are not recommended to deliver plasmids to cells. There were no existing protocols for the transfection of primary human fibroblasts with siRNAs, however, the manufacturer recommended to check Dharmafect 1 and 3. Thus, in a first step, the ability to achieve a silencing effect in fibroblasts was tested by transfecting the positive control silencer siCONTROL Cyclophilin B siRNA into ML-16 and ML-5 cells. This control siRNA has been validated by *Dharmacon* to achieve an efficient knock-down of *Cyclophilin B* transcripts. Cells were harvested at 24, 48, and 72 h after transfection, RNA was extracted, and *Cyclophilin B* (*PPIB*) transcript levels measured by real-time PCR. In both cell lines, a clear down-regulation of *PPIB* transcripts by more than 50% was observed at 48 h and at 72 h after transfection, which gave a first hint that the Dharmafect 1 and 3 reagents might be useful to deliver siRNAs to primary fibroblasts (see appendix page XI, table A.5, and page XII, table A.6). A comparison of the results obtained for Dharmafect 1 and those for Dharmafect 3 revealed a similar efficiency for both reagents. Dharmafect 1 was selected for all further experiments.

In a second step, siRNAs directed against *Htra2-β1* mRNA were transfected into ML-16 to evalute whether they would exert an effect on the Htra2-β1 protein level. Two different siRNA oligos were used: oligo number 3 (target sequence in exon 4/5 of the human *SFRS10* gene), and oligo number 5 (target sequence in exon 7 of the human *SFRS10* gene). Both siRNAs would target not only *Htra2-β1* transcripts, but also any other splice variant except for *Htra2-β2*. However, expression of *SFRS10* in fibroblasts is restricted to the isoforms *Htra2-β1* and *Htra2-β2*, and *Htra2-β2* is not translated into a corresponding protein such that a potential loss of Htra2-β1 in these cells can not be compensated by the replacement of an isoform (chapter 4.1.2.3). Using Dharmafect 1, ML-16 was transfected either with oligo 3 or with oligo 5. Cells were harvested at 48, 72, and 96 h after transfection, protein extracts were prepared and western blot analysis performed using antibodies against Htra2-β1 and β-tubulin. The latter served as control to confirm equal loading of the membrane with protein from each sample.

Data analysis revealed that both delivery of oligo 3 and delivery of oligo 5 led to a knock-down of Htra2-β1 protein levels which was most pronounced at 72 h after transfection (see appendix pages XII-XIV, A.7 to A.10). However, the knock-down was more prominent using oligo 5 (knock-down by 69% with oligo 3 versus knock-down by 91% with oligo 5). Consequently, oligo 5 was selected for further experiments.

To perform the final Htra2-β1 knock-down experiments, ML-16 was selected because this cell line presented the most prominent increase of the *SMN2* splicing pattern among the VPA-treated fibroblasts (chapter 4.1.2.2). The experiment was divided into four different parts: Fibroblasts were (i) incubated <u>without</u> siRNA oligo, <u>without</u> VPA, (ii) transfected <u>with</u> siRNA oligo 5, <u>without</u> addition of VPA, (iii) incubated <u>without</u> siRNA oligo, <u>with</u> VPA, and (iv) transfected <u>with</u> siRNA oligo 5, and incubated <u>with</u> VPA. According to the conditions used to treat fibroblasts with VPA (chapter 4.1.2.1), the drug was added to the respective samples 16 h before harvest. A concentration of 1000 µM was used because this amount induced the most substantial augmentation of the FL-*SMN2* / Δ7-*SMN2* ratio in ML-16 (chapter 4.1.2.2). The following control transfection experiments were included: (i) transfection of the cells with the validated positive control silencer siCONTROL Cyclophilin B siRNA, and (ii) transfection with the siCONTROL Non-Targeting siRNA (negative control which binds to RISC but does not have an mRNA target; used to check for any side effects that are caused exclusively by the presence of an unspecific siRNA oligo in the cell). To validate the transfection efficiency, fibroblasts were transfected with the siCONTROL TOX siRNA. This oligo induces apoptosis as soon as it is delivered to the cell. The rate of apoptosis (corresponding to the transfection efficiency) was determined by an MTT assay. Each of the experimental parts described above was performed in triplicates. Cells were harvested 72 h after transfection, and protein and/or RNA was isolated. The MTT assay was also carried out at 72 h after transfection.



**A**

β-actin

Htra2-β1

+ siRNA 5    - siRNA 5    - siRNA 5    + siRNA 5
+ VPA        + VPA        - VPA        - VPA
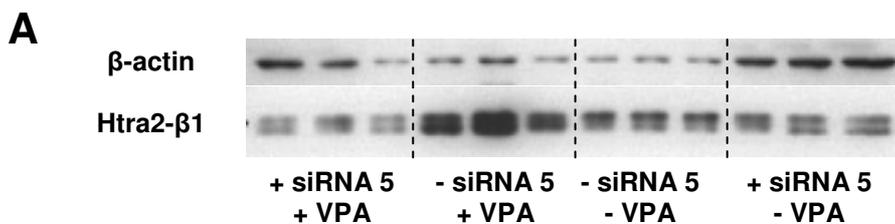
**Figure 15: Knock-down of Htra2-β1 in SMA fibroblast line ML-16 (first experiment). Cells were transfected with siRNA 5 directed against *Htra2-β1* mRNA (with and without VPA) and compared with untransfected cells (with and without VPA). All set-ups were performed in triplicates. The western blot analyis is given in *(A),* and the corresponding bar graph presenting the mean Htra2-β1 protein levels ± SEM is shown in *(B).* The transfection efficiency was 59%, and Htra2-β1 protein levels were knocked down by 54% (+ siRNA 5, - VPA) and 59% (+ siRNA 5, + VPA), respectively. Significant changes are indicated by asterisks (\*\* p<0.01, and \*\*\* p<0.001).**

**B**
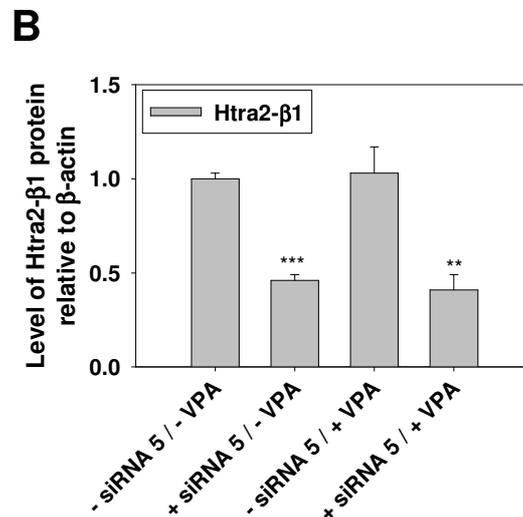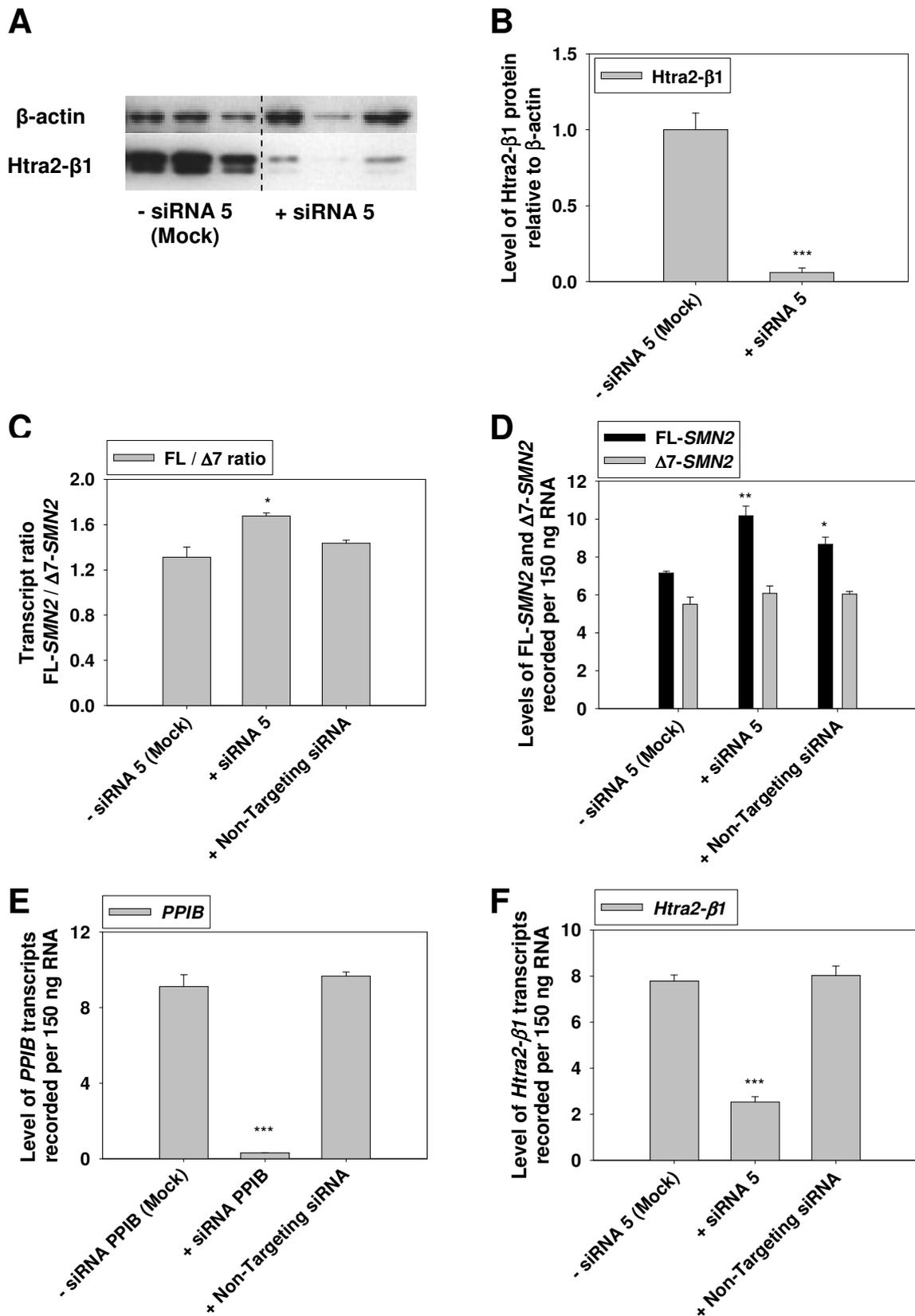
**Figure 16: Knock-down of Htra2-β1 in SMA fibroblast line ML-16 (second experiment). Cells were treated with siRNA 5 directed against *Htra2-β1* mRNA and compared with untreated cells (mock) or cells treated with a negative control siRNA. All set-ups were performed in triplicates. The transfection efficiency was 81%, and Htra2-β1 protein levels were knocked down by 94%. All transcript levels were determined by real-time PCR on a LightCycler and recorded per 150 ng total RNA used for the reverse transcription reaction. Significant changes are indicated by asterisks (*p<0.05, ** p<0.01, *** p<0.001).**

In the first knock-down experiment, a transfection efficiency of only 59% was reached. Western blot analysis was carried out with the protein extracts obtained from the cells treated with siRNA oligo 5 and/or VPA. Htra2-β1 was stained together with β-actin which served as loading control. Data analysis revealed a clear knock-down of Htra2-β1 protein levels in all samples transfected with siRNA oligo 5 (figure 15 A and B). However, the treatment of VPA (without addition of siRNA oligo 5, figure 15 B, third bar) did not lead to increased Htra2-β1 protein levels compared to VPA-untreated cells (figure 15 B, first bar). This suggested that the assay which was established for siRNA treatment (6-well plates, $1 \times 10^5$ cells per well in 2 ml medium) was not suitable to stimulate gene expression with VPA. In comparison, the assay which was successfully applied to increase SMN and Htra2-β1 protein levels with VPA used 10 cm petri dishes and $2 \times 10^5$ cells in 8 ml medium. However, in terms of siRNA studies, the latter conditions are too large-scale. They would be unreasonably expensive, reliability most likely would be questionable, and therefore these conditions could not be applied for the knock-down experiments. Consequently, the final proof for the correlation between elevated Htra2-β1 and increased FL-*SMN2* / Δ7-*SMN2* ratios in SMA fibroblasts under VPA treatment could not be given.

To investigate if the knock-down of Htra2-β1 has any consequences for the *SMN2* splicing pattern in SMA fibroblasts which have not been treated with any drugs, ML-16 fibroblasts were used to perform a second siRNA experiment. The first experiment was not considered further because the transfection efficiency was rather low and thus, a knock-down of Htra2-β1 protein levels by only 54% was achieved (figure 15 B, compare first and second bar for results obtained without VPA treatment). In a second siRNA experiment performed with siRNA oligo 5, a higher transfection efficiency of 81% was obtained. Proteins were extracted for western blotting and/or RNA was isolated to be reverse transcribed, and to carry out quantitative real-time PCR in a second step. Htra2-β1 protein levels were knocked down by 94% (figure 16 A and B), which was a much more pronounced effect than observed in the first experiment.

A subsequent analysis of the FL-*SMN2* / Δ7-*SMN2* transcript ratio in the cell extracts lacking Htra2-β1 applying quantitative real-time PCR (using primers #2075 and #2076 for FL-*SMN2*, and #1449 and #1450 for Δ7-*SMN2*) revealed a slight but significant increase compared to the mock ($p < 0.05$) (figure 16 C). The negative control (performed with siCONTROL Non-targeting siRNA) appeared to be marginally elevated, however, this was not significant.

Moreover, the cells in which Htra2-β1 was knocked down surprisingly presented a significant increase of the FL-*SMN2* transcript level ($p < 0.01$) (figure 16 D). FL transcripts were also slightly augmented in the negative control, although this effect was less pronounced. However, compared to the mock, significance was reached ($p < 0.05$). In contrast, Δ7-*SMN2* transcript levels were found unaffected in both the negative control and the siRNA 5 - transfected cells (figure 16 D).

Quantification of *PPIB* transcript levels by real-time PCR revealed that *PPIB* was efficiently knocked down in the positive control experiment (transfection of fibroblasts with the validated positive control silencer siCONTROL Cyclophilin B siRNA) (figure 16 E). As expected, *PPIB* levels remained unregulated in the negative control. The specificity of the Htra2-β1 knock-down by siRNA oligo 5 was confirmed by real-time PCR analysis of *Htra2-β1* transcript levels (using primers #2690 and #2691). Compared to the mock, *Htra2-β1* transcript levels were found down-regulated in the cells transfected with the siRNA oligo 5, but not in the cells transfected with the negative control siRNA (figure 16 F).

However, these data have to be considered as preliminary and further experiments including the knock-down of Htra2-β1 in other cell lines are required to validate these findings.

The corresponding data for the first and the second Htra2-β1 knock-down experiment are given in the appendix (pages XIV-XVI, tables A.11 to A.14).

### 4.1.3    Treatment of SMA fibroblast cultures with SAHA

The discovery of the propensity of HDAC inhibitors to initiate growth arrest, differentiation, and/or apoptosis of neoplastic cells fostered the systematic development of novel and highly potent compounds which are able to inhibit HDACs at low micromolar concentrations. Some of these substances are already under clinical investigation for cancer treatment, including suberoylanilide hydroxamic acid (SAHA), which belongs to the hydroxamic acid class of HDAC inhibitors, or M344, which is a benzamide (Marks et al. 2004). Early clinical trials in small numbers of subjects could demonstrate that intravenous administration of SAHA is safe and adequate plasma concentrations can be obtained that showed antiproliferative activity in cell culture. Moreover, an inhibition of histone deacetylases was observed in normal and malignant cells, antitumor effects were seen and drug administration revealed that SAHA has a good bioavailability, a favorable pharmacokinetic profile, and is well tolerated (Kelly et al. 2003). To evaluate experimentally whether SAHA is also able to stimulate SMN2 expression *in vitro* and might be another potential candidate for an SMA therapy, the drug was tested using the fibroblast assay described in chapter 4.1.2.1.

#### 4.1.3.1  Impact of SAHA on SMN2 protein levels

Two *SMN1*-deleted fibroblast cell lines (ML-16 and ML-5) derived from patients with SMA were used to investigate the capacity of SAHA to affect human SMN2 protein expression. ML-16 is from a type I SMA patient, and ML-5 is from a type II SMA patient, both of them carrying three *SMN2* copies. Since it has been shown that SAHA is a nanomolar inhibitor of partially purified HDACs, and therefore by far more potent than the aliphatic acids like butyrate and VPA (Richon et al. 1996; Richon et al. 1998), the drug concentrations for fibroblast treatment were chosen to be much lower than those used for the

**Table 17: SMN protein levels (relative to β-tubulin) in SMA fibroblast lines ML-16 and ML-5 after treatment with the second-generation HDAC inhibitor SAHA. Average data (± SEM) from repeated experiments are shown and highest levels are marked in bold.**

| Human SMA fibroblast | | Concentration of SAHA (µM) | | | | | |
|---|---|---|---|---|---|---|---|
| culture | | Mock | 0.05 | 0.5 | 1 | 5 | 10 |
| **ML-16** | (SMA I, 3 *SMN2* copies) | 1.0±0.0 | 1.9±0.4 | 2.4±0.4 | 2.4±0.6 | **3.0±0.6** | 2.8±0.8 |
| **ML-5** | (SMA II, 3 *SMN2* copies) | 1.0±0.0 | 1.7±0.1 | 2.3±0.2 | **2.4±0.7** | 2.0±0.5 | 1.6±0.3 |

experiments with VPA. To cover a broad range, ML-16 and ML-5 were incubated with 0.05, 0.5, 1, 5, and 10 µM SAHA. For each experiment, one of the petri dishes with cells was treated only with the solvent DMSO (mock). The optimal treatment time was evaluated by a time course experiment which was performed in cell line ML-16 and covered 16, 24, 36, and 48 h. A clear effect was only observed at 24 h after SAHA treatment. Consequently, this condition was selected for all further experiments. Like already described for the screening of VPA, after incubation of SMA fibroblasts with SAHA, protein extracts of untreated (mock) and treated fibroblasts were prepared and analyzed by western blotting. The protein β-tubulin served as internal control to confirm equal loading of the membranes. Mean values ± SEM for SMN protein levels relative to β-tubulin obtained from the treatment of different passages of ML-16 and ML-5 with increasing amounts of SAHA are summarized in table 17, and presented as bar graphs in figure 17. Additionally, representative western blots for each SAHA-treated fibroblast culture are presented in figure 17.
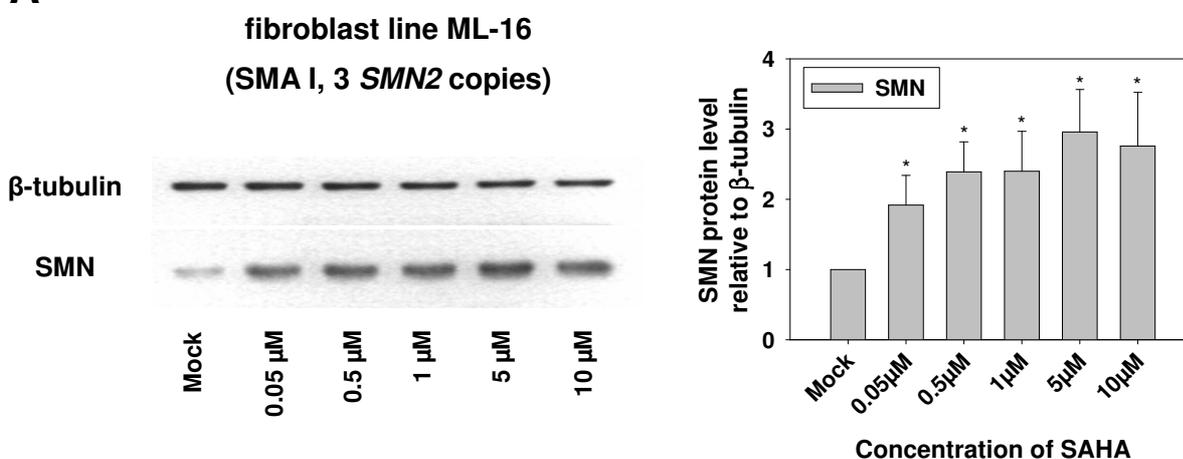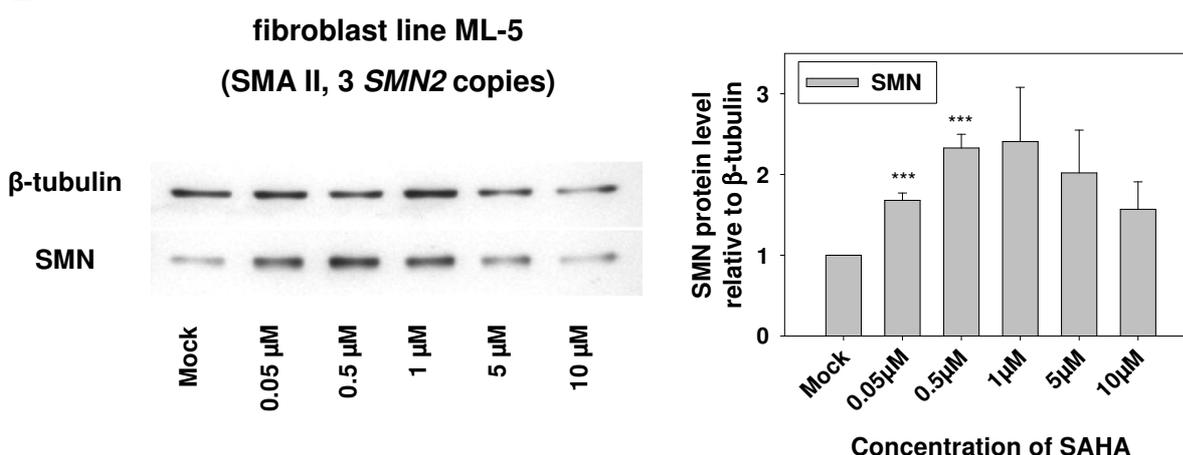


**Figure 17: Increase of the SMN protein level in SMA fibroblast cultures ML-16 and ML-5 treated with solvent (mock) or increasing concentrations of SAHA (0.05, 0.5, 1, 5, and 10 µM) for 24 h. For each cell line, a representative western blot is given which was probed with antibodies against β-tubulin (loading control) and SMN. Mean values ± SEM for the SMN protein level relative to β-tubulin obtained from repeated experiments are summarized in bar graphs. Significant changes are indicated by asterisks (* $p<0.05$; *** $p<0.001$).**

Treatment of ML-16 and ML-5 with SAHA resulted in a significant increase of SMN protein levels in both cell cultures. The maximum level achieved in ML-16 was 3-fold compared to mock at 5 µM SAHA. At 10 µM, a similar increase of the SMN protein level was observed. ML-5 revealed an up to 2.4-fold increase at 1 µM SAHA. In contrast to ML-16, SMN protein levels decreased again when the cells were incubated with higher drug concentrations (5 µM and 10 µM).

### 4.1.3.2 *SMN2* RNA levels under SAHA treatment

To elucidate the pathway SAHA uses to elevate SMN2 protein levels in SMA fibroblasts, and to compare both drugs SAHA and VPA, ML-16 was incubated with SAHA and RNA was isolated 24 h later. After transcription of RNA into cDNA, a semi-quantitative multiplex PCR was carried out to amplify FL-*SMN2* transcripts, Δ7-*SMN2* transcripts, and *GAPDH* as internal standard. Data analysis was performed (i) by determining the FL-*SMN2 versus* Δ7-*SMN2* transcript ratio as a parameter for an effect on exon 7 inclusion and therefore a reversion of the splicing pattern, and (ii) by determining the
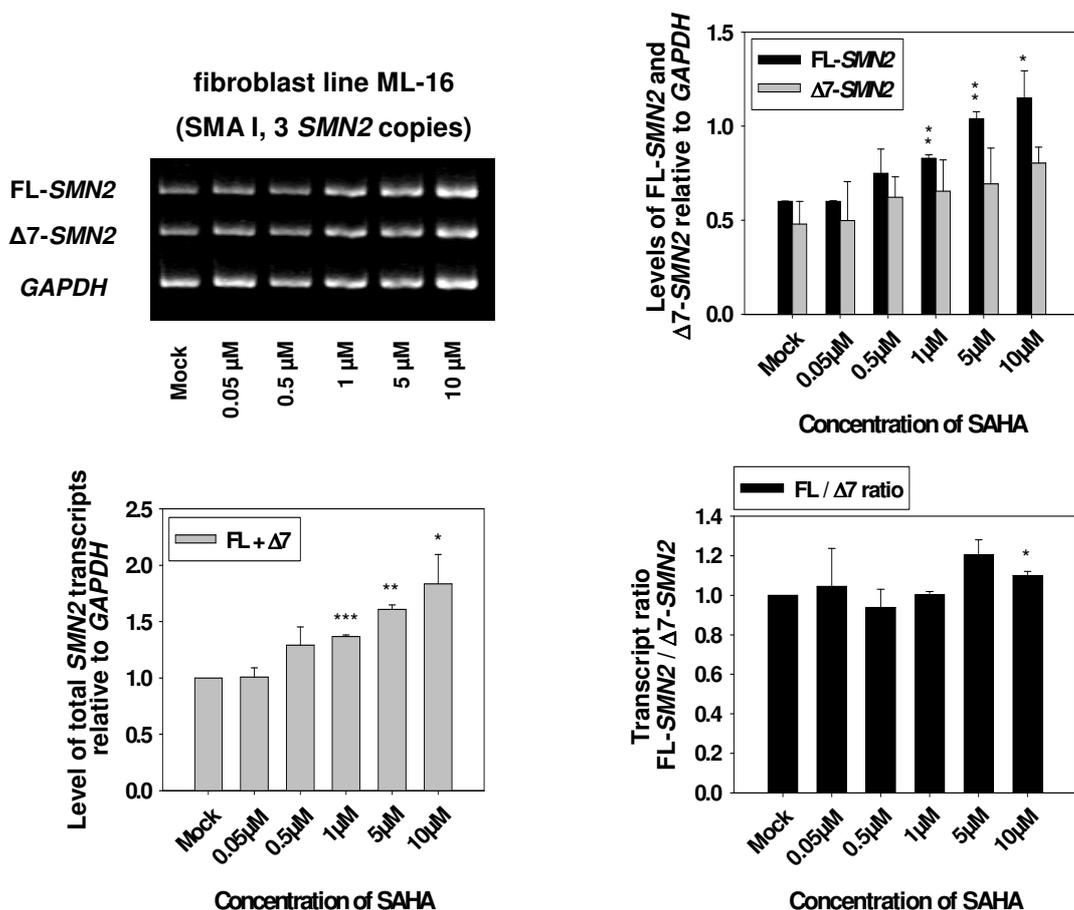


**Figure 18: *SMN2* RNA analysis in SMA fibroblast culture ML-16 after treatment with solvent or increasing concentrations of SAHA (0.05, 0.5, 1, 5, and 10 µM). A representative gel analysis of the semi-quantitative multiplex RT-PCR is given, showing FL-*SMN2*, Δ7-*SMN2*, and the internal standard *GAPDH*. In the bar graphs, mean ± SEM values from repeated experiments are given for the FL-*SMN2* level, the Δ7-*SMN2* level, the level of total *SMN2* transcripts (all of the parameters relative to *GAPDH*), and the FL-*SMN2*/Δ7-*SMN2* ratio. Significant changes are indicated by asterisks (* $p<0.05$; ** $p<0.01$; *** $p<0.001$).**

total amount of *SMN2* transcripts (FL-*SMN2* plu*s* Δ7-*SMN2)* relative to the internal control as parameter for the stimulating effect of VPA on the *SMN2* transcription rate. A representative gel analysis of the RT-PCR and bar graphs which summarize the results obtained for FL-*SMN2*, Δ7-*SMN2*, the FL-*SMN2* versus Δ7-*SMN2* transcript ratio, and the total amount of *SMN2* transcripts is given in figure 18. The corresponding data are given in table 18. Incubation of ML-16 with increasing concentrations of SAHA led to an elevated expression of FL-*SMN2* and Δ7-*SMN2* transcripts, although the changes for Δ7-*SMN2* did not reach significance. FL-*SMN2* levels continuously increased with increasing drug amounts and peaked in an ~1.9-fold up-regulation at 10 µM SAHA. The level of Δ7-*SMN2* reached its maximum at the same concentration showing a ~1.7-fold elevation compared to mock-treated fibroblasts. Consequently, the level of total *SMN2* transcripts was also observed to be significantly elevated under SAHA treatment, suggesting that the overall transcription of the *SMN2* gene was stimulated by the drug.

**Table 18: Levels of FL-*SMN2* RNA, Δ7-*SMN2* RNA, total *SMN2* transcripts FL+Δ7 (relative to *GAPDH*), and the FL/Δ7 ratio in the SMA fibroblast line ML-16. Cells were treated with solvent (mock) or increasing concentrations of SAHA. Average data (± SEM) from repeated experiments are shown, and highest values are marked in bold.**

| Human SMA | | Concentration of SAHA (µM) | | | | | |
|---|---|---|---|---|---|---|---|
| fibroblast culture | | **Mock** | **0.05** | **0.5** | **1** | **5** | **10** |
| | **FL-*SMN2*** | 0.60±0.0 | 0.60±0.0 | 0.75±0.1 | 0.83±0.0 | 1.04±0.0 | **1.15±0.1** |
| **ML-16** | **Δ7-*SMN2*** | 0.48±0.1 | 0.50±0.2 | 0.62±0.1 | 0.66±0.2 | 0.69±0.2 | **0.80±0.1** |
| (SMA I, 3 *SMN2* copies) | **ratio FL/ Δ7** | 1.00±0.0 | 1.04±0.2 | 0.94±0.1 | 1.00±0.0 | **1.20±0.1** | 1.10±0.0 |
| | **FL+ Δ7** | 1.00±0.0 | 1.01±0.1 | 1.29±0.2 | 1.37±0.0 | 1.61±0.0 | **1.83±0.3** |

Analysis of the FL-*SMN2* versus Δ7-*SMN2* ratio revealed slightly increased values at 5 µM and 10 µM SAHA (significant only at 10 µM), whereas the ratio was found unchanged or minimally decreased at the lower drug concentrations. Thus, there is an effect of SAHA on the splicing pattern of *SMN2*, even if the impact is rather weak. This suggests that – at least at the higher SAHA concentrations used in the experiment – two mechanisms contribute to the increase of SMN protein levels in fibroblasts: a stimulation of the *SMN2* transcription rate, and in part a preferential inclusion of *SMN2* exon 7 and a reversion of the *SMN2* splicing pattern toward more FL-*SMN2*.

### 4.1.3.3  Levels of the splicing factor Htra2-β1 under SAHA treatment

The treatment of primary SMA fibroblasts with VPA resulted in an increased transcription of the *SFRS10* gene and elevated levels of the encoded SR-like splicing factor Htra2-β1 (chapter 4.1.2.3). Since Htra2-β1 is able to promote the inclusion of *SMN2* exon 7, this up-regulation might be the cause for the moderate reversion of the pathological *SMN2* splicing pattern obtained under VPA treatment. To check whether SAHA is also able to stimulate the expression of Htra2-β1 and to further investigate if there is a correlation with the weak impact of higher SAHA concentrations (5 µM and 10 µM) on the

FL-*SMN2*/Δ7-*SMN2* transcript ratio, a quantitative western blot analysis was performed on the protein extracts isolated from fibroblast lines ML-16 and ML-5 after treatment with increasing concentrations of SAHA for 24 h. Membranes were re-probed with an anti-Htra2-β1 antibody. As already described, β-tubulin staining was used to confirm loading of the gels with equal protein amounts. The results including representative western blots, and the cumulative data obtained from repeated experiments in different passages of each fibroblast line are given in figure 19 and table 19.
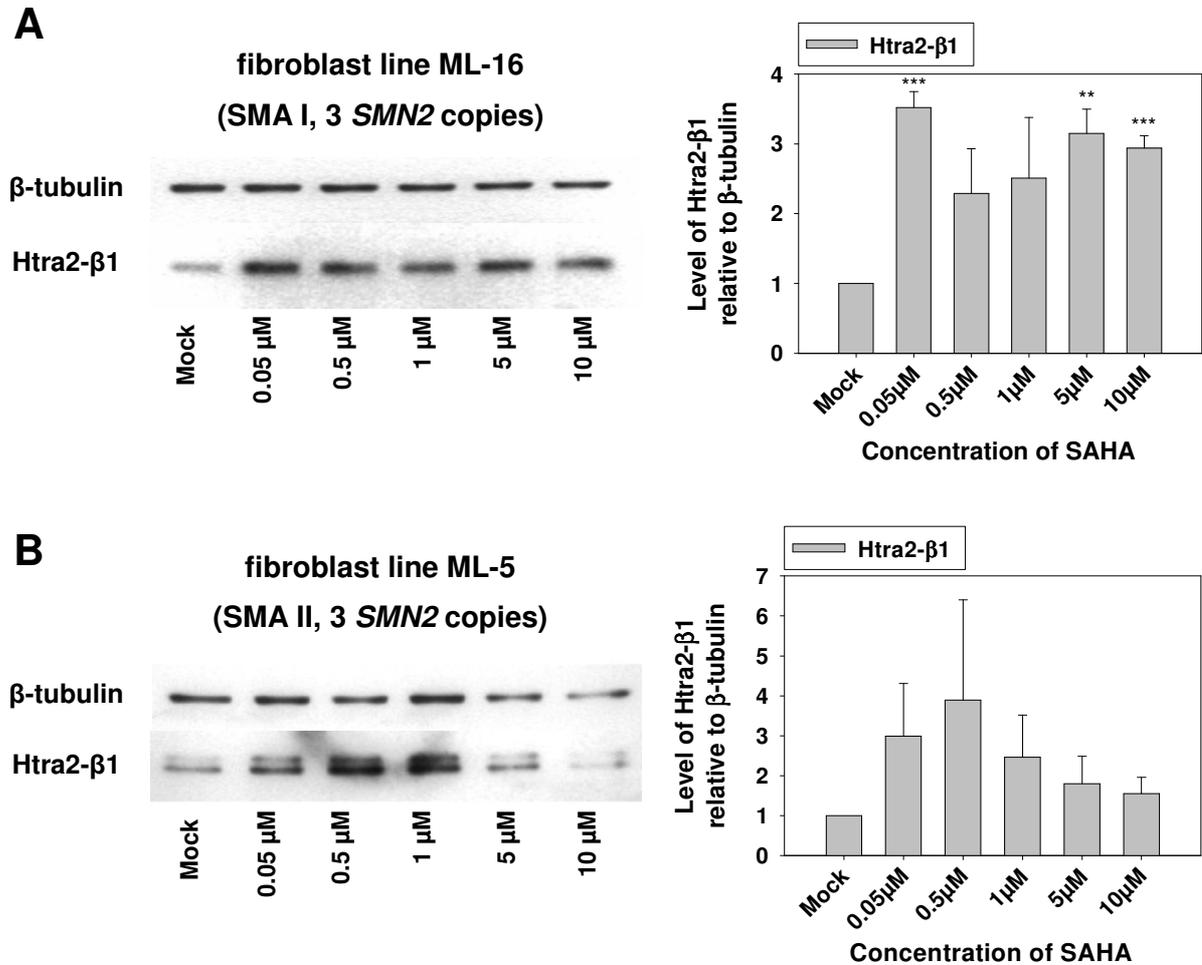


**Figure 19: Level of the splicing factor Htra2-β1 in SMA fibroblast cultures ML-16 *(A)* and ML-5 *(B)* treated with solvent (mock) or increasing concentrations of SAHA (0.05, 0.5, 1, 5, and 10 µM) for 24 h. For each fibroblast line, a representative western blot is given with β-tubulin serving as loading control. Mean values ± SEM for the level of Htra2-β1 relative to β-tubulin obtained from repeated experiments are summarized in bar graphs. Two bands for Htra2-β1 on the western blot result from the phosphorylated and the unphosphorylated form of the protein. Significant changes are indicated by asterisks (** p<0.01; *** p<0.001).**

Treatment of ML-16 and ML-5 with the second-generation HDAC inhibitor SAHA resulted in increased Htra2-β1 protein levels. ML-16 showed a maximum of 3.5-fold compared to untreated cells with markedly elevated levels at all concentrations used throughout the experiment and significant changes at 0.05, 5, and 10 µM SAHA. Thus, the augmentation of Htra2-β1 might be responsible for the increase of the FL-*SMN2*/Δ7-*SMN2* transcript ratio observed at higher SAHA concentrations in ML-16.

However, at lower SAHA concentrations (0.05 µM to 1 µM), the *SMN2* splicing was not shifted toward FL-*SMN2* (chapter 4.1.3.2), although Htra2-β1 levels were clearly increased (figure 19 and table 19). In contrast to ML-16, fibroblast line ML-5 revealed Htra2-β1 levels which peaked at 0.5 µM SAHA and decreased at SAHA concentrations of 1 µM and above. Moreover, the variation between the different investigated passages of ML-5 was much higher than that between the passages of ML-16 as indicated by the much higher SEM values, and the lack of significance in ML-5.

**Table 19: Levels of Htra2-β1 (relative to β-tubulin) in SMA fibroblast lines ML-16 and ML-5 after treatment with the second-generation HDAC inhibitor SAHA. Average data (± SEM) from repeated experiments are shown, and highest levels are marked in bold.**

| Human SMA fibroblast | | Concentration of SAHA (µM) | | | | | |
|---|---|---|---|---|---|---|---|
| culture | | Mock | 0.05 | 0.5 | 1 | 5 | 10 |
| **ML-16** | (SMA I, 3 *SMN2* copies) | 1.0±0.0 | **3.5±0.2** | 2.3±0.6 | 2.5±0.9 | 3.2±0.4 | 2.9±0.2 |
| **ML-5** | (SMA II, 3 *SMN2* copies) | 1.0±0.0 | 3.0±1.3 | **3.9±2.5** | 2.5±1.1 | 1.8±0.7 | 1.6±0.4 |

### 4.1.3.4 Cytotoxicity of SAHA in SMA fibroblast cultures

To elucidate whether SAHA exerts any toxic effect on SMA fibroblasts during the incubation period, an MTT assay was performed and the viability of cells was measured using the ability of living cells to convert thiazolyl blue tetrazolium bromide into detectable violet formazan crystals. Fibroblasts were incubated with solvent (mock) or increasing concentrations of SAHA including 0.05, 0.5, 1, 5, and 10 µM for 24 h. As it is visible in the diagram in figure 20, survival of the cells did not appear to be affected under SAHA treatment, suggesting that the drug was well tolerated by the cells.
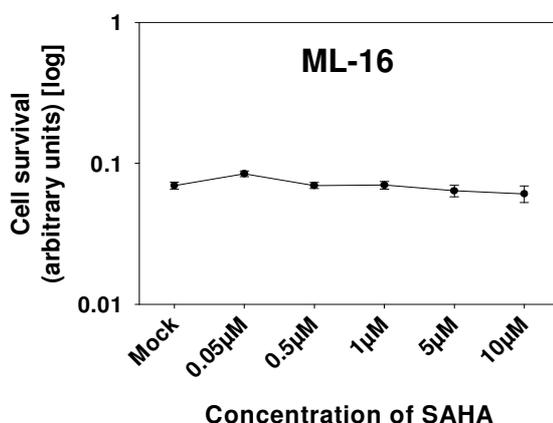


**Figure 20: MTT assay with fibroblast line ML-16. Cells were treated with solvent (mock) or increasing concentrations of SAHA (0.05, 0.5, 1, 5, and 10 µM). Values for the absorption (corresponding to cell survival) are given as mean ± SEM.**

## 4.1.4    Treatment of SMA fibroblast cultures with MS-275

Another second-generation HDAC inhibitor which evolved from the systematic development of and screening for promising compounds which are able to induce histone hyperacetylation and thus act as antitumor agents is MS-275 (Jung et al. 1999; Saito et al. 1999). Structurally, MS-275 is characterized as benzamide. Like SAHA, the compound is very potent, and able to inhibit HDACs at low micromolar concentrations (Saito et al. 1999; Prakash et al. 2001). MS-275 has been shown to have a considerably higher inhibitory activity against class I versus class II HDACs (Miller et al. 2003). Moreover, it inhibits HDAC 1 much more effectively than HDAC 3 (Hu et al. 2003). Similar to SAHA, MS-275 has entered into phase I clinical trials in patients with solid tumors and lymphoma. An increased accumulation of acetylated histones in peripheral blood mononuclear cells was observed at all dose levels after oral administration (Ryan et al. 2005). Further studies are ongoing to optimize the oral treatment schedule.

To check if MS-275 is a candidate for an SMA therapy and able to increase the level of SMN protein derived from the *SMN2* gene *in vitro*, the fibroblast assay described in chapter 4.1.2.1 was applied again. Additionally, due to the facts that MS-275 belongs to another structural class of HDAC inhibitors than VPA and SAHA, and that MS-275 appears to have at least some HDAC selectivity, the investigation of MS-275 was considered as promising to gain general knowledge about the principles that underlie the stimulation of *SMN2* expression.

### 4.1.4.1  Impact of MS-275 on SMN2 protein levels

Similar to SAHA, MS-275 is known to be active at low micromolar levels (Saito et al. 1999; Marks et al. 2004). Therefore, in comparison to the experiments carried out with VPA and butyrate, much lower drug concentrations were selected for the treatment of fibroblast cells including 0.05, 0.25, 0.5, 1, and 5 µM MS-275. Additionally, these concentrations covered a broad range. Each experiment also included mock-treated cells which were incubated with solvent (DMSO) only. Fibroblast line ML-16 (derived from an SMA type I patient with 3 *SMN2* copies) was treated with increasing concentrations of MS-275 for varying time periods including 16 h, 20 h, 24 h, and 48 h. Subsequently, protein extracts

**Table 20: SMN protein levels (relative to β-tubulin) in SMA fibroblast line ML-16 after 24 h - treatment with the second-generation HDAC inhibitor MS-275, a drug from the benzamide class that shows partial HDAC selectivity. Average data (± SEM) from repeated experiments are shown and highest level is marked in bold.**

| Human SMA fibroblast culture | | Concentration of MS-275 (µM) | | | | | |
|---|---|---|---|---|---|---|---|
| | | Mock | 0.05 | 0.25 | 0.5 | 1 | 5 |
| **ML-16** | (SMA I, 3 *SMN2* copies) | 1.0±0.0 | 1.2±0.1 | 1.3±0.1 | **1.4±0.1** | 1.3±0.2 | 0.7±0.1 |

were prepared and western blot analysis was performed using antibodies against SMN and β-tubulin. The latter served as control to confirm that the gels were loaded with equal amounts of each protein sample. The up-regulation of the SMN protein level under MS-275 treatment was significant, but never very pronounced, suggesting that the potential of MS-275 to stimulate the expression of SMN protein derived from the *SMN2* gene is very limited, and by far not sufficient to further consider the drug for a potential SMA therapy. The highest SMN protein level achieved under MS-275 treatment was a 1.4-fold increase at 0.5 µM MS-275 after 24 h of incubation. Treatment of the fibroblasts with 5 µM MS-275 for 24 h even revealed a minimal decrease of the SMN protein level. A representative western blot together with a bar graph for the average data obtained from repeated treatment of different fibroblast passages of ML-16 with MS-275 for 24 h is displayed in figure 21. The corresponding values for the means ± SEM are given in table 20.
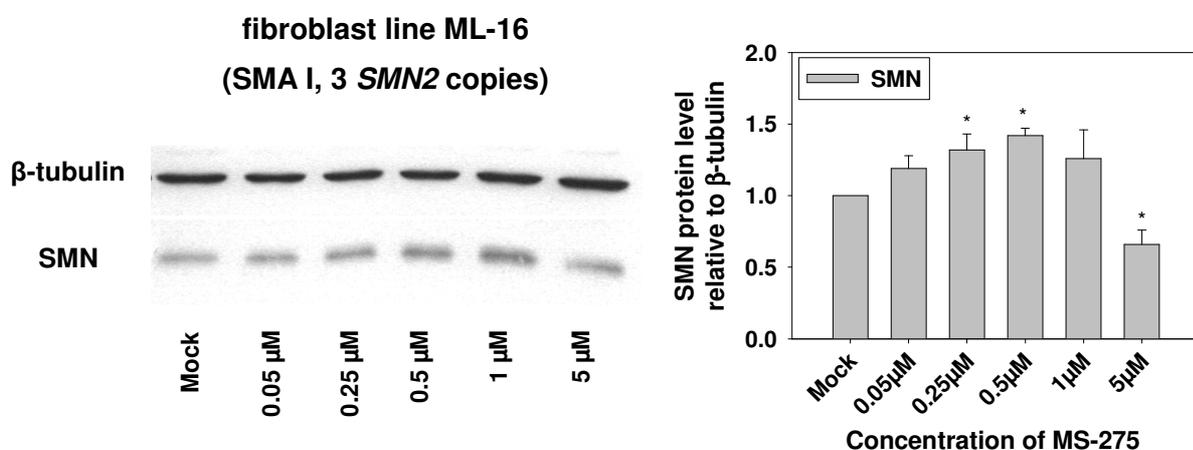


**Figure 21: Treatment of ML-16 with solvent (mock) or increasing concentrations of MS-275 (0.05, 0.25, 0.5, 1, and 5 µM) for 24 h. A representative western blot is given which was probed with antibodies against β-tubulin (loading control) and SMN. Mean values ± SEM for the SMN protein level relative to β-tubulin obtained from repeated experiments in different cell passages are summarized in the bar graph. Significant changes are indicated by asterisks (* p<0.05).**

### 4.1.4.2 *SMN2* RNA expression under MS-275 treatment

To confirm that MS-275 indeed is not able to stimulate the expression or regulate the splicing pattern of the *SMN2* gene in SMA fibroblasts, and to exclude that the lack of an elevated SMN2 protein level under MS-275 treatment is due to an effect on translational processes which inhibits the translation of FL-*SMN2* transcripts, RNA was isolated from ML-16 after treatment with MS-275 for 16 h, 20 h, and 24 h. After reverse transcription, a semi-quantitative PCR was performed to amplify FL-*SMN2* transcripts, Δ7-*SMN2* transcripts, and *GAPDH* as internal control. Regardless of the treatment time and the concentration of MS-275, data analysis revealed neither an increase of the FL-*SMN2* versus Δ7-*SMN2* transcript ratio, nor of the level of FL-*SMN2*, Δ7-*SMN2* or the level of total *SMN2* transcripts. The results rather suggested a down-regulation in particular of FL-*SMN2* and the total *SMN2*
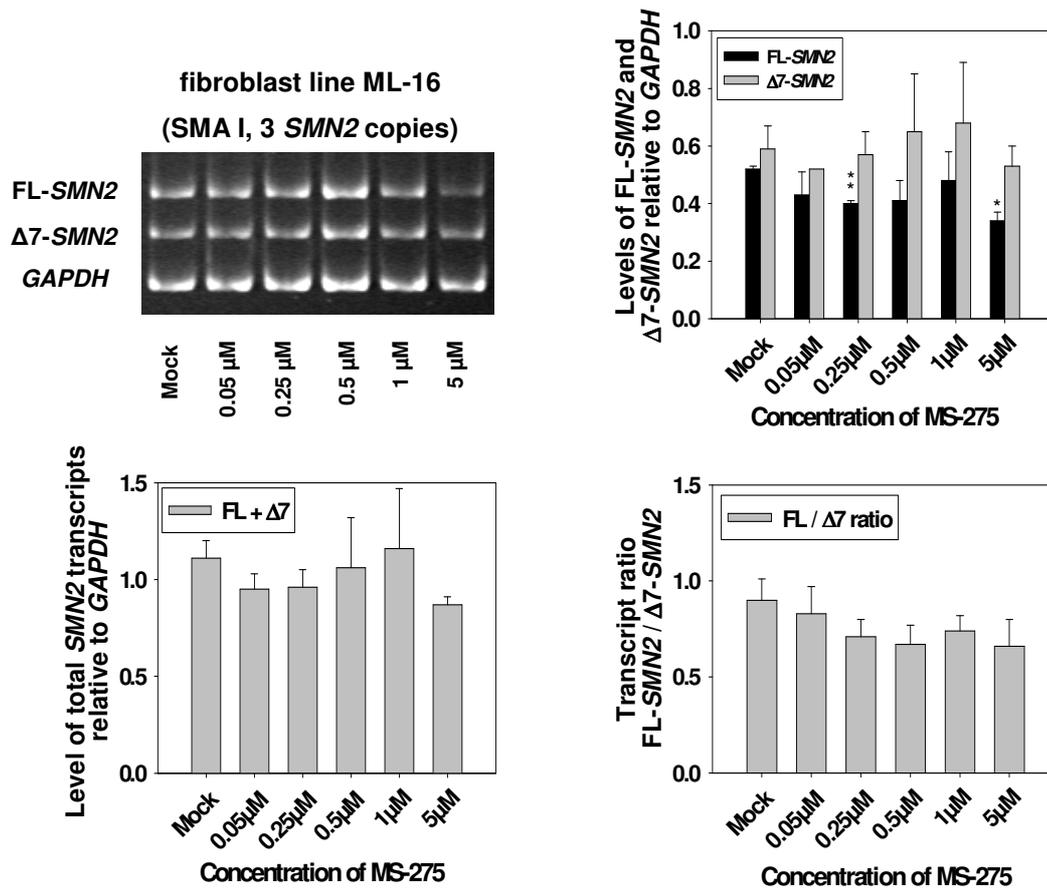
**Figure 22:** *SMN2* RNA analysis in SMA fibroblast culture ML-16 after treatment with solvent or increasing concentrations of MS-275 (0.05, 0.25, 0.5, 1, and 5 µM) for 24 h. A representative gel analysis of the semi-quantitative multiplex RT-PCR is given, showing FL-*SMN2*, Δ7-*SMN2*, and the internal standard *GAPDH*. In the bar graphs, mean ± SEM values from repeated experiments are given for the FL-*SMN2* level, the Δ7-*SMN2* level, the level of total *SMN2* transcripts (all of the parameters relative to *GAPDH*), and the FL-*SMN2*/Δ7-*SMN2* ratio. Significant changes are indicated by asterisks (* p<0.05; ** p<0.01).

**Table 21:** Levels of FL-*SMN2* RNA, Δ7-*SMN2* RNA, total *SMN2* transcripts FL+Δ7 (relative to *GAPDH*), and the FL/Δ7 ratio in the SMA fibroblast line ML-16. Cells were treated with solvent (mock) or increasing concentrations of MS-275 (0.05, 0.25, 0.5, 1, and 5 µM) for 24 h. Average data (± SEM) from repeated experiments are shown, and lowest values are marked in bold.

| Human SMA | | Concentration of MS-275 (µM) | | | | | |
|---|---|---|---|---|---|---|---|
| fibroblast culture | | Mock | 0.05 | 0.25 | 0.5 | 1 | 5 |
| | FL-*SMN2* | 0.52±0.0 | 0.43±0.1 | 0.40±0.0 | 0.41±0.1 | 0.48±0.1 | **0.34±0.0** |
| **ML-16** | Δ7-*SMN2* | 0.59±0.1 | **0.52±0.0** | 0.57±0.1 | 0.65±0.2 | 0.68±0.2 | 0.53±0.1 |
| (SMA I, 3 *SMN2* copies) | ratio FL/ Δ7 | 0.90±0.1 | 0.83±0.1 | 0.71±0.1 | 0.67±0.1 | 0.74±0.1 | **0.66±0.1** |
| | FL+ Δ7 | 1.11±0.1 | 0.95±0.1 | 0.96±0.1 | 1.06±0.3 | 1.16±0.3 | **0.87±0.0** |

transcripts after 24 h of drug treatment which was most visible at 5 µM MS-275. This corresponds with the decrease of the SMN protein level observed at 5 µM MS-275. Since the down-regulation was more pronounced for the FL-*SMN2* transcript and not visible for the Δ7-*SMN2* transcript, a slight decrease of the transcript ratio was measured. This was not significant, but a tendency was visible with increasing concentrations of MS-275, suggesting a negative impact of the drug on *SMN2* exon 7 inclusion. The RT-PCR data obtained after treatment of fibroblasts with MS-275 for 24 h are given in figure 22 and table 21.

### 4.1.4.3  Level of the splicing factor Htra2-β1 under MS-275 treatment

To further characterize the effect of MS-275 on SMA fibroblasts, and to compare the drug with the HDAC inhibitors SAHA, VPA, and butyrate, the level of the splicing factor Htra2-β1 was investigated in protein extracts obtained after incubation of ML-16 with increasing drug concentrations for 24 h. Western blot membranes were re-probed with an antibody against Htra2-β1, and β-tubulin was used
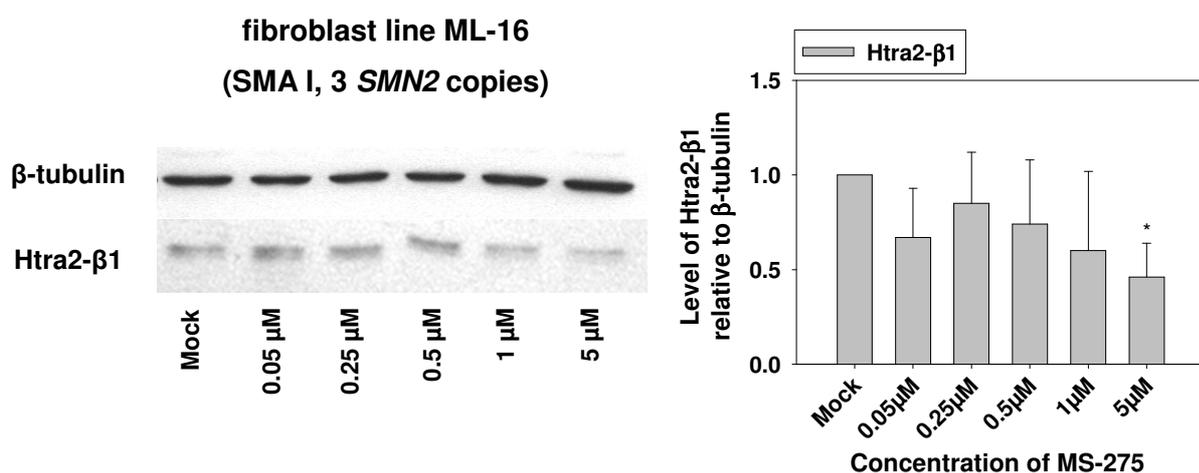


**Figure 23: Level of the splicing factor Htra2-β1 in SMA fibroblast culture ML-16 treated with solvent (mock) or increasing concentrations of MS-275 (0.05, 0.25, 0.5, 1, and 5 µM) for 24 h. A representative western blot is given with β-tubulin serving as loading control. Mean values ± SEM for the level of Htra2-β1 relative to β-tubulin obtained from repeated experiments are summarized in the bar graph. Significant changes are indicated by asterisks (* p<0.05).**

**Table 22: Level of Htra2-β1 (relative to β-tubulin) in SMA fibroblast line ML-16 after treatment with the benzamide MS-275. Average data (± SEM) from repeated experiments are shown, and the lowest level is marked in bold.**

| Human SMA fibroblast | | Concentration of MS-275 (µM) | | | | | |
|---|---|---|---|---|---|---|---|
| | culture | Mock | 0.05 | 0.25 | 0.5 | 1 | 5 |
| **ML-16** | (SMA I, 3 *SMN2* copies) | 1.0±0.0 | 0.67±0.3 | 0.85±0.3 | 0.74±0.3 | 0.60±0.4 | **0.46±0.2** |

as loading control. As demonstrated in figure 23 and table 22, Htra2-β1 levels show the tendency to be slightly decreased under drug treatment, which was most obvious and significant at 5 µM MS-275. This correlates well with the decreased transcript ratio seen on RNA level (chapter 4.1.4.2).

### 4.1.4.4  Cytotoxicity of MS-275 in SMA fibroblast cultures

ML-16 fibroblasts were incubated with increasing concentrations of MS-275 for 24 h to examine whether the drug exerts any toxic effects on these cells. After incubation with the drug, an MTT assay was performed, and cell survival was measured using the ability of viable cells to convert thiazolyl blue tetrazolium bromide into detectable violet formazan crystals. The average data are summarized in figure 24. They clearly demonstrate that MS-275 was not causing increased cell death. Even the highest drug concentration of 5 µM was well tolerated by the cells.
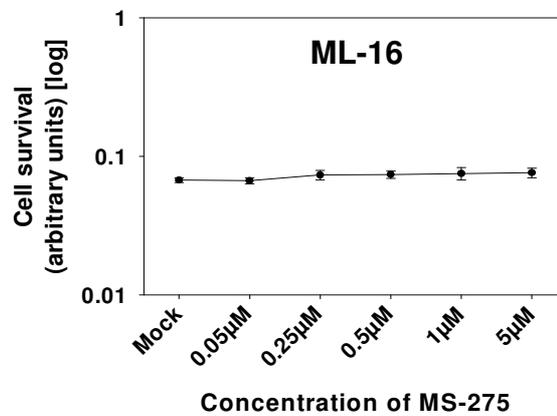


**Figure 24: MTT assay with fibroblast line ML-16. Cells were treated with solvent (mock) or increasing concentrations of MS-275 (0.05, 0.25, 0.5, 1, and 5 µM). Values for the absorption (corresponding to cell survival) are given as mean ± SEM.**

## 4.2 *Ex vivo* experiments with valproic acid in organotypic hippocampal slice cultures (OHSCs) from rat

### 4.2.1 Treatment of OHSCs with valproic acid

SMA is a neuromuscular disorder which is caused by degeneration of α-motor neurons in the spinal cord. Thus, when developing a drug for a potential SMA therapy, it has to be considered that this compound must be able to pass the blood-brain-barrier to reach its therapeutic target, and to stimulate SMN protein expression in neuronal cells. So far, it is unclear whether SAHA and MS-275 are able to cross the blood-brain-barrier in humans. VPA is among a very few HDAC inhibitors which are known to reach the central nervous system (CNS) after oral or intravenous administration. This is also one of the basic requirements for the successful use of the drug in epilepsy therapy. In SMA fibroblasts, it was clearly demonstrated that VPA elevates the level of SMN protein by increasing the transcription of *SMN2* and a partial reversion of the pathological *SMN2* splicing pattern. To investigate in more detail whether VPA is also able to up-regulate SMN protein levels in neuronal tissue would be another important step to further consider the drug as promising for a potential SMA therapy. Most of the native tissues derived from the CNS, however, hardly survive in culture, are not well established and very fragile, or do not provide enough material to perform western blotting and RT-PCR after drug treatment. An extremely potent drug screening and drug validation tool available for CNS disorders is the use of organotypic hippocampal slice cultures (OHSCs) from rat (Stoppini et al. 1991; Savaskan et al. 2000). In contrast to humans, rodents carry one *Smn* gene only, which is not subject to alternative splicing. However, rat OHSCs provide an excellent *ex vivo* system to study the impact of VPA on rat *Smn* (*rSmn*) transcription and rSmn protein levels.

#### 4.2.1.1 Transcriptional activity of *rSmn* under valproic acid treatment

Since humans and rats are known to metabolize VPA differently [the terminal half-life of VPA in humans is 9-18 h and in rats 2-5 h, respectively (Johannessen 2000; Sands et al. 2000)], the experimental conditions used for the treatment of human SMA fibroblasts with VPA (chapter 4.1.2) could not be applied to the treatment of rat tissue. Thus, the optimal drug concentrations and time periods for the stimulation of the OHSCs were initially determined in a set of pilot experiments. Due to the shorter terminal-half life of VPA in rats than in humans, it was most likely that higher drug concentrations are required to achieve a potential effect on *rSmn* transcription. Moreover, in comparison to the experiments performed in fibroblasts, the incubation time of rat OHSCs with VPA was increased, since the drug was expected to need more time for penetration into the tissue slices than into cell monolayers. Consequently, different concentrations of VPA (50 $\mu$M, 500 $\mu$M, and 2000 $\mu$M) were added to the OHSCs which were harvested after 48 h. RNA was isolated and the expression of *rSmn* was analyzed by quantitative real-time RT-PCR using the level of *β-actin* transcripts as internal reference. Since the *rSmn* gene is not subject to alternative splicing, a potential

**A**



**B**
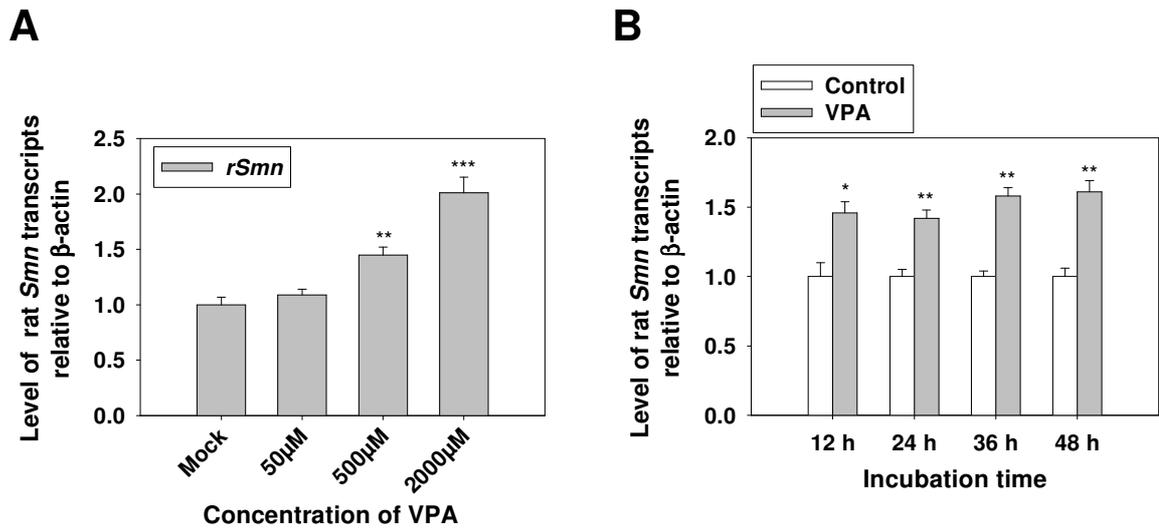


**Figure 25: Level of rat *Smn* (*rSmn*) transcripts in organotypic hippocampal slice cultures from rats after treatment with VPA. RNA analysis was carried out by quantitative real-time RT-PCR on an ABI Prism 7700 TaqMan machine using *β-actin* transcripts as internal control. For each experiment, average data ± SEM from repeated measurements are given. Significant changes are indicated by asterisks (\* p<0.05; \*\* p<0.01; \*\*\* p<0.001). *(A)*. Within a dose-finding experiment, OHSCs were treated with solvent (mock) or increasing concentrations of VPA (50, 500, and 2000 µM) for 48 h. Analysis revealed that 2 mM VPA was the most effective drug concentration to stimulate *rSmn* expression. *(B)*. Incubation of OHSCs with 2 mM VPA for different time periods (12, 24, 36, and 48 h). For each single incubation time, control OHSCs were included and treated with solvent only (mock). A period of 48 h was determined to achieve best results for the treatment of OHSCs with VPA.**

**Table 23: Evaluation of the optimal drug concentration and the optimal incubation period for the treatment of rat OHSCs with the HDAC inhibitor VPA. Average data ± SEM from repeated measurements are shown, and highest levels are marked in bold. For each experiment, control OHSCs were included and treated with solvent only (mock).**

| Dose-finding experiment | Concentration of VPA | Mock | 50 µM | 500 µM | 2000 µM |
|---|---|---|---|---|---|
| | *rSmn* | 1.00±0.1 | 1.09±0.1 | 1.45±0.1 | **2.01±0.1** |
| Evaluation optimal time period | Incubation time with 2 mM VPA | 12 h | 24 h | 36 h | 48 h |
| | *rSmn* (Control vs. VPA) | 1.00±0.1 vs. 1.46±0.1 | 1.00±0.1 vs. 1.42±0.1 | 1.00±0.0 vs. 1.58±0.1 | **1.00±0.1** **vs.** **1.61±0.1** |

VPA-dependent up-regulation of *rSmn* transcripts in rat OHSCs would solely be triggered by transcriptional activation. A significant increase in the expression of *rSmn* mRNA was observed at VPA concentrations of 500 and 2000 µM (figure 25 A and table 23). The maximum increase of the *rSmn* level was 2.0fold compared with mock-treated OHSCs and achieved at 2 mM VPA. After determining the most effective VPA concentration (2 mM), OHSCs were stimulated with this concentration for different time periods (12, 24, 36, and 48 h). Compared with the data obtain after 12 h, the *rSmn* expression was slightly increased at 36 and 48 h, with a maximum elevation of about 1.6fold compared to untreated OHSCs at 48 h (figure 25 B and table 23).

(These experiments were kindly performed by Dr. E. Hahnen at the Institute of Neuropathology, University Erlangen-Nuremberg, Erlangen, Germany. Since 2004, Dr. E. Hahnen is working in our laboratory at the Institute of Human Genetics.)

### 4.2.1.2 Impact of valproic acid on rSmn protein levels

To validate the experiments described above on protein level, OHSCs were stimulated with the optimal concentration of 2 mM VPA for 48 h in a final experiment and analysis of the rSmn protein was performed. Protein extracts were prepared from OHSCs and used for western blotting. The membrane was probed with an antibody against rSmn and an antibody against β-actin. The latter protein served as control to confirm that the gels were loaded with equal amounts of each protein sample. As displayed in figure 26, VPA treatment induced a clear up-regulation of rSmn protein levels in rat OHSCs. Compared to the average rSmn level in the three untreated mock slices (1.00±0.1), an average elevation of 1.8fold±0.0 was achieved after incubation with VPA. This result confirmed the data obtained on RNA level and strongly suggested that VPA is able to increase SMN/rSmn protein levels not only in fibroblasts, but also in neuronal tissue.
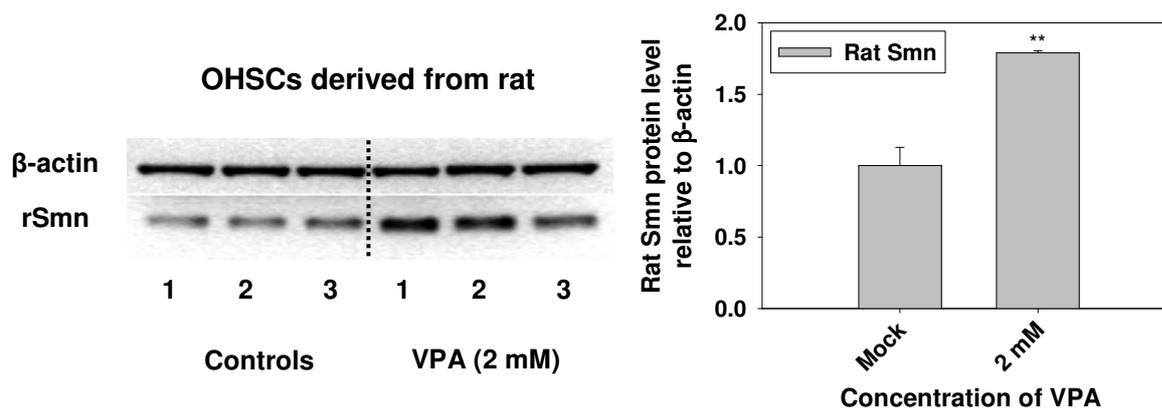


**Figure 26: Treatment of OHSCs with solvent (mock, controls) or 2 mM VPA for 48 h. The western blot shows the analysis of the protein extracts derived from three single rat OHSCs. The membrane was probed with antibodies against β-actin (loading control) and rSmn. The average data ± SEM for the rSmn protein levels in the slices (relative to β-actin) are summarized in the bar graph. Significant changes are indicated by asterisks (** $p < 0.01$).**

### 4.2.1.3 Effect of valproic acid on the level of the splicing factors Tra2-β1 and SF2/ASF in OHSCs

Although *rSmn* is not alternatively spliced and thus a potential over-expression of the splicing factor Htra2-β1 by HDAC inhibitors is of lower interest in rats than in humans, the levels of rat Tra2-β1 and SF2/ASF were studied in VPA-treated OHSCs to compare their regulation with the results obtained in primary human SMA fibroblasts. Western blot membranes obtained from protein extracts of OHSCs incubated with 2 mM VPA for 48 h were re-probed with antibodies against Htra2-β1 (also detects rat Tra2-β1) and SF2/ASF. As described above, β-actin was used as loading control to confirm equal loading of the membranes with protein of each sample. The analysis revealed a moderate increase of the rat Tra2-β1 levels (mock: 1.00±0.1 versus VPA: 1.42±0.2), and a much more pronounced significant elevation of the levels of SF2/ASF (mock: 1.00±0.1 versus VPA: 3.1±0.1). The results are summarized in figure 27.
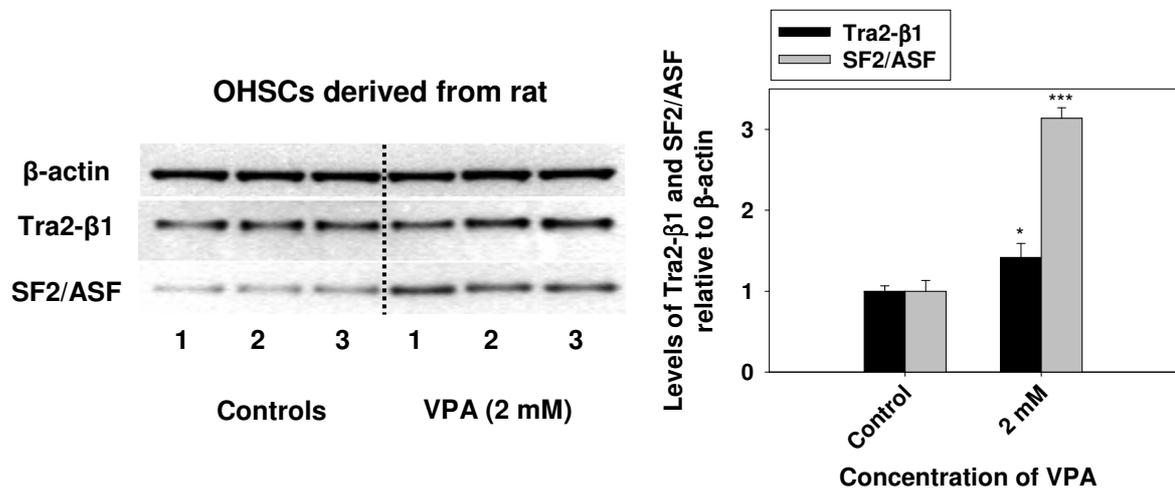


**Figure 27: Treatment of OHSCs with solvent (mock, controls) or 2 mM VPA for 48 h. The western blot shows the analysis of the protein extracts derived from three single rat OHSCs. The membrane was probed with antibodies against β-actin (loading control), Htra2-β1, and SF2/ASF. The average data ± SEM for the splicing factor levels in the rat slices (relative to β-actin) are summarized in the bar graph. Significant changes are indicated by asterisks (\* p<0.05; \*\*\* p<0.001).**

## 4.3    *In vivo* effect of valproic acid on *SMN* gene expression in SMA carriers and SMA patients

Among the investigated compounds, VPA and SAHA markedly elevated the SMN2 protein levels in SMA fibroblasts *in vitro* and thus evolved as promising candidates for a potential SMA therapy. Moreover, it was demonstrated in organotypic hippocampal slice cultures from rat that VPA increases the rSmn protein level in neuronal tissue *ex vivo*. Following the standard protocols for the development of novel therapeutics, the investigation of the *in vivo* effect of these compounds on *SMN* gene expression in an animal model (e.g., an SMA mouse model) would be the next step to follow the *in vitro* and *ex vivo* experiments. However, the terminal half-life of VPA in mice (0.8 h) is completely different compared with that in humans (9-18 h) (Johannessen 2000) which makes the treatment of mice with VPA rather inappropriate to evaluate the *in vivo* drug efficiency. Importantly, VPA is not a novel drug, but a compound which is approved by the Food and Drug Administration (FDA) for application to humans. It is clinically well known and successfully used in long-term therapy of epilepsy as well as for the treatment of mood disorders and migraine (Spina and Perugi 2004). Thus, based on the results obtained with VPA *in vitro* and *ex vivo*, a very straight-forward approach is possible and the drug can directly be administered to humans to study its effect on *SMN* gene activity.

To evaluate whether VPA exerts an effect on *SMN* expression in humans *in vivo*, the collection of tissue samples from drug-treated individuals is required. The only biological material which can easily be collected in sufficient amounts and several times throughout treatment is native blood. This is a tissue not affected by SMA, but both genes *SMN1* and *SMN2* are expressed in blood cells.

One of the most important challenges regarding the analysis of *SMN* RNA levels in blood collected from humans treated with VPA is the evaluation of a suitable endogenous control for the normalization of target transcripts. The comparison of *SMN* transcript levels in blood collected before and throughout drug treatment requires an endogenous control which is stable over time (at least over several weeks). Moreover, expression of the endogenous control gene must not be influenced by VPA. Finally, if the comparison of *SMN* transcript levels among different individuals is planned, the endogenous control gene must be expressed at equal levels in these subjects.

### 4.3.1    Screening for a suitable endogenous control: Expression analysis of selected (housekeeping) genes in blood

To investigate whether VPA or any other HDAC inhibitor is able to increase human *SMN* RNA expression in blood, *SMN* transcript levels have to be compared in samples taken before and throughout drug treatment. A common method to normalize target transcript levels is the simultaneous measurement of the transcript levels of an endogenous control gene in each sample. Subsequently, the levels of the target transcript are calculated relative to those of the endogenous control. To evaluate an endogenous control which is stably expressed over time, stably expressed in different individuals, and whose expression is not influenced by VPA, several candidates have been investigated in more detail.

### 4.3.1.1  Applicability of *CTLA1* transcript levels for the normalization of *SMN* transcripts in peripheral blood

In 2003, a genome-wide genetic analysis of the natural variability in gene expression was carried out in human lymphoblastoid cell lines (Cheung et al. 2003). To identify the genes with the most variable and least variable transcript levels, cDNA microarrays containing about 5,000 randomly selected cDNA clones were used. Based on the data obtained from the cell lines of 35 unrelated individuals, two rankings were composed: one with the top 100 variant genes, and a second one with the top 100 nonvariable genes (personal communication Vivian Cheung).

Although the study was performed in EBV-transformed lymphoblastoid cell lines and not in native blood, the ranking with the nonvariable genes was screened for potential candidates that might serve as endogenous control to normalize *SMN* transcript levels before/throughout VPA treatment during a clinical trial in humans. A housekeeping gene was not identified among the top 100 nonvariable genes. Housekeeping genes are constitutively expressed in all tissues and commonly applied as endogenous controls. However, another promising candidate among the least variable genes was *CTLA1* (*cytotoxic T-lymphocyte-associated serine esterase 1*). *CTLA1* does not belong to the class of housekeeping genes, but is highly expressed in native whole blood (Gene Expression Atlas database). Thus, it was selected to be investigated in more detail.

Since native blood would be the only tissue to be investigated during a clinical trial with HDAC inhibitors, high expression of *CTLA1* in native blood would be sufficient to use this gene as endogenous control. Expression in all human tissues – comparable to a housekeeping gene – is not necessarily required. However, an important prerequisite is the expression of *CTLA1* in all types of blood cells. Thus, expression of the gene was checked in various blood cell fractions using the Human Blood Fractions MTC Panel. The panel contains cDNA preparations from nine different human blood cell fractions together with human placenta control cDNA. Real-time PCR analysis of *CTLA1* expression revealed that two cell populations (resting CD4-positive cells and resting CD19-positive cells) do not express *CTLA1* (figure 28, see appendix page XVII, table B.1 for corresponding data). This result was confirmed with the control cDNA from placenta which is known to be negative for *CTLA1* expression. Consequently, *CTLA1* transcripts are not suitable as endogenous control, because cell type heterogeneity between blood samples collected throughout a clinical trial might become a potential source of variability.

The remaining cell populations clearly expressed *CTLA1*. The transcript levels appeared to be different, however, a quantitative conclusion about the expression level cannot be drawn from the investigated panel. The cDNAs are normalized with three different housekeeping genes (*GAPDH*, *β-actin*, and *α-tubulin*) by the manufacturer, such that from each cell fraction roughly the same cDNA amount was used for investigation of expression. However, according to the manufacturer's information, the normalization of the cDNAs only allows qualitative studies, but is not exact enough to allow for a quantification and comparison of transcript levels. Moreover, the single cDNA fractions are obtained from different donors and different numbers of donors which further restricts the use of the panel only to qualitative purposes.
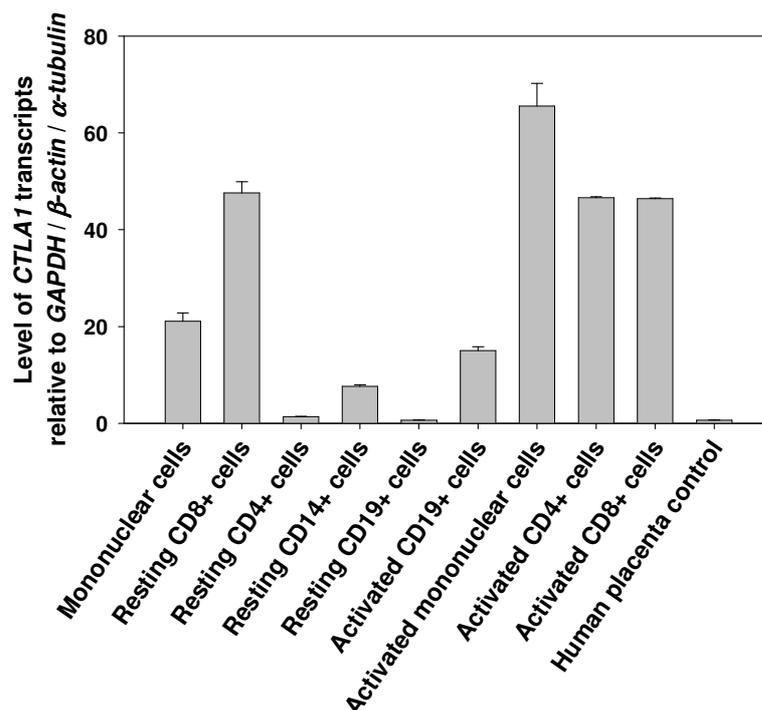
**Figure 28: Real-time PCR analysis of *CTLA1* transcript levels in human blood cell fractions. Measurement of each sample was repeated at least twice, and the resulting data are given as mean ± SEM. "+" is the abbreviation for "positive". The investigation was carried out using the Human Blood Fractions MTC Panel which contains cDNAs from nine different blood cell fractions together with a control cDNA derived from human placenta. *CTLA1* is not expressed in resting CD4+ cells, resting CD19+ cells, and human placenta. Thus, *CTLA1* cannot be used as endogenous control to normalize *SMN* target transcripts in whole blood samples collected throughout a clinical trial with HDAC inhibitors, because cell type heterogeneity between the collected blood samples might become a source for variability.**

## 4.3.1.2 Natural expression variation of the housekeeping genes *RPLP0*, *B2M*, *PPIB*, and *GUSB* in peripheral whole blood

Another approach to identify a suitable endogenous control for the normalization of *SMN* target transcripts in whole blood samples collected throughout a clinical trial covered the investigation of a selected number of housekeeping genes. The application of housekeeping genes for normalization is very common, however, data about the stability of their expression in certain tissues over time and among different individuals are rather rare. Thus, an expression study was set up, including *human acidic ribosomal phosphoprotein P0* (*RPLP0*), *cyclophilin B* (*PPIB*), and *β-glucuronidase* (*GUSB*), all of which have been reported previously to be stably expressed in human peripheral whole blood and cultured peripheral blood mononuclear cells, respectively (Loseke et al. 2003; Dheda et al. 2004; Pachot et al. 2004). Furthermore, *β2-microglobulin* (*B2M*) was included since it is one of the most frequently used endogenous controls. Analysis was performed on RNA isolated from peripheral whole blood using the PAXgene Blood RNA system. The system allows to draw 2.5 ml of blood into a tube which contains a liquid that stabilizes the gene expression pattern in the blood cells at the time point of

collection. The samples were taken from ten control individuals on day 1 and 15. After determination of the RNA concentration with RiboGreen® dye on a microplate reader, equal amounts of RNA were transcribed into cDNA. Subsequently, quantitative real-time PCR was carried out. As presented in the
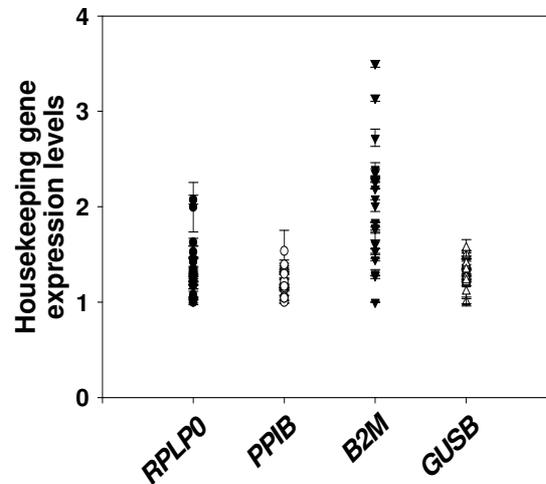


**Figure 29: Expression variation of *human acidic ribosomal phosphoprotein P0* (*RPLP0*), *cyclophilin B* (*PPIB*), *β2-microglobulin* (*B2M*) and *β-glucuronidase* (*GUSB*) in peripheral whole blood. Analysis of the various transcript levels was performed on a total number of 20 blood samples, all of which were collected in PAXgene blood RNA tubes (PreAnalytiX) from ten control individuals who donated blood twice over a period of several weeks. All measurements are repeated at least twice and given as mean ± SEM. The lowest variability was observed for *PPIB* and *GUSB*.**

summary for the 20 blood samples in figure 29, expression levels ranged from 1.00±0.03 to 2.07±0.05 (*RPLP0*), 1.00±0.01 to 1.54±0.22 (*PPIB*), 1.00±0.01 to 3.50±0.04 (*B2M*), and 1.00±0.04 to 1.57±0.09 (*GUSB*), respectively (values are given as mean ± SEM; the data for each single individual are given in the appendix on pages XVII-XVIII, tables B.2 and B.3). Thus, transcript levels of *B2M* revealed the highest variability, followed by *RPLP0*. In comparison, the lowest expression variation among the four investigated housekeeping genes was determined for *PPIB* and *GUSB*.

### 4.3.1.3  Comparison of the expression levels of *PPIB*, *GUSB*, FL-*SMN*, and Δ7-*SMN* in monocytes and lymphocytes

The quantitative analysis of a particular transcript in total RNA samples isolated from whole blood requires that the expression level is about to be equal in the different cell types which contribute to the RNA yield. Differential gene expression in the cell populations might become a source for variability as soon as cell type heterogeneity between the collected blood samples occurs.

Since monocytes and lymphocytes are two major cell fractions which contribute to the amount of total RNA isolated from whole blood, these subpopulations were investigated in more detail to get an idea about how equal the expression level of certain transcripts is. *PPIB* and *GUSB* were selected for analysis because they showed the lowest natural expression variability in previous studies (chapter

4.3.1.2), and to further analyze their suitability as endogenous controls in blood RNA samples. Additionally, the levels of the target transcripts FL-*SMN* and Δ7-*SMN* were checked. The investigation included the collection of whole blood in BD Vacutainer® CPT Cell Preparation Tubes from a number of nine control subjects. Subsequently, peripheral blood mononuclear cells (PBMCs, monocytes and lymphocytes) were isolated, and separated into a fraction containing monocytes and a fraction containing lymphocytes applying magnetic cell sorting (MACS) using an antibody against the monocyte surface marker CD14. This method resulted in a high purity of the two separated cell fractions as confirmed by flow cytometry (see appendix page XVIII, table B.4). After cell separation,
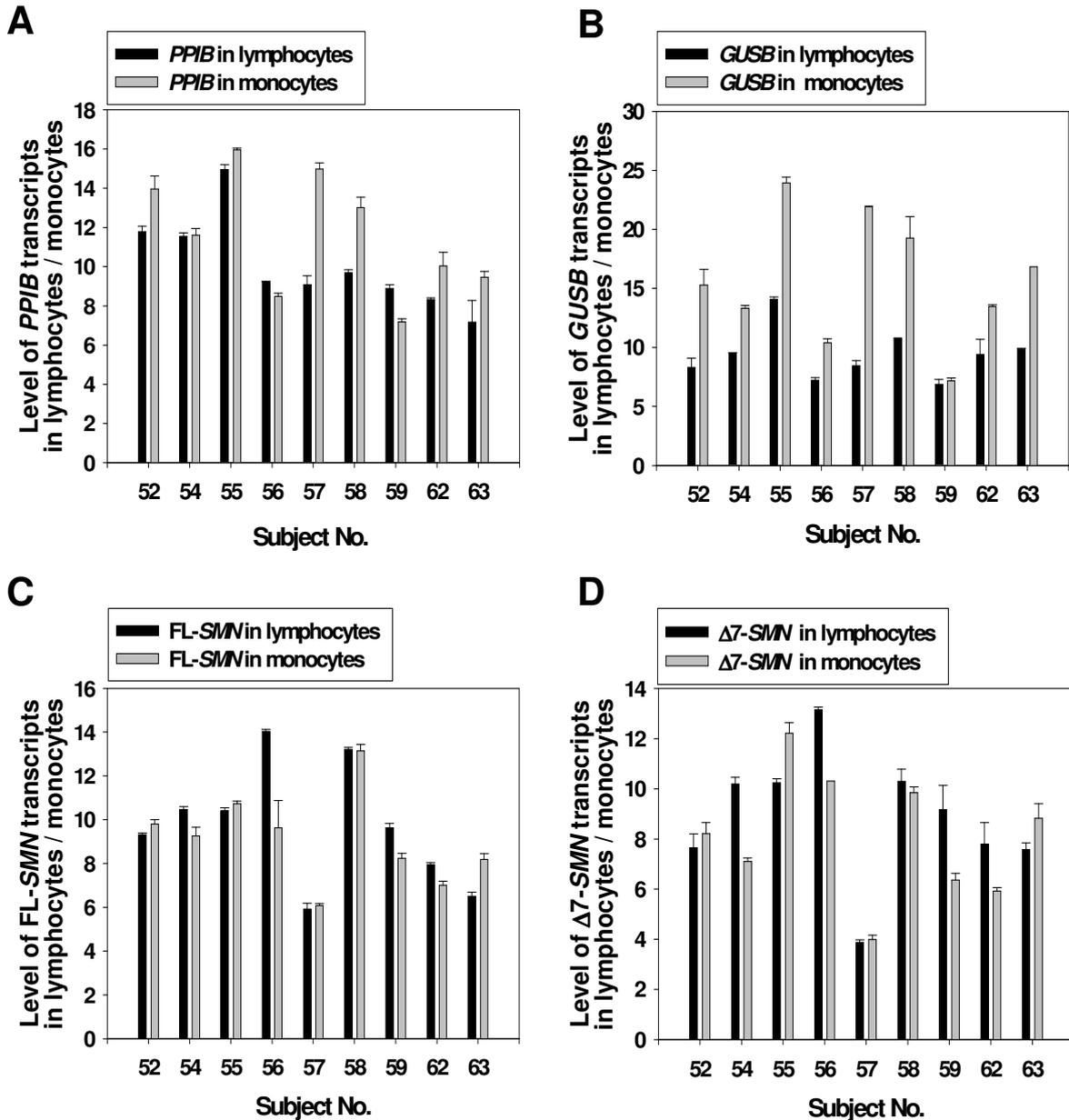


**Figure 30: Quantitative real-time PCR analysis of various transcript levels in monocytes and lymphocytes after isolation of PBMCs from peripheral whole blood, separation of the cell fractions by magnetic cell sorting, mRNA isolation, and reverse transcription. For each subject, investigation included *PPIB* transcripts *(A)*, *GUSB* transcripts *(B)*, FL-*SMN* transcripts *(C)*, and Δ7-*SMN* transcripts *(D)*. A table containing the means ± SEM for each single transcript level is given in the appendix (page XIX, tables B.5 and B.6).**

mRNA was isolated from each of the two fractions using the μMACS mRNA Isolation Kit which is based on magnetic labeling of polyA-mRNA with magnetic MACS Oligo(dT) MicroBeads. Eluted mRNA was measured with RiboGreen® dye on a microplate reader and equal amounts of each sample were used to perform a reverse transcription followed by measurements of the respective transcript level by quantitative real-time PCR. As demonstrated in figure 30 C and D, in most cases, corresponding fractions of lymphocytes and monocytes presented very similar levels of FL-*SMN* and Δ7-*SMN* transcript, respectively. There were only marginal differences between the two cell fractions, suggesting that a potential cell type heterogeneity between collected blood samples would not lead to extensively variable measurements. A more pronounced difference between the FL-*SMN* transcript levels was observed only in subject 56, however, this difference was not significant. For the Δ7-*SMN* levels, a slightly higher variation between monocytes and lymphocytes was measured for subjects 54 ($p<0.01$), 56 ($p<0.05$), and 59 (not significant).

Analysis of *PPIB* transcript levels in monocytes and lymphocytes (figure 30 A) also revealed a very similar expression pattern with minimal differences between most of the corresponding cell fractions, which further argued for the suitability of *PPIB* as endogenous control. Only in the individuals 57 and 58, a more substantial difference was determined ($p<0.01$ for subject 57, and $p<0.05$ for subject 58). In both cases, *PPIB* transcript levels were higher in monocytes than in lymphocytes. In contrast, the analysis of *GUSB* transcripts (figure 30 B) revealed a significantly different expression in corresponding monocyte and lymphocyte fractions in most of the investigated cases, including subjects 52 ($p<0.05$), 54 ($p<0.01$), 55 ($p<0.01$), 57 ($p<0.01$), 58 ($p<0.05$), and 63 ($p<0.001$). A less substantial variation between the two cell fractions was determined only in individuals 56, 59, and 62. In comparison, these results suggested that the application of *GUSB* as endogenous control would bear a higher risk for data variability caused by cell type heterogeneity between collected blood samples than the use of *PPIB*.

### 4.3.1.4  Impact of valproic acid on the expression of *PPIB* and *GUSB* in peripheral whole blood

Another major issue that has to be considered when dealing with VPA is its potential to unspecifically up- or down-regulate the activity of a number of genes. About 2-5% of the expressed genes are estimated to show increased or decreased activity induced by the class of HDAC inhibitors (Pazin and Kadonaga 1997; Butler et al. 2002; Glaser et al. 2003). This might also include housekeeping genes. Thus, a major requirement for an endogenous control to be used for the normalization of RNA data throughout a clinical trial with VPA is the stable expression even under drug treatment. Any positive or negative influence of VPA on the expression of the endogenous control gene would subsequently result in the misinterpretation of the data obtained for *SMN* target transcript levels.

Therefore, further evaluation experiments were carried out with *PPIB* and *GUSB*. The expression of these two genes was analyzed in blood samples received from ten SMA carriers (C1 to C10) treated with VPA within a clinical pilot trial. Compared to the baseline transcript level determined before drug treatment, *PPIB* expression was only little affected by drug therapy in the carriers C6, C7, C9, and C10 (figure 31 A). However, VPA markedly elevated *PPIB* activity in four individuals (carriers C1, C3,

**A**



**B**
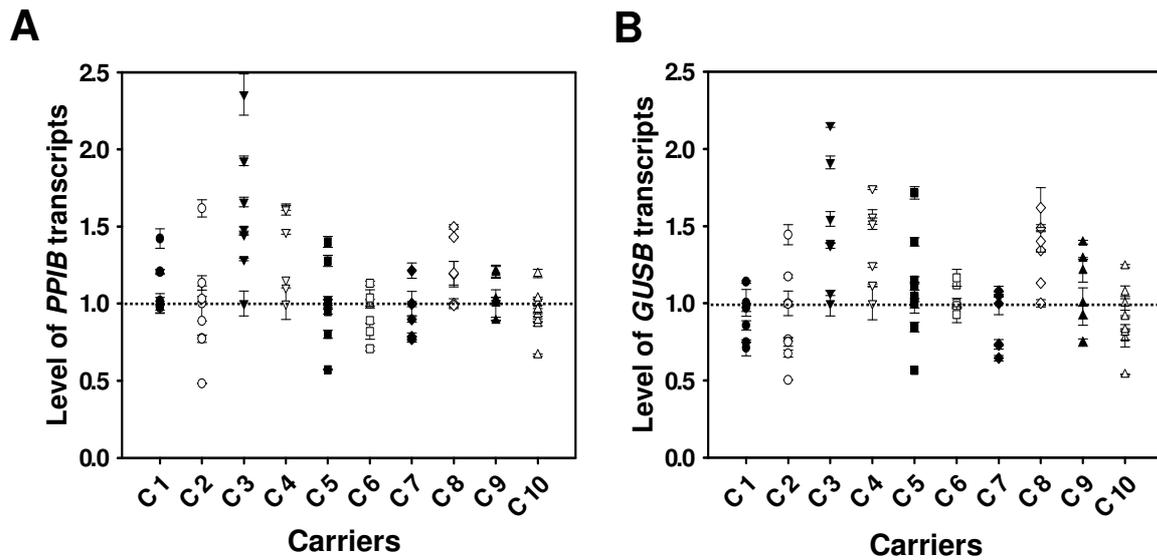


**Figure 31: Analysis of *PPIB (A)* and *GUSB (B)* transcript levels in peripheral whole blood from ten SMA carriers treated with VPA to evaluate potential drug effects on housekeeping gene activity. For each individual, the dotted line indicates the baseline expression determined in three blood samples taken every two weeks before drug treatment (1.0). All transcript levels measured throughout VPA medication are calculated as multiples of 1.0. Values are given as mean ± SEM. A table containing the corresponding data for each single transcript level is given in the appendix (page XX, table B.7).**

C4, and C8), whereas C2 and C5 showed up- or down-regulation of *PPIB* transcript levels under varying VPA serum levels. Analysis of *GUSB* expression revealed an almost unchanged activity in the carriers C1, C6, and C7 (figure 31 B). In a number of four probands (C2, C5, C9 and C10), *GUSB* transcription was stimulated or inhibited during the VPA dosage scheme, and increased mRNA levels were detected in another three carriers (C3, C4, and C8), clearly indicating the potential impact of VPA on the activity of housekeeping genes.

### 4.3.2 Normalization of *SMN* target transcripts as copy number per total RNA amount used for reverse transcription

Among the housekeeping genes *RPLP0*, *B2M*, *PPIB*, and *GUSB*, the latter two showed the lowest natural expression variation. However, between the lowest and the highest respective transcript level a roughly 1.5fold difference was observed which would restrict reliable detection of *SMN* transcript fluctuations to changes more pronounced than that variation. Moreover, in particular *GUSB* was demonstrated to be differentially expressed in monocytes and lymphocytes which might become a source for data variability as soon as cell type heterogeneity between the collected blood samples occurs. Importantly, *in vivo* expression of both *GUSB* and *PPIB* is regulated by VPA as demonstrated in blood taken from SMA carriers which were treated with the drug. Thus, in order to avoid any misinterpretation resulting from the natural variation in housekeeping gene expression and the possibility of altered activity of the endogenous control gene under drug treatment, the normalization

by *PPIB* or *GUSB* was found unsuitable to assess the impact of VPA on human *SMN* gene expression *in vivo*.

An alternative normalization method which is not based on the expression of an endogenous control has been described in 2000 (Bustin 2000). Instead, this method refers to the total RNA amount used for reverse transcription (RT) of each single sample. It was recommended as preferred normalization method for *in vivo* studies dealing with human tissues and is independent of gene expression variation and regulation of endogenous controls. Therefore, the method was selected as first choice to investigate a potential *in vivo* effect of VPA on human *SMN* transcript levels in blood. In a first step, total RNA was isolated from blood using the PAXgene system. DNase digest was included to remove DNA which would interfere with subsequent RNA measurements and the real-time PCR reaction. The exact RNA concentration of each sample was determined in triplicates on a microplate reader using RiboGreen® dye. Subsequently, an amount of 150 ng RNA was used for reverse transcription and FL-*SMN* (primers #2075 and #2076) and Δ7-*SMN* (primers #1449 and #1450) transcript levels were detected by quantitative real-time PCR on a LightCycler machine. For each analyzed sample, results were normalized by recording the copy numbers for FL- and Δ7-*SMN* target transcripts as copy number per ng total RNA used in the RT reaction.

### 4.3.3 Flow cytometric analysis of SMN protein levels in peripheral blood mononuclear cells (PBMCs)

Besides of the analysis of *SMN* RNA levels in blood collected from individuals treated with VPA, it would be of additional interest to study the level of SMN protein under drug treatment. It has been proven in SMA fibroblasts *in vitro* that VPA triggers elevated FL-*SMN2* RNA levels followed by an increase of SMN2 protein. However, RNA is the intermediate product and only analysis of the encoded functional protein in blood taken from drug-treated subjects would provide the final proof whether VPA is also able to regulate SMN levels *in vivo*.

A very common method to quantify protein levels is western blotting. This procedure is well established, but inconvenient and highly time-consuming whenever a large number of samples has to be investigated. Thus, the development of a high-throughput method would be of major benefit to perform SMN protein analysis in blood samples collected from individuals before and throughout the treatment with VPA within a clinical trial. A suitable approach to establish such a procedure is the application of flow cytometry. It would be conceivable to isolate PBMCs from peripheral whole blood samples, to subsequently label the SMN protein within the cells using an antibody which is conjugated to a fluorescent dye, and to finally measure the fluorescence signal (which directly correlates with the SMN protein level) in a certain number of cells on a flow cytometer. In comparison to western blotting, such a method would be faster and require less time to analyze multiple samples derived from different individuals.

To evaluate a method for the quantification of SMN protein levels in blood based on flow cytometry, an immunohistochemistry staining procedure was developed in a first step. Blood was collected in BD Vacutainer® CPT Cell Preparation Tubes, and PBMCs were isolated. Cells were fixed and permeabilized using the Fix&Perm Cell Permeabilization Kit. After subsequent incubation with a

monoclonal anti-SMN FITC-conjugated antibody, successful staining of the SMN protein was checked under a fluorescent microscope. As demonstrated in figure 32 A and B, incubation with the anti-SMN FITC-conjugated antibody resulted in a diffuse staining of the SMN protein in the PBMCs. Additionally, intensively fluorescent dot-like structures called gems were visible. Since gems are exclusively present in the nucleus, this observation indicated that the procedure was able to permeabilize not only the cell membrane, but also the nuclear membrane, and that the anti-SMN FITC-conjugated antibody reached the inner nucleus and bound to the SMN protein localized in the gems. These were two major

**A**



**B**



**C**



**D**
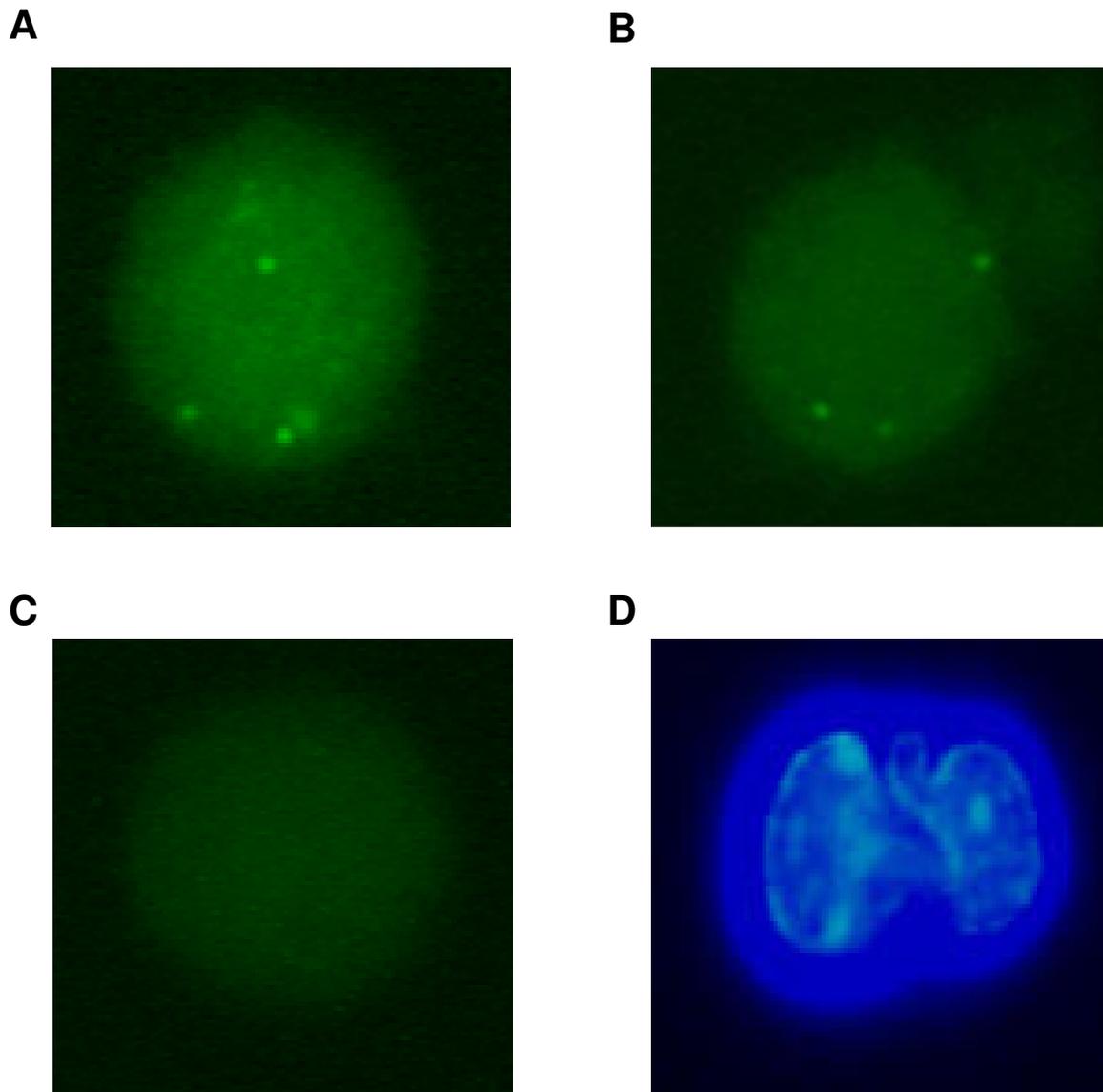


**Figure 32: Immunohistochemistry staining of the SMN protein in PBMCs isolated from peripheral whole blood. Cells were fixed, permeabilized, and subsequently incubated either with a monoclonal anti-SMN FITC-conjugated antibody *(A and B)*, or with an equal amount of the isotype control to check for background staining *(C)*. Analysis by fluorescence microscopy revealed a diffuse staining of SMN together with a staining of the nuclear gems *(A and B)*. Incubation with the isotype control (labeled with FITC but not directed against an antigen) resulted in a weak background staining only *(C)*. The corresponding nucleus from the cell visible in *(C)* was additionally stained with DAPI *(D)* to prove that the background staining was indeed obtained from one of the PBMCs.**

requirements to subsequently apply the method for quantification of SMN protein levels by flow cytometry. In a second step, PBMCs were analyzed on a flow cytometer to check whether this technical equipment is able to distinguish between the fluorescence signal obtained after staining with the anti-SMN FITC-conjugated antibody and the weak signal derived from background staining. Therefore, blood was taken from several individuals, and PBMCs were isolated, fixed, and permeabilized as described above. Incubation was performed with the monoclonal anti-SMN FITC-conjugated antibody, the corresponding isotype control to determine the background staining, and without any antibody to analyze the autofluorescence signal of the cells. Moreover, during the analysis of the PBMCs on the flow cytometer, cells were separated into lymphocytes and monocytes by using fluorescently labeled antibodies against the surface markers CD45 (present on monocytes and lymphocytes) and CD14 (present on monocytes, but not on lymphocytes). Thus, any events counted and analyzed on the flow cytometer could be exactly identified as PBMCs. Additionally, the separation into two cell fractions would allow to check for any potential differences in the regulation of the SMN protein by VPA. Flow cytometric analysis of PBMC samples incubated without antibody, with isotype control, or with anti-SMN FITC-conjugated antibody revealed a moderate but sufficient difference between the detected fluorescence signals (figure 33 and table 24 display the results for one of the blood samples). Figure 33 A presents the autofluorescence results for a PBMC sample, figure 33 B shows the background staining results obtained after incubation of PBMCs from the same individual with the isotype control antibody, and figure 33 C gives the data obtained after incubation with anti-SMN FITC-conjugated antibody. As it is visible in the dot plots, lymphocytes and monocytes could be clearly separated in each sample based on side scatter, forward scatter, and incubation with antibodies against CD45 and CD14 (lymphocytes are positive for CD45 and negative for CD14; monocytes are positive for both CD45 and CD14). The third dot plot in each column analyzes the CD14-PE signal versus the green fluorescence (autofluorescence and signal derived from FITC). Compared to the autofluorescence of the PBMCs, the green fluorescence marginally increases in the isotype control (third dot plot and histograms column A versus third dot plot and histograms column B). However, the increase is much more pronounced in the PBMCs incubated with anti-SMN FITC-conjugated antibody (third dot plot and histograms in column C versus those in columns A and B). This observation was made for lymphocytes and monocytes, suggesting that the flow cytometry equipment is able to distinguish between background staining and specific SMN protein staining. The corresponding data are given in table 24.

**Table 24: Intensity of green fluorescence measured in PBMCs incubated without antibody (autofluorescence), with the respective isotype control, or with the monoclonal anti-SMN FITC-conjugated antibody. Autofluorescence was measured once. The samples to detect the background staining and the specific SMN signal were performed in triplicates, and the results are given as mean ± SEM. The corresponding dot plots and histograms are presented in figure 33.**

|  |  | Autofluorescence | Isotype control | Anti-SMN FITC antibody |
|---|---|---|---|---|
| **Signal for green fluorescence** | **Lymphocytes** | 5.0 | 10.9±0.2 | 25.3±1.0 |
|  | **Monocytes** | 7.9 | 30.4±1.0 | 58.2±2.7 |
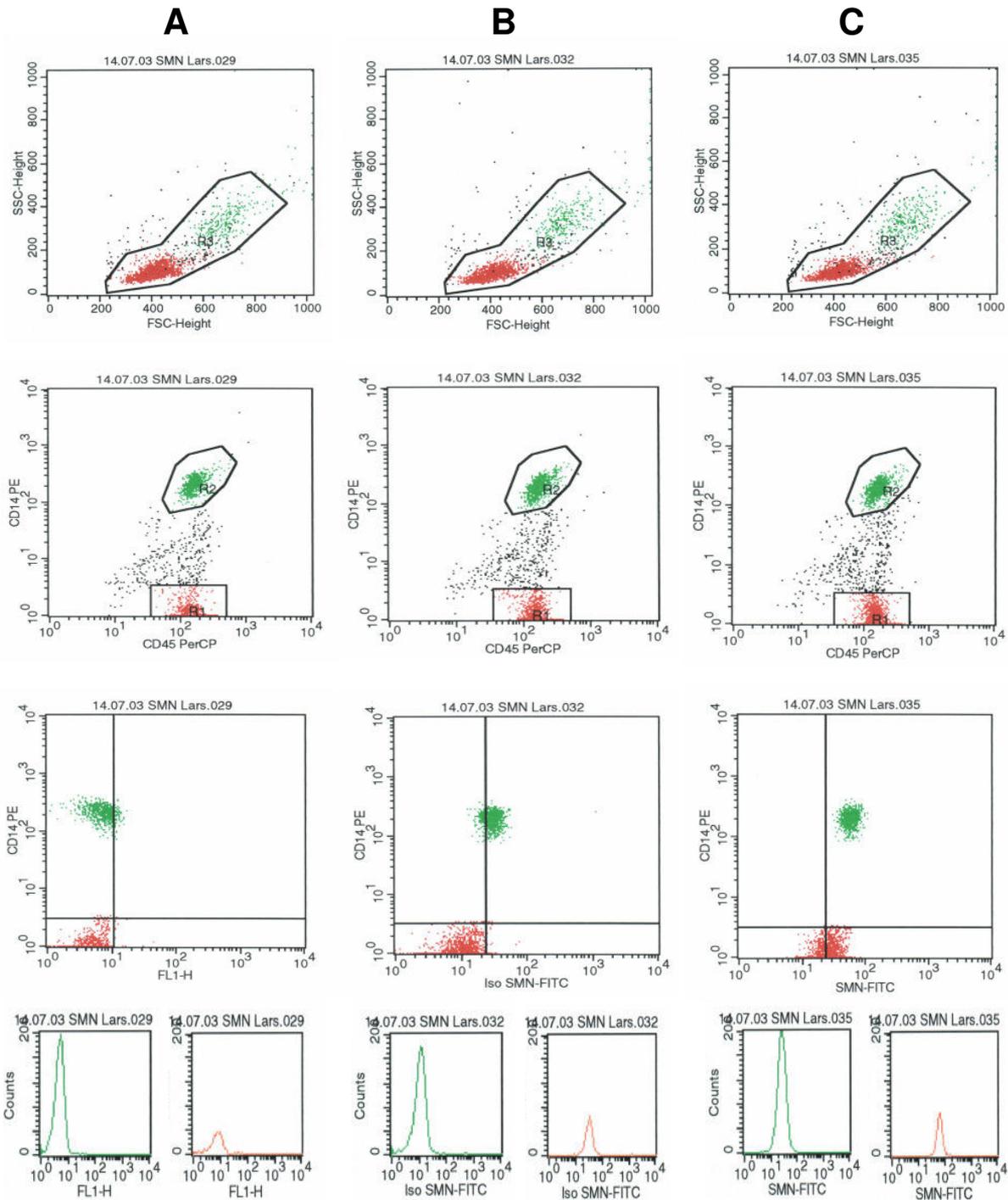
**Figure 33: Flow cytometric analysis of PBMCs after isolation from peripheral whole blood and immunohistochemistry staining of the SMN protein.** *Column (A) is a representative analysis of the autofluorescence of the cells,* *column (B) demonstrates the results for background staining after incubation with an isotype control antibody, and (C) presents the data obtained after incubation with a monoclonal anti-SMN FITC-conjugated antibody. Lymphocytes (red in the dot plots and green in the histogram) and monocytes (green in the dot plots and red in the histogram) were separated using antibodies against the surface markers CD45 and CD14. In each column, the first diagram is a side scatter (SSC) versus forward scatter (FSC) dot plot, the second dot plot shows the fluorescence signal obtained from the CD14-PE labeled antibody versus the signal from the CD45-PerCP labeled antibody, and the third dot plot presents the signal for CD14-PE versus the green fluorescence determined in the samples. The histograms show the cell counts for lymphocytes/monocytes versus the green fluorescence signal.*

Another challenge was the comparability of the data which would be obtained for one and the same individual before and throughout the treatment with VPA. In contrast to RNA samples which can be isolated, stored at -80 °C, and analyzed together within the same real-time PCR run, it would probably be complicated to store intact PBMCs, and keep the SMN protein level constant. Thus, a reliable quantitative analysis of SMN protein levels requires immediate sample measurement. As a suitable tool to compare flow cytometric results obtained at different time points, Sphero Rainbow Calibration Particles were identified. This is a mixture of particles that are dyed to eight different fluorescent intensities. Every Rainbow particle contains a mixture of fluorophores that are excited at any wavelength from 365 to 650 nm. The Rainbow particles have emission spectra that are compatible with many common fluorophores used for immunofluorescent stainings with flow cytometric analysis,
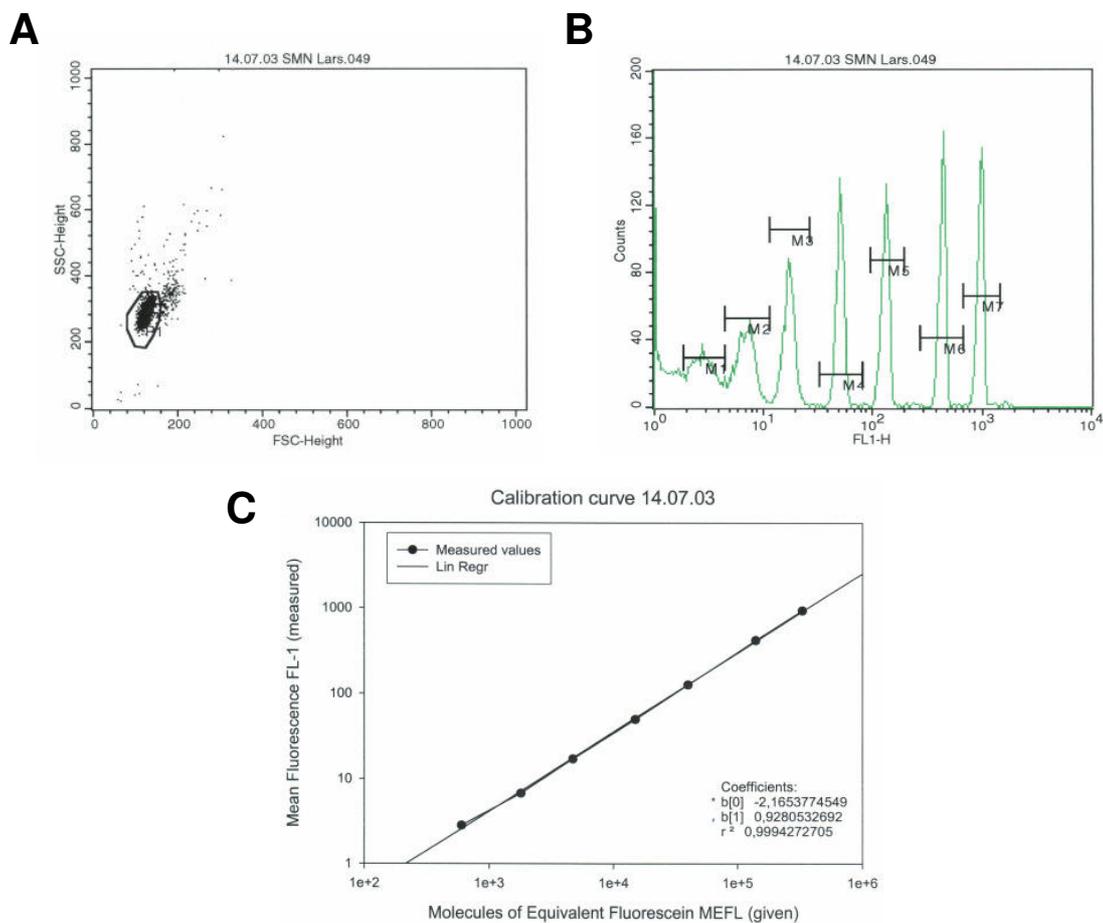


**Figure 34: Measurement of Sphero Rainbow Calibration Particles on a flow cytometer to enable comparability of the data obtained for SMN protein levels in PBMCs at different time points. The particles are identified by their size in the side scatter/forward scatter dot plot *(A)*. They consist of eight different particle fractions, each of which is labeled with a standardized amount of dye that is able to emit green fluorescence similar to the fluorophore FITC. Seven of these fractions were detected by the flow cytometer *(B)*. The mean fluorescence intensity which was measured for each particle fraction and the molecules of equivalent fluorescein which is a standardized value and given by the manufacturer are used to create a standard curve *(C)*. The standard curve serves to transform the green fluorescent intensity measured in the respective PBMC sample into molecules of equivalent fluorescein, a value which makes the samples comparable regardless at which time point they were measured.**

including FITC. Thus, whenever PBMC samples would be measured to determine the SMN protein level in the cells, the particle mixture would be suitable to calibrate the flow cytometer, and to create a standard curve. Subsequently, the standard curve would serve to calculate the SMN protein levels and make them comparable with the data obtained at different time points (figure 34 and appendix page XXI table B.8).

Another problem which, however, could not be solved at the time when the experiments were carried out is the evaluation of an internal standard. To quantify SMN protein levels in PBMCs, the permeabilization of the nuclear membrane is required since a major amount of SMN is localized in the gems. This is a major disadvantage of intracellular stainings, because there is no real guaranty that the degree of permeabilization is always the same. A different degree of permeabilization would most likely have an impact on the amount of anti-SMN FITC-conjugated antibody which is able to diffuse into the nucleus and bind to SMN protein. This would result in a variability of the data obtained for SMN protein levels and quantification would be unreliable. To overcome this problem, a protein which is constitutively expressed exclusively in the nucleus could be detected in parallel. To make sure that the diffusion behavior of the anti-SMN antibody and the antibody against the control protein is as similar as possible, the detection of such a protein requires an antibody which is directly conjugated to FITC. Several proteins were taken into account, including histone H1, emerin, the retinoblastoma protein, and lamin proteins. However, retinoblastoma protein is undetectable in normal PBMCs by flow cytometry, and a primary FITC-conjugated antibody was not available for any constitutively expressed nuclear protein at this time. A primary monoclonal antibody to histone H1 was purchased from *Acris* and the FluoReporter ® FITC Protein Labeling Kit (*Molecular Probes*) was used to label the antibody with FITC. Since the reaction failed, and thus a suitable internal control could not be established, the flow cytometric quantification of SMN protein levels in blood samples collected throughout a clinical trial with VPA was canceled.

### 4.3.4 Comparison of baseline *SMN* transcript levels in peripheral whole blood from controls, SMA carriers, and SMA patients

Prior to a clinical trial with VPA, the expression of *SMN* RNA was characterized in a sample set collected from a total number of 41 untreated subjects including control persons, SMA carriers, and patients with SMA. Native blood is a tissue not affected by SMA and represents the only biological material which can easily be collected from individuals in sufficient amounts to directly monitor the effect of a drug on *SMN* expression. However, studies investigating *SMN* expression in native blood have not been carried out so far.

The cohort under study included ten controls (nine with 2 *SMN1* and one with 3 *SMN1* copies, all of them presenting 0–2 *SMN2* copies), ten SMA carriers (carrying 1 *SMN1* copy and 1–3 *SMN2* copies), six patients with type III SMA (two with 4 *SMN2* and four with 3 *SMN2* copies), ten patients with type II SMA (all of them presenting 3 *SMN2*) and five patients with type I SMA (presenting 2 *SMN2* copies except for one case with 3 *SMN2* copies). To analyze FL-*SMN* and Δ7-*SMN* baseline levels as well as
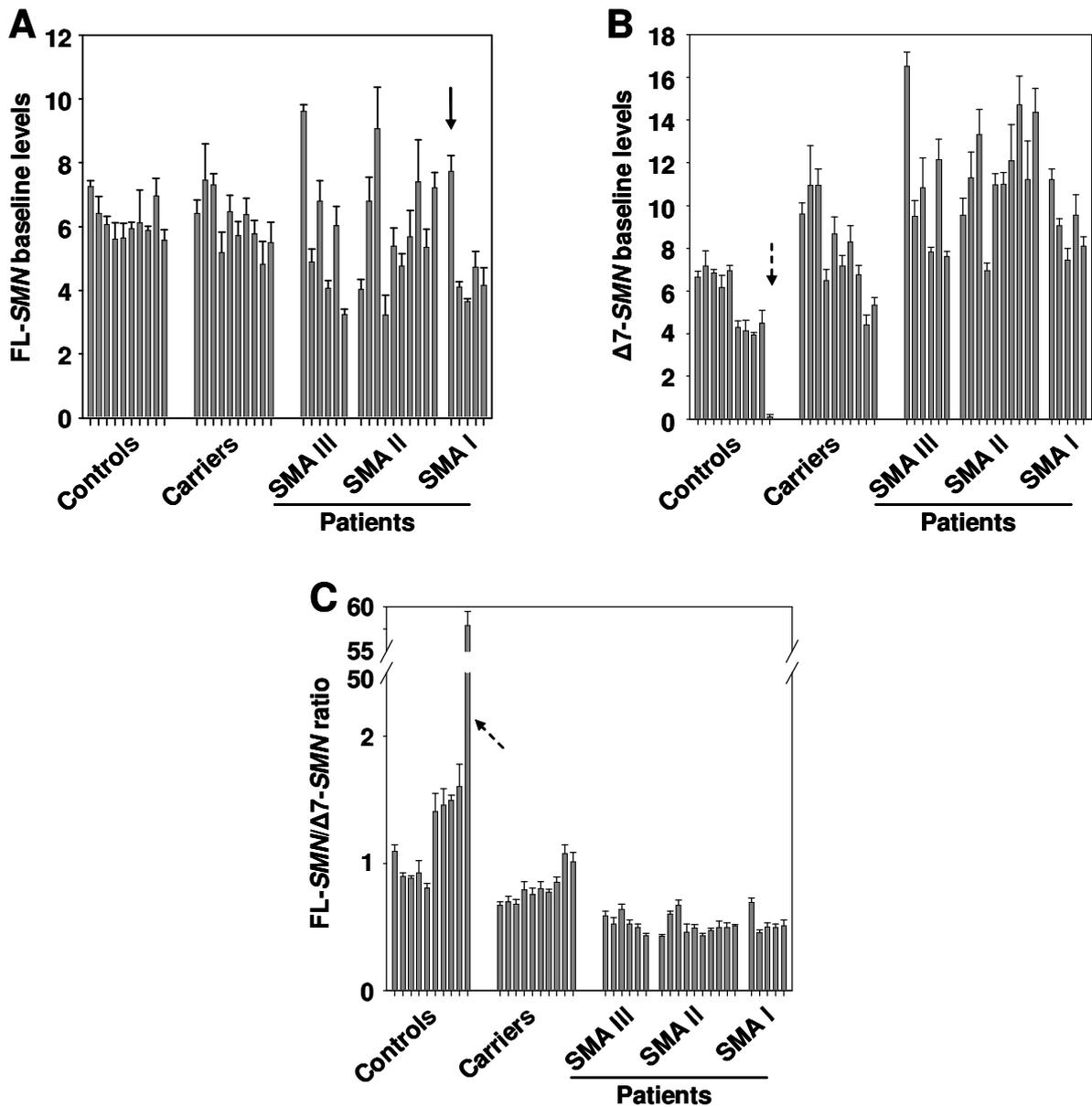
**Figure 35: Comparison of FL-*SMN (A)* and Δ7-*SMN (B)* mRNA baseline levels together with an analysis of the FL-*SMN*/Δ7-*SMN* ratio *(C)* in blood collected from 41 untreated subjects in PAXgene blood RNA tubes. From each subject, blood was taken twice over a time period of several weeks. The average values calculated after repeated real-time PCR measurements of the two blood samples from each individual are given as mean ± SEM. The arrow in *(A)* indicates the FL-*SMN2* level determined for the SMA type I patient with 3 *SMN2* copies. As expected, analysis of the control subject with 2 *SMN1* copies and 0 *SMN2* copies yielded a Δ7-*SMN* transcript amount close to 0 [indicated by the arrow in *(B)*]. The arrow in *(C)* indicates the transcript ratio calculated for the same control, presenting a value of 55.74 ± 3.21 (mean ± SEM) due to almost complete absence of Δ7-*SMN* transcript. The corresponding data and the genotype of each single individual are given in the appendix (page XXI, table B.9).**

the corresponding transcript ratio without drug treatment, peripheral whole blood was taken twice over a time period of several weeks. The average values calculated from the two measurements are compared in figure 35. Unexpectedly, although controls, SMA carriers, and SMA patients differ in the number of functional *SMN1* genes (2-3 *SMN1*, 1 *SMN1*, and homozygous absence of *SMN1*, respectively) and their *SMN2* copy numbers (0-4 *SMN2*), only the type I SMA patients with 2 *SMN2*

copies revealed a significant reduction of FL-*SMN* levels compared to the control and the carrier groups (p always <0.01) (figure 35 A). However, the type I SMA patient with 3 *SMN2* copies stood out from those with 2 *SMN2* copies. Inclusion of this patient into statistical analysis failed to reveal a significant difference between type I SMA patients, carriers, and controls (p=0.052). Controls and carriers (with 2-3 *SMN1* and 1 *SMN1,* respectively) yielded similar amounts of FL-*SMN* transcript with only minor variations among the recruited subjects. In comparison, patients with type I, II, and III SMA (carrying 2-4 *SMN2* copies) displayed a much higher inter-individual variation in FL-*SMN* expression. FL-*SMN* levels measured in peripheral whole blood derived from type I, II, and III patients were not significantly different from each other. Compared to controls, their mRNA levels ranged from lower to even higher values.

In SMA carriers, Δ7-*SMN* mRNA levels were in the range of those observed in controls or higher, with higher levels corresponding to an increased *SMN2* copy number (figure 35 B). Thus, a significant difference between controls and carriers was not observed. The level of Δ7-*SMN* did not discriminate between type I, II, and III SMA patients. However, compared to controls, Δ7-*SMN* levels were significantly higher in SMA patients (p<0.05 for type I patients, and p<0.01 for type II and III patients).

The FL-*SMN*/Δ7-*SMN* transcript ratios in controls overlapped with the values for SMA carriers, which represented similar or slightly lower values, the latter restricted to the individuals carrying 3 *SMN2* genes (figure 35 C). Although a high interindividual variation of the FL- and Δ7-*SMN2* transcript levels was detected in SMA patients even in the presence of identical numbers of *SMN2* (e.g. 3 *SMN2* in all investigated SMA type II patients), the respective FL/Δ7 ratios were in an equal range, and therefore not significantly different from each other. This suggested a varying transcriptional activity of *SMN2* among different subjects. However, the transcript ratios in SMA patients were significantly lower than the ratios determined for controls (p always <0.01; the control without *SMN2* was excluded for analysis) and for carriers (p always < 0.05).

For every investigated parameter (FL-*SMN*, Δ7-*SMN*, and FL/Δ7 ratio), low SEM values demonstrate that there were only marginal differences between the two collected samples of each individual (figure 35).

### 4.3.5    Pilot trial with valproic acid in SMA carriers

#### 4.3.5.1 Impact of valproic acid on *SMN* mRNA levels in peripheral whole blood from SMA carriers

To address the question if VPA is able to increase *SMN* gene expression *in vivo*, ten SMA carriers were enrolled in a clinical pilot trial and treated with VPA. Peripheral whole blood was used to assess FL- and Δ7-*SMN* transcript levels. Among the subjects investigated, VPA treatment resulted in elevated FL-*SMN* mRNA amounts in a number of seven probands, namely C1, C2, C3, C4, C5, C6, and C8 (figure 36 A and table 25). Compared to the baseline FL-*SMN* transcript level determined before VPA medication, a 1.6fold (C6) to 3.4fold (C3) increase was reached. Several weeks after discontinuing VPA medication, FL-*SMN* transcript levels in all drug responders were back on the

**Table 25: Expression of FL-*SMN*, Δ7-*SMN*, and the FL/Δ7 ratio in peripheral whole blood from ten SMA carriers (C1 to C10) treated with VPA. Values are given as mean ± SEM together with the corresponding VPA serum level determined in the same blood sample (n.d. = not detected). Varying total number of values obtained for each parameter among the probands resulted from varying time periods required to adapt VPA serum levels to the therapeutic range. The highest value detected for FL-*SMN*, Δ7-*SMN* and the FL/Δ7 ratio in the respective SMA carrier is indicated in bold.**

| SMA Carrier | | *SMN* transcript levels, FL/Δ7 ratio, and corresponding VPA serum level | | | | | | | | |
|---|---|---|---|---|---|---|---|---|---|---|
| **C1** 1x*SMN1* 1x*SMN2* | **FL-*SMN*** | 1.0±0.1 | 0.8±0.0 | 1.5±0.0 | 1.0±0.0 | 1.6±0.0 | 0.8±0.0 | **1.8±0.1** | 0.8±0.0 | |
| | **Δ7-*SMN*** | 1.0±0.1 | 0.8±0.0 | 1.2±0.0 | 1.0±0.1 | 1.4±0.1 | 0.7±0.2 | **1.5±0.0** | 0.7±0.0 | |
| | **FL/Δ7 ratio** | 1.0±0.1 | 1.0±0.0 | **1.3±0.1** | 1.0±0.0 | 1.1±0.0 | 1.1±0.3 | 1.2±0.0 | 1.1±0.1 | |
| | **VPA (mg/l)** | baseline | n.d. | 53.9 | 65.7 | 79.5 | 104.0 | 84.8 | after | |
| **C2** 1x*SMN1* 1x*SMN2* | **FL-*SMN*** | 1.0±0.1 | 0.8±0.0 | **1.7±0.1** | 0.9±0.0 | 0.4±0.0 | 0.9±0.1 | 1.4±0.0 | 1.6±0.0 | 0.9±0.1 |
| | **Δ7-*SMN*** | 1.0±0.1 | 0.8±0.0 | **1.6±0.1** | 1.1±0.0 | 0.4±0.0 | 0.8±0.1 | 1.2±0.0 | 1.5±0.0 | 1.0±0.1 |
| | **FL/Δ7 ratio** | 1.0±0.1 | 1.0±0.0 | 1.1±0.0 | 0.8±0.0 | 1.0±0.1 | 1.1±0.2 | **1.2±0.0** | 1.1±0.0 | 0.9±0.1 |
| | **VPA (mg/l)** | baseline | n.d. | 26.7 | 45.9 | 62.6 | 75.6 | 57.3 | 61.0 | after |
| **C3** 1x*SMN1* 2x*SMN2* | **FL-*SMN*** | 1.0±0.1 | 1.4±0.0 | 1.9±0.0 | 2.2±0.1 | 1.8±0.1 | 1.3±0.0 | **3.4±0.0** | 1.0±0.0 | |
| | **Δ7-*SMN*** | 1.0±0.1 | 1.5±0.0 | 1.6±0.0 | 2.1±0.0 | 1.8±0.0 | 1.3±0.0 | **2.8±0.0** | 0.9±0.0 | |
| | **FL/Δ7 ratio** | 1.0±0.0 | 0.9±0.0 | 1.2±0.0 | 1.0±0.0 | 1.0±0.1 | 1.0±0.0 | **1.2±0.0** | 1.1±0.1 | |
| | **VPA (mg/l)** | baseline | 30.1 | 64.3 | 48.6 | 60.0 | 58.7 | 53.9 | after | |
| **C4** 1x*SMN1* 2x*SMN2* | **FL-*SMN*** | 1.0±0.1 | 1.2±0.0 | 1.9±0.0 | **2.3±0.0** | 1.8±0.1 | 1.4±0.0 | 1.1±0.1 | | |
| | **Δ7-*SMN*** | 1.0±0.1 | 1.2±0.0 | 1.7±0.0 | **2.0±0.1** | 1.8±0.0 | 1.3±0.0 | 1.2±0.0 | | |
| | **FL/Δ7 ratio** | 1.0±0.0 | 1.0±0.0 | **1.1±0.0** | 1.1±0.1 | 1.0±0.1 | 1.1±0.0 | 0.9±0.1 | | |
| | **VPA (mg/l)** | baseline | 41.4 | 69.7 | 80.5 | 83.3 | 78.8 | after | | |
| **C5** 1x*SMN1* 2x*SMN2* | **FL-*SMN*** | 1.0±0.0 | 1.0±0.0 | 1.7±0.1 | 1.6±0.1 | 0.4±0.0 | 1.2±0.1 | 1.6±0.0 | **2.0±0.0** | 1.2±0.1 |
| | **Δ7-*SMN*** | 1.0±0.1 | 1.0±0.0 | 1.7±0.0 | 1.6±0.2 | 0.5±0.1 | 1.4±0.0 | 1.7±0.0 | **2.4±0.1** | 1.2±0.0 |
| | **FL/Δ7 ratio** | 1.0±0.1 | **1.0±0.0** | 1.0±0.1 | 1.0±0.1 | 0.8±0.1 | 0.9±0.0 | 0.9±0.0 | 0.8±0.0 | 1.0±0.1 |
| | **VPA (mg/l)** | baseline | n.d. | 33.2 | 32.7 | 56.2 | 53.1 | 50.7 | 64.3 | after |
| **C6** 1x*SMN1* 2x*SMN2* | **FL-*SMN*** | 1.0±0.1 | 1.4±0.0 | 0.9±0.1 | **1.6±0.1** | 1.3±0.0 | 1.0±0.0 | 1.1±0.1 | | |
| | **Δ7-*SMN*** | 1.0±0.1 | 1.4±0.1 | 0.9±0.0 | **1.5±0.1** | 1.4±0.0 | 1.2±0.1 | 1.0±0.0 | | |
| | **FL/Δ7 ratio** | 1.0±0.0 | 1.0±0.0 | 1.0±0.1 | **1.1±0.1** | 0.9±0.0 | 0.8±0.1 | 1.1±0.1 | | |
| | **VPA (mg/l)** | baseline | 51.7 | 70.3 | 80.1 | 74.3 | 82.3 | after | | |
| **C7** 1x*SMN1* 2x*SMN2* | **FL-*SMN*** | 1.0±0.1 | 0.7±0.1 | **1.3±0.0** | 1.1±0.0 | 0.6±0.1 | 0.7±0.0 | 0.9±0.0 | | |
| | **Δ7-*SMN*** | 1.0±0.1 | 0.7±0.0 | **1.5±0.0** | 1.2±0.1 | 0.8±0.0 | 0.8±0.0 | 1.0±0.0 | | |
| | **FL/Δ7 ratio** | 1.0±0.0 | **1.0±0.1** | 0.9±0.0 | 0.9±0.0 | 0.8±0.1 | 0.9±0.0 | 0.9±0.1 | | |
| | **VPA (mg/l)** | baseline | n.d. | 76.9 | 92.0 | 128.5 | 80.7 | after | | |
| **C8** 1x*SMN1* 3x*SMN2* | **FL-*SMN*** | 1.0±0.1 | 1.4±0.0 | 1.2±0.0 | 1.4±0.1 | 0.9±0.0 | **1.7±0.0** | 0.9±0.1 | | |
| | **Δ7-*SMN*** | 1.0±0.1 | 1.2±0.1 | 1.0±0.0 | 1.4±0.1 | 0.8±0.0 | **1.5±0.0** | 1.0±0.0 | | |
| | **FL/Δ7 ratio** | 1.0±0.0 | 1.2±0.0 | **1.2±0.0** | 1.0±0.1 | 1.1±0.1 | 1.1±0.0 | 0.9±0.1 | | |
| | **VPA (mg/l)** | baseline | 10.0 | 58.5 | 79.9 | 63.6 | 67.8 | after | | |
| **C9** 1x*SMN1* 3x*SMN2* | **FL-*SMN*** | 1.0±0.2 | 0.7±0.0 | 1.2±0.0 | **1.3±0.0** | 1.0±0.0 | 1.0±0.0 | 0.8±0.1 | | |
| | **Δ7-*SMN*** | 1.0±0.1 | 0.8±0.0 | 1.2±0.0 | **1.4±0.1** | 1.1±0.0 | 1.3±0.1 | 0.9±0.1 | | |
| | **FL/Δ7 ratio** | 1.0±0.1 | 0.9±0.0 | **1.0±0.0** | 0.9±0.0 | 1.0±0.0 | 0.8±0.1 | 0.9±0.0 | | |
| | **VPA (mg/l)** | baseline | 30.7 | 59.9 | 69.1 | 64.3 | 62.4 | after | | |
| **C10** 1x*SMN1* 3x*SMN2* | **FL-*SMN*** | 1.0±0.0 | 1.1±0.0 | 1.1±0.1 | 0.7±0.0 | 0.9±0.0 | **1.2±0.1** | 1.1±0.0 | 1.1±0.0 | 0.5±0.0 |
| | **Δ7-*SMN*** | 1.0±0.1 | 1.1±0.1 | 1.0±0.0 | 0.7±0.0 | 1.1±0.0 | **1.3±0.0** | 1.2±0.0 | 1.2±0.0 | 0.6±0.0 |
| | **FL/Δ7 ratio** | 1.0±0.0 | 1.0±0.0 | **1.1±0.1** | 1.0±0.1 | 0.8±0.0 | 0.9±0.1 | 0.9±0.0 | 0.9±0.0 | 0.8±0.1 |
| | **VPA (mg/l)** | baseline | n.d. | 45.3 | 65.9 | 58.9 | 84.2 | 75.6 | 61.6 | after |

respective baseline level as shown by the very last value given for each of these carriers in table 25. This measurement proved that the observed elevated *SMN* gene expression in the seven probands can indeed be attributed to the treatment with VPA. Interestingly, the degree of up-regulation determined for the FL-*SMN* transcript levels was not clearly correlated to the number of *SMN2* genes present in each carrier (see table 25). The strongest drug response was detected in probands C3, C4, and C5 who all carry 2 *SMN2* copies. C1, C2, C6, and C8, who possess 1 *SMN2* copy and 3 *SMN2* copies, respectively, revealed a weaker increase. Furthermore, fluctuations in the VPA serum level of the responders throughout dose escalation and after reaching the therapeutic range were not clearly reflected by the change of FL-*SMN* mRNA amounts (table 25). Except for C2, who reached the maximal gain of the FL-*SMN* transcript level in an early stage of drug treatment at a relatively low VPA serum level of 26.7 mg/l, the highest elevation was detected in all responders after several weeks of medication and at VPA levels between 53.9 and 84.8 mg/l. However, even while the drug was present, FL-*SMN* transcript levels decreased in between, so that in none of the carriers who responded to the drug a clear correlation between FL-*SMN* mRNA levels and VPA dosage was observed. Due to this fluctuation of transcript levels observed throughout therapy, the increase of FL-*SMN* transcript levels was significant only in the subjects C3 and C4 ($p < 0.05$).

Out of the ten SMA carriers investigated, three subjects did not show markedly changed FL-*SMN* transcript levels upon VPA treatment (figure 36 B). In the blood samples derived from C7, C9, and C10, a maximal elevation of only 1.2fold or 1.3fold was detected, although drug levels in each of these individuals throughout the protocol were similar to those in the responding group. The observation of slight variations including minimal decreases in presence of VPA followed by re-increases of the FL-*SMN* amount corresponds to the behavior already described for the responders.

In each of the ten SMA carriers enrolled in the clinical protocol, up-regulation of the Δ7-*SMN* transcript
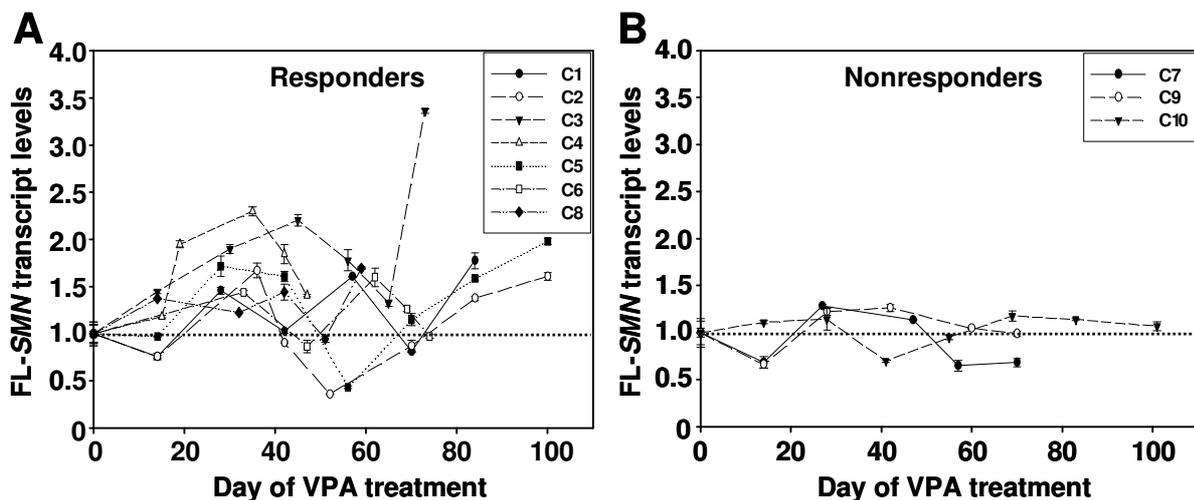


**Figure 36: FL-*SMN* transcript levels in ten SMA carriers treated with VPA in a clinical pilot trial. Transcript measurements *(A, B)* were performed using quantitative real-time PCR, are given as mean ± SEM, and presented as a function of the day of VPA treatment. The baseline FL-*SMN* transcript level was determined for each subject in three blood samples collected in PAXgene blood RNA tubes every two weeks before drug therapy. The mean of these measurements was normalized to 1.0 (dotted line) and is displayed on day 0 of medication. All other values are shown as multiples of the baseline level. For corresponding data and the genotype of each carrier, see also table 25.**

level occurred in parallel with the respective FL-*SMN* transcript level (table 25). Maximal rise of the Δ7-*SMN* mRNA amount in each subject of the responder group (C1, C2, C3, C4, C5, C6, and C8) was detected at the same time point when FL-*SMN* levels peaked and ranged between 2.8fold (C3) and 1.5fold (C1, C6, and C8). In agreement with the results for the FL transcript, significance was reached only for C3 and C4 ($p < 0.05$). The simultaneous gain of both FL- and Δ7-*SMN* transcript levels clearly suggested a general activation of *SMN* transcription processes in peripheral whole blood by VPA. Elevation of the truncated transcript in the responders mostly appeared slightly lower than that of the FL transcript, although these differences were marginal. Consequently, the FL-*SMN* versus Δ7-*SMN* transcript ratio as a parameter for an effect on exon 7 inclusion and therefore a reversion of the splicing pattern was altered only weakly without reaching significance (table 25). In the non-responding group including the probands C7, C9, and C10, almost unchanged FL-*SMN* transcript levels went along with only minimally modified Δ7-*SMN* transcript amounts. The resulting FL-*SMN*/Δ7-*SMN* transcript ratio never increased in these subjects throughout VPA medication.

### 4.3.5.2 Impact of valproic acid on SMN protein levels in peripheral whole blood from SMA carriers

It has been demonstrated in cell culture systems *in vitro*, that VPA is able to elevate both, FL-*SMN* RNA and protein. To prove that VPA acts in the same way in humans *in vivo*, the potential of VPA to increase SMN protein levels in the SMA carriers enrolled in the pilot trial was analyzed. With the exception of proband C6, for 9/10 subjects protein analysis in PBMCs was feasible. From each individual, peripheral whole blood was collected in BD Vacutainer® CPT Cell Preparation Tubes twice: once prior to VPA treatment and once after the VPA serum level was adjusted to the therapeutic
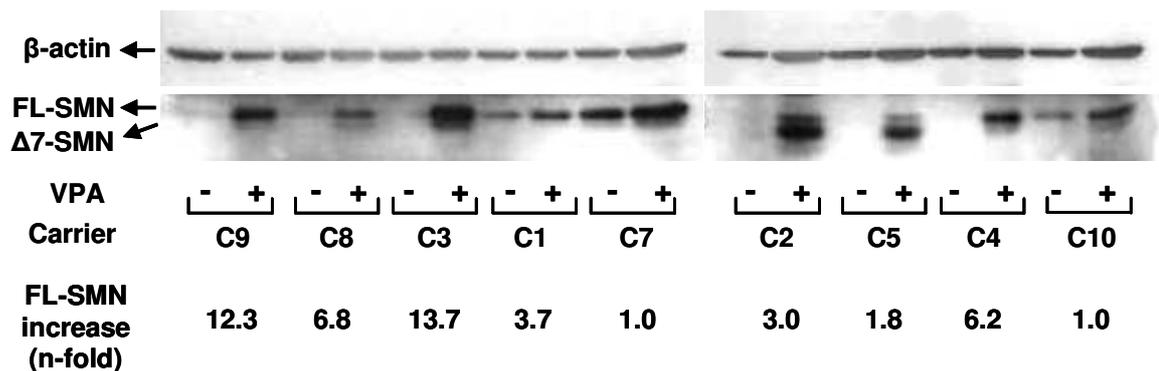


**Figure 37: Analysis of SMN protein levels in nine SMA carriers treated with VPA. Protein extracts were prepared from PBMCs collected once before starting VPA medication and once after individual VPA serum levels were adapted to the therapeutic range. Western blotting was performed with β-actin serving as loading control. For each subject, the baseline SMN protein level is shown in the left lane and the corresponding SMN protein level determined under VPA treatment is presented in the right lane. Two bands visible for SMN result from the FL (upper band) and the Δ7 isoform (lower band). The change in FL protein levels is given as n-fold increase compared to baseline.**

range. PBMCs were isolated and proteins extracted to perform western blotting since flow cytometry analysis could not be applied. Staining of β-actin was used to verify equal protein loading on the blot followed by detection of SMN in a second step. In seven subjects, VPA treatment generated clearly raised FL-SMN protein levels ranging from 1.8fold to 13.7fold as compared to the corresponding control protein sample (figure 37). In agreement with the observations on RNA level, the degree of augmentation did not correspond to the number of *SMN2* copies present in each subject (see table 25). With the exception of C9, all of the individuals showing increased SMN protein levels also revealed a rise of their FL-*SMN* transcript amounts under VPA treatment. In the SMA carriers C7 and C10, VPA therapy did not induce any change of the SMN protein level which matched the respective FL-*SMN* mRNA data. Interestingly, exclusively in C2 and C5, VPA caused a higher rise of the Δ7-SMN protein amount than of the FL-SMN. In contrast, neither for C5 nor for C2 a pronounced effect on splicing was seen on RNA level.

### 4.3.6    Analysis of *SMN2* mRNA levels in peripheral whole blood from patients with type I, II, and III SMA treated with valproic acid

Because shipping of blood samples from the patients' homes to the laboratory was necessary and a collection system that stabilizes proteins was not available, investigations were restricted to RNA analysis. Peripheral whole blood from a total number of 20 patients with SMA who were taking VPA in individual experimental curative approaches was used to investigate *SMN2* activity *in vivo.* Each of the sample sets included two blood samples before starting VPA medication and three additional samples obtained after the VPA dose was adjusted to therapeutic drug serum levels. FL-*SMN2* and Δ7-*SMN2* transcript levels and the corresponding FL-*SMN2*/Δ7-*SMN2* ratio were analyzed and are given in tables 26 to 28 and figure 38.

Among the four patients with type III SMA, subjects P1 and P3 revealed FL-*SMN2* mRNA amounts peaking in a 1.7fold increase upon drug therapy. The remaining two patients surprisingly presented decreased transcript levels as low as 0.4fold (P4) and 0.3fold (P2), respectively, compared to baseline (table 26 and figure 38 A). Similar results were obtained in patients with type II SMA: While 4/11 subjects responded with a considerable elevation of FL transcript levels up to a maximum between 1.9fold (P5 and P6) and 1.5fold (P8), in a number of five patients (P11 to P15) FL-*SMN2* dropped down to amounts ranging between 0.7fold and 0.4fold compared to the values determined before medication (table 28 and figure 38 B). In P9, a fluctuation of FL-*SMN2* above and below baseline level was determined. P10 did not appear to respond to VPA therapy. Analysis of the data obtained from the five patients with SMA type I revealed that subject P16 responded to the drug with an up to 1.9fold augmentation. FL-*SMN2* levels of P17 and P18 remained unchanged, while in P19 and P20 a fluctuation comparable to P9 was obtained (table 27 and figure 38 C). Due to fluctuations of the values throughout therapy, significance was reached only in a single SMA patient, P6 (p<0.05).

According to the observation in SMA carriers, a comparison between the seven clearly responding patients with SMA did not reveal a correlation between FL-*SMN2* elevation and the individual number of *SMN2* genes or the severity of the SMA phenotype (tables 26 to 28). The degree of increase in P1
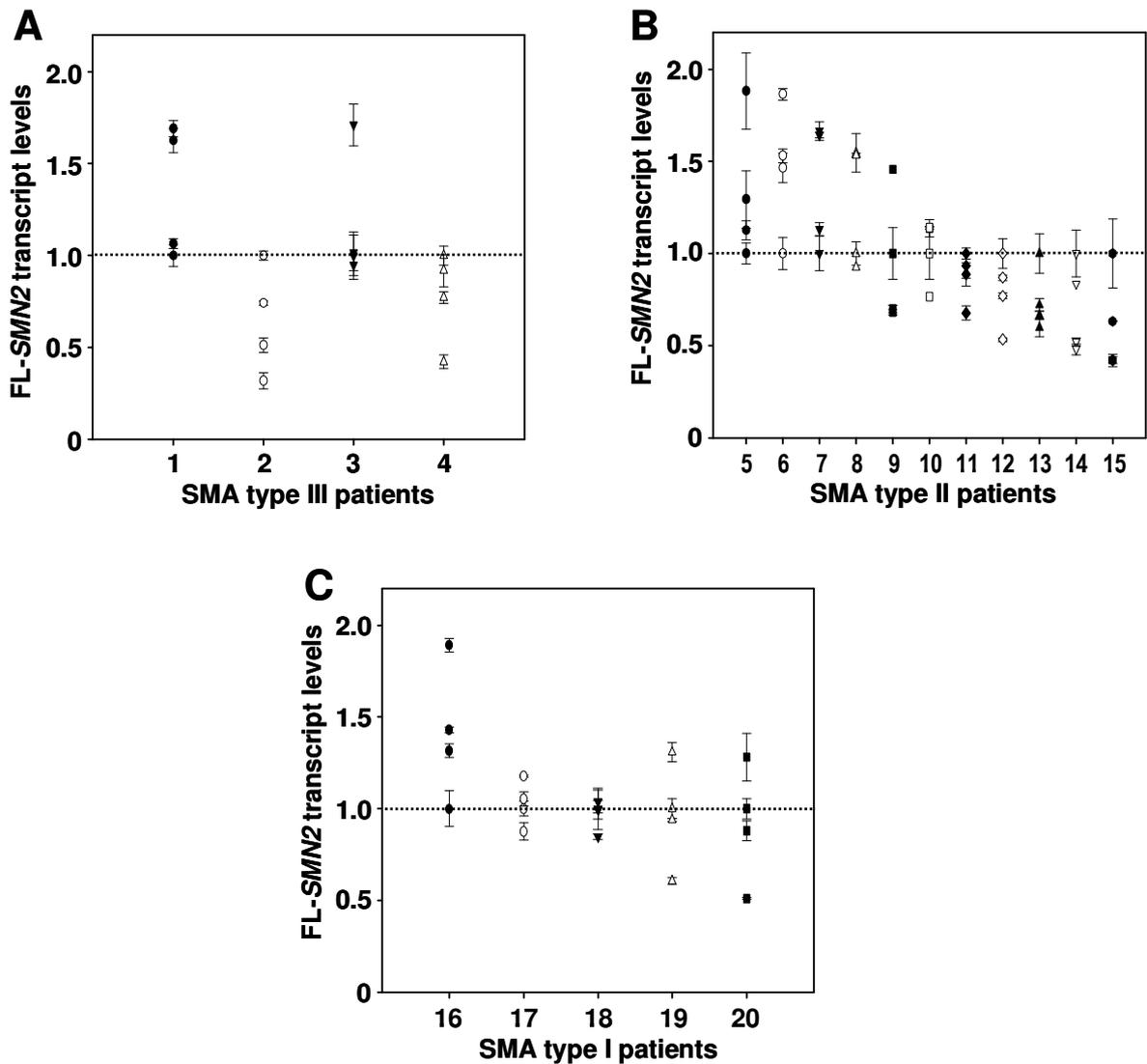
**Figure 38: FL-*SMN2* transcript levels in blood obtained from 20 SMA patients treated with VPA in individual experimental curative approaches throughout Germany according to section 41 of the German Drug Act (AMG). The cohort included four type III SMA patients (A), 11 type II SMA patients (B), and five type I SMA patients (C). All measurements are given as mean ± SEM. For each subject, they include the mean baseline FL-*SMN2* transcript level determined in two blood samples before drug therapy (normalized to 1.0, also indicated by the dotted line) and three additional values obtained throughout medication, shown as multiples of the baseline level.**

and P3 (SMA III, 3 and 4 *SMN2*, respectively) is in a similar range (1.5fold to 1.9fold) like in P5, P6, P7, P8 (SMA II, 3 *SMN2*), and P16 (SMA I, 2 *SMN2*). Furthermore, fluctuations of the VPA serum level throughout therapy were not always correspondingly reflected in the FL-*SMN2* levels which partly varied, and were subject to decreases under VPA treatment. Regulation of the Δ7-*SMN2* transcript levels in the investigated patients with SMA occurred in parallel with the FL-*SMN2* levels, again significant only for P6 (p<0.05) (tables 26 to 28). Consequently, changes in the FL/Δ7 ratio were not detected (tables 26 to 28). Among the responders, only in P1, P5, and P16, FL-*SMN2* appeared to be more strongly elevated than Δ7-*SMN2*, resulting in a maximum increase in ratio by 1.3fold to 1.6fold (significant for P1, p<0.05). This indicates a weak impact of VPA on *SMN2* splicing in these subjects, although the observed effect is rather weak.

**Table 26: Expression of FL-*SMN2*, Δ7-*SMN2*, and FL/Δ7 ratio in peripheral whole blood from four patients with type III SMA (P1 to P4) treated with VPA. Values are given as mean ± SEM together with the corresponding VPA serum level determined in the same blood sample (n.d. = not detected). The most extensively increased/decreased value detected for FL-*SMN2*, Δ7-*SMN2*, and the FL/Δ7 ratio in the respective patient with SMA is indicated in bold.**

| SMA Patient | | *SMN2* transcript levels and corresponding VPA serum levels | | | |
|---|---|---|---|---|---|
| **P1** | **FL-*SMN2*** | 1.0±0.1 | 1.1±0.0 | 1.6±0.1 | **1.7±0.0** |
| SMA III | **Δ7-*SMN2*** | 1.0±0.0 | 0.9±0.0 | 1.2±0.1 | **1.3±0.0** |
| *3xSMN2* | **FL/Δ7 ratio** | 1.0±0.1 | 1.2±0.0 | 1.3±0.0 | **1.3±0.0** |
| | **VPA (mg/l)** | baseline | 61.0 | 99.0 | 84.3 |
| **P2** | **FL-*SMN2*** | 1.0±0.0 | 0.7±0.0 | **0.3±0.0** | 0.5±0.0 |
| SMA III | **Δ7-*SMN2*** | 1.0±0.0 | 0.7±0.1 | **0.3±0.1** | 0.5±0.0 |
| *3xSMN2* | **FL/Δ7 ratio** | 1.0±0.0 | 1.0±0.1 | **1.0±0.3** | 1.0±0.2 |
| | **VPA (mg/l)** | baseline | 78.0 | 84.0 | 84.0 |
| **P3** | **FL-*SMN2*** | 1.0±0.1 | **1.7±0.1** | 1.0±0.1 | 0.9±0.1 |
| SMA III | **Δ7-*SMN2*** | 1.0±0.0 | **1.8±0.0** | 1.1±0.1 | 1.0±0.0 |
| *4xSMN2* | **FL/Δ7 ratio** | 1.0±0.1 | **0.9±0.1** | 0.9±0.0 | 0.9±0.0 |
| | **VPA (mg/l)** | baseline | 82.4 | 62.0 | 79.9 |
| **P4** | **FL-*SMN2*** | 1.0±0.1 | 0.9±0.1 | 0.8±0.0 | **0.4±0.0** |
| SMA III | **Δ7-*SMN2*** | 1.0±0.0 | 0.9±0.1 | 0.8±0.0 | **0.5±0.0** |
| *4xSMN2* | **FL/Δ7 ratio** | 1.0±0.0 | 1.0±0.0 | 1.0±0.1 | **0.8±0.1** |
| | **VPA (mg/l)** | baseline | 58.5 | 82.8 | n.d. |

**Table 27: Expression of FL-*SMN2*, Δ7-*SMN2*, and FL/Δ7 ratio in peripheral whole blood from five patients with type I SMA (P16 to P20) treated with VPA. Values are given as mean ± SEM together with the corresponding VPA serum level determined in the same blood sample (n.d. = not detected). The most extensively increased/decreased value detected for FL-*SMN2*, Δ7-*SMN2*, and the FL/Δ7 ratio in the respective patient with SMA is indicated in bold.**

| SMA Patient | | *SMN2* transcript levels and corresponding VPA serum levels | | | |
|---|---|---|---|---|---|
| **P16** | **FL-*SMN2*** | 1.0±0.1 | 1.4±0.0 | **1.9±0.0** | 1.3±0.0 |
| SMA I | **Δ7-*SMN2*** | 1.0±0.0 | 0.9±0.1 | **1.4±0.0** | 1.0±0.1 |
| *2xSMN2* | **FL/Δ7 ratio** | 1.0±0.1 | **1.6±0.1** | 1.4±0.0 | 1.3±0.1 |
| | **VPA (mg/l)** | baseline | n.d. | 79.0 | 99.0 |
| **P17** | **FL-*SMN2*** | 1.0±0.0 | **1.2±0.0** | 1.1±0.0 | 0.9±0.1 |
| SMA I | **Δ7-*SMN2*** | 1.0±0.0 | **1.1±0.1** | 1.0±0.1 | 0.8±0.1 |
| *2xSMN2* | **FL/Δ7 ratio** | 1.0±0.1 | **1.1±0.1** | 1.1±0.1 | 1.1±0.1 |
| | **VPA (mg/l)** | baseline | 53.0 | 38.0 | 58.0 |
| **P18** | **FL-*SMN2*** | 1.0±0.1 | 1.0±0.1 | 1.0±0.1 | **0.9±0.0** |
| SMA I | **Δ7-*SMN2*** | 1.0±0.1 | 1.0±0.0 | 1.0±0.0 | **0.7±0.0** |
| *2xSMN2* | **FL/Δ7 ratio** | 1.0±0.1 | 1.0±0.0 | 1.0±0.1 | **1.3±0.1** |
| | **VPA (mg/l)** | baseline | 81.3 | 72.2 | 67.6 |
| **P19** | **FL-*SMN2*** | 1.0±0.1 | 0.9±0.0 | **1.3±0.1** | 0.6±0.0 |
| SMA I | **Δ7-*SMN2*** | 1.0±0.0 | 1.0±0.0 | **1.2±0.0** | 0.7±0.0 |
| *3xSMN2* | **FL/Δ7 ratio** | 1.0±0.1 | 0.9±0.0 | **1.1±0.0** | 0.9±0.0 |
| | **VPA (mg/l)** | baseline | 38.0 | 99.0 | 44.0 |
| **P20** | **FL-*SMN2*** | 1.0±0.1 | **1.3±0.1** | 0.5±0.0 | 0.9±0.1 |
| SMA I | **Δ7-*SMN2*** | 1.0±0.1 | **1.0±0.0** | 0.6±0.0 | 0.8±0.0 |
| *3xSMN2* | **FL/Δ7 ratio** | 1.0±0.0 | **1.3±0.1** | 0.8±0.0 | 1.1±0.1 |
| | **VPA (mg/l)** | baseline | 76.2 | n.d. | n.d. |

**Table 28: Expression of FL-*SMN2*, Δ7-*SMN2*, and FL/Δ7 ratio in peripheral whole blood from 11 patients with type II SMA (P5 to P15) treated with VPA. Values are given as mean ± SEM together with the corresponding VPA serum level determined in the same blood sample (n.d. = not detected). The most extensively increased/decreased value detected for FL-*SMN2*, Δ7-*SMN2*, and the FL/Δ7 ratio in the respective patient with SMA is indicated in bold.**

| SMA Patient | *SMN2* transcript levels and VPA levels in serum | | | | | SMA Patient | *SMN2* transcript levels and VPA levels in serum | | | | |
|---|---|---|---|---|---|---|---|---|---|---|---|
| **P5** SMA II *3xSMN2* | FL-*SMN2* | 1.0±0.1 | 1.3±0.2 | 1.1±0.1 | **1.9±0.2** | **P11** SMA II *3xSMN2* | FL-*SMN2* | 1.0±0.0 | 0.9±0.1 | 0.9±0.1 | **0.7±0.0** |
| | Δ7-*SMN2* | 1.0±0.1 | 1.1±0.0 | 1.1±0.0 | **1.5±0.0** | | Δ7-*SMN2* | 1.0±0.0 | 0.9±0.1 | 0.8±0.0 | **0.6±0.0** |
| | FL/Δ7 ratio | 1.0±0.1 | 1.2±0.1 | 1.0±0.1 | **1.3±0.1** | | FL/Δ7 ratio | 1.0±0.0 | 1.0±0.0 | 1.1±0.1 | **1.2±0.1** |
| | VPA (mg/l) | baseline | 71.0 | 68.4 | 84.2 | | VPA (mg/l) | baseline | 78.2 | 56.1 | 47.9 |
| **P6** SMA II *3xSMN2* | FL-*SMN2* | 1.0±0.1 | 1.5±0.1 | **1.9±0.0** | 1.5±0.0 | **P12** SMA II *3xSMN2* | FL-*SMN2* | 1.0±0.1 | 0.8±0.0 | **0.5±0.0** | 0.9±0.0 |
| | Δ7-*SMN2* | 1.0±0.0 | 1.3±0.0 | **1.7±0.1** | 1.4±0.0 | | Δ7-*SMN2* | 1.0±0.1 | 0.7±0.0 | **0.5±0.0** | 0.8±0.0 |
| | FL/Δ7 ratio | 1.0±0.1 | 1.2±0.0 | **1.1±0.1** | 1.1±0.0 | | FL/Δ7 ratio | 1.0±0.1 | **1.1±0.0** | 1.0±0.0 | 1.1±0.1 |
| | VPA (mg/l) | baseline | 63.0 | 69.3 | 90.0 | | VPA (mg/l) | baseline | 63.8 | 57.5 | 68.7 |
| **P7** SMA II *3xSMN2* | FL-*SMN2* | 1.0±0.1 | **1.7±0.0** | 1.6±0.0 | 1.1±0.0 | **P13** SMA II *3xSMN2* | FL-*SMN2* | 1.0±0.1 | 0.7±0.0 | 0.7±0.0 | **0.6±0.0** |
| | Δ7-*SMN2* | 1.0±0.1 | **1.6±0.1** | 1.3±0.0 | 1.1±0.0 | | Δ7-*SMN2* | 1.0±0.1 | 0.8±0.0 | 0.8±0.0 | **0.7±0.0** |
| | FL/Δ7 ratio | 1.0±0.0 | 1.1±0.1 | **1.2±0.0** | 1.0±0.0 | | FL/Δ7 ratio | 1.0±0.0 | 0.9±0.0 | 0.9±0.1 | **0.9±0.0** |
| | VPA (mg/l) | baseline | 54.0 | 58.8 | 73.7 | | VPA (mg/l) | baseline | 62.7 | 83.0 | 79.2 |
| **P8** SMA II *3xSMN2* | FL-*SMN2* | 1.0±0.1 | 1.5±0.1 | **1.5±0.0** | 0.9±0.0 | **P14** SMA II *3xSMN2* | FL-*SMN2* | 1.0±0.1 | 0.8±0.0 | 0.5±0.0 | **0.5±0.0** |
| | Δ7-*SMN2* | 1.0±0.0 | 1.4±0.1 | **1.4±0.0** | 0.8±0.1 | | Δ7-*SMN2* | 1.0±0.1 | 1.0±0.0 | 0.6±0.0 | **0.6±0.0** |
| | FL/Δ7 ratio | 1.0±0.0 | 1.1±0.0 | **1.1±0.0** | 1.1±0.1 | | FL/Δ7 ratio | 1.0±0.0 | 0.8±0.0 | 0.8±0.1 | **0.8±0.0** |
| | VPA (mg/l) | baseline | 69.9 | 54.7 | 98.3 | | VPA (mg/l) | baseline | 88.3 | 73.3 | 72.4 |
| **P9** SMA II *3xSMN2* | FL-*SMN2* | 1.0±0.1 | 0.7±0.0 | **1.5±0.0** | 0.7±0.0 | **P15** SMA II *3xSMN2* | FL-*SMN2* | 1.0±0.2 | 0.6±0.0 | **0.4±0.0** | 0.4±0.0 |
| | Δ7-*SMN2* | 1.0±0.1 | 0.7±0.0 | **1.8±0.1** | 0.6±0.0 | | Δ7-*SMN2* | 1.0±0.2 | 0.7±0.1 | **0.4±0.1** | 0.5±0.1 |
| | FL/Δ7 ratio | 1.0±0.0 | 1.0±0.0 | **0.8±0.0** | 1.1±0.1 | | FL/Δ7 ratio | 1.0±0.0 | 0.9±0.1 | 1.0±0.3 | **0.8±0.1** |
| | VPA (mg/l) | baseline | 95.1 | 68.6 | n.d. | | VPA (mg/l) | baseline | 96.0 | 98.0 | 92.0 |
| **P10** SMA II *3xSMN2* | FL-*SMN2* | 1.0±0.1 | **0.8±0.0** | 1.1±0.0 | 1.1±0.0 | | | | | | |
| | Δ7-*SMN2* | 1.0±0.1 | **0.7±0.1** | 0.9±0.0 | 1.0±0.1 | | | | | | |
| | FL/Δ7 ratio | 1.0±0.0 | 1.1±0.1 | **1.2±0.0** | 1.1±0.1 | | | | | | |
| | VPA (mg/l) | baseline | 83.9 | 73.5 | 80.7 | | | | | | |

# 5      Discussion

*SMN1*, the disease determining gene in SMA, was identified in 1995. This provided the basis for the development of a fast molecular genetic diagnostic test that is available today (Lefebvre et al. 1995; Scheffer et al. 2001). Since the same deletion mutation is found in approximately 94% of all SMA cases (Wirth 2000), identification of the vast majority of patients is relatively easy, and highly reliable. This is one of the most important prerequisites for a successful treatment of SMA.

Meanwhile, comprehensive knowledge regarding the pathological disease mechanisms and the underlying molecular principles was gained, most importantly including the discovery and characterization of the *SMN2* copy gene. *SMN2* is present at least once in each SMA patient. Elevating the activity of *SMN2* and/or altering its splicing pattern by promoting exon 7 inclusion is considered a major target for a causative SMA therapy. However, up to present a cure for SMA is not yet available. The development of a therapy is an exceptional challenge in SMA research.

## 5.1     *In vitro* and *ex vivo* investigations of the first-generation HDAC inhibitor valproic acid

The identification of chemical compounds that inhibit HDACs was a major step toward the development of a therapy for SMA. Initially, HDAC inhibitors were exclusively considered as promising drugs for cancer. They inhibit proliferation and induce differentiation of tumor cells *in vitro* and *in vivo*. These activities are mainly facilitated by hyperacetylation of histone proteins which subsequently leads to an altered chromatin structure and activated gene expression (Cress and Seto 2000; Marks et al. 2001; Marks et al. 2003; Marks et al. 2004).

Importantly, the stimulation of *SMN2* gene expression has been hypothesized to be of benefit for SMA patients. Thus, it seemed reasonable to investigate whether the potency of HDAC inhibitors is not only limited to the regulation of genes that are involved in cancer, but if they are also able to elevate the expression of the *SMN2* gene. The first HDAC inhibitor which was tested in cell lines derived from SMA patients was butyrate, a drug that has long been known to induce hyperacetylation of chromatin in cell culture *in vitro* (Riggs et al. 1977). Incubation of EBV-transformed lymphoblastoid cell lines derived from SMA type I, II, and III patients resulted in increased FL-*SMN2* transcript and SMN protein levels (Chang et al. 2001). It was demonstrated that this augmentation is due to an efficient reversion of the *SMN2* splicing pattern and exon 7 inclusion by butyrate. Moreover, it was shown that the compound elevates the level of SR proteins in the treated cell lines, however, this was not studied in more detail. Administration of butyrate to pregnant mothers of SMA transgenic mice (*Smn*^{-/-}; *SMN2*) improved the survival in their offspring. The authors suggested that the drug exerts its effect on *SMN2* splicing via an indirect pathway. They assumed that butyrate might hyperacetylate histones such that factors are released which finally regulate the alternative splicing of *SMN2* exon 7. It remained unclear whether butyrate also directly affects *SMN2* expression. A quantification of the total amount of *SMN2*

transcripts in butyrate-treated cell lines was not included in the study, leaving it open whether the transcription of the *SMN2* gene was activated.

This was the first study which suggested that HDAC inhibitors might be able to influence *SMN2* expression. However, butyrate is characterized by a very short terminal half-life of only six minutes in human serum. Thus, after systemic administration, butyrate would never reach a target in the human organism in sufficient amounts (Miller et al. 1987; Newmark et al. 1994; Newmark and Young 1995; Engelhard et al. 2001). This includes α-motor neurons in the spinal cord, although the drug would be able to cross the blood-brain barrier (Tsuji 2005). Consequently, butyrate is not suitable for a long-term therapy in SMA patients and was not considered further.

When the results obtained with butyrate were published in 2001, it was also discovered that VPA belongs to the class of drugs which are able to inhibit HDAC activity (Gottlicher et al. 2001; Phiel et al. 2001). *In vitro* experiments with VPA revealed that the compound efficiently hyperacetylates histone proteins in numerous cell culture systems, relieves HDAC-dependent transcriptional repression, and activates the transcription from diverse promoters. Together with these findings, it was observed that VPA inhibits proliferation and induces differentiation in cancer cell lines. Therefore, the drug was suggested as candidate for the treatment of cancer.

However, given the fact that the HDAC inhibitor butyrate was demonstrated to increase FL-*SMN2* transcript and SMN protein levels *in vitro* and in mice *in vivo*, it appeared very exciting to investigate if the HDAC inhibitor VPA possesses a similar potency. In addition, both compounds are short-chain fatty acids and therefore share similar chemical structures. This increases the probability that both drugs target similar classes of enzymes and trigger similar effects. Although in 2001, nothing was known about the HDACs which are responsible for deacetylation of histones in the *SMN2* promotor region and butyrate and VPA do not specifically inhibit one single HDAC, the close relationship between the two compounds seemed very promising that they both might act on *SMN2* expression. Importantly, VPA is a very well-known drug which is approved by the Food and Drug Administration (FDA) and has been used in the treatment of epilepsy for more than three decades (Johannessen and Johannessen 2003). Additionally, VPA is used in the therapy of bipolar disorders, neuropathic pain, and migraine prophylaxis (Johannessen 2000). Currently, the mechanism of action is not completely understood, although especially the antiepileptic effects have been related mainly to γ-aminobutyric acid (GABA), and the interaction of VPA with sodium and calcium channels (Johannessen 2000; Isoherranen et al. 2003). However, based on the finding that only some but not all antiepileptic drugs are able to inhibit HDACs and to hyperacetylate histones (Eyal et al. 2004), it is unlikely that the anticonvulsant activity of VPA is exclusively due to HDAC inhibition, whereas a partial contribution can not be excluded. VPA is characterized by a suitable terminal half-life of 9-18 h in human serum, it rarely shows severe adverse events, crosses the blood-brain-barrier, and possesses an excellent oral bioavailability. This makes VPA adequate for the use in humans and made the drug even more interesting to be investigated for a potential activity on *SMN2* expression.

To study whether VPA is able to regulate *SMN2* expression, the initial experiments were carried out in EBV-transformed lymphoblastoid cell lines derived from SMA patients. They were used because a large number of different cell lines were available in our laboratory. Moreover, EBV cell lines grow very fast, providing enough material for experiments within a relatively short period of time, and conditions that are suitable for drug treatment were given already by Chang and co-workers (Chang et al. 2001).

However, in our hands, treatment of EBV cell lines with VPA did not reveal any regulation of the SMN protein level, regardless of the drug concentration, the cell number, and the incubation time. The results which were already published for butyrate could not be reproduced either. The reason for this observation remains unclear. It is known that the SMN protein interacts with the EBV nuclear antigen 6, a viral protein which is required for the EBV-induced immortalization of primary human B-lymphocytes *in vitro* (Krauer et al. 2004). This viral protein is also known to be a transcriptional regulator. Given the fact that the EBV-transformed cell lines used by Chang *et al.* and in our lab were not purchased from a certain company, but established in the respective lab, it is possible that the immortalization of the lymphocytes was performed with EBV stocks that are not completely identical. Any mutation or other difference related to the EBV nuclear antigen 6 (EBNA-6) could interfere with its interaction with the SMN protein or its function as transcriptional regulator, and result in a differential regulation of SMN expression. Mutations have been demonstrated already for EBNA-4 (Chu et al. 1999). This might finally have impact on the results obtained after drug treatment of the immortalized cell lines. However, these are speculations and a proof cannot be given.

As alternative tool to study whether VPA is able to influence *SMN2* expression *in vitro*, primary fibroblast cultures derived from SMA patients were selected. Due to their origin, these cell lines also provide the genotypic background typical for SMA including homozygous loss of *SMN1*, and one or more *SMN2* copies. Primary SMA fibroblasts do not grow as fast as EBV-transformed lymphoblastoid cell lines, but still they are relatively easy to maintain, and divide with sufficient frequency within a certain time period. The cells are not immortalized by a virus.

The application of primary fibroblasts for drug treatment experiments turned out to be more successful than the use of EBV cell lines as the incubation with butyrate resulted in significantly increased SMN protein levels. Thus, the results from Chang and co-workers were confirmed and butyrate served as positive control to ensure that the fibroblast assay is suitable to investigate the potential impact of a drug on *SMN2* expression. To study VPA, three different primary fibroblast cell lines were treated with the drug, including two cell lines from type I SMA patients with two or three *SMN2* copies and one cell line from a type II SMA patient with three *SMN2* copies. The VPA doses used for the experiments were 0.5, 5, 50, 500, and 1000 µM. Except for 500 and 1000 µM, all concentrations are within the therapeutic range common in epilepsy treatment. Therapy of epilepsy patients with VPA usually requires serum levels of 480-700 µM VPA (corresponding to about 70-100 µg/ml). About 15% of the VPA present in serum cross the blood-brain-barrier, leading to a concentration of 72-105 µM VPA (10.5-15 µg/ml) in brain and spinal liquor (Wieser 1991). The concentrations 0.5-50 µM VPA which were applied to treat primary fibroblasts with VPA correspond to 0.072-7.2 µg VPA/ml. Such concentrations can be reached in human liquor which surrounds the spinal cord and α-motor neurons. Importantly, these concentrations are even lower than the therapeutic VPA serum level, suggesting that they are not toxic and well tolerated. Only 500 and 1000 µM VPA are above the therapeutic range, which has to be considered for interpretation of the results obtained *in vitro*.

In the SMA fibroblast lines incubated with VPA, it was conclusively demonstrated that the compound is able to significantly increase the SMN2 protein level. Compared to untreated cells, drug treatment resulted in a maximum increase ranging between 2.7fold and 3.3fold. The 3.3fold increase was observed at 500 µM VPA in ML-5, however, already at lower concentrations between 0.5 and 50 µM VPA, the cell line presented markedly elevated SMN protein levels. The maximum increase in ML-17

and ML-16 was observed at 50 µM and 5 µM VPA, respectively. Also in these two cell lines, treatment with 0.5 µM VPA already revealed significantly elevated SMN protein levels. Compared to the VPA level common in epilepsy treatment, these data clearly show that an efficient increase of the SMN protein level was achieved even at lower drug concentrations in each of the investigated SMA fibroblast lines. Based on the favorable characteristics of VPA regarding the clinical use in humans and the chance for a causative pharmacological treatment of SMA which arises from the possibility to elevate *SMN2*-derived protein levels, this was an exciting and very promising finding. A more than 2fold increase of the SMN protein level which was achieved in each VPA-treated fibroblast line at 50 µM or a lower drug concentration *in vitro* is assumed to be of benefit to impede the onset or the progression of SMA *in vivo*. Depending on the number of *SMN2* copies, FL-*SMN2* RNA levels in lymphoblastoid cell lines derived from SMA patients range between 20 and 50% compared to controls (Helmken et al. 2003). A similar degree of reduction was observed for the SMN protein level in spinal cord tissue when comparing SMA type I and III fetuses with control fetuses (Lefebvre et al. 1997). In comparison, SMA carriers with one *SMN1* copy and usually 1-3 *SMN2* copies produce about 60-80% FL-*SMN* RNA and protein compared to controls and therefore are asymptomatic (Feldkötter et al. 2002). Thus, doubling of SMN2 protein in SMA patients could be enough to stop or slow down disease progression. However, the experiments with VPA were performed in fibroblasts although α-motor neurons are the affected tissue in SMA patients and therefore present the target for an up-regulation of the SMN2 protein level. It remains to be determined whether the observed effect can also be achieved in these cells and whether this would indeed be sufficient to protect the α-motor neurons from degeneration in SMA patients.

A comparison of the results obtained for VPA with those obtained for butyrate revealed only marginal differences. Both drugs share the ability to increase SMN protein levels at concentrations as low as 0.5 µM, and the maximum up-regulation achieved in the fibroblasts was in a similar range, suggesting that the potency of VPA and butyrate to increase SMN protein levels is very similar.

Among the three human fibroblast lines treated with VPA, the maximum SMN2 protein level was observed at different VPA concentrations (5, 50, and 500 µM VPA, respectively). This is consistent with the inter-individual variability of the VPA metabolism observed among epilepsy patients during therapy (Cloyd 1991). After reaching the maximum, SMN protein levels dropped in ML-17 and ML-5. In ML-16, a second maximum was observed, before protein levels also dropped down at 1000 µM. However, in each of the fibroblast lines, the decrease was marginal. Compared to the respective untreated cells, the SMN protein level was still significantly increased. This suggested that all VPA doses used in the experiment were well tolerated by the cells, which was consistent with the data obtained from the MTT assays showing that cell viability was not significantly affected by VPA. The only exception was incubation of ML-5 with 1000 µM VPA which resulted in a significant decrease of cell viability. Although the corresponding SMN protein level in ML-5 was not severely reduced, this observation might indicate that treatment of the fibroblasts with 1000 µM VPA is the upper concentration limit which is well tolerated by the cells. This also correlates with the fact that 1000 µM VPA is a concentration above the therapeutic range known from epilepsy therapy.

The three fibroblast cell lines incubated with VPA are characterized by different numbers of *SMN2* copies. One cell line carries only 2 *SMN2* copies, while two cell lines have 3 *SMN2* copies. However, an overall correlation between the number of *SMN2* copies and the degree of elevated SMN protein

level was not observed. While such a correlation could be proposed for 0.5, 5, and 500 μM VPA, it is not true at 50 and 1000 μM. This indicates that a direct correlation between the *SMN2* copy number and the percentage increase in SMN levels is either restricted to low VPA concentrations not exceeding 5 μM, or it rather suggests that different factors may act on *SMN2* transcription and/or translation which vary among the drug concentrations and the cell lines. Treatment of a larger number of cell lines with varying *SMN2* copy numbers would be required to clearify this observation.

The expression analysis of *SMN2* in primary SMA fibroblasts after treatment with VPA revealed that augmented SMN protein levels are caused by an increased production of FL-*SMN2* transcripts. Nowadays, the quantification of RNA levels would be performed applying quantitative real-time PCR (Riessland et al. 2006), however, at the time point of investigation, this tool was not yet available in the laboratory. Thus, semi-quantitative multiplex PCR was carried out followed by separation of the PCR products on a gel and densitometric measurement of the bands. The significant elevation of FL-*SMN2* transcripts in each of the three investigated fibroblast lines was facilitated by two different processes: an elevated *SMN2* transcription rate (proven by the augmented amount of total *SMN2* transcripts), and a reversion of the *SMN2* splicing pattern (demonstrated by elevated FL-*SMN2* / Δ7-*SMN2* transcript ratios). VPA is known to influence the expression of a large variety of genes through different pathways (Blaheta and Cinatl 2002). Two of these pathways are most likely responsible for the stimulation of *SMN2* gene transcription. On the one hand, VPA is a powerful inhibitor of histone deacetylases and causes the accumulation of hyperacetylated histones H3 and H4 which releases DNA from the histone proteins. This allows access for transcription factors and activates gene transcription as is was demonstrated already *in vitro* and *in vivo* (Gottlicher et al. 2001; Phiel et al. 2001). Thus, by directly increasing the acetylation status of histones in the *SMN* promoter region, VPA could increase *SMN* RNA expression. On the other hand, the DNA binding activity of the transcription factors AP1 and Sp1 has been proven to be stimulated by VPA (Wlodarczyk et al. 1996; Chen et al. 1997; Chen et al. 1999; Arinze and Kawai 2003). Strikingly, the *SMN2* promoter contains putative binding motifs for both proteins (Echaniz-Laguna et al. 1999; Monani et al. 1999b) which additionally could explain the augmented *SMN2* transcription rate in SMA fibroblasts upon incubation with VPA. Moreover, it is well known that the activity of transcription factors can be modulated by acetylation which subsequently exerts and effect on gene transcription (Cress and Seto 2000; Marks et al. 2001; Marks et al. 2004). VPA could acetylate such a critical transcription factor involved in *SMN2* expression regulation and thereby change its activity. Since the *SMN1* and the *SMN2* promoter are essentially identical (Echaniz-Laguna et al. 1999; Monani et al. 1999b), these observations are not likely to be an *SMN2* promoter-specific effect.

However, the increase in FL-*SMN2* transcript in VPA-treated primary fibroblasts is not purely a function of an activated *SMN2* promoter. If this were the case, the percentage increase of FL-*SMN2* transcript levels and Δ7-*SMN2* transcript levels would be equal, and the transcript ratio would remain unchanged. In contrast, the total amount of *SMN2* transcripts (FL and Δ7) would be unaffected if a drug exerts an effect exclusively on exon 7 inclusion without influencing the promoter activity. Consequently, the data rather suggest that both mechanisms transcriptional stimulation of the *SMN2* gene and reversion of the *SMN2* splicing pattern contribute to the elevated FL-*SMN2* transcript levels observed under VPA treatment. However, due to the observation that the increase in FL / Δ7 transcript ratios in the three investigated SMA cell lines is only moderate and not significant in one of the

fibroblast lines, it can be concluded that the augmented transcriptional activity of *SMN2* is the main mechanism that triggers elevated FL-*SMN2* transcript levels, whereas the impact of VPA on exon 7 inclusion is the secondary effect.

The preferred inclusion of *SMN2* exon 7 in VPA-treated SMA fibroblasts could be a consequence of elevated levels of Htra2-β1 protein. Htra2-β1 is an SR-like splicing factor. It has been demonstrated that *in vitro* over-expression leads to a reversion of the *SMN2* splicing pattern and most importantly also to an increase of the endogenous SMN protein level (Hofmann et al. 2000; Hofmann and Wirth 2002). Since Htra2-β1 was efficiently up-regulated by VPA in all three SMA fibroblast lines reaching maximum levels ranging between 2.7fold and 4.1fold, it most likely explains the achieved reversion of the *SMN2* splicing pattern. However, a comparison of the transcript ratio and the corresponding Htra2-β1 level at each single VPA dose did not reveal a clear correlation between the two parameters. Although the level of Htra2-β1 protein was increased whenever the corresponding FL / Δ7 ratio was found elevated, the maximum for each parameter was observed at different VPA concentrations in ML-16 and ML-5. Such a correlation was obtained only for ML-17. Moreover, increased Htra2-β1 levels did not always trigger an augmented transcript ratio, as demonstrated at 1000 μM VPA in ML-17 (transcript ratio unchanged, Htra2-β1 level increased up to 2.2fold). This suggests that Htra2-β1 might not be the only critical factor which exerts an effect on the *SMN2* splicing pattern in VPA-treated fibroblasts. It is possible that another yet unknown SR or SR-like protein is regulated by VPA and additionally interferes with exon 7 inclusion. However, the splicing factors SF2/ASF and SRp20 which were investigated together with Htra2-β1 and found elevated under VPA treatment are most likely not responsible for this observation. While SF2/ASF binds to *SMN1* RNA and facilitates the correct splicing, the C to T transition in exon 7 abolishes the ability of SF2/ASF to bind *SMN2* RNA (Cartegni and Krainer 2002). For SRp20, only an effect on its own splicing has been shown so far (Jumaa and Nielsen 1997); other genes regulated by SRp20 are yet unknown.

Another observation which could explain the absence of a clear correlation between the elevation of Htra2-β1 protein levels and the increased FL / Δ7 transcript ratio is the high variation of the splicing factor levels obtained in different cell passages from a particular fibroblast line under VPA treatment. The variability of up-regulated Htra2-β1 levels is demonstrated by the high SEM values at each single VPA concentration. Since separate experiments had to be performed to isolate RNA (for *SMN2* expression analysis) and to isolate protein (for an analysis of Htra2-β1 protein levels), it can not be excluded that due to the highly variable up-regulation of Htra2-β1 in different fibroblast passages the data for Htra2-β1 do not exactly reflect the Htra2-β1 level in the passages which were used to isolate RNA and to analyze the transcript ratio.

To approach the correlation between Htra2-β1 and the *SMN2* splicing pattern under VPA treatment in more detail, a procedure was established which allowed knocking down Htra2-β1 protein levels in VPA-treated fibroblasts. This experiment could give the final proof whether the increase in FL-*SMN2* / Δ7-*SMN2* transcript ratios in VPA-treated SMA cell lines is indeed triggered by elevated Htra2-β1 levels. If this were the case, an efficient and specific knock-down of Htra2-β1 should prevent any increase of the transcript ratio. However, the experiment failed. Using the conditions required to knock down Htra2-β1, VPA was unable to stimulate fibroblasts. This was due to the fact that both assays use different cell numbers to work properly (the siRNA assay required $1 \times 10^5$ cells, and the VPA assay in fibroblasts required the double amount of cells). It was not possible to use the VPA assay with $2 \times 10^5$

cells to knock down Htra2-β1, because this was too large-scale for a siRNA experiment. Thus, a final conclusion regarding the correlation between elevated Htra2-β1 and increased *SMN2* transcript ratios could not be drawn, because the Htra2-β1 knock-down and the stimulation of fibroblasts with VPA could not be simultaneously achieved in the SMA fibroblasts.

Interestingly, an efficient knock down of Htra2-β1 protein levels by more than 90% in primary SMA fibroblasts which are not treated with VPA revealed a moderate increase of the FL-*SMN2* / Δ7-*SMN2* transcript ratio. In addition, slightly increased FL-*SMN2* transcript levels were observed, while Δ7-*SMN2* levels remained unchanged, suggesting that the amount of total *SMN2* transcripts and the *SMN2* transcription rate was increased. To a lower degree, the latter result was also obtained in the negative control, indicating that increased transcriptional activity might also be an unspecific effect due to siRNA delivery to the cells. The finding of a slightly increased transcript ratio upon knock down of Htra2-β1 protein levels was very unexpected. Given that Htra2-β1 binds to a specific motif in *SMN2* exon 7 and over-expression of Htra2-β1 efficiently promotes exon 7 inclusion and facilitates a reversion of the *SMN2* splicing pattern (Hofmann et al. 2000), it seems reasonable to assume that the splicing factor Htra2-β1 is responsible for the low amount of ~10-20% FL-*SMN2* transcript produced by the *SMN2* gene. Thus, the lack of Htra2-β1 should further promote exon 7 skipping and result in a substantial decrease of the FL-*SMN2* / Δ7-*SMN2* transcript ratio. However, this was not the case, suggesting that either the very low amount of remaining Htra2-β1 is still sufficient to maintain the generation of FL-*SMN2* transcripts, or mainly other splicing factors are responsible for the ~10-20% of FL-*SMN2* transcripts produced by *SMN2*. Moreover, both scenarios do not explain the slight increase of the transcript ratio. Further experiments in other cell lines are necessary to confirm this observation, and to further elucidate the splicing regulation of the *SMN2* gene.

A comparison of the data for elevated FL-*SMN2* transcript levels with the corresponding data for elevated SMN protein levels revealed that the degree of up-regulation is different in each of the SMA cell lines treated with VPA. In two cell lines, FL-*SMN2* transcript levels were increased up to a maximum of ~2fold, whereas the corresponding SMN protein level peaked in a roughly 3fold elevation. The third fibroblast line presented ~5fold augmented FL-*SMN2* levels versus a ~3fold increase in SMN protein. Additionally, for each fibroblast line, there was a discrepancy between the VPA concentrations required for the maximum FL-*SMN2* RNA level and the maximum SMN protein level. This suggests that VPA differently stimulates transcription and translation of *SMN2*, and that the drug might also interfere with protein stability. Consistent with this observation, a modulated transcription of genes encoding translation factors has already been described for the HDAC inhibitors butyrate and trichostatin A (Goncalves et al. 2005). Furthermore, recent experiments demonstrated that both substances may enhance protein stability such that levels increase without any change of the transcriptional activity of the encoding gene (Chen and Faller 2005), giving rise to the assumption that VPA might act in a similar manner.

It was clearly demonstrated that various SR and SR-like splicing factors (including SF2/ASF, SRp20, and Htra2-β1) are up-regulated by VPA in SMA fibroblasts. Similar effects were achieved with butyrate. The latter finding is consistent with the observation of increased SR proteins in EBV-transformed lymphoblastoid cell lines treated with the drug (Chang et al. 2001). However, SRp20 was found unregulated in the EBV cell lines. This is in contrast to the findings in primary fibroblasts and might be due to a differential regulation of the expression of this protein in different cell lines. For the

increased levels of splicing factors, several explanations can be given. (i) The expression of the splicing factors is activated through inhibition of HDACs by VPA which causes histone hyperacetylation and results in elevated gene transcription. (ii) Transcription factor Sp1 binding motifs are also present in the promoter of Htra2-β1 (Nayler et al. 1998). Thus, increased DNA binding activity of Sp1 under VPA treatment may lead to an increase in Htra2-β1 expression. (iii) Another yet unknown transcription factor might be acetylated by VPA, leading to a modulation of its activity on the *SMN2* promoter (Cress and Seto 2000; Marks et al. 2001; Marks et al. 2004). (iv) It has been demonstrated that SMN regulates its own splicing factor Htra2-β1 such that reduced levels of SMN protein lead to reduced levels of Htra2-β1 but not of other splicing factors, although no protein-protein interaction between SMN and Htra2-β1 occurs (Helmken et al. 2003). One plausible explanation would be that the increase of target transcripts, in this case *SMN2* pre-mRNA, triggers the demand for splicing factors in order to guarantee correct pre-mRNA splicing (Misteli et al. 1997). (v) The altered activity of roughly 2% of the expressed genes observed after VPA treatment (Pazin and Kadonaga 1997) leads to increased levels of a large number of different transcripts in general which requires an elevated level of various splicing factors. (vi) A common pathway (e.g. activation of a kinase or phosphorylation of SR-domains) may be responsible for an elevation of splicing factors containing an SR-domain. The exact mechanism of action remains to be elucidated. In the SMA cell lines treated with VPA, it was shown that the level of *Htra2-β1* and *Htra2-β2* transcripts is elevated under drug treatment. This leads to the conclusion that the expression of the encoding *SFRS10* gene is activated by VPA, which is the trigger for increased Htra2-β1 protein levels. However, to elucidate the pathway responsible for transcriptional activation of *SFRS10*, to investigate the mechanism by which SRp20 and SF2/ASF protein levels are increased, and to check whether even several of the above mentioned possibilities contribute to the augmented splicing factor levels, further experiments are required. The finding that VPA is able to increase the level of various splicing factors opens the perspective that this drug may also have therapeutic implications for diseases other than SMA which are caused by a pathological splicing pattern.

The variability of elevated splicing factor levels obtained upon treatment of different passages from each SMA fibroblast line with a particular VPA concentration was also observed in the experiments with butyrate. Recently, similar results were presented for M344, another HDAC inhibitor (Riessland et al. 2006). This suggests that the variability is either triggered by a pathway specific of substances which belong to the class of HDAC inhibitors, or by the fact that the constant expression of splicing factors is very vulnerable to a critical parameter. It has been demonstrated that splicing is regulated by stress (Shin et al. 2004; Meshorer et al. 2005; Marin-Vinader et al. 2006). This is also true for fibroblasts, as demonstrated by the failure to detect Htra2-β1 protein after electroporation treatment of the cells. Thus, even if the viability of the cells was shown to be unaffected in the MTT assays, it is still conceivable that treatment of fibroblasts with drugs is a stress factor which causes variability in the expression and a variable up-regulation of splicing factor levels. However, this remains speculation.

Remarkably, as already discussed above, the transcription of approximately 2% of expressed genes is regulated by histone acetylation and deacetylation (Van Lint et al. 1996; Pazin and Kadonaga 1997). Consequently, the same number of genes is estimated to show altered activity induced by the class of HDAC inhibitors (Pazin and Kadonaga 1997; Butler et al. 2002; Glaser et al. 2003). Thus, the effect VPA and other HDAC inhibitors exert on the *SMN2* gene is rather unspecific. Exemplarily, this is

confirmed by the transcriptional activation of the *SFRS10* gene in VPA-treated fibroblasts. However, although the expression of a large number of genes is regulated by VPA, the observed severe adverse events observed in long-term therapies are rare (Johannessen 2000).

The results obtained for the treatment of SMA fibroblast lines with VPA were confirmed by Sumner and colleagues in 2003 (Sumner et al. 2003). A number of four fibroblast lines derived from SMA type I patients (two with 1 *SMN2* copy and two with 2 *SMN2* copies, respectively) were used and treated with the drug. Significantly increased FL-*SMN2* transcript and SMN protein levels were obtained in all cell lines 24 h after single drug treatment and after three days of daily drug treatment. The simultaneous measurement of FL-*SMN2* and Δ7-*SMN2* transcripts in one cell line applying quantitative real-time PCR revealed that both transcripts are increased, but the extent of increase in FL transcripts was greater and the *SMN2* transcript ratio was found to be augmented. This matches the results obtained in our laboratory, although Sumner and co-workers used VPA concentrations between 1 and 10 µM which is above the therapeutic range common in epilepsy therapy. Additionally, after a 5-day incubation with daily VPA doses, the number of gems in the nucleus was demonstrated to be increased in all patient cell lines. By a β-lactamase assay in NSC34 cells (neuroblastoma spinal cord cell line derived from mouse) transfected with an *SMN2* promoter-β-lactamase reporter gene vector, Sumner *et al.* also demonstrated that VPA indeed activates the *SMN2* promoter at doses starting at 10 µM. This is consistent with the idea that VPA activates *SMN2* transcription via the inhibition of HDACs and hyperacetylation of histones.

Meanwhile, it was also demonstrated by chromatin immunoprecipitation that rather low levels of the enzyme HDAC 1 and high levels of HDAC 2, but not HDACs 3, 4, or 5 are associated with the human *SMN* gene promoter (Kernochan et al. 2005). This suggests that HDAC 1 and in particular HDAC 2 play an important role in transcriptional regulation of *SMN*. The development of drugs that specifically inhibit HDAC 2 is therefore a future goal in SMA research. Moreover, it was clearly proven that the HDAC inhibitors VPA and SAHA indeed activate the *SMN2* promoter in human fibroblasts via an increase of histone H3 and H4 acetylation levels at the *SMN* gene (Kernochan et al. 2005). Unexpectedly, the greatest increase in acetylation was observed in different regions than those which are associated with HDAC 1 and HDAC 2. This implies that VPA and SAHA have only minimal impact on HDAC 1 and HDAC 2 and mainly act on other HDAC enzymes, although this would be in contrast to the efficient inhibition of HDAC 1 by VPA which was demonstrated earlier (Phiel et al. 2001). However, another suggestion is that the drugs modulate the activity of a transcription factor by acetylation. The transcription factor could subsequently recruit a histone acetyltransferase (HAT) which finally hyperacetylates histones H3 and H4 at the *SMN2* promoter.

Another interesting finding was that VPA, in addition to inhibiting the activity of class I HDAC enzymes, selectively induces proteasomal degradation of HDAC 2, thereby reducing HDAC 2 protein levels (Kramer et al. 2003). VPA induces expression of the Ubc8 E2 ubiquitin conjugase which increases the degradation rate for HDAC 2 at the proteasome. Again, this is inconsistent with the observation that the region in the *SMN2* promoter which binds HDAC 2 does not show a substantial change in histone acetylation upon VPA treatment (Kernochan et al. 2005), but the use of different cell culture systems may be a reasonable explanation to explain the discrepancies. However, the up-regulated expression of the Ubc E2 ubiquitin conjugase under VPA treatment underscores the fact that VPA has impact on the activity of a large number of genes.

Since the results obtained with VPA in SMA fibroblasts *in vitro* were very promising, the drug was considered for further investigations to gain additional knowledge how suitable VPA is for a potential SMA therapy. SMA is caused by degeneration of the α-motor neurons in the spinal cord. Consequently, to reach its therapeutic target, any drug must be able to cross the blood-brain-barrier. It is well known that VPA fulfills this requirement and about 15% of the VPA present in serum reach the brain and spinal liquor (Wieser 1991; Johannessen 2000). Additionally, VPA must be able to stimulate SMN protein expression in neuronal cells. However, further *in vitro* experiments with the drug in motor neuron cultures were not performed because primary human motor neuron cultures that are suitable for drug treatment experiments are not available, and primary motor neuron cultures derived from SMA mice have been described (Rossoll et al. 2003) but are too fragile and would not provide enough material for western blotting (personal communication S. Jablonka and M. Sendtner). An extremely potent *ex vivo* drug screening and drug validation tool available for CNS disorders is the use of organotypic hippocampal slice cultures (OHSCs) from rat (Stoppini et al. 1991; Savaskan et al. 2000). The treatment of OHSCs from early postnatal rats resulted in a significant increase of *rSmn* transcript and rSmn protein levels. Compared to the data from human fibroblasts, the degree of up-regulation appeared to be slightly lower. However, in contrast to humans, rodents carry one *rSmn* gene only which is not subject to alternative splicing. Thus, the observed effect was solely triggered by transcriptional activation of the *rSmn* gene and splicing did not contribute to the augmentation in rSmn protein. To explain the activation of the *rSmn* gene by VPA, the same mechanisms which were discussed for primary fibroblasts have to be taken into account. This includes the hyperacetylation of histones through inhibition of HDACs which are extremely conserved enzymes (Gregoretti et al. 2004) and thus can be inhibited by one and the same drug in different mammalian species. Also, the activity of a transcription factor might be modulated by acetylation. Moreover, in accordance with the human *SMN* promoter, the rat *Smn* promoter containes several putative AP1 and Sp1 binding sites, such that the increased DNA binding activity of AP1 and Sp1 transcription factors under VPA treatment is another possible pathway. The VPA concentration required to achieve the described augmentation of *rSmn* transcripts and rSmn protein was much higher than the drug concentration used to treat fibroblasts. This is due to the extremely different terminal half-lives of VPA in different species (humans: 9-18 h versus rats: 2-5 h) (Johannessen 2000; McCabe 2000; Sands et al. 2000).

A recent investigation further strengthened the data obtained for VPA in rat OHSCs (Hahnen et al. 2006). After drug administration, the cytotoxicity risk was investigated by measuring the propidium iodide (PI) uptake. The incubation of rat OHSCs with 2 mM VPA for 48 h did not show increased PI incorporation, suggesting that the drug was well tolerated by the neuronal tissue. Furthermore, two novel models were applied to validate the activity of VPA. It was demonstrated in motor neuron-enriched cell cultures isolated from rat embryos (Haastert et al. 2005), that 2.6 mM and 6.8 mM VPA increased rSmn protein levels up to 3fold (Hahnen et al. 2006). In human OHSCs which were obtained after surgery from epilepsy patients, 2 mM VPA significantly increased the SMN protein level up to 2fold. The drug concentration in the latter experiment was by far above the therapeutic range, however, recently it has been demonstrated that a lower VPA concentration of 0.2 mM is enough to significantly up-regulate the SMN protein level by more than 40% in human OHSCs (Hauke 2006). These data clearly imply that VPA has the potential to increase SMN protein levels also in human neuronal tissue.

Taken together, the findings from the in *vitro* and *ex vivo* experiments with VPA suggested that the drug is well tolerated in all tested systems, and is able to efficiently increase the SMN / rSmn protein level in SMA fibroblasts and OHSCs derived from rats. In humans, VPA mediates its effect via two pathways, including a transcriptional activation of the *SMN* gene and a reversion of the *SMN2* splicing pattern. These findings were very promising and opened a first realistic possibility for a causative pharmacological treatment of SMA. In the field of human genetics, this would be the first example for a therapy of a monogenic inherited disease by activation of a copy gene through drugs.

## 5.2    *In vitro* investigations of the second-generation HDAC inhibitors SAHA and MS-275

To identify further compounds which have the potency to stimulate *SMN2* expression and therefore are candidates for a potential SMA therapy, two other HDAC inhibitors, SAHA and MS-275, were tested *in vitro*. The design of new substances evolved from the exciting discovery of the correlation between HDAC inhibition and anticancer activity. Additionally, promising *in vitro* results obtained with the first-class HDAC inhibitors (e.g. sodium butyrate, VPA, and phenylbutyrate) in numerous cancer cell lines and the knowledge about critical structural elements which are required by compounds to bind to the catalytic center of HDAC enzymes further moved the field into a new phase of development. Up to present, the second generation HDAC inhibitors are by far not as well studied as VPA. However, in contrast to VPA and butyrate, SAHA and MS-275 need only low micromolar amounts to inhibit HDACs and therefore are much more potent (Richon et al. 1996; Richon et al. 1998; Saito et al. 1999; Prakash et al. 2001; Marks et al. 2004). Although the finding that VPA increases SMN protein levels *in vitro* and *ex vivo* is promising, the clinical potential to increase muscle strength in SMA patients awaits confirmation. Moreover, it is possible that unexpected adverse events will be observed in such a fragile population like SMA patients, and it is conceivable that not all patients respond to the drug in a similar manner. Therefore, drug screening projects aiming at the identification of further promising compounds for a potential SMA therapy are crucial.

The treatment of SMA fibroblasts derived from a type I and a type II SMA patient with SAHA resulted in a significant increase in SMN protein. Levels peaked in a 2.4fold (ML-5) to 3.0fold (ML-16) elevation which is a very similar degree of up-regulation like observed for VPA. In ML-16, the maximum effect was achieved at SAHA concentrations of 5 µM. Interestingly, this is no difference to the treatment of fibroblasts with VPA where SMN levels peaked in a 3.1fold elevation at 5 µM. In ML-5, the 2.4fold elevated SMN level was obtained at 1 µM SAHA. In contrast, 500 µM VPA were required to achieve the maximum SMN increase of 3.3fold. However, treatment of ML-5 with 0.5 and 5 µM VPA, respectively, revealed a 2.3fold to 2.7fold increase in SMN protein which equals the effect observed after incubation of the cells with SAHA. These data suggest that at least in SMA fibroblast cultures similar amounts of the first-generation HDAC inhibitor VPA and of the second-generation HDAC inhibitor SAHA are required to trigger a similar maximum degree of SMN elevation. Only the results for 0.05 µM SAHA suggested that the drug is more potent than VPA because an effect on *SMN2* can be seen already at lower drug concentrations. At 0.05 µM SAHA, a 1.9fold to 1.7fold increase in SMN protein levels was observed. This is approximately in the range that was achieved with the 10fold VPA

concentration of 0.5 µM, however, it was not the maximum up-regulation, and a concentration of 0.05 µM VPA was not investigated such that the outcome of this experiment remains open.

The treatment of fibroblasts with SAHA concentrations higher than 10 µM would most likely not lead to a more pronounced effect on the SMN level. Whereas ML-16 revealed the same up-regulation at 5 and 10 µM SAHA, SMN protein levels appeared to decrease in ML-5 after peaking in the maximum at 1 µM SAHA, implying that the optimal drug concentration for stimulation of the cells was exceeded.

Similar to the data obtained for VPA, the maximum SMN protein level in the two cell lines incubated with SAHA was observed at different drug concentrations, indicating that the drug is differently metabolized by the cell lines. As demonstrated in an MTT assay, the drug was well tolerated by the cells as the viability of the fibroblasts was not affected by any of the SAHA concentrations applied.

It remains to be elucidated whether the concentrations of SAHA which were used in the fibroblast assay are within the therapeutic range which has to be maintained in humans to achieve a sufficient drug concentration in the CNS. After intravenous administration of SAHA to humans, it was demonstrated that histones are hyperacetylated in PBMCs at plasma levels exceeding 2.5 µM (Kelly 2003). Lower concentrations were not tested. Moreover, it is still unclear whether and to which extent the drug is able to cross the blood-brain-barrier in humans, although earlier studies in rodents demonstrated an accumulation of acetylated histones in brain tissue following oral SAHA administration (Hockly et al. 2003).

Given the fact that both compounds VPA and SAHA are HDAC inhibitors, and based on the results obtained for VPA, it was hypothesized that increased SMN protein levels under SAHA treatment are triggered by the same pathways. Indeed, *SMN2* RNA analysis revealed a significant up-regulation of FL-*SMN2* transcript levels after incubation with the drug which explains the augmented generation of SMN protein. Similar to VPA, SAHA activated the transcription of the *SMN2* gene, as clearly demonstrated by augmented amounts of both transcripts FL-*SMN2* and Δ7-*SMN2*. This was confirmed by the increased amount of total *SMN2* transcripts (FL-*SMN2* and Δ7-*SMN2*) measured under SAHA treatment. As discussed earlier, transcriptional activation of *SMN2* can be explained by the inhibition of HDACs and subsequent histone hyperacetylation, together with the possibility of an altered activity of a yet unknown transcription factor by acetylation. Moreover, it was demonstrated that Sp1 and Sp3 proteins can mediate SAHA-induced gene activation (Huang et al. 2000)

Together with the stimulation of *SMN2* expression, SAHA exerted a slight effect on the *SMN2* splicing pattern in SMA fibroblasts treated with 5 and 10 µM of the drug. Again, this correlates with the data for VPA and suggests that both mechanisms transcriptional activation and reversion of the splicing pattern act in concert to increase FL-*SMN2* transcript levels. However, the stimulation of *SMN2* activity appeared to be the main trigger, while preferential *SMN2* exon 7 inclusion was the minor effect and not seen at all drug concentrations. Summarizing the data collected for HDAC inhibitors so far, it seems like all of the compounds which have been demonstrated to increase the SMN protein level in *vitro* act via transcriptional activation of *SMN2* and a reversion of the *SMN2* splicing pattern. In addition to VPA and SAHA, this was also seen for the treatment of SMA fibroblasts with the second generation HDAC inhibitor M344 (Riessland et al. 2006), but even with a more substantially augmented FL-*SMN2* / Δ7-*SMN2* transcript ratio. Furthermore, an extensive promotion of *SMN2* exon 7 inclusion was shown for butyrate in SMA EBV-transformed cell lines, although a potential impact of the drug on *SMN2* transcription was not investigated (Chang et al. 2001). Thus, it can be concluded

that HDAC inhibitors with impact on *SMN2* share similar mechanisms of action to trigger an increase in SMN protein, but there are differences between the drugs to which degree the two single pathways contribute to the final outcome. The differences might result from the unspecific regulation of a number of genes by HDAC inhibitors (Van Lint et al. 1996; Pazin and Kadonaga 1997). It is known that the various drugs do not regulate exactly the same pattern of genes (Pazin and Kadonaga 1997; Butler et al. 2002; Glaser et al. 2003) which most likely includes a different impact on the expression regulation of SR and SR-like proteins. Assuming that not all of the splicing factors which are involved in inclusion/skipping of *SMN2* exon 7 are known up to present, it is possible that in addition to Htra2-β1 other splicing factors are regulated by some of the drugs, leading to a different impact of each compound on exon 7 inclusion. However, this remains speculation for now.

Similar to earlier observations with VPA, treatment of fibroblasts with SAHA also resulted in a different degree of elevated FL-*SMN2* transcript and elevated SMN protein. Moreover, the respective maximum was measured at different SAHA concentrations. While FL-*SMN2* transcript levels in ML-16 were increased up to 1.9fold at 10 µM SAHA, SMN levels peaked at 5 µM and were augmented 3fold. At 10 µM, SAHA still increased SMN levels approximately 3fold, however, there is a discrepancy between RNA and protein levels. Additionally, this is in contrast to the treatment of ML-16 with VPA which revealed a higher increase in transcripts than in protein. This can be interpreted as another hint for a different regulation of transcription and translation by HDAC inhibitors, in particular VPA and SAHA. Differences between the two drugs might occur because they regulate different gene patterns. The exact mechanism for this observation still has to be elucidated and requires further experiments.

The regulation of Htra2-β1 is another characteristic which butyrate, VPA, and SAHA have in common. The treatment of SMA fibroblast line ML-16 with SAHA revealed a maximum of 3.5fold elevated Htra2-β1 protein levels at a concentration as low as 0.05 µM. Compared to treatment of ML-16 with VPA, this effect was achieved with much lower drug amounts. An up-regulation of Htra2-β1 was also seen in ML-5 with a maximum at 5 µM SAHA, although the differences between the results obtained from different passages of ML-5 did not allow to reach significance. Again, increased Htra2-β1 levels and the reversion of the *SMN2* splicing pattern were observed at the same SAHA concentrations. This further argues for the correlation between both parameters. On the other hand, Htra2-β1 was also elevated at SAHA concentrations which did not lead to a preferred *SMN2* exon 7 inclusion, leaving it open whether additional factors with impact on the *SMN2* splicing pattern are regulated by the drug.

Taken together, the *in vitro* results for SAHA in primary SMA fibroblasts clearly demonstrated that the drug efficiently increases SMN protein levels and therefore is another promising candidate for SMA therapy. Recently, it was shown that SAHA elevates the rSmn protein level in OHSCs (Hahnen et al. 2006). The same tool was used to prove that the compound is not cytotoxic for neuronal tissue. Importantly, the treatment of three human OHSCs obtained from epilepsy surgery revealed that SAHA did not alter SMN protein levels in one of the OHSCs, but 32 µM and 64 µM SAHA significantly increased the SMN protein level between 1.6fold and 2.1fold in the OHSCs from the two other individuals. This underscores that SAHA is an HDAC inhibitor which has to be further considered for SMA therapy. However, the present knowledge about adverse events, pharmacokinetics, toxicity, and bioavailability in humans is still sparse, although early clinical trials in a small number of probands has demonstrated good bioavailability, *in vivo* biological activity to inhibit HDACs and hyperacetylate histones, low toxicity and antitumor activity in solid and hematological tumors (Kelly et al. 2003).

Phase II clinical trials in patients with cancer are ongoing (Marks et al. 2004). Profound data in a large number of subjects are required to further validate the suitability of SAHA for the use in humans.

The treatment of SMA fibroblasts with the benzamide MS-275, another second-generation HDAC inhibitor, revealed that the drug is not a candidate for a potential SMA therapy. Although the compound was well tolerated by the cells as demonstrated by an MTT assay, MS-275 failed to efficiently increase the SMN protein level. The maximum up-regulation observed was 1.4fold. Compared to butyrate, VPA, and SAHA, this is only a minimal effect on SMN levels and demonstrated that the drug will not have a chance to move forward to SMA clinical trials. The concentrations used to treat SMA cells ranged between 0.05 and 5 µM MS-275. It is unlikely that these amounts were too low and higher concentrations would elevate the SMN protein level, because a slight but significant decrease below the level of untreated cells was already seen at 5 µM. This was confirmed by significantly down-regulated FL-*SMN2* transcript levels at the same drug concentration.

On RNA level, the FL-*SMN2* transcript levels were found decreased under MS-275 treatment. In contrast, the Δ7-*SMN2* transcript was either unchanged or slightly increased, and an analysis of the amount of total *SMN2* transcripts revealed either no change or a moderate decrease. Due to the lack of a clear tendency and a lack of significance for these observations at any MS-275 concentrations, a clear conclusion regarding the impact of MS-275 on *SMN2* transcription could not be drawn. Moreover, this observation is in contrast to the marginal elevation in SMN protein, however, both effects are minimal and it remains open whether this is indeed due to a differential impact of MS-275 on transcription and translation.

Interestingly, the FL-*SMN2* / Δ7-*SMN2* transcript ratio appeared to decrease with increasing concentrations of MS-275. This is moderate and not significant either, but a clear tendency was seen. Again, the lowest ratio was determined at 5 µM MS-275. Surprisingly, the levels of Htra2-β1 protein decreased in SMA fibroblast line ML-16 incubated with MS-275 which was most pronounced and significant at 5 µM VPA. This could imply that decreasing Htra2-β1 protein levels lead to an increase in *SMN2* exon 7 skipping which may be the reason for decreased FL-*SMN2* transcript levels, augmented Δ7-*SMN2* transcript levels, and the decrease of the transcript ratio. However, this is in contrast the results obtained from the knock-down of Htra2-β1 by the means of siRNA in the same cell line which rather suggested that decreased Htra2-β1 protein levels do not promote *SMN2* exon 7 skipping and a decrease in *SMN2* transcript ratio. Further experiments, in particular additional siRNA studies, are necessary to clarify these contradictory observations.

Recent studies investigated MS-275 using rat OHSCs and the F98 rat glioma cell line (Hahnen et al. 2006). The experiments revealed that MS-275 is not cytotoxic in OHSCs and therefore well tolerated by neuronal rat tissue, however, an increase of *rSmn* transcript levels was neither measured after treatment of rat OHSCs with 4 µM MS-275, nor after incubation of F98 cells with 4 µM of the drug, which confirms the data obtained in SMA fibroblasts.

The comparison of VPA, butyrate, SAHA, and MS-275 underscores once more that different sets of genes are regulated by different HDAC inhibitors. Whereas the first three drugs increase *SMN* expression, MS-275 is unable to do so. Similar observations were made for the regulation of Htra2-β1. This can be explained by a slightly different specificity of the drugs for a subset of HDAC enzymes. Among the three classes of HDACs, only class I (HDACs 1-3, 8) and class II (4-7, 9-11) enzymes are susceptible to HDAC inhibitors (Marks et al. 2004). Both enzyme classes have been shown to be

generally expressed in all tissues examined (de Ruijter et al. 2003). It has been reported earlier that at least in part VPA is able to distinguish between HDAC enzymes and is more selective for class I HDACs (Gottlicher et al. 2001). This is consistent with the finding that VPA only partially inhibits the activity of an HDAC enzyme mix isolated from rat liver (Hahnen et al. 2006). In contrast, SAHA almost completely diminished HDAC activity in the same assay, suggesting that the drug is not specific for a subset of enzymes and acts on both class I and class II HDACs. This was also reported by others (Richon et al. 1998). MS-275 was demonstrated to inhibit the activity of an HDAC mix isolated from rat liver even less than VPA (Hahnen et al. 2006) which indicates pronounced isoenzyme specificity of the drug. Additionally, MS-275 has been shown to have a considerably higher inhibitory activity against HDAC 1 than HDAC 3 (Hu et al. 2003) and an approximately 40,000fold higher inhibitory activity against HDAC 1 than HDAC 8 (Hu et al. 2003; Miller et al. 2003). Thus, it becomes clear that the investigated drugs differ in their ability to inhibit certain subsets of HDAC enzymes. Since not all of the HDACs are associated with each gene promoter, but only a specific combination of enzymes is involved in the deacetylation of histones in a certain promoter region, this explains why some drugs are able to increase the expression of a particular gene, and others are not. Based on the findings that (i) MS-275 is a potent inhibitor of HDAC 1 at submicromolar doses (Hu et al. 2003), (ii) MS-275 is not able to increase *SMN2* / *rSmn* expression levels, and (iii) a clear association between mouse *Smn* /*SMN2* gene promoters and low levels of HDAC 1 has been shown (Kernochan et al. 2005), it can be hypothesized that HDAC 1 does not serve as major target for epigenetic SMA therapy which is important for the future design of isoenzyme-specific drugs for SMA therapy.

## 5.3    *In vivo* effect of valproic acid on *SMN* gene expression in SMA carriers and SMA patients

Given the exciting and promising finding that HDAC inhibitors such as butyrate, VPA, and SAHA are able to increase SMN protein levels in SMA cell lines *in vitro* and in neuronal tissue *ex vivo*, SMA emerges as a very particular example in the field of human genetics providing the therapeutic opportunity of activating a copy gene through pharmacologic drug-based pathways. The features that make SMA a unique therapeutic disease model include: (i) Approximately 94% of all patients with SMA show the same mutation which can be easily identified by simple molecular genetic testing. (ii) Although *SMN1* is homozygously deleted in patients with SMA, a copy gene (*SMN2)* is present in all patients producing minor amounts of a protein completely identical to SMN1. (iii) Several drugs have the potential to significantly elevate the FL-*SMN2* mRNA/protein level. (iv) In particular VPA is a well-known drug approved by the FDA for the treatment of epilepsy and several other diseases. The drug is clinically well experienced, characterized by favorable pharmacological properties, and rarely shows severe adverse events in long-term therapy of epilepsy patients except for teratogenic effects during the first trimenon of pregnancy (Lindhout and Omtzigt 1992; Johannessen and Johannessen 2003). This makes VPA available for a straightforward application to humans. The treatment of mice with VPA to investigate drug safety is not required anymore. Additionally, in mice it may be difficult to evaluate the *in vivo* efficacy of VPA to increase SMN levels, because VPA pharmacokinetics in the mouse is considerably different compared with humans. Although it has been demonstrated that

global histone acetylation is altered after subcutaneous administration of 150 mg VPA to mice (Tremolizzo et al. 2002), this effect is short-lived. Compared with the terminal half-life of VPA in humans (9-18 h), the terminal half-life of VPA in mice is extremely short (0.8 h) (Johannessen 2000). There is a much higher clearance rate for VPA in mice which is due to the low plasma protein binding of the drug (mice ~10% *versus* humans ~90%), the high metabolic capacity (Nau and Loscher 1982), and the higher relative volume of distribution (Loscher and Esenwein 1978). Consequently, it might be difficult to achieve sufficiently high VPA level in mice which might be required to increase SMN levels.

Based on these facts, the effect of VPA on *SMN* gene expression was studied in blood from ten SMA carriers and 20 SMA patients to address the following two questions: (i) Is VPA capable of acting on the *in vivo* FL-*SMN* transcript and protein level, and (ii) how suitable is the use of peripheral whole blood for the development of a biomarker that would allow fast and easy monitoring of the drug response in VPA-treated SMA patients? Since exclusively motor function tests are available so far to detect the clinical outcome of drug treatment (Swoboda et al. 2005), a biomarker would be of high relevance for future clinical trials as well as potential therapies in patients with SMA.

In a first step, a method was established to reliably measure *SMN* transcript levels in human blood samples *in vivo*. In particular the search for a suitable endogenous control which was needed to normalize *SMN* transcript samples was very time-consuming and demonstrated that the quantification of gene expression might be tricky. Analysis gets even more difficult when samples collected from different individuals or collected within a larger period of time have to be compared with each other. The use of various housekeeping genes is very common to normalize target transcript levels, but there are only a few studies dealing with the inter-individual and intra-individual stability of the expression of these genes. After *CTLA1* was excluded as suitable endogenous control, four more genes were investigated in detail. Recent studies suggested that *GUSB*, *PPIB*, and *RPLP0* might be attractive candidates because they were reported to be stably expressed in human peripheral whole blood and cultured PBMCs, respectively (Loseke et al. 2003; Dheda et al. 2004; Pachot et al. 2004). In addition, *B2M* is a housekeeping gene which is very frequently used for the normalization of target transcripts. Therefore, these four genes were selected to be analyzed under the experimental conditions established to study *SMN* RNA expression. The re-investigation of *GUSB*, *PPIB*, and *RPLP0* was required, because each experimental protocol is unique, including the blood collection system, handling of samples, the procedure to extract RNA, and subsequent real-time PCR. The expression analysis demonstrated that only *PPIB* would be a suitable endogenous control. Transcript levels showed the lowest natural expression variability, although a ~1.5fold difference between the lowest and highest transcript level still would restrict the reliable detection of *SMN* transcript fluctuations to changes more pronounced than that. This was considered as major disadvantage, because it was unclear whether an increase in *SMN* transcript levels could be expected *in vivo* and if so, to which degree. *PPIB* also appeared to be equally expressed in the two investigated blood cell fractions which further argued for its suitability as endogenous control. However, as it was also seen for *GUSB*, the expression of *PPIB* was regulated by VPA in blood *in vivo*. This finding was unexpected, but on a second glance it is not too surprising considering that HDAC inhibitors have impact on ~2% of expressed genes (Van Lint et al. 1996; Pazin and Kadonaga 1997). The rather unspecific regulation of a large number of genes is a major issue that comes into the play when dealing with HDAC inhibitors. Importantly, it is most likely impossible to make a prediction about the expression regulation of a

particular gene in a certain individual by a drug. Consequently, *PPIB* was not used as endogenous control. Instead, *SMN* transcripts were normalized by the total RNA amount used for reverse transcription. In 2000, this method has been described for normalization of RNA data and was strongly recommended to be preferred over the use of housekeeping genes as endogenous controls whenever *in vivo* studies are performed dealing with human tissue samples (Bustin 2000). Although the method lacks any endogenous control which corrects pipetting or other errors and therefore requires that all samples to be compared are processed with extreme care and in exactly the same way, the method is independent from any impact of HDAC inhibitors and even independent from natural variations in gene expression. These are major advantages. Thus, given that the use of housekeeping genes for normalization bears a high risk for data misinterpretation, they should not be used as endogenous controls for *in vivo* studies, in particular when dealing with VPA or other HDAC inhibitors.

To investigate the effect of VPA *in vivo*, *SMN* gene expression was studied in blood, although α-motor neurons represent the affected target tissue for a potential SMA therapy. However, α-motor neurons are not available to evaluate an *in vivo* effect of VPA on *SMN* in humans. Based on the observation that VPA increases *SMN* RNA and protein levels in primary fibroblast cultures, on a first glance, the collection of small skin samples from each subject appears to be an alternative. However, due to the surgical procedure which is required to take a skin sample, it would be highly unethical to repeatedly perform skin biopsies in one and the same individual throughout a clinical trial. Even if skin samples were collected before and throughout drug treatment, it is questionable whether enough RNA/protein were extractable for subsequent analysis. Culturing of skin samples following biopsy to achieve more material for analysis would not conserve the gene expression status at time of collection. Consequently, the only tissue accessible in sufficient amounts for repeated analyses is blood. This tissue can serve to explore the general ability of VPA to act on *SMN* gene expression *in vivo*, although the question remains open whether the data obtained from blood reflect the situation in α-motor neurons.

The analysis of baseline *SMN* transcripts in blood derived from a number of 41 untreated individuals revealed no clear difference between the FL-*SMN* transcript levels in controls, SMA carriers, and SMA patients. Regardless whether *SMN1* was present or absent and regardless of the *SMN2* copy number, the FL-*SMN* transcript levels could not be clearly discriminated between patients, carriers, and controls. Only type I SMA patients with 2 *SMN2* copies presented significantly lower FL-*SMN* levels compared with controls and carriers. This observation most likely reflects the fact that nucleated blood cells as a cell type are not affected in SMA. Similar results have already been described for SMN protein in several other unaffected tissues including lung, adrenal gland, kidney, and eye after comparison of control fetuses and fetuses with SMA by the means of immunohistochemistry (Soler-Botija et al. 2005). Thus, an *in vivo* regulation mechanism must exist to force *SMN2* in patients with SMA to compensate for the loss of *SMN1* and to produce large numbers of the FL transcript. Another independent study which was recently carried out in a different cohort including a number of 85 controls, SMA carriers, and SMA patients confirmed that only type I SMA patients with 2 *SMN2* copies show reduced FL-*SMN* transcript levels compared with controls and carriers (Sumner et al. 2006). The finding was further validated by an analysis of SMN protein levels in blood derived from a number of 57 subjects. Again, only SMN protein levels in type I SMA patients with 2 *SMN2* copies were significantly lower than those in controls. In contrast to native blood, a clear correlation between SMA

phenotype and SMN protein expression level was reported for Epstein-Barr-Virus transformed lymphoblastoid cell lines as well as for primary fibroblasts and spinal cord (Coovert et al. 1997; Lefebvre et al. 1997; Helmken et al. 2003). However, studies investigating FL- and Δ7-*SMN* RNA expression in lymphoblastoid cell lines revealed a less pronounced correlation (Gavrilov et al. 1998; Helmken et al. 2003). Further investigations are definitely required for clarification. Interestingly, a clear discrimination between patients with type I, II, and III SMA based on the amount of FL-*SMN2* was not possible either. This seems reasonable, given that one *SMN2* copy produces about 10% of FL-*SMN2* transcript and 90% of Δ7-*SMN2* transcript. Two, three, or even more copies should still generate 10% of FL-*SMN2* and 90% of Δ7-*SMN2*. However, in EBV-transformed cell lines it was observed that, with increasing numbers of *SMN2* genes, the percentage amount of FL transcript increases, whereas the percentage amount of Δ7 transcript decreases (Helmken et al. 2003). In addition, a high inter-individual variation of the FL- and Δ7-*SMN2* transcript levels was detected in native blood even in the presence of identical numbers of *SMN2* (e.g. 3 *SMN2* in all investigated patients with type II SMA). In contrast, the respective FL/Δ7 ratios in all patients were in a similar range. This rather implies a varying transcriptional activity of *SMN2* among different patients and would correlate with the hypothesis that not all *SMN2* genes are functionally equivalent (Coovert et al. 1997; Soler-Botija et al. 2005). However, many more investigations are needed to further elucidate these observations.

The highly significant increase of Δ7-*SMN* transcript levels in SMA type II and III patients compared with controls can be explained by the higher number of *SMN2* genes in these groups of patients. As expected, within the control and the carrier group, Δ7 levels decrease with decreasing *SMN2* copies. This was also seen by Sumner and colleagues (Sumner et al. 2006). Different results were obtained for the comparison of Δ7 levels in controls with those in type I patients. Whereas the cohort investigated in our laboratory revealed a difference, Sumner *et al.* did not observe that. Therefore, the comparison of Δ7 transcript levels in controls and type I patients should be repeated with a cohort including a larger number of type I SMA patients than only five.

Whereas controls and SMA type II and III patients could not be distinguished based on the amount of FL-*SMN* transcript, they revealed different levels of Δ7-*SMN* transcripts. This explains the significantly different FL-*SMN* / Δ7-*SMN* transcript ratios obtained in controls compared with type II and III patients. Due to the above described observation that also in type I patients Δ7 levels were found to be higher than in controls, this cohort revealed the same finding for the transcript ratio like type II and III patients. Thus, the transcript ratio could serve to clearly discriminate between SMA patients and the control group. However, a comparison of the ratios obtained in type I, II, and III patients did not show any differences among these groups, suggesting that splicing efficacy of *SMN2* pre-mRNA transcripts in these cohorts is comparable.

Following the investigation of *SMN* transcript levels in native blood from untreated subjects, blood samples were analyzed from the SMA carriers treated with VPA in a clinical pilot trial and from SMA patients treated with the drug in individual experimental curative approaches all over Germany according to section 41 of the German Drug Act (AMG). Importantly, the lack of a clear difference obtained for FL-*SMN* transcript and protein levels in native blood derived from untreated individuals does not exclude a potential regulation of *SMN* gene expression by VPA. Among the ten SMA carriers that were recruited for the clinical pilot study, VPA treatment revealed elevated FL-*SMN* transcript

levels in seven subjects peaking in maxima ranging from 1.6fold to 3.4fold relative to baseline. In seven out of 20 patients with SMA, a maximal FL-*SMN2* mRNA increase between 1.5fold and 1.9fold was detected. These effects were achieved at therapeutic, well tolerated VPA serum levels and clearly prove that VPA has the potential to act on *SMN* not only *in vitro*, but also in humans *in vivo*. This finding should be very encouraging for the performance of large multicenter clinical trials with VPA in SMA patients. Higher augmentations of FL-*SMN* transcript levels observed for SMA carriers suggest a contribution of both *SMN1* and *SMN2* while slightly milder effects achieved in patients with SMA are most likely due to the presence of *SMN2* only. This led to the conclusion that functional *SMN1* is able to support a drug response, but is not necessarily required to achieve considerable effects. From experiments performed in SMA fibroblasts, it is known that VPA activates *SMN2* transcription and promotes exon 7 inclusion at the same time, thus regulating two mechanisms which eventually cause elevated FL transcript levels. Since the majority of responding carriers and patients displayed constant or only slightly changed FL-*SMN* / Δ7-*SMN* ratios, an induction of *SMN* transcription appears to be the main mechanism of action for VPA in native blood cells *in vivo*. However, in particular with respect to the ratios in P1, P5, and P16, an impact on *in vivo* splicing of *SMN* pre-mRNA cannot be excluded. Fluctuations of the FL-*SMN* transcript levels detected in the responding carriers and patients with SMA throughout the period of VPA medication were similar to observations made using phenylbutyrate (Brahe et al. 2005). Phenylbutyrate is another HDAC inhibitor with a very short terminal half-life of 0.8 to 1 h in humans (Gilbert et al. 2001). It was administered to a very small number of six SMA patients for only seven days within a very preliminary trial to measure *SMN* transcript levels under drug treatment (Brahe et al. 2005). However, the fluctuations are an unexpected finding which can not be conclusively explained up to present. A phenomenon which has been well-known for a long time and might give at least a hint for this observation is nitrate tolerance (Abrams 1980). The treatment of patients suffering from heart failure with organic nitrates may lead to a tolerance and loss of effectiveness of medication in the individual e.g. when the drug is given constantly over a long period. This is due to the down-regulation of enzymes, in particular of the CYP450 group which are needed to release NO from the administered nitrate (Minamiyama et al. 2002). In comparison, VPA was administered to the SMA carriers and patients in retarded form to achieve constant serum levels around the clock. Given that an increase of *SMN* expression requires efficient inhibition of HDAC enzymes by VPA, it could be assumed that constant VPA levels trigger an up-regulation of the targeted HDAC enzymes in certain intervals, thus decreasing the effect on *SMN* gene activity. This is only a hypothesis and remains speculation, however, future clinical trials should include VPA-free intervals to check whether such a dose regimen is able to overcome the observation of fluctuating *SMN* transcript levels.

The elevation of FL-SMN protein in seven SMA carriers up to levels as high as 13.7fold relative to baseline clearly corroborated the response to VPA observed on RNA level and further proved that VPA is not only capable of acting on the SMN protein level *in vitro*, but also *in vivo*. This was the first demonstration for an HDAC inhibitor to be capable of elevating *in vivo* SMN protein levels in humans. The different augmentation degree of FL-*SMN* mRNA and FL-SMN protein in most of the responding subjects is similar to the data obtained with VPA and SAHA, but also other HDAC inhibitors in cell culture (Riessland et al. 2006) and implicates that VPA interferes with transcriptional processes, but also appears to regulate translation and/or stability of SMN. This hypothesis is strongly supported by

the measurements for SMA carrier C9 whose FL transcript levels did not change throughout VPA medication whereas western blot analysis revealed extensively increased FL-SMN protein amounts. Consistent with this observation, a modulated transcription of genes encoding translation factors has already been described for the HDAC inhibitors butyrate and trichostatin A (Goncalves et al. 2005). Furthermore, recent experiments demonstrated that both substances may enhance protein stability such that levels increase without any change of the transcriptional activity of the encoding gene (Chen and Faller 2005), giving rise to the assumption that VPA might act in a similar manner.

The extensive increase of the Δ7-SMN protein in C5 and C2 remains unclear. However, it has been shown that this isoform of the SMN protein is not detrimental and even extends the survival in an SMA mouse model (Le et al. 2005).

In terms of developing a reliable biomarker to monitor the drug response in treated individuals based on the investigation of native blood, the application of PAXgene blood RNA tubes allowed the uncomplicated collection of a relatively small volume of blood (2.5 ml) from each subject. RNA was stabilized in these tubes for several days enabling transport of the samples. Yields were sufficient for many RT-PCR reactions. In order to precisely quantify FL-*SMN* and Δ7-*SMN* transcript levels, LightCycler real-time PCR technology was utilized which allows exact quantification of transcript levels. However, fluctuation of FL-*SMN* transcript levels would clearly hamper reliable monitoring of a drug effect on RNA level. Conclusions could not be drawn from a single blood sample, but only after a whole series of samples from one individual was analyzed. In comparison, protein analysis in general seems to be both more certain and more promising than RNA analysis with PAXgene tubes. Results obtained from the SMA carriers imply that the effect detectable on protein level is much more pronounced. Moreover, as demonstrated in case of proband C9, exclusive RNA analysis might lead to a false negative conclusion which would not happen when focus were on the protein level. Nevertheless, focusing on protein levels as diagnostic tool is much more complicated due to unavailability of a blood collection system which guarantees sample stability and the relatively large amounts of blood required. Thus, diagnostic analysis of proteins is more complicated. Moreover, the collection of 4 ml of blood in BD Vacutainer® CPT Cell Preparation Tubes and subsequent western blot analysis is not applicable as a high-throughput method for a large number of probands enrolled in a protocol. Therefore, another method is needed. At the time of investigation, the development of a flow cytometric method for analysis of SMN protein levels failed which was mainly due to the lack of a directly labeled antibody against a nuclear control protein. When such an antibody becomes available, it would allow to further work on the validation of this bioanalytical method. In addition, another very similar high-throughput method was described recently (Kolb et al. 2006). This approach uses cryo-preserved PBMCs, which are fixed, permeabilized, and subsequently incubated with an anti-SMN antibody. This is followed by incubation with a secondary peroxidase-conjugated goat-anti-mouse antibody, addition of chemiluminescence, and fluorescence signal detection on a microplate reader. The method seems to be suitable for application, although it still has to be validated in a larger number of PBMC samples.

The observation of non-responders among the VPA-treated SMA carriers and the identification of patients with unchanged or decreased FL-*SMN* transcript levels underscores the need for a biomarker. It is well known that HDAC inhibitors are able to decrease gene activity (Marks et al. 2004) which can obviously occur among individuals even when others present gene activation. The

identification of such cases would be of paramount importance in order to restrict drug medication only to responders. However, so far it is not established whether *SMN* expression in blood reflects *SMN* expression in α-motor neurons and correlates with muscle strength in SMA patients. Therefore, large long-term clinical trials in SMA patients that correlate *SMN* expression in blood with individual motor function tests are required to confirm a link between these two parameters.

## 5.4    Future directions

As a result of the progress in understanding the genetic basis and pathophysiology of SMA, several potential strategies to the treatment of SMA have been hypothesized (see figure 5 in chapter 1.5). Below, the different pathways which have been considered as target are listed together with the therapeutic approaches suggested up to present:

1. Elevation of endogenous FL-SMN protein levels generated by *SMN2*

      a) Transcriptional activation of *SMN2* via the gene promoter

           - HDAC inhibitors, including butyrate, VPA, phenylbutyrate, SAHA, and M344

             (Chang et al. 2001; Brichta et al. 2003; Sumner et al. 2003; Andreassi et al. 2004; Kernochan et al. 2005; Brichta et al. 2006; Hahnen et al. 2006; Riessland et al. 2006)

           - compounds that regulate DNA methylation of the *SMN2* promoter, including VPA, and 5-Aza-2'-deoxycytidine

             (Detich et al. 2003; Hauke 2006)

           - interferon, hydroxyurea, quinazolines

             (Baron-Delage et al. 2000; Grzeschik et al. 2005; Jarecki et al. 2005)

      b) Exon 7 inclusion in *SMN2* transcripts

           - HDAC inhibitors, including butyrate, VPA, SAHA, and M344

             (Chang et al. 2001; Brichta et al. 2003; Sumner et al. 2003; Hahnen et al. 2006; Riessland et al. 2006)

           - small synthetic antisense molecules

             (Lim and Hertel 2001; Cartegni and Krainer 2003; Skordis et al. 2003; Singh et al. 2006)

           - aclarubicin, sodium vanadate

             (Andreassi et al. 2001; Zhang et al. 2001)

      c) Translational activation and stabilization of the SMN protein

           - phosphatases and kinases

             (Grimmler et al. 2005a)

           - indoprofen

             (Lunn et al. 2004)

           - aminoglycosides

             (Wolstencroft et al. 2005)

           - proteasome inhibition

             (Chang et al. 2004)

2. Prevention of α-motor neuron degeneration by neuroprotection

    a) Neuroprotective drugs

        - riluzole, gabapentin

         (Miller et al. 2001; Haddad et al. 2003)

    b) Neurotrophic factors

        - cardiotrophin-1

         (Lesbordes et al. 2003)

3. Gene therapy and cell replacement

        - replacement of the *SMN1* gene

         (Azzouz et al. 2004)

        - stem cell therapy

         (Harper et al. 2004)

However, currently there are only a very few strategies under clinical investigation in humans. This is mainly due to problems regarding toxicity, bioavailability, and adverse events. The most advanced therapeutic drug candidates which have been or are considered for completed, ongoing, and planned clinical trials are VPA, phenylbutyrate, hydroxyurea, riluzole, and gabapentin [reviewed in (Sumner 2006)]. Gabapentin was demonstrated to have no or only minimal effect in type II and III SMA patients (Miller et al. 2001; Merlini et al. 2003). Riluzole was tested to be safe in a small number of type I SMA patients, while an improvement of motor abilites was not seen (Russman et al. 2003). However, further studies in a larger number of patients are ongoing. The major disadvantage of phenylbutyrate is the very short terminal half-life of about 1 h in human serum (Gilbert et al. 2001). Hydroxyurea, a drug which has been demonstrated to be benefitial for patients with sickle cell disease, is cytotoxic, and long-term therapy may carry the risk of inducing leukemia (Meyappan et al. 2005). Thus, VPA appears to be the most attractive drug candidate for therapy at present. Based on the *in vitro*, *ex vivo*, and *in vivo* findings for the drug, two large clinical trials are in preparation in the US and in Germany (www.fsma.org and www.initiative-sma.de). For the trial in the US, the enrollment of type II and III SMA patients has already been started. In Germany, the investigation of VPA in type I SMA patients is planned and enrollment is expected to start in fall 2006. These trials will have to elucidate whether the drug is potent enough to prevent α-motor neurons from degeneration and to maintain or to improve motor function in SMA patients. Very recently, the treatment of a small cohort of SMA patients (including seven patients with SMA type III and type IV) with VPA for a mean duration of eight months was reported (Weihl et al. 2006). The treated SMA patients revealed increased quantitative muscle strength and subjective function which is a first hint that VPA might indeed be of clinical benefit.

# 6    Summary

Proximal spinal muscular atrophy (SMA) is a common neuromuscular disorder causing infant death in 50% of all patients. Homozygous absence of the *survival motor neuron gene* (*SMN1*) is the primary cause of SMA, while SMA severity is mainly determined by the number of *SMN2* copies. One *SMN2* copy produces only about 10% of full-length (FL) protein identical to SMN1, whereas the majority of *SMN2* transcripts are aberrantly spliced due to a silent mutation within an exonic splicing enhancer in exon 7. However, correct splicing can be restored by over-expression of the SR-like splicing factor Htra2-β1.

In the present work, it is demonstrated that in fibroblast cultures derived from SMA patients treated with therapeutic doses (0.5-50 $\mu$M) of the histone deacetylase (HDAC) inhibitor valproic acid (VPA) the level of SMN protein increased ~3fold. Augmented SMN protein levels could be attributed to elevated FL-*SMN2* transcript levels which were triggered by two different mechanisms: a transcriptional activation of the *SMN2* gene, and a preferred exon 7 inclusion in *SMN2* transcripts. The latter observation was most likely due to increased levels of the splicing factor Htra2-β1. In addition to Htra2-β1, VPA increased the expression of further SR proteins which may have important implications for other disorders affected by alternative splicing. Importantly, the drug was able to elevate *rSmn* transcript and protein levels *ex vivo* through transcriptional activation in organotypic hippocampal brain slices from rats. This demonstrated that VPA also exerts an effect on neuronal tissue, the target for a potential SMA therapy.

Since VPA is a drug highly successfully used in long-time epilepsy therapy, these findings opened the exciting perspective for a first causal therapy of an inherited disease by elevating the *SMN2* transcription level and restoring its correct splicing.

The evaluation of two second-generation HDAC inhibitors in SMA fibroblasts *in vitro* revealed that SAHA, a drug that belongs to the hydroxamic acids, also efficiently elevated SMN protein levels 2.4fold to 3fold. Therefore, SAHA was identified as another attractive candidate for SMA therapy. In contrast, the data obtained for MS-275, an HDAC inhibitor of the benzamide class, demonstrated that the drug does not possess enough potency to substantially elevate SMN protein levels *in vitro*. Thus, MS-275 will not have a chance to move forward to SMA clinical trials.

Based on the promising data for VPA *in vitro* and *ex vivo* and given that VPA is already approved for application to humans, a first pilot trial with VPA was carried out in ten SMA carriers (parents of patients with SMA) aiming to evaluate drug potency to increase *SMN* transcript and protein levels *in vivo*. In order to further validate the outcome of the study, *SMN2* gene expression was analyzed in peripheral whole blood derived from 20 patients with SMA (5x type I, 11x type II, 4x type III) treated with VPA in individual experimental curative approaches all over Germany according to section 41 of the German Drug Act (AMG). Moreover, the value of these screenings was determined for the development of a clinical biomarker to monitor the response to VPA and other HDAC inhibitors in treated individuals. Such a biomarker would be highly useful for clinical trials and future therapies in SMA patients.

Drug treatment revealed elevated full-length *SMN* RNA and protein levels in blood from 7/10 SMA carriers. Importantly, SMN protein levels increased far more substantially (up to 13.8fold) than the

levels of the intermediate product, FL-*SMN* RNA, that showed an increase of up to 3.4fold. These observations provided first proof of the *in vivo* activation of a therapeutic target gene by VPA in an inherited disease. Among the investigated SMA patients, FL-*SMN2* RNA levels were increased 1.5fold to 1.9fold in seven subjects, whereas 13 patients presented unchanged or even decreased transcript levels. This data suggested that some individuals are responders to VPA, while others are most likely nonresponders or even negative-responders.

However, so far it is unknown whether *SMN* expression in blood reflects *SMN* expression in α-motor neurons and correlates with muscle strength. Therefore, systematic long-term clinical trials in SMA patients that correlate *SMN* expression in blood with individual motor function tests are required in the future to address the question whether *SMN* transcript and protein levels in blood may serve as biomarker, and to study the effect of VPA on motor function.

# 7      Zusammenfassung

Die proximale spinale Muskelatrophie (SMA) ist eine häufige neuromuskuläre Erkrankung, die bei der Hälfte aller Patienten bereits im Kindesalter zum Tod führt. Die Krankheit entsteht durch homozygoten Verlust des *survival motor neuron* Gens (*SMN1*). Der Schweregrad der SMA wird vor allem durch die Anzahl der *SMN2*-Kopien bestimmt. Eine *SMN2*-Kopie produziert nur zu etwa 10% ein Volllänge-Protein, welches mit SMN1 identisch ist. Der größte Anteil der *SMN2*-Transkripte wird auf Grund einer stillen Mutation innerhalb eines exonischen Spleißverstärkers in Exon 7 alternativ gespleißt. Durch Überexpression des SR-ähnlichen Spleißfaktors Htra2-β1 kann das korrekte Spleißmuster von *SMN2* jedoch fast vollständig wiederhergestellt werden.

In der vorliegenden Arbeit wird gezeigt, dass in Fibroblastenkulturen von SMA-Patienten, die mit dem Histondeacetylase (HDAC) - Inhibitor Valproinsäure (VPA) behandelt wurden, der SMN-Proteinspiegel ~3-fach ansteigt. Dieser Anstieg des SMN-Proteinspiegels konnte auf die vermehrte Produktion von Volllänge-*SMN2*-Transkripten zurückgeführt werden, welche durch zwei Mechanismen bedingt war: eine gesteigerte Transkriptionsaktivität des *SMN2*-Gens und den vermehrten Einschluss von Exon 7 in *SMN2*-Transkripte. Die letztere Beobachtung ließ sich mit hoher Wahrscheinlichkeit durch eine Erhöhung des Htra2-β1-Proteinspiegels erklären. Zusätzlich zu Htra2-β1 steigerte VPA auch die Expression weiterer SR-Proteine, was möglicherweise von großer Bedeutung für andere durch alternatives Spleißen hervorgerufene Erkrankungen sein könnte. In einem weiteren äußerst wichtigen Experiment konnte gezeigt werden, dass VPA auch *ex vivo* in organotypischen hippokampalen Hirnschnittkulturen der Ratte durch transkriptionelle Aktivierung den *rSmn*-Transkript- und Proteinspiegel erhöht. Damit konnte bewiesen werden, dass die Substanz auch in neuronalem Gewebe – dem Zielgewebe bei einer potentiellen SMA-Therapie – einen Effekt auf den SMN-Proteinspiegel erzielen kann.

Da VPA ein Arzneistoff ist, der erfolgreich in der Langzeittherapie der Epilepsie eingesetzt wird, eröffneten diese Ergebisse eine interessante Perspektive für eine erste kausale Therapie einer Erbkrankheit durch Steigerung der Transkriptionsrate und Wiederherstellung des korrekten Spleißens des *SMN2*-Gens.

Die Untersuchung zweier HDAC-Inhibitoren der zweiten Generation in SMA-Fibroblastenkulturen *in vitro* führten zu dem Ergebnis, dass SAHA, eine Substanz aus der Klasse der Hydroxamsäuren, ebenfalls in der Lage ist, den SMN-Proteinspiegel 2,4-fach bis 3-fach zu erhöhen. Damit konnte SAHA als weitere attraktive Kandidatensubstanz für eine SMA-Therapie identifiziert werden. Im Gegensatz dazu ließen die Daten zu MS-275, einem HDAC-Inhibitor der Benzamid-Klasse, erkennen, dass diese Substanz nicht das Potenzial hat, den SMN-Proteinspiegel *in vitro* beträchtlich zu erhöhen. Daraus konnte geschlussfolgert werden, dass MS-275 für klinische Studien bezüglich SMA nicht in Frage kommen wird.

Basierend auf den vielversprechenden Daten zu VPA *in vitro* und *ex vivo* sowie auf Grund der Tatsache, dass VPA für die Anwendung am Menschen bereits zugelassen ist, wurde eine erste Pilotstudie mit VPA bei 10 SMA-Anlageträgern (Eltern von SMA-Patienten) durchgeführt, um zu untersuchen, ob VPA den *SMN*-Transkript- und Proteinspiegel auch *in vivo* zu erhöhen vermag. Um das Ergebnis dieser Studie zu untermauern, wurde zudem die Expression des *SMN2*-Gens in Blut von

20 SMA-Patienten (5x Typ I, 11x Typ II, 4x Typ III) analysiert, die in Deutschland im Rahmen individueller Heilversuche entsprechend Paragraph 41 des Arzneimittelgesetzes (AMG) mit VPA behandelt wurden. Die resultierenden Daten wurden außerdem im Hinblick auf die Entwicklung eines klinischen Biomarkers untersucht, welcher Auskunft darüber geben kann, ob Patienten, die mit VPA oder andere HDAC-Inhibitoren behandelt werden, auf diese Substanzen ansprechen oder nicht. Ein Biomarker dieser Art wäre extrem wichtig für klinische Studien und zukünftige Therapien in SMA-Patienten.

Die Behandlung mit VPA führte bei 7 von 10 SMA-Anlageträgern zu erhöhten Volllänge-SMN-RNA- und Proteinspiegeln im Blut. Von großer Bedeutung war die Beobachtung, dass die SMN-Proteinspiegel weitaus stärker anstiegen (bis zu 13,8-fach) als die Spiegel des Intermediärproduktes, der Volllänge-*SMN*-RNA. Für letztere konnte ein bis zu 3,4-facher Anstieg gemessen werden. Diese Ergebnisse lieferten den ersten Beweis dafür, dass VPA auch *in vivo* die Aktivität eines Genes zu steigern vermag, welchem eine essentielle Rolle bei der möglichen Therapie einer Erbkrankheit zukommt. Die Analyse der Blutproben der behandelten SMA-Patienten ergab 1,5-fach bis 1,9-fach erhöhte Volllänge-*SMN2*-RNA-Spiegel bei 7 Individuen, während 13 Patienten unveränderte oder sogar erniedrigte Transkriptspiegel zeigten. Diese Daten führten zu der Schlussfolgerung, dass einige Personen auf VPA ansprechen, andere allerdings keine Reaktion oder sogar einen negativen Effekt zeigen.

Bisher ist allerdings nicht untersucht worden, ob die Expression des *SMN*-Gens im Blut die Expression des *SMN*-Gens in den α-Motoneuronen reflektiert und mit der Muskelkraft korreliert. In der Zukunft sind deshalb klinische Langzeitstudien mit SMA-Patienten erforderlich, in denen die Expression des *SMN*-Gens im Blut mit Muskelkraftmessungen korreliert wird, so dass geklärt werden kann, ob die *SMN*-Transkript- und Proteinspiegel im Blut tatsächlich als Biomarker dienen können, und ob VPA einen positiven Einfluss auf die Muskelkraft hat.

# 8          Publications, lectures, poster contributions, and awards

## 8.1          Original publications

**Brichta L**, Hofmann Y, Hahnen E, Siebzehnrubl FA, Raschke H, Blumcke I, Eyupoglu IY and Wirth B (2003) Valproic acid increases the SMN2 protein level: a well-known drug as a potential therapy for spinal muscular atrophy. *Hum Mol Genet*. 12: 2481-9

Wirth B, **Brichta L**, Schrank B, Lochmuller H, Blick S, Baasner A and Heller R (2006) Mildly affected patients with spinal muscular atrophy are partially protected by an increased SMN2 copy number. *Hum Genet*. 119: 422-8

**Brichta L**, Holker I, Haug K, Klockgether T and Wirth B (2006) In vivo activation of SMN in spinal muscular atrophy carriers and patients treated with valproate. *Ann Neurol*. 59: 970-5

Riessland M, **Brichta L**, Hahnen E and Wirth B (2006) The benzamide M344, a novel histone deacetylase inhibitor, significantly increases SMN2 RNA/protein levels in spinal muscular atrophy (SMA) cells. *Hum Genet.* May 2006 [Epub ahead of print]

Hahnen E, Eyupoglu IY, **Brichta L**, Haastert K, Trankle C, Siebzehnrubl FA, Riessland M, Holker I, Claus P, Romstock J, Buslei R, Wirth B and Blumcke I (2006) In vitro and ex vivo evaluation of second-generation histone deacetylase inhibitors for the treatment of spinal muscular atrophy. *J Neurochem.* May 2006 [Epub ahead of print]

Fyfe JC, Menotti-Raymond M, David VA, **Brichta L**, Schaffer AA, Agarwala R, Murphy WJ, Wedemeyer WJ, Gregory BL, Buzzell BG, Drummond MC, Wirth B and O'Brien SJ (2006) An ~140kb deletion associated with feline spinal muscular atrophy implies an essential LIX1 function for motor neuron survival. *Genome Res.* In press

## 8.2          Reviews and book chapters

Wirth B, **Brichta L** and Hahnen E (2006) Spinal muscular atrophy: from gene to therapy. *Semin Pediatr Neurol*. In press

Wirth B, **Brichta L** and Hahnen E (2006) Spinal muscular atrophy and therapeutic prospects. In Jeanteur P. (Ed.), *Alternative splicing and disease.* Springer-Verlag Berlin, Heidelberg, pp. 109-132. In press

## 8.3 Printed lecture contributions

Wirth B, **Brichta L**, Hofmann Y, Haug K. (2003) Spinal muscular atrophy: Perspectives of a therapy by restoring the splicing pattern of *SMN2*. *Eur J Hum Genet.* 11, Suppl. 1:46 (S20) (European Human Genetics Conference, Symposium Splicing and Disease, Birmingham)

**Brichta L**, Hofmann Y, Hahnen E, Siebzehnrübl FA, Raschke H, Blumcke I, Eyupoglu IY, Wirth B. (2004) Valproic acid increases the SMN2 protein level: A potential therapy for spinal muscular atrophy. *Abstract book* (7th Annual International SMA Research Group Meeting, Washington DC)

**Brichta L**, Hofmann Y, Hahnen E, Siebzehnrübl FA, Raschke H, Blumcke I, Eyupoglu IY, Wirth B. (2004) Valproic acid increases the SMN2 protein level: A well-known drug as a potential therapy for spinal muscular atrophy. *Medgen.* 15:270 (S7 03) (Annual Meeting of the German Society of Human Genetics, Symposium Splicing and Disease, Marburg)

**Brichta L**, Haug K, Sun Y, Stier S, Klockgether T, Wirth B. (2004) Pilot study of *in vivo* effects of valproic acid on *SMN* gene expression in SMA carriers. *Eur J Hum Genet.* 12, Suppl. 1:65 (C02) (European Human Genetics Conference, Clinical Genetics Session, München)

**Brichta L**, Haug K, Sun Y, Stier S, Holker I, Hahnen E, Klockgether T, Wirth B. (2004) Pilot study of *in vivo* effects of valproic acid on *SMN* gene expression in SMA carriers. *Abstract book* (8th Annual International SMA Research Group Meeting, Chicago)

**Brichta L** (2004) Einfluss von Valproinsäure auf den SMN2-Proteinlevel – eine gut bekannte Substanz als mögliche Therapie der spinalen Muskelatrophie. *Abstract book* (Preisträgervortrag für den 1. Preis des Felix-Jerusalem-Preises der DGM, Annual Meeting of the German Society for Clinical Neurophysiology and funktionelle Bildgebung, Jena)

**Brichta L**, Holker I, Wirth B. (2005) Valproic acid treatment of SMA patients: implications for evaluation of a clinical biomarker. *Abstract book* (9th Annual International SMA Research Group Meeting, Philadelphia)

Lyding S, Dohna-Schwake C, **Brichta L**, Hahnen E, Wirth B, Voit T. (2005) SMA type I: Prospective placebo-controlled double-blinded clinical treatment study with valproic acid. *Abstract book* (9th Annual International SMA Research Group Meeting, Philadelphia)

**Brichta L**, Holker I, Haug K, Klockgether T, Wirth B. (2006) *In vivo* activation of *SMN* in SMA carriers and patients treated with valproic acid. *Medgen.* 18:31 (W4 03) (Annual Meeting of the German Society of Human Genetics, Neurogenetics Session, Heidelberg)

**Brichta L**, Holker I, Haug K, Klockgether T, Wirth B. (2006) Evidence of *in vivo* increase of *SMN* RNA and protein in SMA carriers and patients treated with valproic acid. *Eur J Hum Genet.* 14, Suppl. 1:93 (C52) (European Human Genetics Conference, Therapy for Genetic Disease Session, Amsterdam)

**Brichta L**, Holker I, Haug K, Klockgether T, Wirth B. (2006) Evidence of *in vivo* increase of *SMN* RNA and protein in SMA carriers and patients treated with valproic acid. *Abstract book* (10th Annual International SMA Research Group Meeting, Montréal)

Riessland M, **Brichta L**, Hahnen E, Wirth B. (2006) The benzamide M344, a novel histone deacetylase inhibitor, significantly increases SMN2 RNA/protein levels in spinal muscular atrophy (SMA) cells. *Abstract book* (10th Annual International SMA Research Group Meeting, Montréal)

## 8.4     Printed poster contributions

**Brichta L**, Hofmann Y, Raschke H, Sun Y, Haug K, Wirth B. (2003) Potential therapeutical approach for spinal muscular atrophy (SMA): Valproic acid up-regulates SMN protein levels in SMA fibroblast cell cultures. *Abstract book* (International Neuroscience Symposium: Molecular Basis of CNS Disorders, Bonn)

Haug K, **Brichta L**, Sun Y, Klockgether T, Wirth B. (2003) Clinical study with valproic acid in SMA carriers. *Abstract book* (7th Annual International SMA Research Group Meeting, Washington DC)

**Brichta L**, Hofmann Y, Hahnen E, Siebzehnrubl FA, Raschke H, Blumcke I, Eyupoglu IY, Wirth B. (2003) Valproic acid increases SMN2 protein and splicing factor levels: A potential therapy for spinal muscular atrophy and other diseases associated with exon skipping. *Abstract book* (Eukaryotic mRNA processing, Cold Spring Harbor)

Haug K; **Brichta L**, Sun Y, Stier S, Klockgether T, Wirth B. (2003) Clinical study with valproic acid in SMA carriers. *Medgen* 15:297 (P018) (Annual Meeting of the German Society of Human Genetics, Marburg)

**Brichta L**, Hofmann Y, Hahnen E, Siebzehnrübl FA, Raschke H, Blumcke I, Eyupoglu IY, Wirth B. (2004) Valproic acid – an HDAC inhibitor may provide a first causative cure for spinal muscular atrophy by increasing *SMN2* expression. *Abstract book* (Chromatin 2004, Luxembourg)

**Brichta L**, Holker I, Haug K, Hahnen E, Klockgether T, Wirth B. (2005) Valproic acid treatment of spinal muscular atrophy patients as a chance to increase *SMN2* gene expression and improve motor abilities. *Medgen* 17:62 (P018) (Annual Meeting of the German Society of Human Genetics, Halle)

Hahnen E, Eyüpoglu IY, **Brichta L**, Siebzehnrübl FA, Riessland M, Tränkle C, Buslei R, Wirth B, Blümcke I. (2005) Therapy of spinal muscular atrophy : Hydroxamid acids increase survival of motor neuron protein levels. *Medgen* 17:113 (P234) (Annual Meeting of the German Society of Human Genetics, Halle)

Hahnen E, Eyüpoglu IY, **Brichta L**, Haastert K, Tränkle C, Siebzehnrübl FA, Riessland M, Holker I; Claus P, Romstöck J, Buslei R, Blümcke I, Wirth B. (2006) *In vitro* and *ex vivo* evaluation of second generation histone deacetylase inhibitors fort he treatment of spinal muscular atrophy. *Medgen* 18:113 (P291) (Annual Meeting of the German Society of Human Genetics, Heidelberg)

Riessland M, **Brichta L**, Hahnen E, Wirth B. (2006) The benzamide M344, a novel histone deacetylase inhibitor, significantly increases SMN2 RNA/protein levels in spinal muscular atrophy (SMA) cells. *Medgen* 18:113 (P293) (Annual Meeting of the German Society of Human Genetics, Heidelberg)

## 8.5    Awards

2003
Poster Award
**Brichta L**, Hofmann Y, Raschke H, Sun Y, Haug K, Wirth B. (2003) Potential therapeutical approach for spinal muscular atrophy (SMA): Valproic acid up-regulates SMN protein levels in SMA fibroblast cell cultures. *Abstract book* (International Neuroscience Symposium: Molecular Basis of CNS Disorders, Bonn)

2004
$1^{st}$ Prize of the Felix-Jerusalem-Myopathy-Award of the "Deutsche Gesellschaft für Muskelkranke, DGM" (German Society of Muscle Disease Patients), awarded for the following work:
"Valproic acid increases the SMN2 protein level: A well-known drug as potential therapy for spinal muscular atrophy"

2005
Attendy of the $55^{th}$ Meeting of Nobel Prize Winners in Lindau, $2^{nd}$ Interdisciplinary Meeting, from June $26^{th}$ to July $1^{st}$, 2005
(selected as student representative by the Medical Faculty of the University of Cologne)

2006
Young Investigator Award of the Medical Faculty of the University of Cologne, provided by Novartis

# 9      References

Abrams J (1980) Nitrate tolerance and dependence. A critical assessment. *Nouv Presse Med.* 9:2499-504

Agalioti T, Chen G and Thanos D (2002) Deciphering the transcriptional histone acetylation code for a human gene. *Cell.* 111:381-92

Akiyama Y, Maesawa C, Ogasawara S, Terashima M and Masuda T (2003) Cell-type-specific repression of the maspin gene is disrupted frequently by demethylation at the promoter region in gastric intestinal metaplasia and cancer cells. *Am J Pathol.* 163:1911-9

Alland L, Muhle R, Hou H, Jr., Potes J, Chin L, Schreiber-Agus N and DePinho RA (1997) Role for N-CoR and histone deacetylase in Sin3-mediated transcriptional repression. *Nature.* 387:49-55

Allfrey VG, Faulkner R and Mirsky AE (1964) Acetylation and Methylation of Histones and Their Possible Role in the Regulation of Rna Synthesis. *Proc Natl Acad Sci U S A.* 51:786-94

Andreassi C, Angelozzi C, Tiziano FD, Vitali T, De Vincenzi E, Boninsegna A, Villanova M, Bertini E, Pini A, Neri G and Brahe C (2004) Phenylbutyrate increases SMN expression in vitro: relevance for treatment of spinal muscular atrophy. *Eur J Hum Genet.* 12:59-65

Andreassi C, Jarecki J, Zhou J, Coovert DD, Monani UR, Chen X, Whitney M, Pollok B, Zhang M, Androphy E and Burghes AH (2001) Aclarubicin treatment restores SMN levels to cells derived from type I spinal muscular atrophy patients. *Hum Mol Genet.* 10:2841-9

Arents G, Burlingame RW, Wang BC, Love WE and Moudrianakis EN (1991) The nucleosomal core histone octamer at 3.1 A resolution: a tripartite protein assembly and a left-handed superhelix. *Proc Natl Acad Sci U S A.* 88:10148-52

Arinze IJ and Kawai Y (2003) Sp family of transcription factors is involved in valproic acid-induced expression of Galphai2. *J Biol Chem.* 278:17785-91

Avner P and Heard E (2001) X-chromosome inactivation: counting, choice and initiation. *Nat Rev Genet.* 2:59-67

Azzouz M, Le T, Ralph GS, Walmsley L, Monani UR, Lee DC, Wilkes F, Mitrophanous KA, Kingsman SM, Burghes AH and Mazarakis ND (2004) Lentivector-mediated SMN replacement in a mouse model of spinal muscular atrophy. *J Clin Invest.* 114:1726-31

Baccon J, Pellizzoni L, Rappsilber J, Mann M and Dreyfuss G (2002) Identification and characterization of Gemin7, a novel component of the survival of motor neuron complex. *J Biol Chem*. 277:31957-62

Baker BS (1989) Sex in flies: the splice of life. *Nature*. 340:521-4

Baron-Delage S, Abadie A, Echaniz-Laguna A, Melki J and Beretta L (2000) Interferons and IRF-1 induce expression of the survival motor neuron (SMN) genes. *Mol Med*. 6:957-68

Battaglia G, Princivalle A, Forti F, Lizier C and Zeviani M (1997) Expression of the SMN gene, the spinal muscular atrophy determining gene, in the mammalian central nervous system. *Hum Mol Genet*. 6:1961-71

Bechade C, Rostaing P, Cisterni C, Kalisch R, La Bella V, Pettmann B and Triller A (1999) Subcellular distribution of survival motor neuron (SMN) protein: possible involvement in nucleocytoplasmic and dendritic transport. *Eur J Neurosci*. 11:293-304

Bergin A, Kim G, Price DL, Sisodia SS, Lee MK and Rabin BA (1997) Identification and characterization of a mouse homologue of the spinal muscular atrophy-determining gene, survival motor neuron. *Gene*. 204:47-53

Bertrandy S, Burlet P, Clermont O, Huber C, Fondrat C, Thierry-Mieg D, Munnich A and Lefebvre S (1999) The RNA-binding properties of SMN: deletion analysis of the zebrafish orthologue defines domains conserved in evolution. *Hum Mol Genet*. 8:775-82

Black DL (2003) Mechanisms of alternative pre-messenger RNA splicing. *Annu Rev Biochem*. 72:291-336

Blaheta RA and Cinatl J, Jr. (2002) Anti-tumor mechanisms of valproate: a novel role for an old drug. *Med Res Rev*. 22:492-511

Blencowe BJ (2000) Exonic splicing enhancers: mechanism of action, diversity and role in human genetic diseases. *Trends Biochem Sci*. 25:106-10

Boffa LC, Vidali G, Mann RS and Allfrey VG (1978) Suppression of histone deacetylation in vivo and in vitro by sodium butyrate. *J Biol Chem*. 253:3364-6

Bradford MM (1976) A rapid and sensitive method for the quantitation of microgram quantities of protein utilizing the principle of protein-dye binding. *Anal Biochem*. 72:248-54

Brahe C (2000) Copies of the survival motor neuron gene in spinal muscular atrophy: the more, the better. *Neuromuscul Disord*. 10:274-5

Brahe C, Servidei S, Zappata S, Ricci E, Tonali P and Neri G (1995) Genetic homogeneity between childhood-onset and adult-onset autosomal recessive spinal muscular atrophy. *Lancet*. 346:741-2

Brahe C, Vitali T, Tiziano FD, Angelozzi C, Pinto AM, Borgo F, Moscato U, Bertini E, Mercuri E and Neri G (2005) Phenylbutyrate increases SMN gene expression in spinal muscular atrophy patients. *Eur J Hum Genet*. 13:256-9

Brahe C, Zappata S, Velona I, Bertini E, Servidei S, Tonali P and Neri G (1993) Presymptomatic diagnosis of SMA III by genotype analysis. *Am J Med Genet*. 45:408-11

Brahms H, Meheus L, de Brabandere V, Fischer U and Luhrmann R (2001) Symmetrical dimethylation of arginine residues in spliceosomal Sm protein B/B' and the Sm-like protein LSm4, and their interaction with the SMN protein. *Rna*. 7:1531-42

Braunstein M, Sobel RE, Allis CD, Turner BM and Broach JR (1996) Efficient transcriptional silencing in Saccharomyces cerevisiae requires a heterochromatin histone acetylation pattern. *Mol Cell Biol*. 16:4349-56

Brichta L, Hofmann Y, Hahnen E, Siebzehnrubl FA, Raschke H, Blumcke I, Eyupoglu IY and Wirth B (2003) Valproic acid increases the SMN2 protein level: a well-known drug as a potential therapy for spinal muscular atrophy. *Hum Mol Genet*. 12:2481-9

Brichta L, Holker I, Haug K, Klockgether T and Wirth B (2006) In vivo activation of SMN in spinal muscular atrophy carriers and patients treated with valproate. *Ann Neurol*. 59:970-5

Briese M, Esmaeili B and Sattelle DB (2005) Is spinal muscular atrophy the result of defects in motor neuron processes? *Bioessays*. 27:946-57

Brownell JE, Zhou J, Ranalli T, Kobayashi R, Edmondson DG, Roth SY and Allis CD (1996) Tetrahymena histone acetyltransferase A: a homolog to yeast Gcn5p linking histone acetylation to gene activation. *Cell*. 84:843-51

Brzustowicz LM, Lehner T, Castilla LH, Penchaszadeh GK, Wilhelmsen KC, Daniels R, Davies KE, Leppert M, Ziter F, Wood D and et al. (1990) Genetic mapping of chronic childhood-onset spinal muscular atrophy to chromosome 5q11.2-13.3. *Nature*. 344:540-1

Buhler D, Raker V, Luhrmann R and Fischer U (1999) Essential role for the tudor domain of SMN in spliceosomal U snRNP assembly: implications for spinal muscular atrophy. *Hum Mol Genet*. 8:2351-7

Burge CB, Tuschl PA and Sharp PA (1999) Splicing of precursors to mRNAs by the spliceosomes, in:R.F. Gesteland, J.F.Atkins (Eds.), The RNA World. *Cold Spring Harbour Laboratory Press, Cold Spring Harbour, New York*. 525-560

Burghes AH (1997) When is a deletion not a deletion? When it is converted. *Am J Hum Genet*. 61:9-15

Burglen L, Lefebvre S, Clermont O, Burlet P, Viollet L, Cruaud C, Munnich A and Melki J (1996) Structure and organization of the human survival motor neurone (SMN) gene. *Genomics*. 32:479-82

Burglen L, Seroz T, Miniou P, Lefebvre S, Burlet P, Munnich A, Pequignot EV, Egly JM and Melki J (1997) The gene encoding p44, a subunit of the transcription factor TFIIH, is involved in large-scale deletions associated with Werdnig-Hoffmann disease. *Am J Hum Genet*. 60:72-9

Burlet P, Huber C, Bertrandy S, Ludosky MA, Zwaenepoel I, Clermont O, Roume J, Delezoide AL, Cartaud J, Munnich A and Lefebvre S (1998) The distribution of SMN protein complex in human fetal tissues and its alteration in spinal muscular atrophy. *Hum Mol Genet*. 7:1927-33

Burlingame RW, Love WE, Wang BC, Hamlin R, Nguyen HX and Moudrianakis EN (1985) Crystallographic structure of the octameric histone core of the nucleosome at a resolution of 3.3 A. *Science*. 228:546-53

Bussaglia E, Clermont O, Tizzano E, Lefebvre S, Burglen L, Cruaud C, Urtizberea JA, Colomer J, Munnich A, Baiget M and et al. (1995) A frame-shift deletion in the survival motor neuron gene in Spanish spinal muscular atrophy patients. *Nat Genet*. 11:335-7

Bustin M (1999) Regulation of DNA-dependent activities by the functional motifs of the high-mobility-group chromosomal proteins. *Mol Cell Biol*. 19:5237-46

Bustin M (2001a) Chromatin unfolding and activation by HMGN(*) chromosomal proteins. *Trends Biochem Sci*. 26:431-7

Bustin M (2001b) Revised nomenclature for high mobility group (HMG) chromosomal proteins. *Trends Biochem Sci*. 26:152-3

Bustin M and Reeves R (1996) High-mobility-group chromosomal proteins: architectural components that facilitate chromatin function. *Prog Nucleic Acid Res Mol Biol*. 54:35-100

Bustin SA (2000) Absolute quantification of mRNA using real-time reverse transcription polymerase chain reaction assays. *J Mol Endocrinol*. 25:169-93

Butler LM, Zhou X, Xu WS, Scher HI, Rifkind RA, Marks PA and Richon VM (2002) The histone deacetylase inhibitor SAHA arrests cancer cell growth, up-regulates thioredoxin-binding protein-2, and down-regulates thioredoxin. *Proc Natl Acad Sci U S A*. 99:11700-5

Byrd JC and Alho H (1987) Differentiation of PC12 pheochromocytoma cells by sodium butyrate. *Brain Res*. 428:151-5

Campbell L, Hunter KM, Mohaghegh P, Tinsley JM, Brasch MA and Davies KE (2000) Direct interaction of Smn with dp103, a putative RNA helicase: a role for Smn in transcription regulation? *Hum Mol Genet*. 9:1093-100

Carissimi C, Saieva L, Baccon J, Chiarella P, Maiolica A, Sawyer A, Rappsilber J and Pellizzoni L (2006) Gemin8 is a novel component of the survival motor neuron complex and functions in snRNP assembly. *J Biol Chem*. 281:8126-34

Carnegie GK, Sleeman JE, Morrice N, Hastie CJ, Peggie MW, Philp A, Lamond AI and Cohen PT (2003) Protein phosphatase 4 interacts with the survival of motor neurons complex and enhances the temporal localisation of snRNPs. *J Cell Sci*. 116:1905-13

Carrozza MJ, Utley RT, Workman JL and Cote J (2003) The diverse functions of histone acetyltransferase complexes. *Trends Genet*. 19:321-9

Cartegni L, Hastings ML, Calarco JA, Stanchina E and Krainer AR (2006) Determinants of Exon 7 Splicing in the Spinal Muscular Atrophy Genes, SMN1 and SMN2. *Am J Hum Genet*. 78:63-77

Cartegni L and Krainer AR (2002) Disruption of an SF2/ASF-dependent exonic splicing enhancer in SMN2 causes spinal muscular atrophy in the absence of SMN1. *Nat Genet*. 30:377-84

Cartegni L and Krainer AR (2003) Correction of disease-associated exon skipping by synthetic exon-specific activators. *Nat Struct Biol*. 10:120-5

Carter TA, Bonnemann CG, Wang CH, Obici S, Parano E, De Fatima Bonaldo M, Ross BM, Penchaszadeh GK, Mackenzie A, Soares MB, Kunkel LM and Gilliam TC (1997) A multicopy transcription-repair gene, BTF2p44, maps to the SMA region and demonstrates SMA associated deletions. *Hum Mol Genet*. 6:229-36

Chan YB, Miguel-Aliaga I, Franks C, Thomas N, Trulzsch B, Sattelle DB, Davies KE and van den Heuvel M (2003) Neuromuscular defects in a Drosophila survival motor neuron gene mutant. *Hum Mol Genet*. 12:1367-76

Chang HC, Hung WC, Chuang YJ and Jong YJ (2004) Degradation of survival motor neuron (SMN) protein is mediated via the ubiquitin/proteasome pathway. *Neurochem Int*. 45:1107-12

Chang JG, Hsieh-Li HM, Jong YJ, Wang NM, Tsai CH and Li H (2001) Treatment of spinal muscular atrophy by sodium butyrate. *Proc Natl Acad Sci U S A*. 98:9808-13

Charroux B, Pellizzoni L, Perkinson RA, Shevchenko A, Mann M and Dreyfuss G (1999) Gemin3: A novel DEAD box protein that interacts with SMN, the spinal muscular atrophy gene product, and is a component of gems. *J Cell Biol*. 147:1181-94

Charroux B, Pellizzoni L, Perkinson RA, Yong J, Shevchenko A, Mann M and Dreyfuss G (2000) Gemin4. A novel component of the SMN complex that is found in both gems and nucleoli. *J Cell Biol*. 148:1177-86

Chen G, Yuan P, Hawver DB, Potter WZ and Manji HK (1997) Increase in AP-1 transcription factor DNA binding activity by valproic acid. *Neuropsychopharmacology*. 16:238-45

Chen G, Yuan PX, Jiang YM, Huang LD and Manji HK (1999) Valproate robustly enhances AP-1 mediated gene expression. *Brain Res Mol Brain Res*. 64:52-8

Chen JS and Faller DV (2005) Histone deacetylase inhibition-mediated post-translational elevation of p27KIP1 protein levels is required for G1 arrest in fibroblasts. *J Cell Physiol*. 202:87-99

Chen Q, Baird SD, Mahadevan M, Besner-Johnston A, Farahani R, Xuan J, Kang X, Lefebvre C, Ikeda JE, Korneluk RG and MacKenzie AE (1998) Sequence of a 131-kb region of 5q13.1 containing the spinal muscular atrophy candidate genes SMN and NAIP. *Genomics*. 48:121-7

Cheung VG, Conlin LK, Weber TM, Arcaro M, Jen KY, Morley M and Spielman RS (2003) Natural variation in human gene expression assessed in lymphoblastoid cells. *Nat Genet*. 33:422-5

Chisholm A and Tessier-Lavigne M (1999) Conservation and divergence of axon guidance mechanisms. *Curr Opin Neurobiol*. 9:603-15

Cho M, Uemura H, Kim SC, Kawada Y, Yoshida K, Hirao Y, Konishi N, Saga S and Yoshikawa K (2001) Hypomethylation of the MN/CA9 promoter and upregulated MN/CA9 expression in human renal cell carcinoma. *Br J Cancer*. 85:563-7

Chu PG, Chang KL, Chen WG, Chen YY, Shibata D, Hayashi K, Bacchi C, Bacchi M and Weiss LM (1999) Epstein-Barr virus (EBV) nuclear antigen (EBNA)-4 mutation in EBV-associated malignancies in three different populations. *Am J Pathol*. 155:941-7

Claus P, Bruns AF and Grothe C (2004) Fibroblast growth factor-2(23) binds directly to the survival of motoneuron protein and is associated with small nuclear RNAs. *Biochem J*. 384:559-65

Clermont O, Burlet P, Benit P, Chanterau D, Saugier-Veber P, Munnich A and Cusin V (2004) Molecular analysis of SMA patients without homozygous SMN1 deletions using a new strategy for identification of SMN1 subtle mutations. *Hum Mutat*. 24:417-27

Clermont O, Burlet P, Lefebvre S, Burglen L, Munnich A and Melki J (1995) SMN gene deletions in adult-onset spinal muscular atrophy. *Lancet*. 346:1712-3

Cloyd J (1991) Pharmacokinetic pitfalls of present antiepileptic medications. *Epilepsia*. 32 Suppl 5:S53-65

Cobben JM, van der Steege G, Grootscholten P, de Visser M, Scheffer H and Buys CH (1995) Deletions of the survival motor neuron gene in unaffected siblings of patients with spinal muscular atrophy. *Am J Hum Genet*. 57:805-8

Coovert DD, Le TT, McAndrew PE, Strasswimmer J, Crawford TO, Mendell JR, Coulson SE, Androphy EJ, Prior TW and Burghes AH (1997) The survival motor neuron protein in spinal muscular atrophy. *Hum Mol Genet*. 6:1205-14

Cress WD and Seto E (2000) Histone deacetylases, transcriptional control, and cancer. *J Cell Physiol*. 184:1-16

de Ruijter AJ, van Gennip AH, Caron HN, Kemp S and van Kuilenburg AB (2003) Histone deacetylases (HDACs): characterization of the classical HDAC family. *Biochem J*. 370:737-49

Deimling von F, Scharf JM, Liehr T, Rothe M, Kelter AR, Albers P, Dietrich WF, Kunkel LM, Wernert N and Wirth B (1999) Human and mouse RAD17 genes: identification, localization, genomic structure and histological expression pattern in normal testis and seminoma. *Hum Genet*. 105:17-27

Detich N, Bovenzi V and Szyf M (2003) Valproate induces replication-independent active DNA demethylation. *J Biol Chem*. 278:27586-92

Dheda K, Huggett JF, Bustin SA, Johnson MA, Rook G and Zumla A (2004) Validation of housekeeping genes for normalizing RNA expression in real-time PCR. *Biotechniques*. 37:112-4, 116, 118-9

DiDonato CJ, Chen XN, Noya D, Korenberg JR, Nadeau JH and Simard LR (1997) Cloning, characterization, and copy number of the murine survival motor neuron gene: homolog of the spinal muscular atrophy-determining gene. *Genome Res*. 7:339-52

DiDonato CJ, Lorson CL, De Repentigny Y, Simard L, Chartrand C, Androphy EJ and Kothary R (2001) Regulation of murine survival motor neuron (Smn) protein levels by modifying Smn exon 7 splicing. *Hum Mol Genet*. 10:2727-36

DiDonato CJ, Morgan K, Carpten JD, Fuerst P, Ingraham SE, Prescott G, McPherson JD, Wirth B, Zerres K, Hurko O and et al. (1994) Association between Ag1-CA alleles and severity of autosomal recessive proximal spinal muscular atrophy. *Am J Hum Genet*. 55:1218-29

Dixon DA, Balch GC, Kedersha N, Anderson P, Zimmerman GA, Beauchamp RD and Prescott SM (2003) Regulation of cyclooxygenase-2 expression by the translational silencer TIA-1. *J Exp Med*. 198:475-81

Doenecke D and Gallwitz D (1982) Acetylation of histones in nucleosomes. *Mol Cell Biochem*. 44:113-28

Eberharter A and Becker PB (2002) Histone acetylation: a switch between repressive and permissive chromatin. Second in review series on chromatin dynamics. *EMBO Rep*. 3:224-9

Echaniz-Laguna A, Miniou P, Bartholdi D and Melki J (1999) The promoters of the survival motor neuron gene (SMN) and its copy (SMNc) share common regulatory elements. *Am J Hum Genet*. 64:1365-70

Egger G, Liang G, Aparicio A and Jones PA (2004) Epigenetics in human disease and prospects for epigenetic therapy. *Nature*. 429:457-63

Eggert C, Chari A, Laggerbauer B and Fischer U (2006) Spinal muscular atrophy: the RNP connection. *Trends Mol Med*. 12:113-21

Ehrlich M and Wang RY (1981) 5-Methylcytosine in eukaryotic DNA. *Science*. 212:1350-7

Eickbush TH and Moudrianakis EN (1978) The histone core complex: an octamer assembled by two sets of protein-protein interactions. *Biochemistry*. 17:4955-64

Engelhard HH, Duncan HA, Kim S, Criswell PS and Van Eldik L (2001) Therapeutic effects of sodium butyrate on glioma cells in vitro and in the rat C6 glioma model. *Neurosurgery*. 48:616-24; discussion 624-5

Eperon IC, Makarova OV, Mayeda A, Munroe SH, Caceres JF, Hayward DG and Krainer AR (2000) Selection of alternative 5' splice sites: role of U1 snRNP and models for the antagonistic effects of SF2/ASF and hnRNP A1. *Mol Cell Biol*. 20:8303-18

Espert L, Eldin P, Gongora C, Bayard B, Harper F, Chelbi-Alix MK, Bertrand E, Degols G and Mechti N (2006) The exonuclease ISG20 mainly localizes in the nucleolus and the Cajal (Coiled) bodies and is associated with nuclear SMN protein-containing complexes. *J Cell Biochem*. March 2006:[Epub ahead of print]

Eyal S, Yagen B, Sobol E, Altschuler Y, Shmuel M and Bialer M (2004) The activity of antiepileptic drugs as histone deacetylase inhibitors. *Epilepsia*. 45:737-44

Fakan S, Leser G and Martin TE (1984) Ultrastructural distribution of nuclear ribonucleoproteins as visualized by immunocytochemistry on thin sections. *J Cell Biol*. 98:358-63

Faustino NA and Cooper TA (2003) Pre-mRNA splicing and human disease. *Genes Dev*. 17:419-37

Feinberg AP and Tycko B (2004) The history of cancer epigenetics. *Nat Rev Cancer*. 4:143-53

Feinberg AP and Vogelstein B (1983a) Hypomethylation distinguishes genes of some human cancers from their normal counterparts. *Nature*. 301:89-92

Feinberg AP and Vogelstein B (1983b) Hypomethylation of ras oncogenes in primary human cancers. *Biochem Biophys Res Commun*. 111:47-54

Feldkötter M, Schwarzer V, Wirth R, Wienker TF and Wirth B (2002) Quantitative Analyses of SMN1 and SMN2 Based on Real-Time LightCycler PCR: Fast and Highly Reliable Carrier Testing and Prediction of Severity of Spinal Muscular Atrophy. *Am J Hum Genet*. 70:358-68

Felgner PL, Gadek TR, Holm M, Roman R, Chan HW, Wenz M, Northrop JP, Ringold GM and Danielsen M (1987) Lipofection: a highly efficient, lipid-mediated DNA-transfection procedure. *Proc Natl Acad Sci U S A*. 84:7413-7

Felsenfeld G and Groudine M (2003) Controlling the double helix. *Nature*. 421:448-53

Feng W, Gubitz AK, Wan L, Battle DJ, Dostie J, Golembe TJ and Dreyfuss G (2005) Gemins modulate the expression and activity of the SMN complex. *Hum Mol Genet*. 14:1605-11

Finnin MS, Donigian JR, Cohen A, Richon VM, Rifkind RA, Marks PA, Breslow R and Pavletich NP (1999) Structures of a histone deacetylase homologue bound to the TSA and SAHA inhibitors. *Nature*. 401:188-93

Fischer DD, Cai R, Bhatia U, Asselbergs FA, Song C, Terry R, Trogani N, Widmer R, Atadja P and Cohen D (2002) Isolation and characterization of a novel class II histone deacetylase, HDAC10. *J Biol Chem*. 277:6656-66

Friesen WJ and Dreyfuss G (2000) Specific sequences of the Sm and Sm-like (Lsm) proteins mediate their interaction with the spinal muscular atrophy disease gene product (SMN). *J Biol Chem*. 275:26370-5

Frugier T, Tiziano FD, Cifuentes-Diaz C, Miniou P, Roblot N, Dierich A, Le Meur M and Melki J (2000) Nuclear targeting defect of SMN lacking the C-terminus in a mouse model of spinal muscular atrophy. *Hum Mol Genet*. 9:849-58

Furumai R, Komatsu Y, Nishino N, Khochbin S, Yoshida M and Horinouchi S (2001) Potent histone deacetylase inhibitors built from trichostatin A and cyclic tetrapeptide antibiotics including trapoxin. *Proc Natl Acad Sci U S A*. 98:87-92

Furumai R, Matsuyama A, Kobashi N, Lee KH, Nishiyama M, Nakajima H, Tanaka A, Komatsu Y, Nishino N, Yoshida M and Horinouchi S (2002) FK228 (depsipeptide) as a natural prodrug that inhibits class I histone deacetylases. *Cancer Res*. 62:4916-21

Galm O, Herman JG and Baylin SB (2006) The fundamental role of epigenetics in hematopoietic malignancies. *Blood Rev*. 20:1-13

Gangwani L, Flavell RA and Davis RJ (2005) ZPR1 is essential for survival and is required for localization of the survival motor neurons (SMN) protein to Cajal bodies. *Mol Cell Biol*. 25:2744-56

Gangwani L, Mikrut M, Theroux S, Sharma M and Davis RJ (2001) Spinal muscular atrophy disrupts the interaction of ZPR1 with the SMN protein. *Nat Cell Biol*. 3:376-83

Gao L, Cueto MA, Asselbergs F and Atadja P (2002) Cloning and functional characterization of HDAC11, a novel member of the human histone deacetylase family. *J Biol Chem*. 277:25748-55

Gavrilov DK, Shi X, Das K, Gilliam TC and Wang CH (1998) Differential SMN2 expression associated with SMA severity. *Nat Genet*. 20:230-1

Gennarelli M, Lucarelli M, Capon F, Pizzuti A, Merlini L, Angelini C, Novelli G and Dallapiccola B (1995) Survival motor neuron gene transcript analysis in muscles from spinal muscular atrophy patients. *Biochem Biophys Res Commun*. 213:342-8

Giesemann T, Rathke-Hartlieb S, Rothkegel M, Bartsch JW, Buchmeier S, Jockusch BM and Jockusch H (1999) A role for polyproline motifs in the spinal muscular atrophy protein SMN. Profilins bind to and colocalize with smn in nuclear gems. *J Biol Chem*. 274:37908-14

Gilbert J, Baker SD, Bowling MK, Grochow L, Figg WD, Zabelina Y, Donehower RC and Carducci MA (2001) A phase I dose escalation and bioavailability study of oral sodium phenylbutyrate in patients with refractory solid tumor malignancies. *Clin Cancer Res*. 7:2292-300

Gilliam TC, Brzustowicz LM, Castilla LH, Lehner T, Penchaszadeh GK, Daniels RJ, Byth BC, Knowles J, Hislop JE, Shapira Y and et al. (1990) Genetic homogeneity between acute and chronic forms of spinal muscular atrophy. *Nature*. 345:823-5

Glaser KB, Staver MJ, Waring JF, Stender J, Ulrich RG and Davidsen SK (2003) Gene expression profiling of multiple histone deacetylase (HDAC) inhibitors: defining a common gene set produced by HDAC inhibition in T24 and MDA carcinoma cell lines. *Mol Cancer Ther*. 2:151-63

Goncalves J, Malta-Vacas J, Louis M, Brault L, Bagrel D, Monteiro C and Brito M (2005) Modulation of translation factor's gene expression by histone deacetylase inhibitors in breast cancer cells. *Clin Chem Lab Med*. 43:151-6

Gottlicher M, Minucci S, Zhu P, Kramer OH, Schimpf A, Giavara S, Sleeman JP, Lo Coco F, Nervi C, Pelicci PG and Heinzel T (2001) Valproic acid defines a novel class of HDAC inhibitors inducing differentiation of transformed cells. *Embo J*. 20:6969-78

Grant PA (2001) A tale of histone modifications. *Genome Biol*. 2:REVIEWS0003

Gray SG and Ekstrom TJ (2001) The human histone deacetylase family. *Exp Cell Res*. 262:75-83

Greger V, Debus N, Lohmann D, Hopping W, Passarge E and Horsthemke B (1994) Frequency and parental origin of hypermethylated RB1 alleles in retinoblastoma. *Hum Genet*. 94:491-6

Greger V, Passarge E, Hopping W, Messmer E and Horsthemke B (1989) Epigenetic changes may contribute to the formation and spontaneous regression of retinoblastoma. *Hum Genet*. 83:155-8

Gregoretti IV, Lee YM and Goodson HV (2004) Molecular evolution of the histone deacetylase family: functional implications of phylogenetic analysis. *J Mol Biol*. 338:17-31

Grimmler M, Bauer L, Nousiainen M, Korner R, Meister G and Fischer U (2005a) Phosphorylation regulates the activity of the SMN complex during assembly of spliceosomal U snRNPs. *EMBO Rep*. 6:70-6

Grimmler M, Otter S, Peter C, Muller F, Chari A and Fischer U (2005b) Unrip, a factor implicated in cap-independent translation, associates with the cytosolic SMN complex and influences its intracellular localization. *Hum Mol Genet*. 14:3099-111

Gronroos E, Hellman U, Heldin CH and Ericsson J (2002) Control of Smad7 stability by competition between acetylation and ubiquitination. *Mol Cell*. 10:483-93

Grzeschik SM, Ganta M, Prior TW, Heavlin WD and Wang CH (2005) Hydroxyurea enhances SMN2 gene expression in spinal muscular atrophy cells. *Ann Neurol*. 58:194-202

Gu W and Roeder RG (1997) Activation of p53 sequence-specific DNA binding by acetylation of the p53 C-terminal domain. *Cell*. 90:595-606

Gubitz AK, Mourelatos Z, Abel L, Rappsilber J, Mann M and Dreyfuss G (2002) Gemin5, a novel WD repeat protein component of the SMN complex that binds Sm proteins. *J Biol Chem*. 277:5631-6

Haastert K, Grosskreutz J, Jaeckel M, Laderer C, Bufler J, Grothe C and Claus P (2005) Rat embryonic motoneurons in long-term co-culture with Schwann cells-a system to investigate motoneuron diseases on a cellular level in vitro. *J Neurosci Methods*. 142:275-84

Haddad H, Cifuentes-Diaz C, Miroglio A, Roblot N, Joshi V and Melki J (2003) Riluzole attenuates spinal muscular atrophy disease progression in a mouse model. *Muscle Nerve*. 28:432-7

Hahnen E, Eyupoglu IY, Brichta L, Haastert K, Trankle C, Siebzehnrubl FA, Riessland M, Hölker I, Claus P, Romstock J, Buslei R, Wirth B and Blümcke I (2006) In vitro and ex vivo evaluation of second-generation histone deacetylase inhibitors for the treament of spinal muscular atrophy. *J Neurochem.* May 2006 [Epub ahead of print]

Hahnen E, Forkert R, Marke C, Rudnik-Schoneborn S, Schonling J, Zerres K and Wirth B (1995) Molecular analysis of candidate genes on chromosome 5q13 in autosomal recessive spinal muscular atrophy: evidence of homozygous deletions of the SMN gene in unaffected individuals. *Hum Mol Genet*. 4:1927-33

Hahnen E, Schonling J, Rudnik-Schoneborn S, Raschke H, Zerres K and Wirth B (1997) Missense mutations in exon 6 of the survival motor neuron gene in patients with spinal muscular atrophy (SMA). *Hum Mol Genet*. 6:821-5

Hahnen E, Schonling J, Rudnik-Schoneborn S, Zerres K and Wirth B (1996) Hybrid survival motor neuron genes in patients with autosomal recessive spinal muscular atrophy: new insights into molecular mechanisms responsible for the disease. *Am J Hum Genet*. 59:1057-65

Harper JM, Krishnan C, Darman JS, Deshpande DM, Peck S, Shats I, Backovic S, Rothstein JD and Kerr DA (2004) Axonal growth of embryonic stem cell-derived motoneurons in vitro and in motoneuron-injured adult rats. *Proc Natl Acad Sci U S A*. 101:7123-8

Hasan S, Stucki M, Hassa PO, Imhof R, Gehrig P, Hunziker P, Hubscher U and Hottiger MO (2001) Regulation of human flap endonuclease-1 activity by acetylation through the transcriptional coactivator p300. *Mol Cell*. 7:1221-31

Hassig CA, Fleischer TC, Billin AN, Schreiber SL and Ayer DE (1997) Histone deacetylase activity is required for full transcriptional repression by mSin3A. *Cell*. 89:341-7

Hauke J (2006) Analyse der epigenetischen Regulation des survival motor neuron gens 2. *University of Cologne, Cologne, Diplomarbeit*.

Hebert MD, Szymczyk PW, Shpargel KB and Matera AG (2001) Coilin forms the bridge between Cajal bodies and SMN, the spinal muscular atrophy protein. *Genes Dev*. 15:2720-9

Heinzel T, Lavinsky RM, Mullen TM, Soderstrom M, Laherty CD, Torchia J, Yang WM, Brard G, Ngo SD, Davie JR, Seto E, Eisenman RN, Rose DW, Glass CK and Rosenfeld MG (1997) A complex containing N-CoR, mSin3 and histone deacetylase mediates transcriptional repression. *Nature*. 387:43-8

Helmken C, Hofmann Y, Schoenen F, Oprea G, Raschke H, Rudnik-Schoneborn S, Zerres K and Wirth B (2003) Evidence for a modifying pathway in SMA discordant families: reduced SMN level decreases the amount of its interacting partners and Htra2-beta1. *Hum Genet*. 114:11-21

Hockly E, Richon VM, Woodman B, Smith DL, Zhou X, Rosa E, Sathasivam K, Ghazi-Noori S, Mahal A, Lowden PA, Steffan JS, Marsh JL, Thompson LM, Lewis CM, Marks PA and Bates GP (2003) Suberoylanilide hydroxamic acid, a histone deacetylase inhibitor, ameliorates motor deficits in a mouse model of Huntington's disease. *Proc Natl Acad Sci U S A*. 100:2041-6

Hoffmann J (1893) Dritter Beitrag zur Lehre von der hereditären progressiven spinalen Muskelatrophie im Kindesalter. *Dtsch Z Nervenheilk*. 18:217-222.

Hofmann Y, Lorson CL, Stamm S, Androphy EJ and Wirth B (2000) Htra2-beta 1 stimulates an exonic splicing enhancer and can restore full-length SMN expression to survival motor neuron 2 (SMN2). *Proc Natl Acad Sci U S A*. 97:9618-23

Hofmann Y and Wirth B (2002) hnRNP-G promotes exon 7 inclusion of survival motor neuron (SMN) via direct interaction with Htra2-beta1. *Hum Mol Genet*. 11:2037-49

Hsieh-Li HM, Chang JG, Jong YJ, Wu MH, Wang NM, Tsai CH and Li H (2000) A mouse model for spinal muscular atrophy. *Nat Genet*. 24:66-70

Hu E, Dul E, Sung CM, Chen Z, Kirkpatrick R, Zhang GF, Johanson K, Liu R, Lago A, Hofmann G, Macarron R, de los Frailes M, Perez P, Krawiec J, Winkler J and Jaye M (2003) Identification of novel isoform-selective inhibitors within class I histone deacetylases. *J Pharmacol Exp Ther*. 307:720-8

Hua Y and Zhou J (2004a) Rpp20 interacts with SMN and is re-distributed into SMN granules in response to stress. *Biochem Biophys Res Commun*. 314:268-76

Hua Y and Zhou J (2004b) Survival motor neuron protein facilitates assembly of stress granules. *FEBS Lett*. 572:69-74

Huang L, Sowa Y, Sakai T and Pardee AB (2000) Activation of the p21WAF1/CIP1 promoter independent of p53 by the histone deacetylase inhibitor suberoylanilide hydroxamic acid (SAHA) through the Sp1 sites. *Oncogene*. 19:5712-9

Hubbert C, Guardiola A, Shao R, Kawaguchi Y, Ito A, Nixon A, Yoshida M, Wang XF and Yao TP (2002) HDAC6 is a microtubule-associated deacetylase. *Nature*. 417:455-8

Isoherranen N, Yagen B and Bialer M (2003) New CNS-active drugs which are second-generation valproic acid: can they lead to the development of a magic bullet? *Curr Opin Neurol*. 16:203-11

Iwahashi H, Eguchi Y, Yasuhara N, Hanafusa T, Matsuzawa Y and Tsujimoto Y (1997) Synergistic anti-apoptotic activity between Bcl-2 and SMN implicated in spinal muscular atrophy. *Nature*. 390:413-7

Jablonka S, Schrank B, Kralewski M, Rossoll W and Sendtner M (2000) Reduced survival motor neuron (Smn) gene dose in mice leads to motor neuron degeneration: an animal model for spinal muscular atrophy type III. *Hum Mol Genet*. 9:341-6

Jarecki J, Chen X, Bernardino A, Coovert DD, Whitney M, Burghes A, Stack J and Pollok BA (2005) Diverse small-molecule modulators of SMN expression found by high-throughput compound screening: early leads towards a therapeutic for spinal muscular atrophy. *Hum Mol Genet*. 14:2003-18

Jenuwein T and Allis CD (2001) Translating the histone code. *Science*. 293:1074-80

Johannessen CU (2000) Mechanisms of action of valproate: a commentatory. *Neurochem Int*. 37:103-10

Johannessen CU and Johannessen SI (2003) Valproate: past, present, and future. *CNS Drug Rev*. 9:199-216

Jones DO, Cowell IG and Singh PB (2000) Mammalian chromodomain proteins: their role in genome organisation and expression. *Bioessays*. 22:124-37

Jones KW, Gorzynski K, Hales CM, Fischer U, Badbanchi F, Terns RM and Terns MP (2001) Direct interaction of the spinal muscular atrophy disease protein SMN with the small nucleolar RNA-associated protein fibrillarin. *J Biol Chem*. 276:38645-51

Jones PL, Veenstra GJ, Wade PA, Vermaak D, Kass SU, Landsberger N, Strouboulis J and Wolffe AP (1998) Methylated DNA and MeCP2 recruit histone deacetylase to repress transcription. *Nat Genet*. 19:187-91

Jumaa H and Nielsen PJ (1997) The splicing factor SRp20 modifies splicing of its own mRNA and ASF/SF2 antagonizes this regulation. *Embo J*. 16:5077-85

Jung M, Brosch G, Kolle D, Scherf H, Gerhauser C and Loidl P (1999) Amide analogues of trichostatin A as inhibitors of histone deacetylase and inducers of terminal cell differentiation. *J Med Chem*. 42:4669-79

Jurica MS and Moore MJ (2003) Pre-mRNA splicing: awash in a sea of proteins. *Mol Cell*. 12:5-14

Kandasamy K, Joseph K, Subramaniam K, Raymond JR and Tholanikunnel BG (2005) Translational control of beta2-adrenergic receptor mRNA by T-cell-restricted intracellular antigen-related protein. *J Biol Chem*. 280:1931-43

Kashima T and Manley JL (2003) A negative element in SMN2 exon 7 inhibits splicing in spinal muscular atrophy. *Nat Genet*. 34:460-3

Kedersha NL, Gupta M, Li W, Miller I and Anderson P (1999) RNA-binding proteins TIA-1 and TIAR link the phosphorylation of eIF-2 alpha to the assembly of mammalian stress granules. *J Cell Biol*. 147:1431-42

Kelly WK, Richon VM, O'Connor O, Curley T, MacGregor-Curtelli B, Tong W, Klang M, Schwartz L, Richardson S, Rosa E, Drobnjak M, Cordon-Cordo C, Chiao JH, Rifkind R, Marks PA and Scher H (2003) Phase I clinical trial of histone deacetylase inhibitor: suberoylanilide hydroxamic acid administered intravenously. *Clin Cancer Res*. 9:3578-88

Kelter AR, Herchenbach J and Wirth B (2000) The transcription factor-like nuclear regulator (TFNR) contains a novel 55-amino-acid motif repeated nine times and maps closely to SMN1. *Genomics*. 70:315-26

Kernochan LE, Russo ML, Woodling NS, Huynh TN, Avila AM, Fischbeck KH and Sumner CJ (2005) The role of histone acetylation in SMN gene expression. *Hum Mol Genet*.
Kerr DA, Nery JP, Traystman RJ, Chau BN and Hardwick JM (2000) Survival motor neuron protein modulates neuron-specific apoptosis. *Proc Natl Acad Sci U S A*. 97:13312-7

Khochbin S, Verdel A, Lemercier C and Seigneurin-Berny D (2001) Functional significance of histone deacetylase diversity. *Curr Opin Genet Dev*. 11:162-6

Kijima M, Yoshida M, Sugita K, Horinouchi S and Beppu T (1993) Trapoxin, an antitumor cyclic tetrapeptide, is an irreversible inhibitor of mammalian histone deacetylase. *J Biol Chem*. 268:22429-35

Kolb SJ, Gubitz AK, Olszewski RF, Jr., Ottinger E, Sumner CJ, Fischbeck KH and Dreyfuss G (2006) A novel cell immunoassay to measure survival of motor neurons protein in blood cells. *BMC Neurol.* 6:6

Kornberg RD (1974) Chromatin structure: a repeating unit of histones and DNA. *Science.* 184:868-71

Kouzarides T (2000) Acetylation: a regulatory modification to rival phosphorylation? *Embo J.* 19:1176-9

Kramer OH, Zhu P, Ostendorff HP, Golebiewski M, Tiefenbach J, Peters MA, Brill B, Groner B, Bach I, Heinzel T and Gottlicher M (2003) The histone deacetylase inhibitor valproic acid selectively induces proteasomal degradation of HDAC2. *Embo J.* 22:3411-20

Krauer KG, Buck M, Belzer DK, Flanagan J, Chojnowski GM and Sculley TB (2004) The Epstein-Barr virus nuclear antigen-6 protein co-localizes with EBNA-3 and survival of motor neurons protein. *Virology.* 318:280-94

Kruh J (1982) Effects of sodium butyrate, a new pharmacological agent, on cells in culture. *Mol Cell Biochem.* 42:65-82

Kurihara N, Menaa C, Maeda H, Haile DJ and Reddy SV (2001) Osteoclast-stimulating factor interacts with the spinal muscular atrophy gene product to stimulate osteoclast formation. *J Biol Chem.* 276:41035-9

La Bella V, Cisterni C, Salaun D and Pettmann B (1998) Survival motor neuron (SMN) protein in rat is expressed as different molecular forms and is developmentally regulated. *Eur J Neurosci.* 10:2913-23

Laemmli UK (1970) Cleavage of structural proteins during the assembly of the head of bacteriophage T4. *Nature.* 227:680-5

Laherty CD, Yang WM, Sun JM, Davie JR, Seto E and Eisenman RN (1997) Histone deacetylases associated with the mSin3 corepressor mediate mad transcriptional repression. *Cell.* 89:349-56

Laird PW and Jaenisch R (1994) DNA methylation and cancer. *Hum Mol Genet.* 3 Spec No:1487-95

Le TT, Pham LT, Butchbach ME, Zhang HL, Monani UR, Coovert DD, Gavrilina TO, Xing L, Bassell GJ and Burghes AH (2005) SMNDelta7, the major product of the centromeric survival motor neuron (SMN2) gene, extends survival in mice with spinal muscular atrophy and associates with full-length SMN. *Hum Mol Genet.* 14:845-57

Leder A and Leder P (1975) Butyric acid, a potent inducer of erythroid differentiation in cultured erythroleukemic cells. *Cell.* 5:319-22

Lefebvre S, Burglen L, Reboullet S, Clermont O, Burlet P, Viollet L, Benichou B, Cruaud C, Millasseau P, Zeviani M and et al. (1995) Identification and characterization of a spinal muscular atrophy-determining gene. *Cell*. 80:155-65

Lefebvre S, Burlet P, Liu Q, Bertrandy S, Clermont O, Munnich A, Dreyfuss G and Melki J (1997) Correlation between severity and SMN protein level in spinal muscular atrophy. *Nat Genet*. 16:265-9

Lefebvre S, Burlet P, Viollet L, Bertrandy S, Huber C, Belser C and Munnich A (2002) A novel association of the SMN protein with two major non-ribosomal nucleolar proteins and its implication in spinal muscular atrophy. *Hum Mol Genet*. 11:1017-27

Lesbordes JC, Cifuentes-Diaz C, Miroglio A, Joshi V, Bordet T, Kahn A and Melki J (2003) Therapeutic benefits of cardiotrophin-1 gene transfer in a mouse model of spinal muscular atrophy. *Hum Mol Genet*. 12:1233-9

Lim SR and Hertel KJ (2001) Modulation of survival motor neuron pre-mRNA splicing by inhibition of alternative 3' splice site pairing. *J Biol Chem*. 276:45476-83

Lindhout D and Omtzigt JG (1992) Pregnancy and the risk of teratogenicity. *Epilepsia*. 33 Suppl 4:S41-8

Liu Q and Dreyfuss G (1996) A novel nuclear structure containing the survival of motor neurons protein. *Embo J*. 15:3555-65

Liu Q, Fischer U, Wang F and Dreyfuss G (1997) The spinal muscular atrophy disease gene product, SMN, and its associated protein SIP1 are in a complex with spliceosomal snRNP proteins. *Cell*. 90:1013-21

Lorson CL and Androphy EJ (1998) The domain encoded by exon 2 of the survival motor neuron protein mediates nucleic acid binding. *Hum Mol Genet*. 7:1269-75

Lorson CL and Androphy EJ (2000) An exonic enhancer is required for inclusion of an essential exon in the SMA-determining gene SMN. *Hum Mol Genet*. 9:259-65

Lorson CL, Hahnen E, Androphy EJ and Wirth B (1999) A single nucleotide in the SMN gene regulates splicing and is responsible for spinal muscular atrophy. *Proc Natl Acad Sci U S A*. 96:6307-11

Lorson CL, Strasswimmer J, Yao JM, Baleja JD, Hahnen E, Wirth B, Le T, Burghes AH and Androphy EJ (1998) SMN oligomerization defect correlates with spinal muscular atrophy severity. *Nat Genet*. 19:63-6

Loscher W and Esenwein H (1978) Pharmacokinetics of sodium valproate in dog and mouse. *Arzneimittelforschung*. 28:782-7

Loseke S, Grage-Griebenow E, Wagner A, Gehlhar K and Bufe A (2003) Differential expression of IFN-alpha subtypes in human PBMC: evaluation of novel real-time PCR assays. *J Immunol Methods*. 276:207-22

Luger K, Mader AW, Richmond RK, Sargent DF and Richmond TJ (1997) Crystal structure of the nucleosome core particle at 2.8 A resolution. *Nature*. 389:251-60

Lunn MR, Root DE, Martino AM, Flaherty SP, Kelley BP, Coovert DD, Burghes AH, Man NT, Morris GE, Zhou J, Androphy EJ, Sumner CJ and Stockwell BR (2004) Indoprofen upregulates the survival motor neuron protein through a cyclooxygenase-independent mechanism. *Chem Biol*. 11:1489-93

Mailman MD, Heinz JW, Papp AC, Snyder PJ, Sedra MS, Wirth B, Burghes AH and Prior TW (2002) Molecular analysis of spinal muscular atrophy and modification of the phenotype by SMN2. *Genet Med*. 4:20-6

Marin-Vinader L, Shin C, Onnekink C, Manley JL and Lubsen NH (2006) Hsp27 enhances recovery of splicing as well as rephosphorylation of SRp38 after heat shock. *Mol Biol Cell*. 17:886-94

Marks P, Rifkind RA, Richon VM, Breslow R, Miller T and Kelly WK (2001) Histone deacetylases and cancer: causes and therapies. *Nat Rev Cancer*. 1:194-202

Marks PA, Miller T and Richon VM (2003) Histone deacetylases. *Curr Opin Pharmacol*. 3:344-51

Marks PA, Richon VM, Miller T and Kelly WK (2004) Histone deacetylase inhibitors. *Adv Cancer Res*. 91:137-68

Marmorstein R (2004) Structural and chemical basis of histone acetylation. *Novartis Found Symp*. 259:78-98; discussion 98-101, 163-9

Matsuyama A, Shimazu T, Sumida Y, Saito A, Yoshimatsu Y, Seigneurin-Berny D, Osada H, Komatsu Y, Nishino N, Khochbin S, Horinouchi S and Yoshida M (2002) In vivo destabilization of dynamic microtubules by HDAC6-mediated deacetylation. *Embo J*. 21:6820-31

McCabe PH (2000) New anti-epileptic drugs for the 21st century. *Expert Opin Pharmacother*. 1:633-74

McCaffrey PG, Newsome DA, Fibach E, Yoshida M and Su MS (1997) Induction of gamma-globin by histone deacetylase inhibitors. *Blood*. 90:2075-83

McWhorter ML, Monani UR, Burghes AH and Beattie CE (2003) Knockdown of the survival motor neuron (Smn) protein in zebrafish causes defects in motor axon outgrowth and pathfinding. *J Cell Biol.* 162:919-31

Meinke PT and Liberator P (2001) Histone deacetylase: a target for antiproliferative and antiprotozoal agents. *Curr Med Chem.* 8:211-35

Meister G, Buhler D, Laggerbauer B, Zobawa M, Lottspeich F and Fischer U (2000) Characterization of a nuclear 20S complex containing the survival of motor neurons (SMN) protein and a specific subset of spliceosomal Sm proteins. *Hum Mol Genet.* 9:1977-86

Meister G, Buhler D, Pillai R, Lottspeich F and Fischer U (2001) A multiprotein complex mediates the ATP-dependent assembly of spliceosomal U snRNPs. *Nat Cell Biol.* 3:945-9

Meister G and Fischer U (2002) Assisted RNP assembly: SMN and PRMT5 complexes cooperate in the formation of spliceosomal UsnRNPs. *Embo J.* 21:5853-63

Melki J, Abdelhak S, Sheth P, Bachelot MF, Burlet P, Marcadet A, Aicardi J, Barois A, Carriere JP, Fardeau M and et al. (1990) Gene for chronic proximal spinal muscular atrophies maps to chromosome 5q. *Nature.* 344:767-8

Melki J, Burlet P, Clermont O, Pascal F, Paul B, Abdelhak S, Sherrington R, Gurling H, Nakamura Y, Weissenbach J and et al. (1993) Refined linkage map of chromosome 5 in the region of the spinal muscular atrophy gene. *Genomics.* 15:521-4

Melki J, Lefebvre S, Burglen L, Burlet P, Clermont O, Millasseau P, Reboullet S, Benichou B, Zeviani M, Le Paslier D and et al. (1994) De novo and inherited deletions of the 5q13 region in spinal muscular atrophies. *Science.* 264:1474-7

Merlini L, Solari A, Vita G, Bertini E, Minetti C, Mongini T, Mazzoni E, Angelini C and Morandi L (2003) Role of gabapentin in spinal muscular atrophy: results of a multicenter, randomized Italian study. *J Child Neurol.* 18:537-41

Meshorer E, Bryk B, Toiber D, Cohen J, Podoly E, Dori A and Soreq H (2005) SC35 promotes sustainable stress-induced alternative splicing of neuronal acetylcholinesterase mRNA. *Mol Psychiatry.* 10:985-97

Meyappan JD, Lampl M and Hsu LL (2005) Parents' assessment of risk in sickle cell disease treatment with hydroxyurea. *J Pediatr Hematol Oncol.* 27:644-50

Michishita E, Park JY, Burneskis JM, Barrett JC and Horikawa I (2005) Evolutionarily conserved and nonconserved cellular localizations and functions of human SIRT proteins. *Mol Biol Cell.* 16:4623-35

Miguel-Aliaga I, Culetto E, Walker DS, Baylis HA, Sattelle DB and Davies KE (1999) The Caenorhabditis elegans orthologue of the human gene responsible for spinal muscular atrophy is a maternal product critical for germline maturation and embryonic viability. *Hum Mol Genet*. 8:2133-43

Miller AA, Kurschel E, Osieka R and Schmidt CG (1987) Clinical pharmacology of sodium butyrate in patients with acute leukemia. *Eur J Cancer Clin Oncol*. 23:1283-7

Miller RG, Moore DH, Dronsky V, Bradley W, Barohn R, Bryan W, Prior TW, Gelinas DF, Iannaccone S, Kissel J, Leshner R, Mendell J, Mendoza M, Russman B, Samaha F and Smith S (2001) A placebo-controlled trial of gabapentin in spinal muscular atrophy. *J Neurol Sci*. 191:127-31

Miller S, Dykes D and Polesky H (1988) A simple salting out procedure for extracting DNA from human nucleated cells. *Nucl. Acid. Res.* 1216:1215

Miller TA, Witter DJ and Belvedere S (2003) Histone deacetylase inhibitors. *J Med Chem*. 46:5097-116

Minamiyama Y, Takemura S, Nishino Y and Okada S (2002) Organic nitrate tolerance is induced by degradation of some cytochrome P450 isoforms. *Redox Rep*. 7:339-42

Misteli T, Caceres JF and Spector DL (1997) The dynamics of a pre-mRNA splicing factor in living cells. *Nature*. 387:523-7

Miyajima H, Miyaso H, Okumura M, Kurisu J and Imaizumi K (2002) Identification of a cis-acting element for the regulation of SMN exon 7 splicing. *J Biol Chem*. 277:23271-7

Miyaso H, Okumura M, Kondo S, Higashide S, Miyajima H and Imaizumi K (2003) An intronic splicing enhancer element in SMN Pre-mRNA. *J Biol Chem*.
Mohaghegh P, Rodrigues NR, Owen N, Ponting CP, Le TT, Burghes AH and Davies KE (1999) Analysis of mutations in the tudor domain of the survival motor neuron protein SMN. *Eur J Hum Genet*. 7:519-25

Monani UR, Lorson CL, Parsons DW, Prior TW, Androphy EJ, Burghes AH and McPherson JD (1999a) A single nucleotide difference that alters splicing patterns distinguishes the SMA gene SMN1 from the copy gene SMN2. *Hum Mol Genet*. 8:1177-83

Monani UR, McPherson JD and Burghes AH (1999b) Promoter analysis of the human centromeric and telomeric survival motor neuron genes (SMNC and SMNT). *Biochim Biophys Acta*. 1445:330-6

Monani UR, Pastore MT, Gavrilina TO, Jablonka S, Le TT, Andreassi C, DiCocco JM, Lorson C, Androphy EJ, Sendtner M, Podell M and Burghes AH (2003) A transgene carrying an A2G missense

mutation in the SMN gene modulates phenotypic severity in mice with severe (type I) spinal muscular atrophy. *J Cell Biol*. 160:41-52

Monani UR, Sendtner M, Coovert DD, Parsons DW, Andreassi C, Le TT, Jablonka S, Schrank B, Rossol W, Prior TW, Morris GE and Burghes AH (2000) The human centromeric survival motor neuron gene (SMN2) rescues embryonic lethality in Smn(-/-) mice and results in a mouse with spinal muscular atrophy. *Hum Mol Genet*. 9:333-9

Mosmann T (1983) Rapid colorimetric assay for cellular growth and survival: application to proliferation and cytotoxicity assays. *J Immunol Methods*. 65:55-63

Mouaikel J, Narayanan U, Verheggen C, Matera AG, Bertrand E, Tazi J and Bordonne R (2003) Interaction between the small-nuclear-RNA cap hypermethylase and the spinal muscular atrophy protein, survival of motor neuron. *EMBO Rep*. 4:616-22

Mourelatos Z, Abel L, Yong J, Kataoka N and Dreyfuss G (2001) SMN interacts with a novel family of hnRNP and spliceosomal proteins. *Embo J*. 20:5443-52

Mullis KB and Faloona FA (1987) Specific synthesis of DNA in vitro via a polymerase-catalyzed chain reaction. *Methods Enzymol*. 155:335-50

Munsat TL and Davies KE (1992) International SMA consortium meeting. (26-28 June 1992, Bonn, Germany). *Neuromuscul Disord*. 2:423-8

Nagy L, Kao HY, Chakravarti D, Lin RJ, Hassig CA, Ayer DE, Schreiber SL and Evans RM (1997) Nuclear receptor repression mediated by a complex containing SMRT, mSin3A, and histone deacetylase. *Cell*. 89:373-80

Nakajima H, Kim YB, Terano H, Yoshida M and Horinouchi S (1998) FR901228, a potent antitumor antibiotic, is a novel histone deacetylase inhibitor. *Exp Cell Res*. 241:126-33

Nakamura N and Takenaga K (1998) Hypomethylation of the metastasis-associated S100A4 gene correlates with gene activation in human colon adenocarcinoma cell lines. *Clin Exp Metastasis*. 16:471-9

Nan X, Ng HH, Johnson CA, Laherty CD, Turner BM, Eisenman RN and Bird A (1998) Transcriptional repression by the methyl-CpG-binding protein MeCP2 involves a histone deacetylase complex. *Nature*. 393:386-9

Narayanan U, Ospina JK, Frey MR, Hebert MD and Matera AG (2002) SMN, the spinal muscular atrophy protein, forms a pre-import snRNP complex with snurportin1 and importin beta. *Hum Mol Genet*. 11:1785-95

Nau H and Loscher W (1982) Valproic acid: brain and plasma levels of the drug and its metabolites, anticonvulsant effects and gamma-aminobutyric acid (GABA) metabolism in the mouse. *J Pharmacol Exp Ther*. 220:654-9

Nayler O, Cap C and Stamm S (1998) Human transformer-2-beta gene (SFRS10): complete nucleotide sequence, chromosomal localization, and generation of a tissue-specific isoform. *Genomics*. 53:191-202

Newmark HL, Lupton JR and Young CW (1994) Butyrate as a differentiating agent: pharmacokinetics, analogues and current status. *Cancer Lett*. 78:1-5

Newmark HL and Young CW (1995) Butyrate and phenylacetate as differentiating agents: practical problems and opportunities. *J Cell Biochem Suppl*. 22:247-53

Noll M and Kornberg RD (1977) Action of micrococcal nuclease on chromatin and the location of histone H1. *J Mol Biol*. 109:393-404

Nover L, Scharf KD and Neumann D (1989) Cytoplasmic heat shock granules are formed from precursor particles and are associated with a specific set of mRNAs. *Mol Cell Biol*. 9:1298-308

Ogino S and Wilson RB (2002) Genetic testing and risk assessment for spinal muscular atrophy (SMA). *Hum Genet*. 111:477-500

Ohtani-Fujita N, Fujita T, Aoike A, Osifchin NE, Robbins PD and Sakai T (1993) CpG methylation inactivates the promoter activity of the human retinoblastoma tumor-suppressor gene. *Oncogene*. 8:1063-7

Olins AL and Olins DE (1974) Spheroid chromatin units (v bodies). *Science*. 183:330-2

Oudet P, Gross-Bellard M and Chambon P (1975) Electron microscopic and biochemical evidence that chromatin structure is a repeating unit. *Cell*. 4:281-300

Pachot A, Blond JL, Mougin B and Miossec P (2004) Peptidylpropyl isomerase B (PPIB): a suitable reference gene for mRNA quantification in peripheral whole blood. *J Biotechnol*. 114:121-4

Pagliardini S, Giavazzi A, Setola V, Lizier C, Di Luca M, DeBiasi S and Battaglia G (2000) Subcellular localization and axonal transport of the survival motor neuron (SMN) protein in the developing rat spinal cord. *Hum Mol Genet*. 9:47-56

Park JW, Voss PG, Grabski S, Wang JL and Patterson RJ (2001) Association of galectin-1 and galectin-3 with Gemin4 in complexes containing the SMN protein. *Nucleic Acids Res*. 29:3595-602

Pazin MJ and Kadonaga JT (1997) What's up and down with histone deacetylation and transcription? *Cell*. 89:325-8

Pellizzoni L, Baccon J, Charroux B and Dreyfuss G (2001a) The survival of motor neurons (SMN) protein interacts with the snoRNP proteins fibrillarin and GAR1. *Curr Biol*. 11:1079-88

Pellizzoni L, Baccon J, Rappsilber J, Mann M and Dreyfuss G (2001b) Purification of native SMN complexes and identification of Gemin6 as a novel component. *J Biol Chem*. 277:7540-5

Pellizzoni L, Charroux B, Rappsilber J, Mann M and Dreyfuss G (2001c) A functional interaction between the survival motor neuron complex and RNA polymerase II. *J Cell Biol*. 152:75-85

Pellizzoni L, Kataoka N, Charroux B and Dreyfuss G (1998) A novel function for SMN, the spinal muscular atrophy disease gene product, in pre-mRNA splicing. *Cell*. 95:615-24

Pellizzoni L, Yong J and Dreyfuss G (2002) Essential Role for the SMN Complex in the Specificity of snRNP Assembly. *Science*. 298:1775-9

Perrine SP, Ginder GD, Faller DV, Dover GH, Ikuta T, Witkowska HE, Cai SP, Vichinsky EP and Olivieri NF (1993) A short-term trial of butyrate to stimulate fetal-globin-gene expression in the beta-globin disorders. *N Engl J Med*. 328:81-6

Peterson CL and Laniel MA (2004) Histones and histone modifications. *Curr Biol*. 14:R546-51

Phiel CJ, Zhang F, Huang EY, Guenther MG, Lazar MA and Klein PS (2001) Histone deacetylase is a direct target of valproic acid, a potent anticonvulsant, mood stabilizer, and teratogen. *J Biol Chem*. 276:36734-41

Piecyk M, Wax S, Beck AR, Kedersha N, Gupta M, Maritim B, Chen S, Gueydan C, Kruys V, Streuli M and Anderson P (2000) TIA-1 is a translational silencer that selectively regulates the expression of TNF-alpha. *Embo J*. 19:4154-63

Pillai RS, Grimmler M, Meister G, Will CL, Luhrmann R, Fischer U and Schumperli D (2003) Unique Sm core structure of U7 snRNPs: assembly by a specialized SMN complex and the role of a new component, Lsm11, in histone RNA processing. *Genes Dev*. 17:2321-33

Prakash S, Foster BJ, Meyer M, Wozniak A, Heilbrun LK, Flaherty L, Zalupski M, Radulovic L, Valdivieso M and LoRusso PM (2001) Chronic oral administration of CI-994: a phase 1 study. *Invest New Drugs*. 19:1-11

Raclin V, Veber PS, Burglen L, Munnich A and Melki J (1997) De novo deletions in spinal muscular atrophy: implications for genetic counselling. *J Med Genet*. 34:86-7

Richards EJ and Elgin SC (2002) Epigenetic codes for heterochromatin formation and silencing: rounding up the usual suspects. *Cell*. 108:489-500

Richon VM, Emiliani S, Verdin E, Webb Y, Breslow R, Rifkind RA and Marks PA (1998) A class of hybrid polar inducers of transformed cell differentiation inhibits histone deacetylases. *Proc Natl Acad Sci U S A*. 95:3003-7

Richon VM, Webb Y, Merger R, Sheppard T, Jursic B, Ngo L, Civoli F, Breslow R, Rifkind RA and Marks PA (1996) Second generation hybrid polar compounds are potent inducers of transformed cell differentiation. *Proc Natl Acad Sci U S A*. 93:5705-8

Riddle DL (1997) C.elegans II. *Cold Spring Harbor Laboratory Press*. Cold Spring Harbor, NY

Riessland M, Brichta L, Hahnen E and Wirth B (2006) The benzamide M344, a novel histone deacetylase inhibitor, significantly increases SMN2 RNA/protein levels in spinal muscular atrophy cells. *Hum Genet*. May 2006:[Epub ahead of print]

Riggs MG, Whittaker RG, Neumann JR and Ingram VM (1977) n-Butyrate causes histone modification in HeLa and Friend erythroleukaemia cells. *Nature*. 268:462-4

Rochette CF, Gilbert N and Simard LR (2001) SMN gene duplication and the emergence of the SMN2 gene occurred in distinct hominids: SMN2 is unique to Homo sapiens. *Hum Genet*. 108:255-66

Rodenhiser D and Mann M (2006) Epigenetics and human disease: translating basic biology into clinical applications. *Cmaj*. 174:341-8

Rodrigues NR, Owen N, Talbot K, Ignatius J, Dubowitz V and Davies KE (1995) Deletions in the survival motor neuron gene on 5q13 in autosomal recessive spinal muscular atrophy. *Hum Mol Genet*. 4:631-4

Rossoll W, Jablonka S, Andreassi C, Kroning AK, Karle K, Monani UR and Sendtner M (2003) Smn, the spinal muscular atrophy-determining gene product, modulates axon growth and localization of beta-actin mRNA in growth cones of motoneurons. *J Cell Biol*. 163:801-12

Rossoll W, Kroning AK, Ohndorf UM, Steegborn C, Jablonka S and Sendtner M (2002) Specific interaction of Smn, the spinal muscular atrophy determining gene product, with hnRNP-R and gry-rbp/hnRNP-Q: a role for Smn in RNA processing in motor axons? *Hum Mol Genet*. 11:93-105

Roth SY, Denu JM and Allis CD (2001) Histone acetyltransferases. *Annu Rev Biochem*. 70:81-120

Rothe F, Gueydan C, Bellefroid E, Huez G and Kruys V (2006) Identification of FUSE-binding proteins as interacting partners of TIA proteins. *Biochem Biophys Res Commun*. 343:57-68

Roy N, Mahadevan MS, McLean M, Shutler G, Yaraghi Z, Farahani R, Baird S, Besner-Johnston A, Lefebvre C, Kang X and et al. (1995a) The gene for neuronal apoptosis inhibitory protein is partially deleted in individuals with spinal muscular atrophy. *Cell*. 80:167-78

Roy N, McLean MD, Besner-Johnston A, Lefebvre C, Salih M, Carpten JD, Burghes AH, Yaraghi Z, Ikeda JE, Korneluk RG and et al. (1995b) Refined physical map of the spinal muscular atrophy gene (SMA) region at 5q13 based on YAC and cosmid contiguous arrays. *Genomics*. 26:451-60

Rudnik-Schöneborn S, Rohrig D, Morgan G, Wirth B and Zerres K (1994) Autosomal recessive proximal spinal muscular atrophy in 101 sibs out of 48 families: clinical picture, influence of gender, and genetic implications. *Am J Med Genet*. 51:70-6

Russman BS, Iannaccone ST and Samaha FJ (2003) A phase 1 trial of riluzole in spinal muscular atrophy. *Arch Neurol*. 60:1601-3

Ryan QC, Headlee D, Acharya M, Sparreboom A, Trepel JB, Ye J, Figg WD, Hwang K, Chung EJ, Murgo A, Melillo G, Elsayed Y, Monga M, Kalnitskiy M, Zwiebel J and Sausville EA (2005) Phase I and pharmacokinetic study of MS-275, a histone deacetylase inhibitor, in patients with advanced and refractory solid tumors or lymphoma. *J Clin Oncol*. 23:3912-22

Saito A, Yamashita T, Mariko Y, Nosaka Y, Tsuchiya K, Ando T, Suzuki T, Tsuruo T and Nakanishi O (1999) A synthetic inhibitor of histone deacetylase, MS-27-275, with marked in vivo antitumor activity against human tumors. *Proc Natl Acad Sci U S A*. 96:4592-7

Sakai T, Toguchida J, Ohtani N, Yandell DW, Rapaport JM and Dryja TP (1991) Allele-specific hypermethylation of the retinoblastoma tumor-suppressor gene. *Am J Hum Genet*. 48:880-8

Sandman K, Pereira SL and Reeve JN (1998) Diversity of prokaryotic chromosomal proteins and the origin of the nucleosome. *Cell Mol Life Sci*. 54:1350-64

Sands SA, Guerra V and Morilak DA (2000) Changes in tyrosine hydroxylase mRNA expression in the rat locus coeruleus following acute or chronic treatment with valproic acid. *Neuropsychopharmacology*. 22:27-35

Sanger F, Nicklen S and Coulson AR (1977) DNA sequencing with chain-terminating inhibitors. *Proc Natl Acad Sci U S A*. 74:5463-7

Savaskan NE, Eyupoglu IY, Brauer AU, Plaschke M, Ninnemann O, Nitsch R and Skutella T (2000) Entorhinal cortex lesion studied with the novel dye fluoro-jade. *Brain Res*. 864:44-51

Scharf JM, Endrizzi MG, Wetter A, Huang S, Thompson TG, Zerres K, Dietrich WF, Wirth B and Kunkel LM (1998) Identification of a candidate modifying gene for spinal muscular atrophy by comparative genomics. *Nat Genet*. 20:83-6

Scheffer H, Cobben JM, Matthijs G and Wirth B (2001) Best practice guidelines for molecular analysis in spinal muscular atrophy. *Eur J Hum Genet*. 9:484-91

Schmutz J, Martin J, Terry A, Couronne O, Grimwood J, Lowry S, Gordon LA, Scott D, Xie G, Huang W, Hellsten U, Tran-Gyamfi M, She X, Prabhakar S, Aerts A, Altherr M, Bajorek E, Black S, Branscomb E, Caoile C, Challacombe JF, Chan YM, Denys M, Detter JC, Escobar J, Flowers D, Fotopulos D, Glavina T, Gomez M, Gonzales E, Goodstein D, Grigoriev I, Groza M, Hammon N, Hawkins T, Haydu L, Israni S, Jett J, Kadner K, Kimball H, Kobayashi A, Lopez F, Lou Y, Martinez D, Medina C, Morgan J, Nandkeshwar R, Noonan JP, Pitluck S, Pollard M, Predki P, Priest J, Ramirez L, Retterer J, Rodriguez A, Rogers S, Salamov A, Salazar A, Thayer N, Tice H, Tsai M, Ustaszewska A, Vo N, Wheeler J, Wu K, Yang J, Dickson M, Cheng JF, Eichler EE, Olsen A, Pennacchio LA, Rokhsar DS, Richardson P, Lucas SM, Myers RM and Rubin EM (2004) The DNA sequence and comparative analysis of human chromosome 5. *Nature*. 431:268-74

Schrank B, Gotz R, Gunnersen JM, Ure JM, Toyka KV, Smith AG and Sendtner M (1997) Inactivation of the survival motor neuron gene, a candidate gene for human spinal muscular atrophy, leads to massive cell death in early mouse embryos. *Proc Natl Acad Sci U S A*. 94:9920-5

Sharma A, Lambrechts A, Hao le T, Le TT, Sewry CA, Ampe C, Burghes AH and Morris GE (2005) A role for complexes of survival of motor neurons (SMN) protein with gemins and profilin in neurite-like cytoplasmic extensions of cultured nerve cells. *Exp Cell Res*. 309:185-97

Shin C, Feng Y and Manley JL (2004) Dephosphorylated SRp38 acts as a splicing repressor in response to heat shock. *Nature*. 427:553-8

Shpargel KB and Matera AG (2005) Gemin proteins are required for efficient assembly of Sm-class ribonucleoproteins. *Proc Natl Acad Sci U S A*. 102:17372-7

Simard LR, Rochette C, Semionov A, Morgan K and Vanasse M (1997) SMN(T) and NAIP mutations in Canadian families with spinal muscular atrophy (SMA): genotype/phenotype correlations with disease severity. *Am J Med Genet*. 72:51-8

Singh NK, Singh NN, Androphy EJ and Singh RN (2006) Splicing of a critical exon of human survival motor neuron is regulated by a unique silencer element located in the last intron. *Mol Cell Biol*. 26:1333-46

Singh NN, Androphy EJ and Singh RN (2004a) An extended inhibitory context causes skipping of exon 7 of SMN2 in spinal muscular atrophy. *Biochem Biophys Res Commun*. 315:381-8

Singh NN, Androphy EJ and Singh RN (2004b) In vivo selection reveals combinatorial controls that define a critical exon in the spinal muscular atrophy genes. *Rna*. 10:1291-305

Skordis LA, Dunckley MG, Yue B, Eperon IC and Muntoni F (2003) Bifunctional antisense oligonucleotides provide a trans-acting splicing enhancer that stimulates SMN2 gene expression in patient fibroblasts. *Proc Natl Acad Sci U S A*. 100:4114-9

Soares VM, Brzustowicz LM, Kleyn PW, Knowles JA, Palmer DA, Asokan S, Penchaszadeh GK, Munsat TL and Gilliam TC (1993) Refinement of the spinal muscular atrophy locus to the interval between D5S435 and MAP1B. *Genomics*. 15:365-71

Soler-Botija C, Cusco I, Caselles L, Lopez E, Baiget M and Tizzano EF (2005) Implication of fetal SMN2 expression in type I SMA pathogenesis: protection or pathological gain of function? *J Neuropathol Exp Neurol*. 64:215-23

Spina E and Perugi G (2004) Antiepileptic drugs: indications other than epilepsy. *Epileptic Disord*. 6:57-75

Spotswood HT and Turner BM (2002) An increasingly complex code. *J Clin Invest*. 110:577-82

Sterner DE and Berger SL (2000) Acetylation of histones and transcription-related factors. *Microbiol Mol Biol Rev*. 64:435-59

Stoilov P, Daoud R, Nayler O and Stamm S (2004) Human tra2-beta1 autoregulates its protein concentration by influencing alternative splicing of its pre-mRNA. *Hum Mol Genet*. 13:509-24

Stoppini L, Buchs PA and Muller D (1991) A simple method for organotypic cultures of nervous tissue. *J Neurosci Methods*. 37:173-82

Strahl BD and Allis CD (2000) The language of covalent histone modifications. *Nature*. 403:41-5

Strasswimmer J, Lorson CL, Breiding DE, Chen JJ, Le T, Burghes AH and Androphy EJ (1999) Identification of survival motor neuron as a transcriptional activator-binding protein. *Hum Mol Genet*. 8:1219-26

Sumner CJ (2006) Therapeutics development for spinal muscular atrophy. *NeuroRx*. 3:235-45

Sumner CJ, Huynh TN, Markowitz JA, Perhac JS, Hill B, Coovert DD, Schussler K, Chen X, Jarecki J, Burghes AH, Taylor JP and Fischbeck KH (2003) Valproic acid increases SMN levels in spinal muscular atrophy patient cells. *Ann Neurol*. 54:647-54

Sumner CJ, Kolb SJ, Harmison GG, Jeffries NO, Schadt K, Finkel RS, Dreyfuss G and Fischbeck KH (2006) SMN mRNA and protein levels in peripheral blood: biomarkers for SMA clinical trials. *Neurology*. 66:1067-73

Sun Y, Grimmler M, Schwarzer V, Schoenen F, Fischer U and Wirth B (2005) Molecular and functional analysis of intragenic SMN1 mutations in patients with spinal muscular atrophy. *Hum Mutat*. 25:64-71

Swoboda KJ, Prior TW, Scott CB, McNaught TP, Wride MC, Reyna SP and Bromberg MB (2005) Natural history of denervation in SMA: relation to age, SMN2 copy number, and function. *Ann Neurol*. 57:704-12

Taunton J, Hassig CA and Schreiber SL (1996) A mammalian histone deacetylase related to the yeast transcriptional regulator Rpd3p. *Science*. 272:408-11

Tear G (1999) Axon guidance at the central nervous system midline. *Cell Mol Life Sci*. 55:1365-76

Terns MP and Terns RM (2001) Macromolecular complexes: SMN--the master assembler. *Curr Biol*. 11:R862-4

The-*C.elegans*-Sequencing-Consortium (1998) Genome sequence of the nematode C. elegans: a platform for investigating biology. *Science*. 282:2012-8

Thomas JO (1999) Histone H1: location and role. *Curr Opin Cell Biol*. 11:312-7

Thomas JO and Kornberg RD (1975) An octamer of histones in chromatin and free in solution. *Proc Natl Acad Sci U S A*. 72:2626-30

Thompson TG, Morrison KE, Kleyn P, Bengtsson U, Gilliam TC, Davies KE, Wasmuth JJ and McPherson JD (1993) High resolution physical map of the region surrounding the spinal muscular atrophy gene. *Hum Mol Genet*. 2:1169-76

Tini M, Benecke A, Um SJ, Torchia J, Evans RM and Chambon P (2002) Association of CBP/p300 acetylase and thymine DNA glycosylase links DNA repair and transcription. *Mol Cell*. 9:265-77

Tremolizzo L, Carboni G, Ruzicka WB, Mitchell CP, Sugaya I, Tueting P, Sharma R, Grayson DR, Costa E and Guidotti A (2002) An epigenetic mouse model for molecular and behavioral neuropathologies related to schizophrenia vulnerability. *Proc Natl Acad Sci U S A*. 99:17095-100

Tsuji A (2005) Small molecular drug transfer across the blood-brain barrier via carrier-mediated transport systems. *NeuroRx*. 2:54-62

Turner BM (2000) Histone acetylation and an epigenetic code. *Bioessays*. 22:836-45

Turner BM, Birley AJ and Lavender J (1992) Histone H4 isoforms acetylated at specific lysine residues define individual chromosomes and chromatin domains in Drosophila polytene nuclei. *Cell*. 69:375-84

Ueda H, Manda T, Matsumoto S, Mukumoto S, Nishigaki F, Kawamura I and Shimomura K (1994a) FR901228, a novel antitumor bicyclic depsipeptide produced by Chromobacterium violaceum No. 968. III. Antitumor activities on experimental tumors in mice. *J Antibiot (Tokyo)*. 47:315-23

Ueda H, Nakajima H, Hori Y, Fujita T, Nishimura M, Goto T and Okuhara M (1994b) FR901228, a novel antitumor bicyclic depsipeptide produced by Chromobacterium violaceum No. 968. I. Taxonomy, fermentation, isolation, physico-chemical and biological properties, and antitumor activity. *J Antibiot (Tokyo)*. 47:301-10

Ueda H, Nakajima H, Hori Y, Goto T and Okuhara M (1994c) Action of FR901228, a novel antitumor bicyclic depsipeptide produced by Chromobacterium violaceum no. 968, on Ha-ras transformed NIH3T3 cells. *Biosci Biotechnol Biochem*. 58:1579-83

Urnov FD, Yee J, Sachs L, Collingwood TN, Bauer A, Beug H, Shi YB and Wolffe AP (2000) Targeting of N-CoR and histone deacetylase 3 by the oncoprotein v-erbA yields a chromatin infrastructure-dependent transcriptional repression pathway. *Embo J*. 19:4074-90

van der Steege G, Grootscholten PM, Cobben JM, Zappata S, Scheffer H, den Dunnen JT, van Ommen GJ, Brahe C and Buys CH (1996) Apparent gene conversions involving the SMN gene in the region of the spinal muscular atrophy locus on chromosome 5. *Am J Hum Genet*. 59:834-8

van der Steege G, Grootscholten PM, van der Vlies P, Draaijirs TG, Osinga J, Cobben JM, Scheffer H and Buys CH (1995) PCR-based DNA test to confirm clinical diagnosis of autosomal recessive spinal muscular atrophy. *Lancet*. 345:985-986

Van Lint C, Emiliani S and Verdin E (1996) The expression of a small fraction of cellular genes is changed in response to histone hyperacetylation. *Gene Expr*. 5:245-53

Vidali G, Boffa LC, Bradbury EM and Allfrey VG (1978) Butyrate suppression of histone deacetylation leads to accumulation of multiacetylated forms of histones H3 and H4 and increased DNase I sensitivity of the associated DNA sequences. *Proc Natl Acad Sci U S A*. 75:2239-43

Viollet L, Bertrandy S, Bueno Brunialti AL, Lefebvre S, Burlet P, Clermont O, Cruaud C, Guenet JL, Munnich A and Melki J (1997) cDNA isolation, expression, and chromosomal localization of the mouse survival motor neuron gene (Smn). *Genomics*. 40:185-8

Voss MD, Hille A, Barth S, Spurk A, Hennrich F, Holzer D, Mueller-Lantzsch N, Kremmer E and Grasser FA (2001) Functional cooperation of Epstein-Barr virus nuclear antigen 2 and the survival motor neuron protein in transactivation of the viral LMP1 promoter. *J Virol*. 75:11781-90

Vousden KH (2000) p53: death star. *Cell*. 103:691-4

Wallrath LL (1998) Unfolding the mysteries of heterochromatin. *Curr Opin Genet Dev*. 8:147-53

Wan L, Battle DJ, Yong J, Gubitz AK, Kolb SJ, Wang J and Dreyfuss G (2005) The survival of motor neurons protein determines the capacity for snRNP assembly: biochemical deficiency in spinal muscular atrophy. *Mol Cell Biol*. 25:5543-51

Wang CH, Xu J, Carter TA, Ross BM, Dominski MK, Bellcross CA, Penchaszadeh GK, Munsat TL and Gilliam TC (1996) Characterization of survival motor neuron (SMNT) gene deletions in asymptomatic carriers of spinal muscular atrophy. *Hum Mol Genet*. 5:359-65

Weihl CC, Connolly AM and Pestronk A (2006) Valproate may improve strength and function in patients with type III/IV spinal muscle atrophy. *Neurology*. June 2006:[Epub ahead of print]

Weintraub H and Groudine M (1976) Chromosomal subunits in active genes have an altered conformation. *Science*. 193:848-56

Werdnig G (1891) Zwei frühinfantile hereditäre Fälle von progressiver Muskelatrophie unter dem Bilde der Dystrophie, aber auf neurotischer Grundlage. *Archiv für Psychiatrie und Nervenkrankheiten*. 22:437-480

Widom J (1998) Chromatin structure: linking structure to function with histone H1. *Curr Biol*. 8:R788-91

Wieser HG (1991) Comparison of valproate concentrations in human plasma, CSF and brain tissue after administration of different formulations of valproate or valpromide. *Epilepsy Res*. 9:154-9

Will CL and Luhrmann R (2001) Spliceosomal UsnRNP biogenesis, structure and function. *Curr Opin Cell Biol*. 13:290-301

Williams BY, Hamilton SL and Sarkar HK (2000) The survival motor neuron protein interacts with the transactivator FUSE binding protein from human fetal brain. *FEBS Lett*. 470:207-10

Winkler C, Eggert C, Gradl D, Meister G, Giegerich M, Wedlich D, Laggerbauer B and Fischer U (2005) Reduced U snRNP assembly causes motor axon degeneration in an animal model for spinal muscular atrophy. *Genes Dev*. 19:2320-30

Wirth B (2000) An update of the mutation spectrum of the survival motor neuron gene (SMN1) in autosomal recessive spinal muscular atrophy (SMA). *Hum Mutat*. 15:228-37

Wirth B, Brichta L, Schrank B, Lochmuller H, Blick S, Baasner A and Heller R (2006) Mildly affected patients with spinal muscular atrophy are partially protected by an increased SMN2 copy number. *Hum Genet*. 119:422-8

Wirth B, Herz M, Wetter A, Moskau S, Hahnen E, Rudnik-Schoneborn S, Wienker T and Zerres K (1999) Quantitative analysis of survival motor neuron copies: identification of subtle SMN1 mutations in patients with spinal muscular atrophy, genotype-phenotype correlation, and implications for genetic counseling. *Am J Hum Genet*. 64:1340-56

Wirth B, Pick E, Leutner A, Dadze A, Voosen B, Knapp M, Piechaczek-Wappenschmidt B, Rudnik-Schoneborn S, Schonling J, Cox S and et al. (1994) Large linkage analysis in 100 families with autosomal recessive spinal muscular atrophy (SMA) and 11 CEPH families using 15 polymorphic loci in the region 5q11.2-q13.3. *Genomics*. 20:84-93

Wirth B, Rudnik-Schoneborn S, Hahnen E, Rohrig D and Zerres K (1995) Prenatal prediction in families with autosomal recessive proximal spinal muscular atrophy (5q11.2-q13.3): molecular genetics and clinical experience in 109 cases. *Prenat Diagn*. 15:407-17

Wirth B, Schmidt T, Hahnen E, Rudnik-Schoneborn S, Krawczak M, Muller-Myhsok B, Schonling J and Zerres K (1997) De novo rearrangements found in 2% of index patients with spinal muscular atrophy: mutational mechanisms, parental origin, mutation rate, and implications for genetic counseling. *Am J Hum Genet*. 61:1102-11

Wlodarczyk BC, Craig JC, Bennett GD, Calvin JA and Finnell RH (1996) Valproic acid-induced changes in gene expression during neurulation in a mouse model. *Teratology*. 54:284-97

Wolstencroft EC, Mattis V, Bajer A, Young PJ and Lorson CL (2005) A non-sequence specific requirement for SMN protein activity: the role of aminoglycosides in inducing elevated SMN protein levels. *Hum Mol Genet*. 14:1199-210

Wood WB (1988) The nematode Caenorhabditis elegans. *Cold Spring Harbor Laboratory Press*. Cold Spring Harbor, NY

Wu J and Grunstein M (2000) 25 years after the nucleosome model: chromatin modifications. *Trends Biochem Sci*. 25:619-23

Yang XJ (2004) The diverse superfamily of lysine acetyltransferases and their roles in leukemia and other diseases. *Nucleic Acids Res*. 32:959-76

Yang XJ and Gregoire S (2005) Class II histone deacetylases: from sequence to function, regulation, and clinical implication. *Mol Cell Biol*. 25:2873-84

Yoshida M, Kijima M, Akita M and Beppu T (1990) Potent and specific inhibition of mammalian histone deacetylase both in vivo and in vitro by trichostatin A. *J Biol Chem*. 265:17174-9

Yoshida M, Nomura S and Beppu T (1987) Effects of trichostatins on differentiation of murine erythroleukemia cells. *Cancer Res*. 47:3688-91

Young PJ, Day PM, Zhou J, Androphy EJ, Morris GE and Lorson CL (2002a) A direct interaction between the survival motor neuron protein and p53 and its relationship to spinal muscular atrophy. *J Biol Chem*. 277:2852-9

Young PJ, DiDonato CJ, Hu D, Kothary R, Androphy EJ and Lorson CL (2002b) SRp30c-dependent stimulation of survival motor neuron (SMN) exon 7 inclusion is facilitated by a direct interaction with hTra2 beta 1. *Hum Mol Genet*. 11:577-87

Young PJ, Francis JW, Lince D, Coon K, Androphy EJ and Lorson CL (2003) The Ewing's sarcoma protein interacts with the Tudor domain of the survival motor neuron protein. *Brain Res Mol Brain Res*. 119:37-49

Young PJ, Jensen KT, Burger LR, Pintel DJ and Lorson CL (2002c) Minute virus of mice NS1 interacts with the SMN protein, and they colocalize in novel nuclear bodies induced by parvovirus infection. *J Virol*. 76:3892-904

Young PJ, Jensen KT, Burger LR, Pintel DJ and Lorson CL (2002d) Minute virus of mice small nonstructural protein NS2 interacts and colocalizes with the Smn protein. *J Virol*. 76:6364-9

Young PJ, Le TT, thi Man N, Burghes AH and Morris GE (2000) The relationship between SMN, the spinal muscular atrophy protein, and nuclear coiled bodies in differentiated tissues and cultured cells. *Exp Cell Res*. 256:365-74

Young PJ, Newman A, Jensen KT, Burger LR, Pintel DJ and Lorson CL (2005) Minute virus of mice small non-structural protein NS2 localizes within, but is not required for the formation of, Smn-associated autonomous parvovirus-associated replication bodies. *J Gen Virol*. 86:1009-14

Yu Q, Cok SJ, Zeng C and Morrison AR (2003) Translational repression of human matrix metalloproteinases-13 by an alternatively spliced form of T-cell-restricted intracellular antigen-related protein (TIAR). *J Biol Chem*. 278:1579-84

Zerres K and Davies KE (1999) 59th ENMC International Workshop: Spinal Muscular Atrophies: recent progress and revised diagnostic criteria 17-19 April 1998, Soestduinen, The Netherlands. *Neuromuscul Disord*. 9:272-8

Zerres K and Rudnik-Schoneborn S (1995) Natural history in proximal spinal muscular atrophy. Clinical analysis of 445 patients and suggestions for a modification of existing classifications. *Arch Neurol*. 52:518-23

Zerres K, Rudnik-Schoneborn S, Forkert R and Wirth B (1995) Genetic basis of adult-onset spinal muscular atrophy. *Lancet*. 346:1162

Zhang HL, Pan F, Hong D, Shenoy SM, Singer RH and Bassell GJ (2003) Active transport of the survival motor neuron protein and the role of exon-7 in cytoplasmic localization. *J Neurosci*. 23:6627-37

Zhang ML, Lorson CL, Androphy EJ and Zhou J (2001) An in vivo reporter system for measuring increased inclusion of exon 7 in SMN2 mRNA: potential therapy of SMA. *Gene Ther*. 8:1532-8

Zhu J, Mayeda A and Krainer AR (2001) Exon identity established through differential antagonism between exonic splicing silencer-bound hnRNP A1 and enhancer-bound SR proteins. *Mol Cell*. 8:1351-61

Zou J, Barahmand-pour F, Blackburn ML, Matsui Y, Chansky HA and Yang L (2004) Survival motor neuron (SMN) protein interacts with transcription corepressor mSin3A. *J Biol Chem*. 279:14922-8

# Appendix

*- Data tables which are presented in the results section will not be recurring here -*

# A.   *In vitro* experiments with histone deacetylase (HDAC) inhibitors in cell lines derived from SMA patients

**A.1: Levels of *Htra2-β1* transcripts and *Htra2-β2* transcripts in SMA fibroblast lines treated with VPA.**

| Human SMA fibroblast culture | | Concentration of VPA (µM) | | | | | |
|---|---|---|---|---|---|---|---|
| | | **Mock** | **0.5** | **5** | **50** | **500** | **1000** |
| **ML-17** (SMA I, 2 *SMN2* copies) | ***Htra2-β1*** | 1.00 | 2.95 | 1.98 | 2.06 | 1.40 | 1.45 |
| **ML-16** (SMA I, 3 *SMN2* copies) | ***Htra2-β1*** | 1.00 | 2.76 | 3.02 | 4.00 | 3.43 | 2.66 |
| **ML-5** (SMA II, 3 *SMN2* copies) | ***Htra2-β1*** | 1.00 | 1.58 | 1.80 | 1.86 | 0.99 | 0.93 |
| | ***Htra2-β2*** | 1.00 | 1.82 | 2.79 | 3.76 | 0.98 | 0.84 |

**A.2: Transfection efficiencies obtained for different passages of SMA fibroblast line ML-16 after electroporation using the Amaxa Nucleofector technology. Various electroporation programs were applied to deliver the pmaxGFP plasmid (encoding green fluorescent protein) into the cells. Transfected cells were subsequently identified by their green fluorescence on a flow cytometer. P11 was the youngest investigated cell passage, and P13 the oldest investigated cell passage.**

| Passage of ML-16 | Nucleofector Kit | Electroporation program | Amount of pmaxGFP (µg) | Transfected cells (%) |
|---|---|---|---|---|
| **P 11** | Basic | U23 | 2 | 85.3 |
| | Basic | A24 | 1 | 35.3 |
| | Basic | T16 | 1 | 45.3 |
| | Basic | U12 | 1 | 52.0 |
| | Basic | V13 | 1 | 75.7 |
| | Basic | U23 | 1 | 65.5 |
| | NHDF | V13 | 1 | 49.8 |
| | NHDF | U23 | 1 | 62.7 |
| **P 12** | Basic | V13 | 2 | 63.2 |
| | Basic | U23 | 2 | 70.7 |
| | NHDF | V13 | 2 | 71.1 |
| | NHDF | U23 | 2 | 65.5 |
| **P 13** | Basic | V13 | 2 | 54.6 |
| | Basic | U23 | 2 | 59.6 |
| | NHDF | V13 | 2 | 62.9 |
| | NHDF | U23 | 2 | 55.5 |

## A



**24 h**          **48 h**          **72 h**

β-tubulin

SMN

without siRNA
+ siRNA oligo 3
+ siRNA oligo 5
+ Non-Targeting siRNA
without siRNA
+ siRNA oligo 3
+ siRNA oligo 5
+ Non-Targeting siRNA
without siRNA
+ siRNA oligo 3
+ siRNA oligo 5
+ Non-Targeting siRNA

**+ Basic, + U23**

## B



**24 h**          **48 h**          **72 h**

Htra2-β1

without siRNA
+ siRNA oligo 3
+ siRNA oligo 5
+ Non-Targeting siRNA
without siRNA
+ siRNA oligo 3
+ siRNA oligo 5
+ Non-Targeting siRNA
without siRNA
+ siRNA oligo 3
+ siRNA oligo 5
+ Non-Targeting siRNA
POSITIVE CONTROL

**+ Basic, + U23**

**A.3: Western blot analysis of protein extracts prepared from fibroblast line ML-16 at 24, 48, and 72 h after electroporation (Amaxa Nucleofector technology) using the electroporation program U23 and the Basic Nucleofector Kit for Primary Mammalian Fibroblasts. *(A)* Initial experiments to evaluate a suitable siRNA oligo directed against Htra2-β1 (siRNA oligo 3 or siRNA oligo 5) and to evaluate a suitable incubation time (24, 48, or 72 h) to obtain a sufficient knock-down of the Htra2-β1 protein level. Fibroblasts incubated without any siRNA oligo and incubated with Non-targeting siRNA were included as controls. All of the samples were treated with Nucleofector Solution (Basic Kit) and the electroporation program U23. Western blot analysis revealed signals for β-tubulin and SMN, however, Htra2-β1 could not be detected. *(B)* The threefold amount of each protein extract used in *(A)* was loaded on a gel and a western blot analysis was carried out including a positive control (protein extract derived from ML-16 fibroblasts which were neither treated with Nucleofector solution, nor with an electroporation program). Htra2-β1 protein was clearly detected in the positive control, whereas the protein was undetectable in all the other samples. Ponceau staining of the nitrocellulose membranes was performed to ensure that approximately equal protein amounts of each sample were loaded onto the gel and transferred to the membrane.**
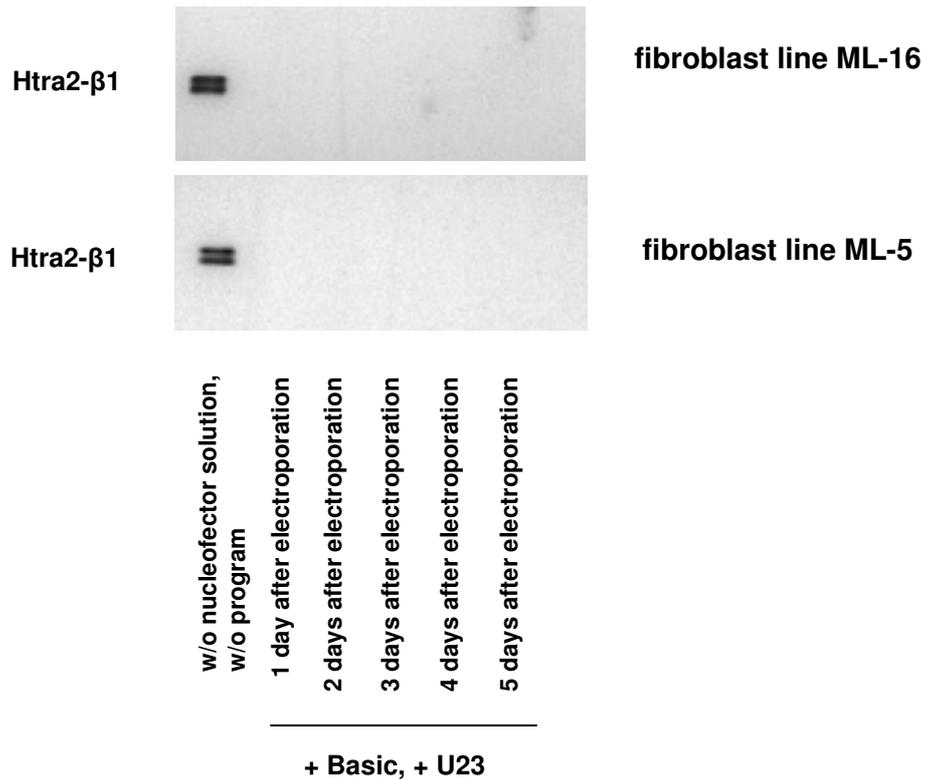
**A.4: Western blot analysis of protein extracts prepared from ML-16 and ML-5 at 1, 2, 3, 4, and 5 days after electroporation (Amaxa Nucleofector technology) using the electroporation program U23 and the Basic Nucleofector Kit for Primary Mammalian Fibroblasts. Fibroblasts from the same respective cell passage of ML-16 or ML-5 that were neither treated with Nucleofector solution nor with an electroporation program served as positive control (first lane in each Western blot). Staining of the nitrocellulose membranes with Ponceau was performed to ensure that approximately equal protein amounts of each sample were loaded onto the gel and transferred to the membrane.**

**A.5: Levels of *PPIB* (*Cyclophilin B*) transcripts in the SMA fibroblast lines ML-16 and ML-5 after transfection with the validated positive control silencer siCONTROL Cyclophilin B siRNA using the <u>Dharmafect 1</u> lipofection reagent. Transcript levels were repeatedly measured by quantitative real-time PCR at 24, 48, and 72 h after transfection, and are given as mean ± SEM. Lowest *PPIB* levels are marked in bold.**

| Human SMA fibroblast culture | *PPIB* transcript level | | | | | |
|---|---|---|---|---|---|---|
| | 24 h after transfection | | 48 h after transfection | | 72 h after transfection | |
| | Mock | +siRNA | Mock | +siRNA | Mock | +siRNA |
| **ML-16** (SMA I, 3 *SMN2* copies) | 1.00±0.03 | 1.01±0.01 | 1.00±0.02 | **0.34±0.01** | 1.00±0.05 | 0.41±0.03 |
| **ML-5** (SMA II, 3 *SMN2* copies) | 1.00±0.03 | 0.73±0.00 | 1.00±0.12 | **0.44±0.06** | 1.00±0.02 | 0.47±0.03 |

**A.6: Levels of** *PPIB* **(***Cyclophilin B***) transcripts in the SMA fibroblast lines ML-16 and ML-5 after transfection with the validated positive control silencer siCONTROL Cyclophilin B siRNA using the** <u>Dharmafect 3</u> **lipofection reagent. Transcript levels were repeatedly measured by quantitative real-time PCR at 24, 48, and 72 h after transfection, and are given as mean ± SEM. Lowest** *PPIB* **levels are marked in bold.**

| Human SMA fibroblast culture | *PPIB* transcript level | | | | | |
|---|---|---|---|---|---|---|
| | 24 h after transfection | | 48 h after transfection | | 72 h after transfection | |
| | Mock | +siRNA | Mock | +siRNA | Mock | +siRNA |
| **ML-16** (SMA I, 3 *SMN2* copies) | 1.00±0.03 | 1.45±0.04 | 1.00±0.02 | **0.38±0.01** | 1.00±0.05 | 0.46±0.03 |
| **ML-5** (SMA II, 3 *SMN2* copies) | 1.00±0.03 | 0.99±0.04 | 1.00±0.12 | 0.44±0.06 | 1.00±0.02 | **0.39±0.01** |
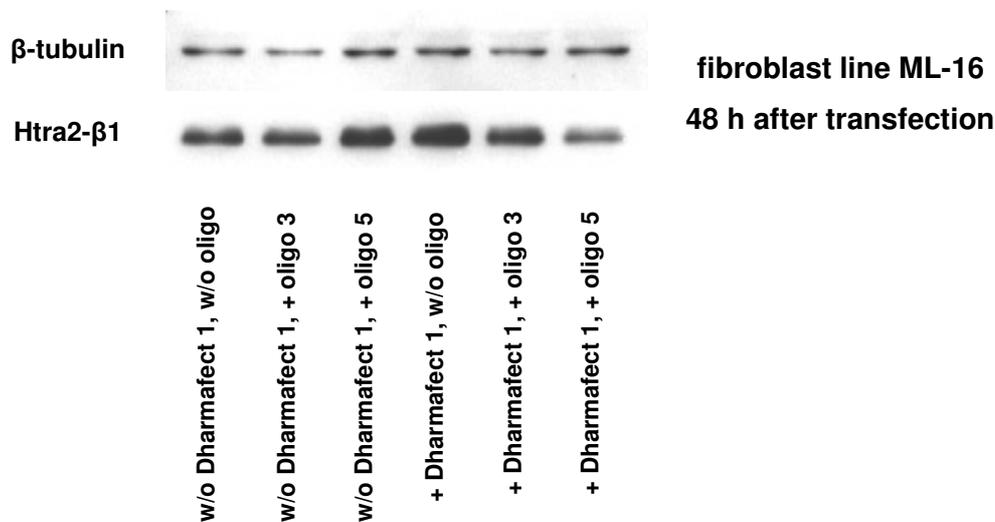


**A.7: Western blot analysis of protein extracts prepared from ML-16 at** <u>48 h after transfection</u> **with the siRNA oligos 3 and 5 using Dharmafect 1. Both siRNA oligos target Htra2-β1 mRNA. Controls included ML-16 fibroblasts which were neither treated with Dharmafect 1 nor with siRNA (first lane), fibroblasts which were treated with oligo 3 / oligo 5 without addition of Dharmafect 1 (second and third lane), and fibroblasts which were treated with Dharmafect 1 but not with siRNA oligos (fourth lane).**

β-tubulin

Htra2-β1

**fibroblast line ML-16**

**72 h after transfection**

w/o Dharmafect 1, w/o oligo

w/o Dharmafect 1, + oligo 3

w/o Dharmafect 1, + oligo 5

+ Dharmafect 1, w/o oligo

+ Dharmafect 1, + oligo 3

+ Dharmafect 1, + oligo 5
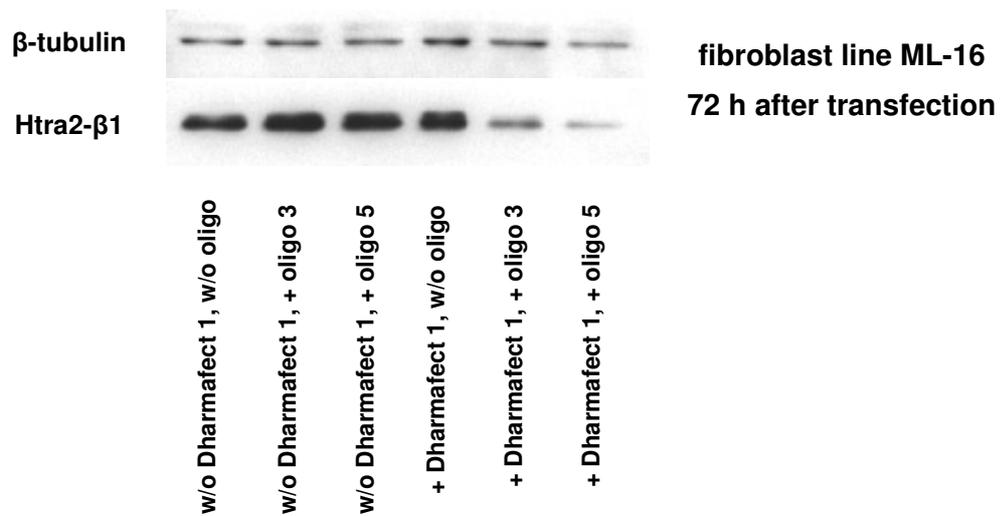
**A.8: Western blot analysis of protein extracts prepared from ML-16 at 72 h after transfection with the siRNA oligos 3 and 5 using Dharmafect 1. Both siRNA oligos target Htra2-β1 mRNA. Controls included ML-16 fibroblasts which were neither treated with Dharmafect 1 nor with siRNA (first lane), fibroblasts which were treated with oligo 3 / oligo 5 without addition of Dharmafect 1 (second and third lane), and fibroblasts which were treated with Dharmafect 1 but not with siRNA oligos (fourth lane).**

β-tubulin

Htra2-β1

**fibroblast line ML-16**

**96 h after transfection**

w/o Dharmafect 1, w/o oligo

w/o Dharmafect 1, + oligo 3

w/o Dharmafect 1, + oligo 5

+ Dharmafect 1, w/o oligo

+ Dharmafect 1, + oligo 3

+ Dharmafect 1, + oligo 5
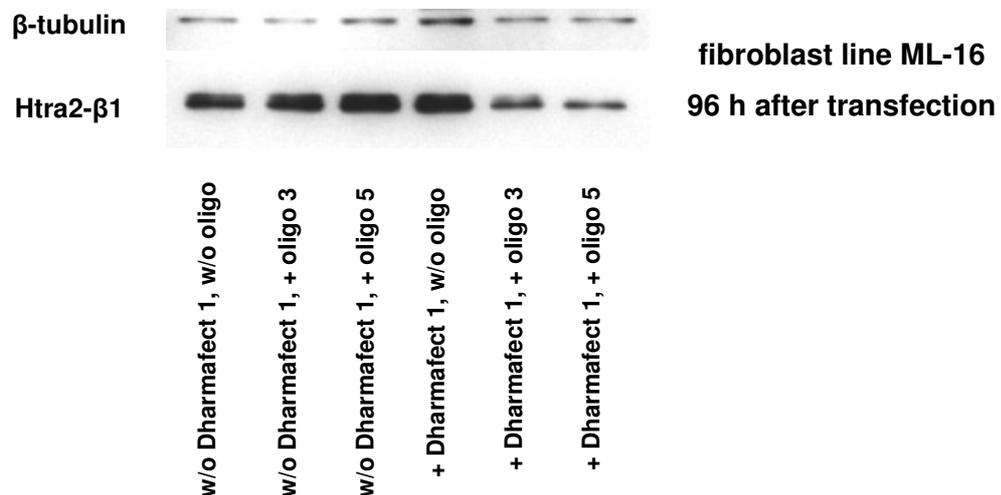
**A.9: Western blot analysis of protein extracts prepared from ML-16 at 96 h after transfection with the siRNA oligos 3 and 5 using Dharmafect 1. Both siRNA oligos target Htra2-β1 mRNA. Controls included ML-16 fibroblasts which were neither treated with Dharmafect 1 nor with siRNA (first lane), fibroblasts which were treated with oligo 3 / oligo 5 without addition of Dharmafect 1 (second and third lane), and fibroblasts which were treated with Dharmafect 1 but not with siRNA oligos (fourth lane).**

**A.10: Levels of Htra2-β1 protein in the SMA fibroblast line ML-16 after transfection with the siRNA oligos 3 and 5 using Dharmafect 1 lipofection reagent. Both siRNA oligos target Htra2-β1 mRNA. Cells were harvested at 48, 72, and 96 h after transfection, protein extracts were prepared, and western blot analysis was performed using β-tubulin as loading control. Lowest Htra2-β1 protein levels are marked in bold.**

| Human SMA fibroblast culture | | Htra2-β1 protein level | | | |
|---|---|---|---|---|---|
| | | Mock | 48 h after transfection | 72 h after transfection | 96 h after transfection |
| **ML-16** (SMA I, 3 *SMN2* copies) | **Oligo 3** | 1 | 1.16 | **0.31** | 0.60 |
| | **Oligo 5** | 1 | 0.51 | **0.09** | 0.38 |

**A.11: Absorption data obtained from <u>MTT assays</u> in fibroblast line ML-16 after transfection with siCONTROL TOX siRNA using Dharmafect 1 compared to untransfected cells (mock). The experiment served to determine the transfection efficiency. Cells transfected with the siCONTROL TOX siRNA underwent apoptosis. Thus, the rate of apoptosis corresponds to the transfection efficiency. Experiments were performed in triplicates and data are given as mean ± SEM.**

| Human SMA fibroblast culture | | Absorption | |
|---|---|---|---|
| | | Mock | + siCONTROL TOX |
| **ML-16** (SMA I, 3 *SMN2* copies) | **1st experiment** | 0.080±0.003 | 0.033±0.002 |
| | **2nd experiment** | 0.075±0.003 | 0.014±0.007 |

**A.12: Htra2-β1 protein levels determined after western blotting of protein extracts obtained from the <u>first knock-down experiment</u> in fibroblast line ML-16. Cells were transfected with or without siRNA oligo 5 against Htra2-β1 mRNA and harvested at 72 h after transfection. Prior to harvest, a part of the cells was additionally incubated with VPA for 16 h. Experiments were performed in triplicates and results are given as mean ± SEM.**

| Human SMA fibroblast culture | Htra2-β1 protein level | |
|---|---|---|
| | - siRNA, - VPA | 1.00±0.03 |
| **ML-16**<br>(SMA I, 3 *SMN2* copies) | + siRNA, - VPA | 0.46±0.03 |
| | - siRNA, + VPA | 1.03±0.14 |
| | + siRNA, + VPA | 0.41±0.08 |

**A.13: Htra2-β1 protein levels determined after western blotting of protein extracts obtained from the <u>second knock-down experiment</u> in fibroblast line ML-16. Cells were transfected with or without siRNA oligo 5 against Htra2-β1 mRNA and harvested at 72 h after transfection. Experiments were performed in triplicates and results are given as mean ± SEM.**

| Human SMA fibroblast culture | Htra2-β1 protein level | |
|---|---|---|
| **ML-16**<br>(SMA I, 3 *SMN2* copies) | - siRNA (Mock) | 1.00±0.11 |
| | + siRNA | 0.06±0.03 |

**A.14:** *SMN2*, *PPIB*, and *Htra2-β1* transcript levels determined by real-time PCR in RNA samples obtained from the <u>second knock-down experiment</u> in fibroblast line ML-16. Cells were incubated without siRNA (Mock) or transfected with the respective silencing siRNA or the siCONTROL Non-targeting siRNA and harvested at 72 h after transfection. The values given for FL-*SMN2*, Δ7-*SMN2*, FL / Δ7 ratio, and *Htra2-β1* were determined in the samples transfected with siRNA oligo 5 directed against *Htra2-β1* mRNA, and the *PPIB* transcript levels were determined after transfection of the fibroblasts with the positive control silencer siCONTROL Cyclophilin B siRNA. Experiments were performed in triplicates and results are given as mean ± SEM.

| Human SMA fibroblast culture | | Transcript levels | | |
|---|---|---|---|---|
| | | - siRNA (Mock) | + silencing siRNA | + Non-targeting siRNA |
| **ML-16** (SMA I, 3 *SMN2* copies) | **FL-*SMN2*** | 7.16±0.10 | 10.17±0.51 | 8.67±0.38 |
| | **Δ7-*SMN2*** | 5.50±0.38 | 6.08±0.39 | 6.04±0.15 |
| | **FL / Δ7 ratio** | 1.31±0.09 | 1.68±0.03 | 1.44±0.03 |
| | ***PPIB*** | 9.11±0.63 | 0.30±0.02 | 9.67±0.22 |
| | ***Htra2-β1*** | 7.78±0.26 | 2.53±0.24 | 8.03±0.40 |

## B.  *In vivo* effect of valproic acid on *SMN* gene expression in SMA carriers and SMA patients

**B.1: Analysis of *CTLA1* expression in different blood cell fractions which are delivered with the Human Blood Fractions MTC Panel. Human placenta control served as negative control. Values from repeated measurements are given as mean ± SEM. "+" is the abbreviation for "positive".**

| Blood cell fraction | *CTLA1* transcript level |
|---|---|
| Mononuclear cells | 21.13±1.68 |
| Resting CD8+ cells | 47.62±2.30 |
| Resting CD4+ cells | 1.38±0.08 |
| Resting CD14+ cells | 7.65±0.29 |
| Resting CD19+ cells | 0.67±0.05 |
| Activated CD19+ cells | 15.01±0.78 |
| Activated mononuclear cells | 65.57±4.67 |
| Activated CD4+ cells | 46.67±0.14 |
| Activated CD8+ cells | 46.42±0.13 |
| Human placenta control | 0.66±0.03 |

**B.2: *RPLP0* and *PPIB* transcript levels in 20 blood samples obtained from ten control individuals who donated blood twice over a period of several weeks. Values from repeated measurements are given as mean ± SEM.**

| Subject No. | *RPLP0* | | *PPIB* | |
|---|---|---|---|---|
| | Sample 1 | Sample 2 | Sample 1 | Sample 2 |
| 50 | 1.05±0.01 | 2.00±0.26 | 1.15±0.03 | 1.54±0.22 |
| 51 | 1.00±0.02 | 1.26±0.04 | 1.06±0.07 | 1.17±0.01 |
| 52 | 1.31±0.03 | 1.18±0.00 | 1.34±0.00 | 1.18±0.06 |
| 53 | 1.22±0.00 | 1.46±0.00 | 1.00±0.01 | 1.15±0.01 |
| 54 | 1.21±0.07 | 1.18±0.04 | 1.30±0.06 | 1.13±0.06 |
| 56 | 1.29±0.02 | 1.63±0.04 | 1.15±0.01 | 1.38±0.06 |
| 57 | 1.42±0.05 | 1.53±0.07 | 1.32±0.01 | 1.19±0.06 |
| 58 | 1.07±0.04 | 1.26±0.01 | 1.22±0.07 | 1.30±0.00 |
| 59 | 1.19±0.01 | 1.35±0.02 | 1.04±0.00 | 1.17±0.01 |
| 60 | 1.00±0.03 | 2.07±0.05 | 1.04±0.02 | 1.39±0.01 |

**B.3:** *B2M* and *GUSB* transcript levels in 20 blood samples obtained from ten control individuals who donated blood twice over a period of several weeks. Values from repeated measurements are given as mean ± SEM.

| Subject No. | B2M | | GUSB | |
|:---:|:---:|:---:|:---:|:---:|
| | Sample 1 | Sample 2 | Sample 1 | Sample 2 |
| 50 | 1.84±0.00 | 3.50±0.04 | 1.34±0.05 | 1.29±0.23 |
| 51 | 1.62±0.12 | 2.36±0.04 | 1.00±0.04 | 1.11±0.13 |
| 52 | 1.30±0.05 | 2.01±0.06 | 1.47±0.01 | 1.22±0.00 |
| 53 | 1.54±0.02 | 2.72±0.09 | 1.19±0.02 | 1.21±0.03 |
| 54 | 2.09±0.00 | 1.78±0.06 | 1.40±0.05 | 1.25±0.03 |
| 56 | 1.45±0.01 | 2.19±0.01 | 1.39±0.04 | 1.39±0.06 |
| 57 | 2.39±0.07 | 2.26±0.01 | 1.54±0.00 | 1.38±0.08 |
| 58 | 1.00±0.01 | 1.28±0.00 | 1.50±0.00 | 1.41±0.05 |
| 59 | 1.77±0.01 | 2.30±0.01 | 1.27±0.01 | 1.23±0.01 |
| 60 | 1.61±0.05 | 3.14±0.03 | 1.34±0.00 | 1.57±0.09 |

**B.4:** Purity of the lymphocyte and the monocyte fraction after isolation of PBMCs from peripheral whole blood and separation of two the cell fractions by magnetic cell sorting (MACS). The fractions were analyzed on a flow cytometer using anti-CD14 and anti-CD45 fluorescently labeled antibodies. Whenever enough material was available, 10,000 events were counted and analyzed. The table presents the number of lymphocytes / monocytes together with the number of contaminating cells that were identified among the counted events within one sample. Due to the very limited number of PBMCs obtained from individuals 57 and 63, the purity was not checked in the corresponding separated cell fractions.

| Subject No. | Fraction of lymphocytes | | Fraction of monocytes | |
|:---:|:---:|:---:|:---:|:---:|
| | Number of lymphocytes | Number of monocytes (contamination) | Number of lymphocytes (contamination) | Number of monocytes |
| 52 | 9318 | 171 | 126 | 7866 |
| 54 | 8243 | 49 | 162 | 2470 |
| 55 | 9331 | 118 | 239 | 7122 |
| 56 | 8678 | 270 | 37 | 8204 |
| 58 | 9527 | 29 | 58 | 8602 |
| 59 | 8729 | 59 | 60 | 416 |
| 62 | 9515 | 74 | 435 | 3443 |

**B.5:** _PPIB_ and _GUSB_ transcript levels in corresponding monocytes and lymphocytes fractions derived from nine control individuals. Levels were measured after isolation of PBMCs from peripheral whole blood, separation of the cells by magnetic cell sorting, mRNA isolation, and reverse transcription. Values obtained after repeated measurements are given as mean ± SEM.

| Subject No. | PPIB | | GUSB | |
| --- | --- | --- | --- | --- |
| | Lymphocytes | Monocytes | Lymphocytes | Monocytes |
| 52 | 11.78±0.28 | 13.96±0.67 | 8.31±0.78 | 15.27±1.33 |
| 54 | 11.55±0.17 | 11.61±0.34 | 9.49±0.07 | 13.31±0.24 |
| 55 | 14.96±0.25 | 15.96±0.08 | 14.07±0.19 | 23.93±0.50 |
| 56 | 9.23±0.02 | 8.48±0.16 | 7.21±0.22 | 10.39±0.33 |
| 57 | 9.07±0.46 | 14.98±0.32 | 8.44±0.45 | 21.92±0.05 |
| 58 | 9.69±0.16 | 13.01±0.53 | 10.82±0.00 | 19.27±1.81 |
| 59 | 8.88±0.19 | 7.18±0.16 | 6.86±0.43 | 7.16±0.26 |
| 62 | 8.32±0.08 | 10.04±0.70 | 9.41±1.27 | 13.47±0.15 |
| 63 | 7.17±1.11 | 9.46±0.30 | 9.85±0.07 | 16.83±0.00 |

**B.6:** FL-_SMN_ and Δ7-_SMN_ transcript levels in corresponding monocytes and lymphocytes fractions derived from nine control individuals. Levels were measured after isolation of PBMCs from peripheral whole blood, separation of the cells by magnetic cell sorting, mRNA isolation, and reverse transcription. Values obtained after repeated measurements are given as mean ± SEM.

| Subject No. | FL-SMN | | Δ7-SMN | |
| --- | --- | --- | --- | --- |
| | Lymphocytes | Monocytes | Lymphocytes | Monocytes |
| 52 | 9.32±0.07 | 9.81±0.19 | 7.65±0.56 | 8.22±0.43 |
| 54 | 10.47±0.13 | 9.26±0.40 | 10.19±0.27 | 7.11±0.13 |
| 55 | 10.42±0.13 | 10.73±0.13 | 10.24±0.16 | 12.22±0.42 |
| 56 | 14.03±0.10 | 9.63±1.25 | 13.16±0.10 | 10.31±0.00 |
| 57 | 5.92±0.27 | 6.08±0.09 | 3.88±0.10 | 3.99±0.18 |
| 58 | 13.21±0.10 | 13.15±0.29 | 10.30±0.49 | 9.85±0.23 |
| 59 | 9.64±0.19 | 8.24±0.22 | 9.16±0.98 | 6.36±0.27 |
| 62 | 7.95±0.10 | 7.01±0.19 | 7.80±0.86 | 5.92±0.14 |
| 63 | 6.50±0.19 | 8.19±0.26 | 7.58±0.26 | 8.83±0.58 |

**B.7: Expression levels of *PPIB* and *GUSB* in peripheral whole blood from ten SMA carriers (C1 to C10) treated with VPA. Values are given as mean ± SEM together with the corresponding VPA serum level determined in the same blood sample (n.d. = not detected). Varying total number of values obtained for each parameter among the probands resulted from varying time periods required to adapt VPA serum levels to the therapeutic range. The most extensively increased/decreased value detected for *PPIB* and *GUSB* in the respective SMA carrier is indicated in bold.**

| SMA Carrier | *PPIB* and *GUSB* transcript levels together with the corresponding VPA serum level | | | | | | | |
|---|---|---|---|---|---|---|---|---|
| **C1** 1x*SMN1* 1x*SMN2* | *PPIB* | 1.0±0.1 | 1.0±0.0 | 1.2±0.0 | 1.0±0.0 | **1.4±0.1** | 1.0±0.0 | 1.2±0.0 |
| | *GUSB* | 1.0±0.1 | 0.7±0.1 | 1.0±0.0 | 0.9±0.0 | 1.0±0.0 | 0.7±0.0 | **1.1±0.0** |
| | VPA (mg/l) | baseline | n.d. | 53.9 | 65.7 | 79.5 | 104.0 | 84.8 |
| **C2** 1x*SMN1* 1x*SMN2* | *PPIB* | 1.0±0.1 | 0.8±0.0 | **1.6±0.1** | 1.0±0.0 | **0.5±0.0** | 0.8±0.0 | 0.9±0.0 | 1.1±0.0 |
| | *GUSB* | 1.0±0.1 | 0.7±0.0 | **1.4±0.1** | 0.8±0.0 | **0.5±0.0** | 0.7±0.0 | 1.0±0.0 | 1.2±0.0 |
| | VPA (mg/l) | baseline | n.d. | 26.7 | 45.9 | 62.6 | 75.6 | 57.3 | 61.0 |
| **C3** 1x*SMN1* 2x*SMN2* | *PPIB* | 1.0±0.1 | 1.4±0.0 | 1.3±0.0 | 1.7±0.0 | 1.9±0.0 | 1.5±0.0 | **2.4±0.1** |
| | *GUSB* | 1.0±0.1 | 1.4±0.0 | 1.1±0.0 | 1.5±0.0 | 1.9±0.0 | 1.4±0.0 | **2.2±0.0** |
| | VPA (mg/l) | baseline | 30.1 | 64.3 | 48.6 | 60.0 | 58.7 | 53.9 |
| **C4** 1x*SMN1* 2x*SMN2* | *PPIB* | 1.0±0.1 | 1.2±0.0 | 1.1±0.0 | **1.6±0.0** | 1.6±0.0 | 1.5±0.0 |
| | *GUSB* | 1.0±0.1 | 1.1±0.0 | 1.2±0.0 | 1.6±0.0 | **1.7±0.0** | 1.5±0.0 |
| | VPA (mg/l) | baseline | 41.4 | 69.7 | 80.5 | 83.3 | 78.8 |
| **C5** 1x*SMN1* 2x*SMN2* | *PPIB* | 1.0±0.0 | 0.8±0.0 | 1.3±0.0 | 1.0±0.0 | **0.6±0.0** | 1.0±0.0 | 0.9±0.0 | **1.4±0.0** |
| | *GUSB* | 1.0±0.0 | 0.8±0.0 | 1.4±0.0 | 1.1±0.0 | **0.6±0.0** | 1.2±0.0 | 1.0±0.0 | **1.7±0.0** |
| | VPA (mg/l) | baseline | n.d. | 33.2 | 32.7 | 56.2 | 53.1 | 50.7 | 64.3 |
| **C6** 1x*SMN1* 2x*SMN2* | *PPIB* | 1.0±0.0 | **1.1±0.0** | 0.8±0.1 | 1.0±0.1 | 0.9±0.0 | 0.7±0.0 |
| | *GUSB* | 1.0±0.0 | 1.0±0.0 | 1.0±0.0 | 1.1±0.0 | **1.2±0.1** | 0.9±0.1 |
| | VPA (mg/l) | baseline | 51.7 | 70.3 | 80.1 | 74.3 | 82.3 |
| **C7** 1x*SMN1* 2x*SMN2* | *PPIB* | 1.0±0.1 | 0.8±0.0 | 1.0±0.0 | **1.2±0.1** | 0.8±0.0 | 0.9±0.0 |
| | *GUSB* | 1.0±0.1 | 0.6±0.0 | **1.1±0.0** | 1.0±0.0 | 0.7±0.0 | 0.7±0.0 |
| | VPA (mg/l) | baseline | n.d. | 76.9 | 92.0 | 128.5 | 80.7 |
| **C8** 1x*SMN1* 3x*SMN2* | *PPIB* | 1.0±0.0 | 1.2±0.1 | 1.2±0.1 | **1.5±0.0** | 1.0±0.0 | 1.4±0.0 |
| | *GUSB* | 1.0±0.0 | 1.3±0.0 | 1.5±0.0 | 1.4±0.1 | 1.1±0.0 | **1.6±0.1** |
| | VPA (mg/l) | baseline | 10.0 | 58.5 | 79.9 | 63.6 | 67.8 |
| **C9** 1x*SMN1* 3x*SMN2* | *PPIB* | 1.0±0.1 | 0.9±0.0 | 1.2±0.0 | 1.0±0.0 | **1.2±0.0** | 1.0±0.0 |
| | *GUSB* | 1.0±0.1 | **0.7±0.0** | 1.2±0.1 | 1.3±0.0 | **1.4±0.0** | 0.9±0.1 |
| | VPA (mg/l) | baseline | 30.7 | 59.9 | 69.1 | 64.3 | 62.4 |
| **C10** 1x*SMN1* 3x*SMN2* | *PPIB* | 1.0±0.0 | 0.9±0.0 | 0.9±0.0 | 0.7±0.0 | 0.9±0.0 | 1.0±0.0 | 1.0±0.0 | **1.2±0.0** |
| | *GUSB* | 1.0±0.0 | 0.8±0.1 | 0.8±0.0 | **0.5±0.0** | 0.8±0.0 | 1.1±0.0 | 0.9±0.0 | **1.2±0.0** |
| | VPA (mg/l) | baseline | n.d. | 45.3 | 65.9 | 58.9 | 84.2 | 75.6 | 61.6 |

**B.8: Values obtained from the measurement of Sphero Rainbow Calibration particles on a flow cytometer. The Molecules of Equivalent Fluorescein are given and correspond to one of eight different particle fractions, each of which is labeled with a standardized amount of dye that is able to emit green fluorescence similar to the fluorophore FITC. Seven of these fractions were detected by the flow cytometer such that the mean fluorescence intensity of the respective fraction was analyzed.**

| Molecules of Equivalent Fluorescein (MEFL, given) | 600 | 1,800 | 4,700 | 15,000 | 40,000 | 140,000 | 330,000 |
|---|---|---|---|---|---|---|---|
| Mean Fluorescence (FL-1, measured) | 2.83 | 6.77 | 16.93 | 49.19 | 126.26 | 419.27 | 926.57 |

**B.9: Comparison of FL-*SMN* and Δ7-*SMN* mRNA baseline levels together with an analysis of the FL-*SMN*/Δ7-*SMN* ratio in blood collected from 41 untreated subjects. From each subject, blood was taken twice over a time period of several weeks. The average values calculated after repeated measurements of the two blood samples are given as mean ± SEM. The order of the individuals used in this table corresponds to the order of the individuals in figure 35 in the results section.**

|  | Genotype | FL-*SMN* | Δ7-*SMN* | FL / Δ7 ratio |
|---|---|---|---|---|
| **Controls** | 3 *SMN1*, 2 *SMN2* | 7.26±0.17 | 6.65±0.28 | 1.10±0.05 |
|  | 2 *SMN1*, 2 *SMN2* | 6.42±0.53 | 7.18±0.70 | 0.90±0.03 |
|  | 2 *SMN1*, 2 *SMN2* | 6.06±0.26 | 6.85±0.16 | 0.88±0.02 |
|  | 2 *SMN1*, 2 *SMN2* | 5.62±0.50 | 6.17±0.58 | 0.92±0.10 |
|  | 2 *SMN1*, 2 *SMN2* | 5.65±0.45 | 6.97±0.23 | 0.81±0.04 |
|  | 2 *SMN1*, 1 *SMN2* | 5.95±0.19 | 4.32±0.30 | 1.41±0.14 |
|  | 2 *SMN1*, 1 *SMN2* | 6.13±1.01 | 4.15±0.48 | 1.46±0.13 |
|  | 2 *SMN1*, 1 *SMN2* | 5.89±0.13 | 3.95±0.11 | 1.49±0.04 |
|  | 2 *SMN1*, 1 *SMN2* | 6.97±0.53 | 4.40±0.59 | 1.61±0.17 |
|  | 2 *SMN1*, 0 *SMN2* | 5.57±0.32 | 0.10±0.10 | 55.74±3.21 |
| **Carriers** | 1 *SMN1*, 3 *SMN2* | 6.41±0.42 | 9.60±0.52 | 0.67±0.03 |
|  | 1 *SMN1*, 3 *SMN2* | 7.45±1.13 | 10.94±1.85 | 0.70±0.05 |
|  | 1 *SMN1*, 3 *SMN2* | 7.31±0.35 | 10.96±0.75 | 0.68±0.04 |
|  | 1 *SMN1*, 2 *SMN2* | 5.19±0.64 | 6.49±0.51 | 0.79±0.06 |
|  | 1 *SMN1*, 2 *SMN2* | 6.47±0.51 | 8.67±0.79 | 0.76±0.05 |
|  | 1 *SMN1*, 2 *SMN2* | 5.73±0.43 | 7.18±0.50 | 0.80±0.05 |

| | Genotype | FL-*SMN* | Δ7-*SMN* | FL / Δ7 ratio |
|---|---|---|---|---|
| **Carriers** | 1 *SMN1*, 2 *SMN2* | 6.38±0.50 | 8.31±0.76 | 0.77±0.02 |
| | 1 *SMN1*, 2 *SMN2* | 5.77±0.43 | 6.76±0.44 | 0.85±0.04 |
| | 1 *SMN1*, 1 *SMN2* | 4.82±0.72 | 4.41±0.48 | 1.08±0.07 |
| | 1 *SMN1*, 1 *SMN2* | 5.50±0.64 | 5.36±0.34 | 1.01±0.07 |
| **SMA III Patients** | 4 *SMN2* | 9.61±0.20 | 16.51±0.65 | 0.59±0.04 |
| | 4 *SMN2* | 4.90±0.39 | 9.49±0.74 | 0.52±0.05 |
| | 3 *SMN2* | 6.80±0.64 | 10.84±1.38 | 0.64±0.04 |
| | 3 *SMN2* | 4.08±0.23 | 7.83±0.21 | 0.52±0.03 |
| | 3 *SMN2* | 6.02±0.61 | 12.14±0.96 | 0.50±0.03 |
| | 3 *SMN2* | 3.25±0.16 | 7.60±0.26 | 0.43±0.02 |
| **SMA II Patients** | 3 *SMN2* | 4.04±0.30 | 9.56±0.78 | 0.42±0.01 |
| | 3 *SMN2* | 6.80±0.75 | 11.31±1.19 | 0.60±0.02 |
| | 3 *SMN2* | 9.06±1.30 | 13.32±1.18 | 0.67±0.04 |
| | 3 *SMN2* | 3.24±0.61 | 6.96±0.34 | 0.46±0.07 |
| | 3 *SMN2* | 5.40±0.56 | 10.96±0.52 | 0.49±0.03 |
| | 3 *SMN2* | 4.77±0.39 | 11.01±0.54 | 0.43±0.02 |
| | 3 *SMN2* | 5.68±0.82 | 12.09±1.70 | 0.47±0.02 |
| | 3 *SMN2* | 7.40±1.32 | 14.71±1.35 | 0.49±0.05 |
| | 3 *SMN2* | 5.36±0.56 | 11.20±1.82 | 0.49±0.03 |
| | 3 *SMN2* | 7.22±0.47 | 14.35±1.14 | 0.51±0.01 |
| **SMA I Patients** | 3 *SMN2* | 7.73±0.50 | 11.21±0.50 | 0.69±0.04 |
| | 2 *SMN2* | 4.11±0.17 | 9.07±0.32 | 0.45±0.02 |
| | 2 *SMN2* | 3.66±0.09 | 7.45±0.55 | 0.50±0.03 |
| | 2 *SMN2* | 4.72±0.51 | 9.55±0.97 | 0.50±0.03 |
| | 2 *SMN2* | 4.16±0.55 | 8.11±0.42 | 0.51±0.05 |

# Erklärung

Ich versichere, dass ich die von mir vorgelegte Dissertation selbständig angefertigt, die benutzten Quellen und Hilfsmittel vollständig angegeben und die Stellen der Arbeit - einschließlich Tabellen, Karten und Abbildungen - , die anderen Werken im Wortlaut oder dem Sinn nach entnommen sind, in jedem Einzelfall als Entlehnung kenntlich gemacht habe; dass diese Dissertation noch keiner anderen Fakultät oder Universität zur Prüfung vorgelegen hat; dass sie - abgesehen von unten angegebenen Teilpublikationen - noch nicht veröffentlicht worden ist sowie, dass ich eine solche Veröffentlichung vor Abschluss des Promotionsverfahrens nicht vornehmen werde. Die Bestimmungen der Promotionsordnung sind mir bekannt. Die von mir vorgelegte Dissertation ist von Frau Professor Brunhilde Wirth betreut worden.

*Teilpublikationen:*

**Brichta L**, Hofmann Y, Hahnen E, Siebzehnrubl FA, Raschke H, Blumcke I, Eyupoglu IY and Wirth B (2003) Valproic acid increases the SMN2 protein level: a well-known drug as a potential therapy for spinal muscular atrophy. *Hum Mol Genet.* 12: 2481-9

**Brichta L**, Holker I, Haug K, Klockgether T and Wirth B (2006) In vivo activation of SMN in spinal muscular atrophy carriers and patients treated with valproate. *Ann Neurol.* 59: 970-5

Hahnen E, Eyupoglu IY, **Brichta L**, Haastert K, Trankle C, Siebzehnrubl FA, Riessland M, Holker I, Claus P, Romstock J, Buslei R, Wirth B and Blumcke I (2006) In vitro and ex vivo evaluation of second-generation histone deacetylase inhibitors for the treatment of spinal muscular atrophy. *J Neurochem.* May 2006 [Epub ahead of print]

Köln, 30. Juni 2006                                             Lars Brichta

# Curriculum Vitae - Lars Brichta

| | |
|---|---|
| Geburtsdatum: | 06. Mai 1977 |
| Geburtsort: | Lutherstadt Eisleben |
| Staatsangehörigkeit: | deutsch |
| Familienstand: | ledig |

## Schulausbildung

| | |
|---|---|
| 1983 - 1987 | Grundschule Siersleben |
| 1987 - 1991 | Polytechnische Oberschule „Adolf Hennecke" Siersleben |
| 1991 - 1995 | Gottfried-August-Bürger-Gymnasium Benndorf |
| | Abschluss: Allgemeine Hochschulreife, Prädikat „sehr gut" (1,0) |

## Wehrdienst

| | |
|---|---|
| 1995 - 1996 | Sanitäter in der Dr.-Dorothea-Erxleben-Kaserne in Halle sowie in der Sachsen-Anhalt-Kaserne in Weißenfels |

## Hochschulstudium

| | |
|---|---|
| 1996 - 2000 | Martin-Luther-Universität Halle-Wittenberg |
| | Studium der Pharmazie |
| | Stipendiat der Studienstiftung des deutschen Volkes |
| Oktober 2000 - März 2001 | Novartis Pharma AG in Basel, Schweiz |
| | Department of Bone Metabolism-Biology (Dr. T. Buhl) |
| | Diplomarbeit mit dem Thema: |
| | „Analytical interferences and pharmacokinetic interactions between acebutolol with its active metabolite diacetolol and polyethylene glycol 400 applying LC ESI MS/MS" |
| | Abschluss: Diplompharmazeut, Prädikat „sehr gut" |
| April 2001 - September 2001 | Pharmaziepraktikum in der Heide-Apotheke, Halle |
| November 2001 | Approbation als Apotheker |
| | Pharmazeutische Prüfung mit dem Prädikat „sehr gut" (1,07) |

**Beruflicher Werdegang**

Januar 2002 - Juli 2002    Forschungsaufenthalt an den
National Institutes of Health (NIH) in Bethesda, USA
National Institute of Diabetes, Digestive and Kidney Diseases
(NIDDK), Laboratory of Bioorganic Chemistry (Dr. J. Wess)
Molekularbiologische Arbeiten an Muscarinrezeptoren

Martin-Luther-Stipendium der Universität Halle-Wittenberg


seit August 2002    Universität zu Köln sowie
Rheinische Friedrich-Wilhelms-Universität Bonn,
Institute für Humangenetik (Prof. Dr. B. Wirth)
Anfertigung einer Dissertation mit dem Thema:
„Molecular genetic investigations of histone deacetylase
inhibitors as potential neurotherapeutics for autosomal
recessive proximal spinal muscular atrophy (SMA)"

**Sonstiges**

1985 - 1992    Musikschule Eisleben
Unterricht im Fach Cello,
Abschlussprüfung mit dem Prädikat „gut"


Bonn, 30. Juni 2006                                Lars Brichta